Electronics and Computing in Textiles
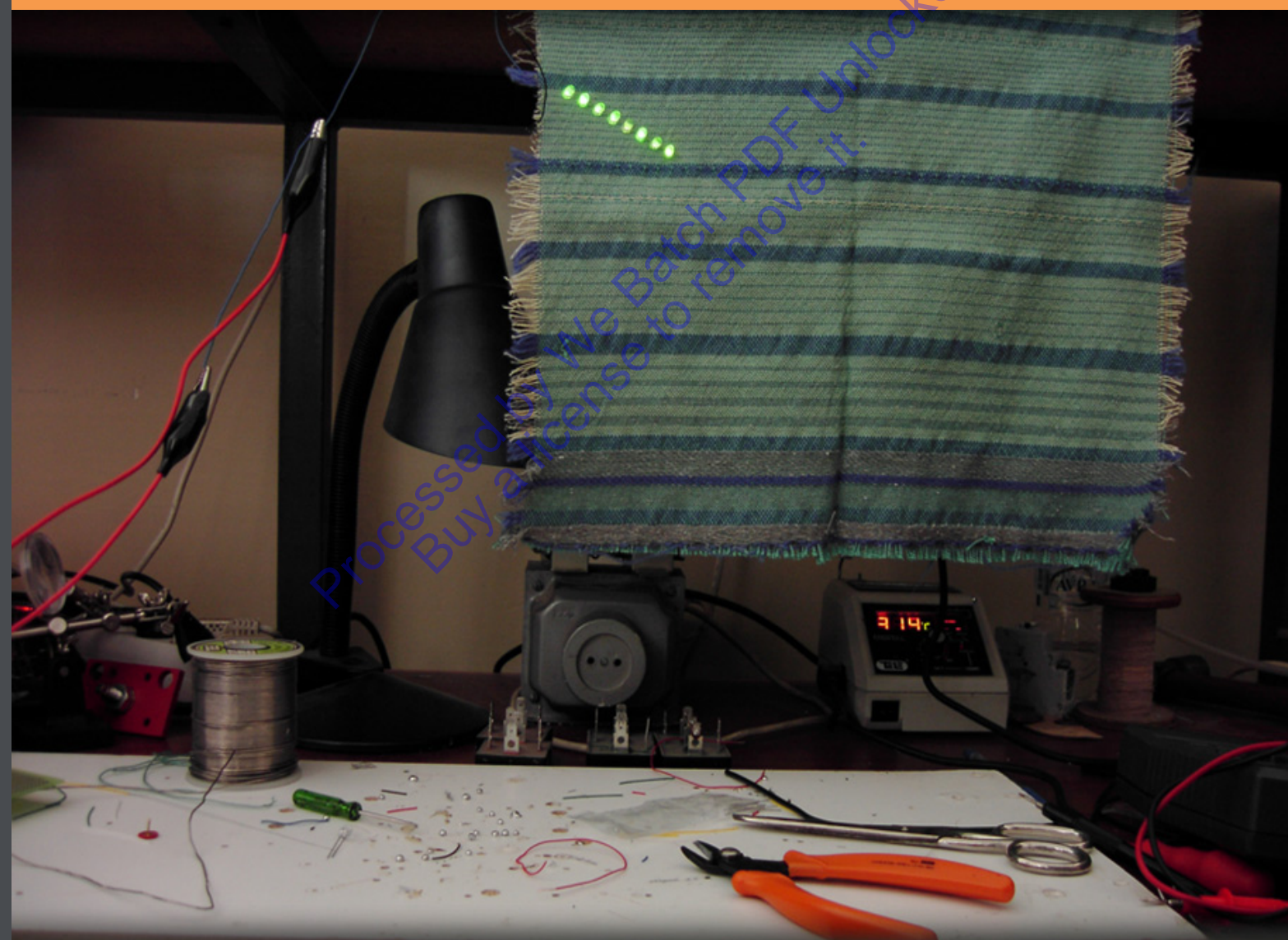
Editor: Savvas Vassiliadis

Editor: Savvas Vassiliadis

Contributors:

M. Rangoussi and A. Çay, A. Kallivretaki, D. Domvoglou, S. Potirakis, N.-A. Tatlas

N. Stathopoulos, S. Savaidis and S. Mitilinaios, Kl. Prekas

D. Goustouridis and E.D. Kyriakis-Bitzaros, M. Blaga, S. Boz and M.Ç. Erdoğan

Electronics and Computing in Textiles

Electronics and Computing in Textiles

Editor: Savvas Vassiliadis

Contributors:

M. Rangoussi and A. Çay, A. Kallivretaki, D. Domvoglou, S. Potirakis, N.-A. Tatlas

N. Stathopoulos, S. Savaidis and S. Mitilinaios, Kl. Prekas

D. Goustouridis and E.D. Kyriakis-Bitzaros, M. Blaga, S. Boz and M.Ç. Erdoğan

Contents

Download free eBooks at bookboon.com

Preface

The book "Electronics and Computing in Textiles" has a strong cross-disciplinary character. Textiles (including clothing) represent a mature industrial sector, however it engages many scientific fields. Process, mechanical, electrical, electronics and computer engineering, in parallel to the physics and chemistry, as well as to the materials science contribute in the evolution and the progress of the Textile engineering.

Textile sector benefits from the interaction between the disciplines. Newly developed materials and methods, new machines and models are added to the potential of the textile engineering. The result is obvious: advanced textile and clothing items, more comfortable and with better appearance as well as with improved mechanical and sensorial properties. It is also very impressive that these advanced products are delivered in the market under much better cost characteristics than in the past.

The increased interaction and synergy between the various disciplines has generated the strong stream of the technical textiles. They are fibrous and textile products created for technical applications and use. Medical, military, aeronautical, automotive and structural are considered as typical technical textiles. Recently the electronics and the computing engineering influence on an increasing basis the textile processes and products. The multifunctional textiles are complex products designed with the aim to combine the textile character with one or more others, e.g. the electrical. This fact enables the presentation of the point of view of this book. It examines the dependencies and the relationships between the electronics and the computing on the one hand and the textiles on the other, in order to serve the study and the understanding of the related materials, systems and processes. It is worth to mention that the approach of this book is very innovative and unique, since there is a lack of related sources with the aforementioned contents and structure.

This book is a result of the collaboration of many authors. Every chapter corresponding to a different topic, has been written by one or more scientists of the respective specialization. The majority of the chapters are written by electrical and computers engineers, who specialize and apply the electrical, electronic and computing engineering topics into the textile fields. Few other chapters give the opposite point of view, where the textile engineers describe how the electronic and computing systems exist now in their fields and influence the productivity and the production issues. One of the research activities of the Department of Electronics of TEI Piraeus, Greece is the support of the electronics and computing issues applied in the textile and clothing sector. Therefore the authors of the first group are mainly from the academic staff of it. The authors of the second group are well known and specialized members of the academic community of the universities of Iasi, Romania and Ege, Turkey.

I would like to thank my colleagues, who accepted my invitation to participate in this innovative book. As co-authors they share their knowledge and experience for the benefit of the readers and consequently they have contributed in the successful publication of this book. It was a unique positive experience to coordinate this group of friendly and dedicated persons. I would be happy to receive any comments or errors reports from our readers. Its the only way to correct and to improve the level of this book.

Dr. Savvas Vassiliadis
TEI Piraeus, Athens, Greece
September 2012
svas@teipir.gr

Introduction

The unique properties of the fibrous materials have been recognized thousands of years ago and they became the basic material for the clothing and domestic uses. Later they have been used for technical applications in parallel to the clothing ones. The textile (and clothing) engineering deals with the study and development of the fibrous materials, their process, integration and treatment in order to deliver a product in the market. The development of new materials and processes with new and increased properties made possible the design of new products and on the other hand the detection of user needs initiated the development of new materials and processes. The technology push and pull principle finds many excellent applications examples in the textile sector.

The textile technology combines, besides the mathematics, physics and chemistry, numerous engineering fields such as mechanical, chemical, electrical, process, materials etc. Especially the modern textile technology with intensive orientation to multifunctional and smart materials, as well as to the wearable systems and e-textiles, brings together the neighboring engineering fields for the achievement of the expected advanced result. A modern and successful textile engineer must establish a multiple profile with the fibre, fabrics and textile process engineering in the kernel surrounded by the links to the other disciplines. Thus it is very important to offer to the textile engineers a thorough overview of the related fields with emphasis on the modern aspects of them. It is expected that the textile engineers will be familiarized with the potential of the other fields and the tools offered by them in solving textile problems. This is exactly the point of view of this book. Electronic and Computing specialists give a reader friendly overview of their specific fields and combine it with related textile applications. They initiate exactly understanding of the content of the particular areas as well as of the typical applications in the textile field. In order to offer an idea of the penetration of the Electronic and Computing technology in the textile sector, two chapters describe the use of electronic and computing systems in the knitting and clothing sector.

The first chapter is dedicated to the artificial neural networks (ANN). The ANN is a powerful tool used in complex problems and procedures. The ANN is itself a non-linear and stochastic model. They are very successful in system identification, modelling and prediction applications, pattern recognition and classification as well as in data clustering, filtering and compression. These application fields are common in many of the textile technology problems. After the systematic introduction to the ANN's a couple of interesting examples of textile interest is presented.

Chapter 2 presents the computational mechanical modelling principles and their application in the properties prediction of the complex textile structures. The estimation of the properties and the behaviour of the textile structures was rough and based on the empirical experience of the engineers. Today especially for the technical applications the predictions precision requirements are higher and the empirical approach is not enough. Analytical expressions for the description of the mechanical behaviour do not exist due to the geometrical and materials non-linearities. Therefore the mechanical computational modelling of the textile structures becomes essential and very useful. Basic methods and characteristic examples are presented for a variety of models.

In Chapter 3 the e-textiles related concepts are presented. The reader gets familiar on the basic theoretical aspects of the electrical conductivity and the electrical properties of the textile materials. The more advanced topic on the textile sensors and actuators is following and a reference is made on the power supply methods of the e-textiles systems. Finally the incorporation of the microprocessors and the installation of communication networks are given.

The acoustics and the sound absorption issues on the textile field is the subject of the Chapter 4. The chapter starts with an introduction in the theory of sound and noise. Further the sound measurement is thoroughly described. The next topic is about the sound absorption, reflection and refraction which is followed by the method of measurement of sound absorption measurements. In order to come gradually in the nature of the fabrics, the sound absorption mechanisms in porous materials are presented. Finally the textile applications of the acoustics and sound absorption are given and discussed.

In the Chapter 5 the signal processing field is presented and it is followed by the respective applications in the textile area. After a short introduction, the theory of the signals and the digitization is presented. Thereafter the basic characteristics and method of the signal processing in its various forms are thorough discussed. Special attention is paid on the discreet time signals and systems case. Finally the digital image processing issues are offered to the reader and after the completion of the information provided, the application in the textile field is closing the chapter.

The Chapter 6 is an extended chapter embracing the radio frequencies theory and applications. The chapter starts with a through introduction and continues in the transmission lines theory and their electrical characteristics. Various operational conditions are examined and the Smith chart is presented. In the next paragraph a coaxial cable T-resonator is described. The following topic is the one on the antennas. The description and analysis of the radiation patterns, the gain and bandwidth are given. The microstrip antennae are presented. Finally applications of the textile area are discussed.

Chapter 7 gives an overview of the programmable logic controllers. These control devices are very much used in the various textile processing stages. In every machine the operation is based and controlled by one or usually more PLC's. The introduction on the PLC's is followed by the presentation of their technical characteristics. In the next stage the various kinds of inputs and outputs are given. The examination of the PLC's is continued by the software development and the operation of the PLC's issues. As it happens in the previous chapters a case study from the textile industry is presented.

The Chapter 8 covers the topic of the wireless body area networks and the sensors networking. It starts with an introduction and an examination of the needs of that kind of networks. In a next paragraph the structure of the wireless body area networks is examined with a reference on the various modules used. The next part contains the areas of usage of the wireless body area networks and the communication protocols and platforms. Finally an extended collection of known R&D projects of the current field is reported.

Chapter 9 provides the knitted fabrics engineering, especially the knitters point of view. The knitting principles and the knitting machines are presented. The next step is the presentation of the production of the knitted garments. Following to that the electronic elements and devises in use are described. As a main computing field the CAD and the CAM systems are extensively observed. With that structure the chapter gives a very good approach of the application of electronic and computing systems in the knitting field.

In Chapter 10 the electronic and computer applications in the clothing design and production are given. After the introduction, the chapter continues on the issues related with the electronics and computing in the modelling department. In the next part the electronics and computing in the cutting department are presented. As it is expected the next paragraph is dedicated in the electronics and computing in the sewing room. The chapter contains also an extended reference on the computerized movers for the transportation of the intermediate and final products in the clothing industry. The last part presents the important computerized management and control issues.

We hope that the innovative structure of this book will help the engineers of the various fields to understand each other better and easier. It also gives them the opportunity to obtain the maximization of the performance of the team work, when engineers from different disciplines cooperate with textile specialists. Any comments and suggestions for the future editions are considered as serious contributions for the upgrade of the level of the book and thus they are highly appreciated.

1. Non linear approaches in textiles: the Artificial Neural Networks example

by

M. Rangoussi and A. Çay

Department of Electronics Engineering, Technological Education Institute of Piraeus, Greece
Department of Textile Engineering, Ege University, Izmir, Turkey

1.1 Introduction

1.1.1 Engineering and Modeling

Engineering designs and constructs all kinds of devices, equipment, technical systems, large production units or public works aiming to improve the quality of human life and to raise the living standards. Engineering also designs and construct all tools, machinery and methods necessary for these tasks. To accomplish its mission, engineering makes use of all the great results of science and technology, along with the innovative thinking of engineers all over the world. The outcomes of all this effort comprise the so-called 'man-made' or 'artificial' component of the world that surrounds us, as opposed to the 'natural' component (earth, fauna, flora, human beings and climate). Now-a-days, engineering works cover all dimensions from micro- and nano- to giga- and terra- scales and expand their range of activities to the space and faraway planets and stars.

Textiles is one of the most ancient and most close to the human being engineering fields: it goes back to ancient Egypt, where the Pharaohs wore elaborate hand gloves made from cotton threads, to ancient China and probably even further back in human prehistory. For thousands of years, textiles have been clothing the human body for protection and survival, for distinction of hierarchy, role and responsibility, for celebration or mourning, for the joy of life and the sorrow of death.

Apart from clothing, yarns and fabrics have found millions of other uses, ranging from traditional investment of interiors (tents, furniture, buildings, cars, airplanes), sails for vessels or media for stocking goods to the most exciting modern uses (aesthetics and fashion, healthcare, military and safety) and further on to the smart, multi-functional textiles of the modern era, equipped with sensors and 'gifted' with artificial intelligence so as to respond to our needs or feelings!

A major tool in the effort of scientists and engineers to understand nature and its laws and exploit this knowledge to construct better artificial devices and systems has been the analysis and modeling of systems. This is achieved by means of mathematical and physical sciences, at various levels of abstraction and at various levels of approximation as well. Models of real life systems and of their functionality have evolved from early forms of architectural miniatures of landscapes, buildings, bridges, airports, factories, vehicles, etc. made of clay, cork, plastic or other materials, to the modern, electronic, three-dimensional models created by sophisticated computer graphics software.

It is important to keep in mind that it is the mathematics relations, simple or complex, lying behind all such software, that govern the drawing of the geometrical forms and shapes, texture and lighting effects that produce the exquisite, photo-realistic models on a computer screen. In turn, these mathematics relations have been formulated by scientists on the basis of analysis of the real system they had carried out, in an attempt to approximate its functionality by a set of relations of the minimum complexity possible; yet, it should adequately resemble the real system.

Although intuitively an accurate and detailed model is expected to be more useful, often an approximate, simplified model is to be preferred, as it lends itself to immediate use while it retains the key characteristics of the system it models. It is parsimonious, in the sense that it is not overloaded with details that cannot be appreciated by the user of the model. Still, it provides us with a clear-cut view of the real-world prototype it models.

What is the practical value of a model? It has to do with prediction. A model helps the designer predict the behavior, static or dynamic, of the device or system being designed, before taking the cost and dedicating the effort to actually construct it. This results in considerable savings of effort and cost. Loops of testing, corrections and changes for the improvement of the initial design are common practice in the design and construction of products or services. Fortunately, models allow us to loop through correction steps at a considerably low level of cost and take the construction cost for the real-world system only after the design has been finalized.

In textiles engineering, models built to describe the properties, characteristic measures and dynamic behavior of yarns, fabrics and final products have been valuable design tools. Of great practical value are models that predict the properties and behavior of the produced fabric based on the properties of the yarns and weaving pattern employed.

1.1.2   Is this a deterministic or a stochastic world?

In their strife to obtain 'good' models, scientists have gradually shifted from the deterministic to the so-called stochastic approach. The difference between the two terms is essential to the way the world around us is perceived and interpreted by humans; in fact, expressed under various forms, the dilemma whether this is a deterministic or a stochastic world has long been discussed and argued by science, philosophy and religion. Leaving that aspect of the discussion to the knowledgeable, engineering proceeds to exploit the best of the two approaches, selecting per case the one that produces adequately good models for the problem at hand.

- The deterministic approach heeds that the world around us, its natural and artificial components alike, can be fully and exactly described by mathematics relations. At an increased level of complexity – often prohibitively high for all practical purposes – equations and inequalities, linear or nonlinear, can describe in full detail all that happens around us, including laws of nature, behavior of beings and functionalities of constructed, artificial systems. Scientists formulate the sets of such relations by study and analysis of the real-world systems and phenomena; next, engineers simplify them enough to be manageable by contemporary mathematics and software – but not too much, so as to retain the essential features of the real-world prototype they model. The level of approximation in the description of systems and phenomena thus obtained is varying and it is decided per occasion by the engineers.

- The stochastic approach heeds that there exist factors affecting behaviors and functionalities of beings and systems that cannot be fully described by equations, as they are essentially random in nature. Noise, either acoustic or electronic, mechanical friction, the behavior of the atmosphere as transport media for wireless communications are but a few typical examples of factors that render a system random or stochastic. Laws of nature are no exception, either. The set of all possible outcomes or values of a random factor form an ensemble; the random factor is described by measures averaged over the ensemble of all its possible forms, rather than with exact equations per case. Stochastic equations are thus obtained to describe or model stochastic systems and the notion of probability (that one of all possible outcomes contained in the ensemble will eventually occur at a given time) comes into picture.

Major engineering tasks such as detection of events, pattern recognition and object classification receive stochastic answers under the stochastic approach. A certain fabric flaw probably (or with probability p %) is caused by a certain machinery fault, a certain fabric is more likely (higher probability) to belong to class A than to class B, or it will exhibit a given property with probability p %. In contrast, the deterministic approach provides 'binary' or 'crisp' answers of the type: belongs / does not belong, exists / does not exist, will exhibit / will not exhibit, etc. Both types of answers may be correct or wrong; the stochastic approach, however, is closer to the way a human expert would make and express decisions.

1.1.3   Is this a linear or a non-linear world?

This is clearly a non-linear world, all scientists answer in concordance. Non-linearity is the rule without exception in nature and all natural factors: materials, constructions, beings and behaviors. Linearity is an abstraction adopted by our perception in order to simplify nature at a level where we would be able to comprehend, describe and interpret it. A straight line or a perfect plane, as these are defined in Euclidean geometry, are not to be seen anywhere in nature; yet, they are successful simplifications or approximations of a tight string or a calm water or other liquid media level.

Inasmuch as they bear a correspondence to the real-world objects, such approximations are valuable help for common people and scientists alike: the former use linear approximations to cope with everyday life problems and calculations of distance, area, value, time, etc., while the later exploit them to express and test theories and communicate results. Scientists have another good reason to seek linear approximations: linear mathematics have traditionally been far more advanced than non-linear mathematics, the later having progressed to a level of practical interest only recently. Tools and methods at the avail of scientists and engineers have been linear in their vast majority, prompting them to attempt to 'linearize' essentially non-linear problems.

It can be argued that linearity is a matter of 'distance' one takes from the object or behavior under study. Indeed, if one 'zooms in' to the surface of an object made of a given material, irregularities, aberrations, flaws and fluctuations – inherent to all materials – will appear; upon 'zooming out' enough, flaws disappear and the ideal straight line or plane view prevails. In fact, there are areas or parts or aspects of the object under study where the linear approximation is 'reasonable', i.e. it lies at a smaller distance or 'leaves small error' to the real, non-linear nature of the object, and other parts where such condition does not hold. Different linear approximations may be required at different parts of the object. A sigmoid line, for example, may be crudely approximated by three different straight lines as in Figure 1.1; this is a piece-wise linear approximation. These three lines constitute a linear model of the actual sigmoid line.
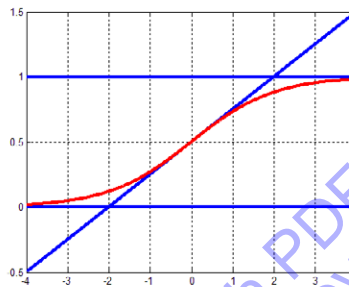

Figure 1.1: The non-linear sigmoid function (red curve) is approximated by three straight lines (blue lines).
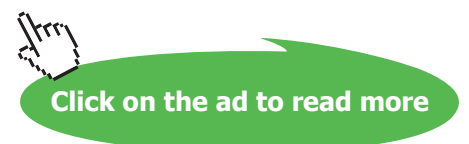The horizontal line at y = 0 is a good approximation for x < -2; the 'diagonal' line for -2 < x < 2; the horizontal line at y = 1 for x > 2.

It may be argued that a linear approximation by five different lines would be preferable, as it would leave smaller error; however, this is a more complex model that requires more computations. In general, there is a trade-off between approximation (model) complexity and approximation error, calling for a balanced decision.

When a real-world problem is cast into a linear model via a linear approximation procedure, linear mathematics (typically coded into a software tool) are employed to yield the solution, which is tested at a simulation level and the model is corrected accordingly. These steps loop until some criterion is met. The final solution is then materialized by the construction of the actual object. Yarn, tissue, fabric and final textile product design and construction are no exception to this approach.

1.2   Artificial Neural Networks (ANNs)

1.2.1   Is it all hype?

A part of it is – was, rather – hype, but certainly not all, scientists reply today. There's true value in them; only, one has to know what to expect. Only a couple of decades ago, excitement over the merits of these new tools drove expectations too high: they were claimed to be universal problem solvers. Interestingly enough, now that the dust has cleared, they still hold a title of universality – this time by strict mathematical proof: they are universal function approximators. If only for this property, ANNs deserve a formal introduction. In light of the discussion held in the previous section,

Artificial Neural Networks are non-linear, stochastic mathematical models.

1.2.2   ANN types and structures

They are inspired by – and named after – the neural system of biological organizations, a network built from *neurons*, *axons*, *dendrites* and connection points know as *synapses*, as neuroscience explains. Through this network, information flows in the form of electric signals from the peripheral sensors to the brain (*sensing* direction) and control orders flow from the brain to the peripherals (*actuating* direction). Similarities do not hold any further, however; the nervous system and the brain are far too complex to be fully understood or modeled by science as yet, while ANNs are governed by simple – even if non-linear – relations.

Artificial, as opposed to biological, neural networks are built of nodes called *neurons* or *processing elements (PEs)* which are interconnected by links bearing *weights*. Each node receives a vector of inputs, processes them non-linearly in the general case and produces a single output. Figure 1.2 shows a simplified example of a node that accepts a vector of three inputs $[x_0, x_1, x_2]$, weights them by $[w_0, w_1, w_2]$, respectively, processes their sum z by the non-linear 'activation function' (a sigmoid, a hard-limiter or other) to produce a single output y.
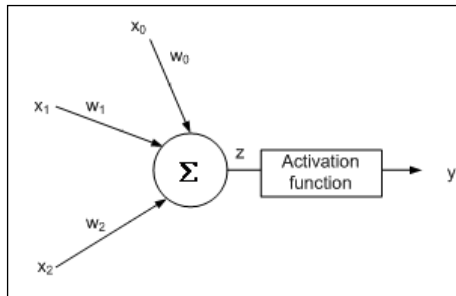
Figure 1.2: A simplified example of a node or PE or neuron of an ANN: input x are weighted by weights w.
The weighted average z is processed by the non-linear activation function to produce output z.

Nodes are organized into *layers* arrayed into a sequence; output values of a layer serve as input values to the next layer. In general, an ANN is a *multi-layer* construction. In an ANN of L layers, the first (L-1) layers are called *hidden* while the last, L-th layer is the *output layer*. Figure 1.3 shows a simplified example of an ANN with three layers of nodes (input, hidden, output).
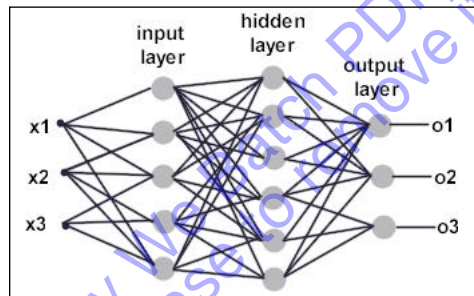
Figure 1.3: A simplified example of a three-layer ANN (input, hidden, output). Input vectors are three-dimensional ($[x_1, x_2, x_3]$).
All inputs are 'fed' to all input layer nodes. All nodes of a layer are connected to all nodes of the next layer.
Weights at connections are not shown for simplicity.

It is interesting that networks with as little as only two layers (one hidden and one output) can solve really complex problems. In fact, it has been proved that a two-layered network, appropriately structured and trained, can *approximate arbitrarily well any function* that has a finite number of discontinuities, thus gaining the title of universal approximators for the ANN family. How is this achieved? What other kinds of problems can ANNs solve?

Input data, typically in the form of vectors of measurements X, are introduced to the first layer. Data proceed through – while being processed by – the ANN, from layer to layer, to the *output layer*, where they form the vector of output values or (stochastic) decisions Y. Data flow between successive layers can be unidirectional (from a given layer to the next one in sequence) in a *feedforward network* or bidirectional (proceeding forward to the next layer *and* looping back to the previous one) in a *feedback network*.

Although more sophisticated forms exist, the *typical* processing relation performed by the nodes of layer L_i, in a feedforward network, in order to transforms the data vector X_i into the data vector X_{i+1}, is *a weighted average passed through a non-linear function*, formulated as

$$X_{i+1} = f_i(a_i X_i + b_i). \hspace{4cm} (1.1)$$

Here $f_i(\cdot)$ denotes the *non-linear transfer function* of layer L_i, common to all nodes in this layer but possibly varying across different layers. The log-sigmoid, the hard-limiter and the hyperbolic tangent are typical non-linear function examples. The linear option is retained for $f_i(\cdot)$ if a *linear layer* is necessary for solving a given problem. $\{a_i\}$ denotes the vector of *weights* and $\{b_i\}$ the vectors of additive constants (offsets or *biases*) that render the linear combination affine.

Network 'architecture' (i.e., the number of layers, number of nodes per layer, possible connections among nodes and layers, weights and non-linear functions employed) complexity is commensurate with the complexity of the system the ANN is asked to model. A variety of different architectures have been proposed and successfully implemented so far. Perceptrons, multilayer perceptrons, feedforward and feedback, generalized regression, associative, hebbian learning, radial basis, linear vector quantizer and many other network types are available for testing and use. Selection of the best architecture is empirical; rules of thumb rather than closed form solutions are available.

Download free eBooks at bookboon.com

1.2.3   ANN functionalities

In a feedforward network, input data vector X undergoes a series of L such transformations that change both the values and the number of the vector components, until it is handed out as output vector Y:

$$X=X_1 \rightarrow \boxed{L_1} \rightarrow X_2 \rightarrow \boxed{L_2} \rightarrow X_3 \rightarrow \cdots \rightarrow X_i \rightarrow \boxed{L_i} \rightarrow X_{i+1} \rightarrow \cdot\cdot \rightarrow X_L \rightarrow \boxed{L_L} \rightarrow Y$$
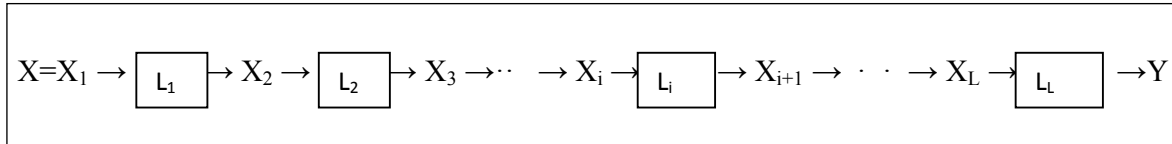
If viewed as one global system, the ANN structure proposes a relation between input vector X and output vector Y, of the form

$$Y = F(X), \tag{1.2}$$

where $F(\cdot)$ represents the *nested* application of the $f_i(\cdot)s$ across successive layers L_1 to L_L:

$$Y = F(X) = f_L(X_L) = f_L(f_{L-1}(X_{L-1})) = \qquad \cdots \qquad = f_L(f_{L-1}(f_{L-2}(\cdots(f_2(f_1(X_1)))\cdots))). \tag{1.3}$$

Although each $f_i(\cdot)$ is a simple function or model, the 'cumulative' effect across all layers in a multi-layered network produces rather complex functions. What is the kind of problems that such functions – and, consequently, ANNs can address successfully? They can be grouped under three major categories:

1. *Function approximation*, including system identification, modeling and prediction,
2. *Pattern classification*, including pattern recognition and decision making, and
3. *Data processing*, including clustering, filtering and compression.

It is worth to note that under these three categories falls a considerable majority of engineering problems, either directly or after suitable manipulation. How are these demanding tasks accomplished by an ANN? It has to do with the *adaptation property* of ANNs. It would be a rather simple task to build up an ANN model and code it into software, if it weren't for the fact that it is an adaptive model: weights $\{a_i\}$ and biases $\{b_i\}$ are repeatedly adjusted to best suit the data at hand, via an algorithm that is typically iterative, until an optimality criterion is met. A variety of iterative algorithms have been proposed so far; different algorithms are better suited to different types of problems. What is crucial here is the fact that these iterative algorithms have been proved to converge to a solution given an adequate set of sample data for training.

The development of an ANN approach in order to solve a given engineering problem proceeds in three phases: (a) initial selection of the ANN type, architecture and training algorithm, (b) training phase and (c) testing phase.

- During the training phase the ANN 'learns' the rules that govern the system under investigation through a set of examples (the training set) presented to its input; each input vector within the training set is associate with a correct output (answer). The iterative algorithm employed to 'train' the ANN adapts its weights iteratively, based on the difference between actual and correct output (error). Weights are adjusted until error is minimized; upon convergence the training phase ends.

- During the testing phase, which represents the actual ANN long-term functionality of interest, unknown examples are presented to its input; using the weight values adjusted through training, the ANN processes each unknown input and produces the corresponding output. This output value may represent things as different as class membership, probability of an event, estimated value of a parameter, etc. Correct outputs produced in response to unknown inputs prove the ANN's ability to 'generalize', i.e. to extract 'knowledge' or 'rules' from the set of examples that are then applied to unknown cases. The 'generalization' property ultimately shows that

    - the ANN type, architecture and training algorithm chosen are suitable for the problem at hand; and
    - the training set used was 'rich' (representative of all possible cases) enough to guarantee successful operation during testing phase.

What if 'generalization' is not achieved? This means that either the training set was not rich enough or the ANN selection was not successful (in total or in its parametrization). In the former case a different approach may be more suitable than ANNs since more data are not often easy to acquire; in the latter case the process loops back to redesign the net or its parametrization or the training algorithm and to go through the training phase once more.

All in all, the ANN approach is both complex and sensitive; it is worth taking the pain to resort to it only after straightforward, linear methods have failed to address the problem at hand or when there is strong evidence of non-linearity in the data, coming from prior information.

1.3   ANNs in textiles engineering

Artificial Neural Networks, in both their functions as approximators and as classifiers, have found use and successful application in a variety of problems arising in textiles engineering. They have been used to 'estimate' values of yarn-, fiber- or fabric-related properties on the basis of simple, measurable structural parameters, before the actual construction or fabrication step takes place. They have been used to detect failures, faults, or other events of interest from signals recorded or images taken during the yarn, fiber of fabric production process. It can be safely stated that within the textiles engineering area, ANNs have been exploited in all classic engineering problems, such as detection, classification, modeling, estimation and pattern analysis. In the following paragraphs, two such examples are outlined.

1.3.1 A function approximation problem example: prediction of fabric air permeability

Air permeability of fabrics is an important property in textiles because it determines both the comfort of the final product (garment) and the behavior of the fabric during the vacuum drying phase of its processing. Therefore, prediction of the air permeability of a fabric before its actual construction is a task of practical interest. Air permeability is known to depend on the material of the yarn and the micro-structural parameters of the fabric, through rather complex, non-linear relations. Porosity of the fabric offers a path to calculate air permeability; unfortunately, there is no standardized method to calculate or directly measure porosity, especially for dense fabrics. On the other hand, micro-structural parameters of the fabric such as warp and weft densities or mass per unit area of fabric can be measured with adequate accuracy.

Linear multiple regression analysis, carried out in order to investigate the degree of linearity of the relation among air permeability and the three aforementioned micro-structural parameters, reveals that an 85% of the variability in air permeability values can be linearly explained by the variability in the three parameters while the rest 15% calls for a non-linear approach. In that case an ANN can be designed and trained to predict air permeability values (output) from input vectors that contain micro-structural parameter measurement data.

A Generalized Regression Neural Network (GRNN) is employed for this task. This is a member of the Radial Basis Function ANNs that are known to be universal approximators appropriate for problems that present radial symmetry of the data space, as is the case at hand. Another advantage is that the GRNN training iterative algorithms converge rapidly. A GRNN contains two layers of neurons, each consisting of N neurons, where N is the cardinality of the training set (number of the input - output pairs available). The first (hidden) layer consists of radial basis function (RBF) neurons while the second (output) layer consists of linear neurons of special structure, allowing for real-valued outputs. A single, real-valued output value is employed here; it is the air permeability value predicted by the ANN on the basis of the three micro-structural parameters of the fabric under design. Indeed, after training with a set including various types of fabrics, the specific ANN exhibits satisfactory generalization, meaning that it can accurately predict air permeability values of fabrics not included in its training set – yet, of micro-structural parameters within the same range as those in the training set.

Figure 1.4 shows prediction results on a set of fabrics of six (6) different knitting patterns across five (5) different parameters yielding thirty (30) different fabric sample cases. Twenty four (24) samples are used for training and six (6) for testing. Air permeability values are on the vertical axis while fabric sample case index is on the horizontal axis. Upper plot shows excellent agreement between real (red stars) and ANN predicted (blue circles) air permeability values across the 24 cases of the training set, here used as the testing set. Lower plot shows the corresponding good agreement for the 6 cases of the testing set that are not used for training.

Calculation of the average error (difference between real and estimated air permeability output value) across different samples reveals that only 3.3% of the total variability in the air permeability value is not 'explained' by the non-linear, ANN approach, as compared to the 15% of variability left 'unexplained' by the linear method.
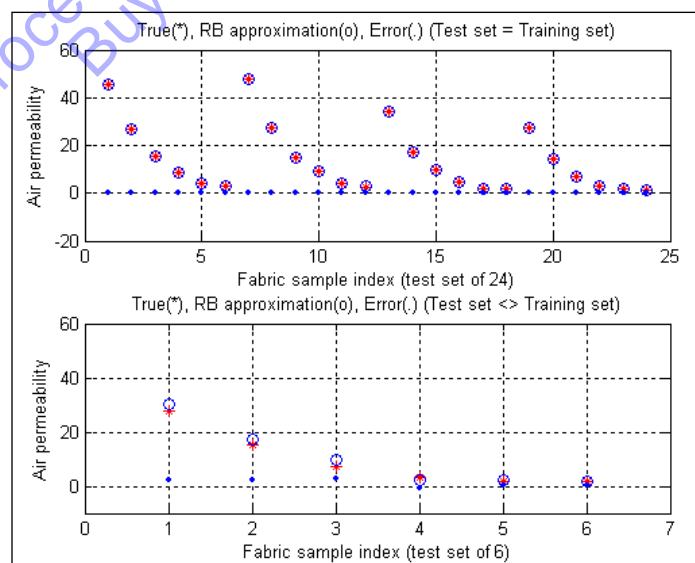

Figure 1.4: Air permeability real (red stars) and ANN predicted (blue circles) values for 30 fabric samples of different micro-structural parameters. Upper plot: training set used as testing set (24 cases). Lower plot: testing set unknown (6 cases).

In a feedforward network, input data vector X undergoes a series of L such transformations that change both the values and the number of the vector components, until it is handed out as output vector Y:

1.3.2 A classification problem example: classification of faults in circular knitting machines

The automated supervision of the knitting process is of high interest so as to avoid (i) the waste of material and (ii) the increase of production cost. Knitted fabrics produced by circular knitting machines that involve numerous moving parts may come out defective as a result of failure of the machine; depending on the type of failure, the product may be of reduced quality and price or altogether unsuitable for further use. Automated detection and classification of the various types of knitting machine failures is therefore of great practical interest. Indeed, if issued in real time, an alarm or call for technical support and repair will result in considerable time and cost savings. Yarn tension signal is a quantity that can be monitored for early machine failure detection. Figure 1.5 shows a yarn tension signal recording under normal (upper plot) and abnormal (lower plot) operating conditions of the knitting machine.

Correlation the different types of mechanical failures with the possible corresponding differences in the respective tension signals would allow for the classification of the machine fault type based on the classification of the event present in the recorded tension signal. This is a complex and demanding task for human experts; it is therefore expected to be demanding under automated performance as well. The non-linear ANN approach is investigated for the detection and the classification tasks.
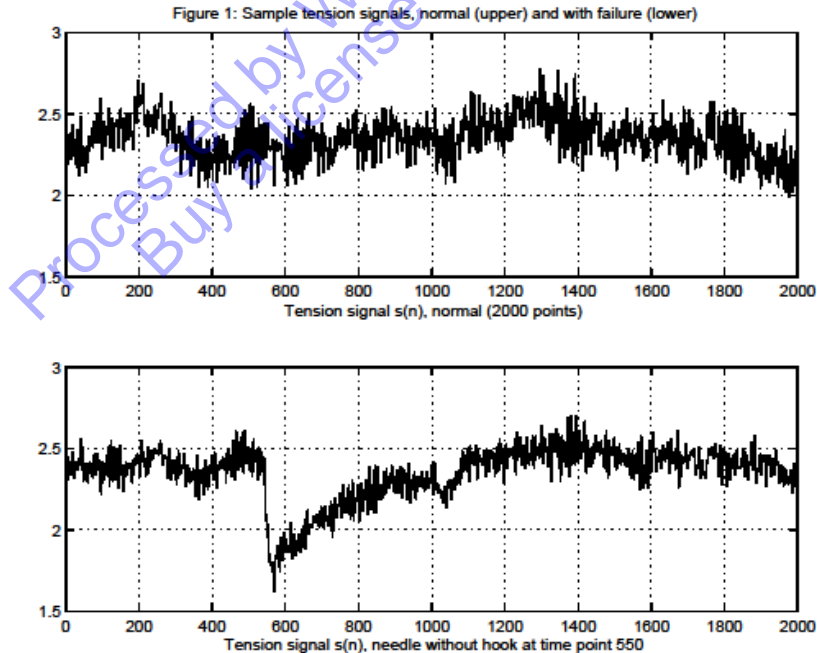

Figure 1: Sample tension signals, normal (upper) and with failure (lower)

Figure 1.5: Yarn tension signal recording under normal (upper plot) and abnormal (lower plot – needle without a hook) knitting machine operating conditions.

As a first step, a set of 'features' or characteristic quantities have to be extracted from the signal. This step reduces the dimensionality of the problem from the dimension of the recorded signal length down to that of the number 'features' selected and extracted. These features, however, should retain and convey all information present in the signal that will subsequently allow for the classification of the signals into different classes. Taking into account the non-stationary nature of the yarn tension signal, a set of time-frequency analysis features are selected; these are based on the (pseudo-) Wigner-Ville Distribution (WVD) of the yarn tension signal. It is a two dimensional distribution of the signal power across time and frequency axes, that extends the notion of Fourier Transform spectrum of stationary signals to cover the case of non-stationary signals. Figure 1.6 shows this two dimensional WVD feature for the yarn tension signal cases of Figure 1.5 (left: normal, right: needle without a hook).
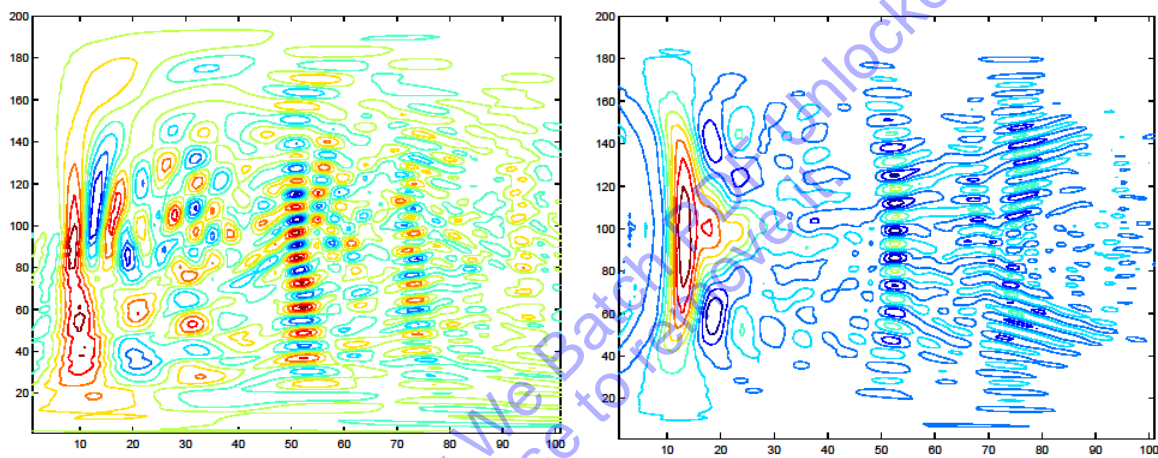
Figure 1.6: Two dimensional Wigner-Ville Distribution feature computed from the yarn tension signal of Figure 1.5
(left: normal operation, right: needle without a hook).

The plots in Figure 1.6 are contours obtained by cross-sectioning the two dimensional, landscape-like WVD characteristic quantities. Horizontal axis is frequency while vertical axis is time, centered on the failure time point of figure 5 (lower plot, n=550). Color depicts signal power at a given time-frequency neighborhood, scale increasing from blue to red. After suitable reduction back to one dimension, feature vectors are obtained and presented to a Learning Vector Quantizer (LVQ) type of ANN classifier. The LVQ ANN architecture is selected for its ability to handle input vectors of high dimensionality, as is the case at hand; yet, at the cost of longer training iterations. It is a two-layered architecture with a first, competitive layer that classifies inputs in sub-classes and a second, linear layer that groups sub-classes into target classes. The target class index is the single output.

The LVQ designed for this problem is trained to classify input vectors into (a) two and (b) three distinct classes of machine failures. Correct classification scores are varying between 75% and 90%, case-dependent. These are satisfactory results given the complexity of the task and the fact that they are obtained directly, without any ANN architectural parameter trimming. However, they reveal the sensitivity and the amount of computational effort required by the ANN approach.

1.4   Discussion

Non-linear methods have been attracting research interest in complex engineering problems where the linear approach is not adequate. Artificial Neural networks are but an example; Fuzzy Logic, Support Vector Machines, Genetic Algorithms, Soft Computing and many other alternatives are open for investigation as to their appropriateness to handle a given problem. These methods are valuable when tackling complex, demanding problems; yet, they are computationally demanding, they may converge to optimal or to suboptimal solutions while their performance is case-dependent. The right choice is possible only after the engineer has deeply studied and understood the nature of the problem at hand and has formed a clear view of the type of answer and the accuracy of answer sought. The cost of resorting to non-linear approaches has always to be taken into account and justified: there still exists the possibility that the linear method returns a solution whose quality and accuracy are satisfactory!

1.5   Literature

Araujo, M., Catarino, A., Hong, H., "Process Control in for Total Quality in Circular Knitting," AUTEX Research Journal, vol. 1, No 1, pp. 21–29, 1999.

Araujo, M., Catarino, A., Hong, H., "Quality Control in Circular Knitting by Monitoring Yarn Input Tension," Proceedings of the 79th World Conference of The Textile Institute, Chennai, India, vol. 1, pp. 167–182, February 1999.

Backer, S. (1951). The relationship between the structural geometry of a textile fabric and its physical properties, Part IV: Intercise geometry and air permeability, Textile Research J., vol. 2, pp. 703–714.

Bhattacharjee, D., Kothari, V.K. (2007). A neural network system for prediction of thermal resistance of textile fabrics. Textile Research Journal, 77 (1), pp 4–12.

Brasquet, C., LeCloirec, P. (2000). Pressure drop through textile fabrics-experimental data modeling using classical models and neural networks. Chemical Engineering Science, 55, pp. 2767–2778.

Cay, A., Vassiliadis, S., Rangoussi, M. & Tarakcioglu, I. (2007). Prediction of the air permeability of woven fabrics using neural networks. Intl. J. of Clothing Science and Technology, 19 (1), pp 18–35.

Chen, S., Cowan, C.F.N., and Grant, P.M. (1991). Orthogonal least-squares learning algorithm for radial basis function networks, IEEE Transactions on Neural Networks, vol. 2(2), pp. 302–309.

Claasen, T.A.C.M., Mecklenbrauker, W.F.G., (1980). "The Wigner Distribution – A tool for time-frequency analysis," Philips J. Res., vol. 35, Parts I, II, III.

Cohen, L., (1986). "Generalized Phase-Space Distribution Functions," Journal of Math. and Physics, vol. 7, pp. 781–786.

Crochiere, R.E., Rabiner, L.R., (1983). "Multirate Digital Signal Processing," Prentice-Hall, New Jersey, USA.

Cybenko, G. (1989). Approximations by superpositions of sigmoidal functions. Mathematics of Control, Signals, and Systems, no. 4, pp. 303–314.

Gurumurthy, B.R. (2007). Prediction of fabric compressive properties using artificial neural networks. Autex Research Journal, 7 (1), pp. 19–31.

Elman, J.L. (1990). Finding structure in time, Cognitive Science, vol. 14, pp. 179–211.

Ertugul, S. & Ucar, N. (2000). Predicting bursting strength of cotton plain knitted fabrics using intelligent techniques. Textile Research Journal, 70 (10), pp. 845–851.

Guruprasad, R. & Behera, B.K. (2010). Soft computing in Textiles. Indian Journal of Fibre and Textile Research, vol. 35, pp. 75–84.

Haykin, S. (1998). Neural Networks: A Comprehensive Foundation, Prentice Hall, ISBN 0132733501, New York.

Hertz, J., Krogh, A. & Palmer, R.G. (1991). Introduction to the Theory of Neural Computation, Addison-Wesley Longman Publishing Co., Boston, MA, USA.

Hornik, K., Stinchcombe, M. & White, H. (1989). Multilayer Feedforward Networks are universal approximators. Neural Networks, vol. 2, pp. 359–366.

Jain, A.K., (1997). "Fundamentals of Digital Image Processing," Prentice-Hall.

Janssen, A.J.E.M., (1982). "On the locus and spread of Time-Frequency Pseudo-Density Functions," Philips J. Res., vol. 37, pp. 79–110.

Keeler, J. (1992). Vision of Neural Networks and Fuzzy Logic for Prediction and Optimisation of Manufacturing Processes, In: Applications of Artificial Neural Networks III, vol. 1709, pp. 447–456.

Kohonen, T., (1990). "Self-Organization and Associative Memory," 2nd ed., Springer-Verlag, New York.

Kohonen, T., (1990). "Improved versions of LVQ," Proceedings of Intl. J. Conf. on Neural Networks '90, vol. 1, pp. 545–550.

Lin, D.-T. (1994). The Adaptive Time-Delay Neural Network: Characterization and Applications to Pattern Recognition, Prediction and Signal Processing. PhD thesis, University of Maryland, USA.

Lin, J.-J. (2007). Prediction of yarn shrinkage using neural nets. Textile Research Journal, 77(5), pp. 336–342.

Lippman, R.P. (1987). An introduction to computing with neural nets. IEEE ASSP Magazine, pp. 4–22.

Majumdar, P. K. (2004). Predicting the breaking elongation of ring spun cotton yarns using mathematical, statistical and artificial neural network models. Textile Research Journal, 74(7), pp. 652–655.

Matlab, (2005). MATLAB 7 R14, Neural Network Toolbox User's Guide, The MathWorks Inc., Natick, MA, USA.

Ramesh, M.C., Rjamanickam, R. & Jayaraman, S. (1995). The prediction of yarn tensile properties by using artificial neural networks. Journal of Text. Inst., vol. 86, no.3, pp. 459–469.

Rich, E. & Knight, K. (1991). Artificial Intelligence, McGraw-Hill, New York, USA, pp. 487–524.

Stylios, G. & Sotomi, J.O., (1996). Thinking sewing machines for intelligent garment manufacture. Intl. Journal of Clothing Science and Technology, vol. 8 (1/2), pp. 44–55.

Stylios, G. & Parsons-Moore, R. (1993). Seam pucker prediction using neural computing. Intl. Journal of Clothing Science and Technology, vol. 5, no. 5, pp. 24–27.

Vassiliadis, S., Rangoussi, M., Araujo, M. (2002). "Feature extraction and classification of faults in circular knitting machines based on time-frequency techniques," Proc. 2nd AUTEX World Textile Conference, pp. 203–213, Bruges, Belgium.

Zadeh, L. (1994). Soft Computing and Fuzzy Logic, IEEE Software, vol. 11, no. 1-6, pp. 48–56.

2 Computational Modelling of Textile Structures

by

A. Kallivretaki, S. Vassiliadis and Ch. Provatidis

Department of Electronics Engineering, TEI of Piraeus, Greece
School of Mechanical Engineering, National Technical University of Athens, Greece

2.1 Introduction to the computational modelling

Several engineering sectors, as mechanical, civil, electrical and electronic engineering, present a modern design culture focusing on the optimization of the product performance. The optimization procedure lies on the selection of the appropriate dimensional and physical characteristics of the product for the achievement of the desirable performance accounting also the resource limitations and the production cost. It is a repetitive procedure consisting of the development of a product model with the defined properties (design parameters), examination of the product performance and modification of the design parameters for the improvement of the performance – cost ratio. Since the sample production is a cost and time-consuming process, the modern engineering design was implemented computer-based tools for the development and the performance prediction of the sample.

The evolutions in software programming and in the computer hardware performance increased the capabilities of computer-aided tools. The Computer Aided Design (CAD) serves the geometrical representation of the objects and the Computer Aided Engineering (CAE), among other functions, supports the mechanical analysis of the modelled structure. CAD and CAE software products, nowadays, are available in the market and they offer plethora of design capabilities, advanced numerical techniques and special facilities for the solution of the engineering problems.

The mechanical engineering field adopted advanced CAD and CAE software packages for the evolution of consumer products, heavy equipment, industrial components, machinery manufacturing, micro electromechanical systems as well as medical products. The computer based tools improve the aesthetics and ergonomics of product designs by generating advanced shapes, complex surfaces, and patterns. They allow fast design and performance prediction of large scale component assemblies. Static and dynamic structural analysis as well as thermal, fluid and acoustic analysis, support the solution of the mechanical problems.

2.2 The computational modelling in the textile sector

The textile modelling has already met the first computer-based tools focusing on the aesthetic design. Thus some of them are already available as commercial packages for industrial use. To mention some of them,

- *Textile Vision*: Is specified in the visualization of woven textile patterns in two-dimensional sheets (Figure 2.1).
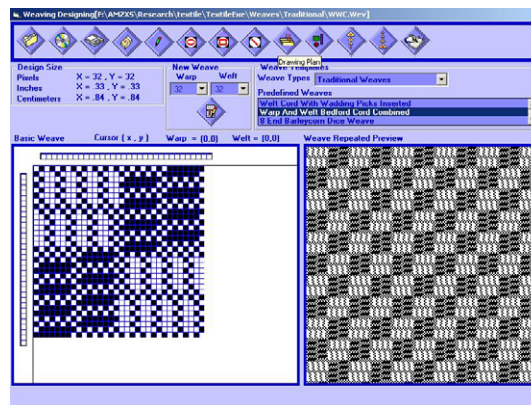
Figure 2.1: Design tools for weave creation (source: Textile Vision software).

- *JacqCAD MASTERS*: Offers extensive features to assist in designing, editing, creating loom control files, and punching of textile designs.
- *Optitex 2D/3D CAD*: Supports solutions from pattern design to manufacturing and retailing process. Offers integrated software solution that uses a combination of both 2D patterns and 3D technology to deliver virtually real sewn products.

- *DesignScope Victor*: Focuses on the mapping of textile patterns in three-dimensional structures (Figure 2.2). The mapping technique includes advanced displaying capabilities as the visual properties of the yarn, light and shadow on the yarn, light and shadow of the pleats and creases, fabric density and transparencies.
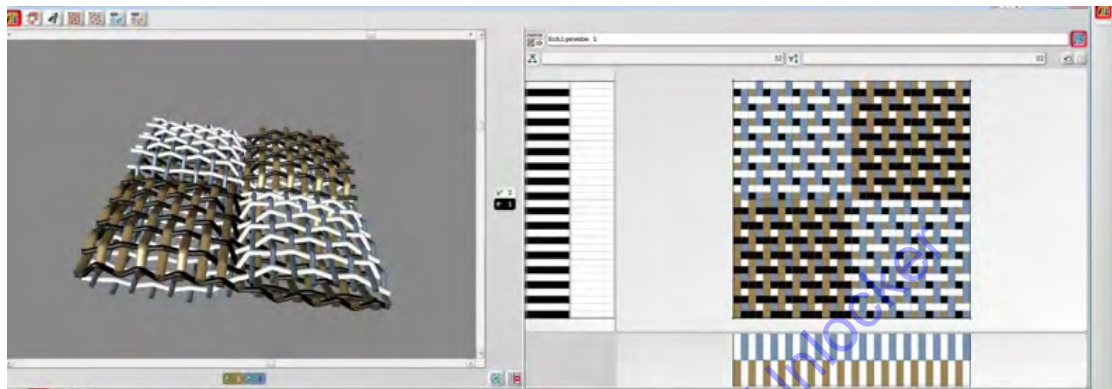
Figure 2.2: 3D Weave modules of "DesignScope victor" software.

Apart from the aesthetic design tools, the textile society inquired mechanical design tools in order to predict the performance of the textile structures. The first researches, conducted in 1940s, focused on the two-dimensional representation of the fabric unit cell (see figure 2.3) and the implementation of analytical methods for the mechanical analysis of them. The basic target of the researchers in that period was the correlation of the structural properties (dimensional and physical) with the mechanical properties and the fabric hand.
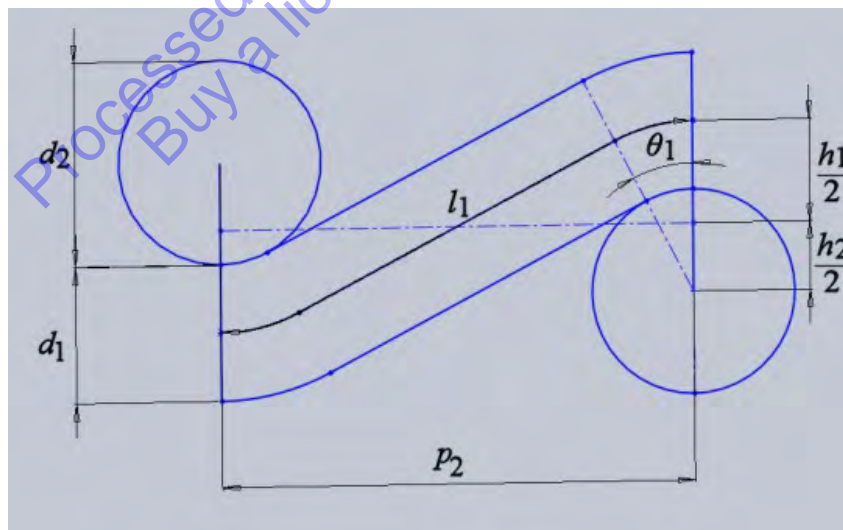
Figure 2.3: Plain woven geometry proposed by Peirce (Peirce 1937).

Nowadays, the development of the textile industry and its dynamic expansion in advanced technical applications converted the design of the textile structures to a complex engineering procedure. In particular, the expansion of the composite structures (including woven or knitted reinforcement) in automotive and aerospace industry necessitated the accurate prediction of their performance. Thus the engineering design tools are adapted gradually for the evolution of the textile design procedure (Hearle 2004, Lomov 2001).

Since the structural hierarchy of a textile comprises the fibres – yarns – fabric unit cells – fabric, the corresponding modelling phases were developed.

2.3   The basic principles of the Finite Element Method

The Finite Element Method (FEM) is, nowadays, the prevalent computational tool for the mechanical analysis of structures. The FEM is a numerical technique for the approximate solution of a wide area of engineering problems based on the discretization of the considered structure.

The implementation of the FEM consists of two principal stages: (a) the mathematical formulation of the physical problem and (b) the numerical solution of the mathematical model. The mathematical formulation is based on certain assumptions regarding the geometry, loading and boundary conditions in order to receive the governing equations. The governing equations are partial differential equations subjected to boundary conditions. Since an analytical closed form solution is unachievable, an approximate solution is desired based on the advanced numerical techniques of FEM.

A simplified description of the FEM concept is the subdivision of the structure into components of simple geometry, the finite elements. The response of the finite elements derives from the displacements of specific points of the elements, the nodes. Thus the total response of the structure is then approximated to the one obtained by the discrete model when assembling the finite element mesh. The basics for the comprehension of the FEM concept when implementing in structural mechanics problems are the following.

- Finite Elements: Are the subdivisions of the continuum structure. Increasing the density of the mesh, the accuracy of the solution and computational cost are increased.
- Nodes: The nodes are the points of the elements where the degrees of freedom are defined. Moreover the nodes define the element geometry and connectivity, using common nodes in the adjacent elements.
- Degrees of freedom (dofs): Correspond to the displacements (translational and rotational) that the nodes of the model present.
- Boundary conditions (BC): Are the values of the dofs that the boundary nodes of the model receive due to the supports.

The basic Element types considering the constitutive properties are:

- Bar (axial loading in members, modelling of trusses)
- Beam (axial and vertical loading, modelling of frames)
- Plate (plane stress and plane strain)
- Shell (plane and normal loading)
- Solid (loading in 3 dimensions)

2.4 Geometrical representation of the textile structures

2.4.1 Geometry of yarn

The ideal structure of a multifilament twisted yarn is considered in the current approach. The basic assumptions are:

- circular cross-sections of the yarn and the constituent filaments
- the filaments follow a uniform helical path retaining constant distance from the yarn axis
- close packing arrangement of filaments.

The geometry of a filament within the yarn structure is easily obtained defining the filament diameter, the helix diameter and pitch.
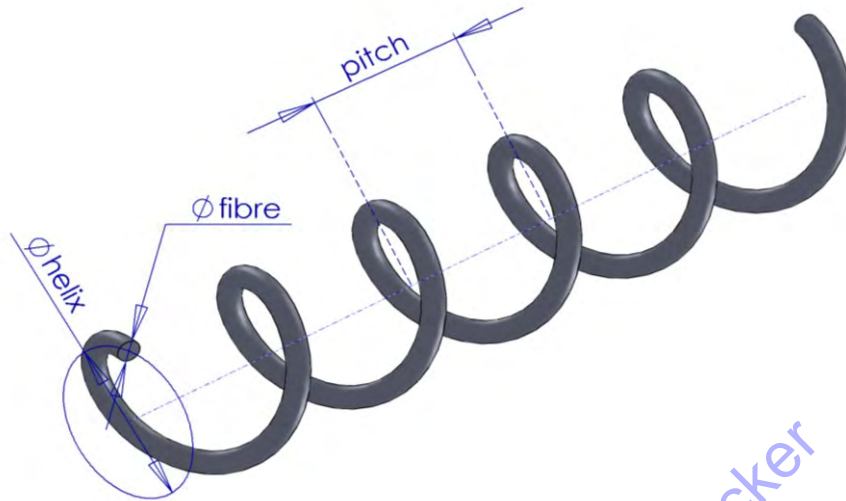
Figure 2.4: The helical path of a filament.

The pitch of the helix is defined by the yarn twist (pitch=1/twist) while the helix diameter is calculated geometrically considering the filament position within the yarn and the filament diameter (d_f). Thus for the first layer of filaments the helix diameter is:

$$d\,(1)= d_f/\cos(\pi/4)$$

while for the i layer (i>1) of filaments the helix diameter is:

$$d\,(i)= d\,(i-1)+2\,d_f$$

The steps for the geometrical representation of an ideal yarn consisting of three layers of filaments are shown in the Figure 2.5.
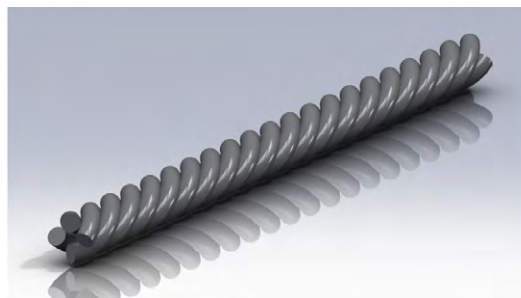
1 layer of fibres
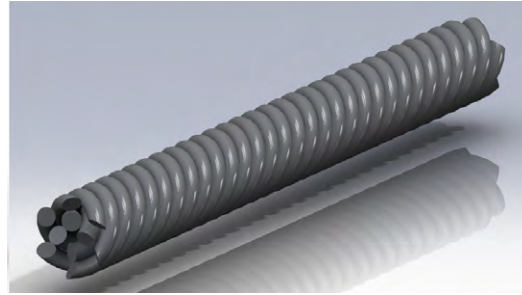
2 layers of fibres
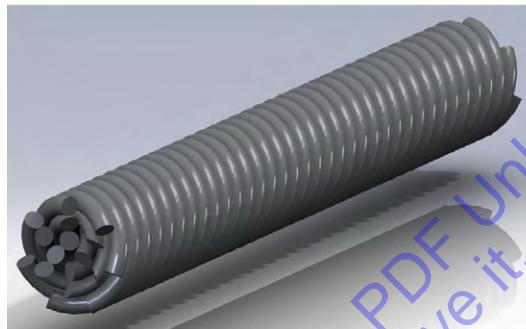
3 layers of fibres

Figure 2.5: Geometrical representation of an ideal multifilament twisted yarn.

The cross section of the yarn derives from the section view of the model to a plane normal to the yarn axis as shown in the Figure 2.6.
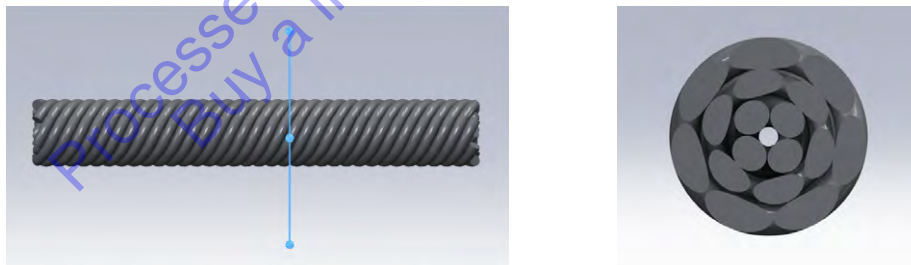
Figure 2.6: Cross section of the modelled yarn.

2.4.2   Geometry of the woven structures

The geometrical modelling of the plain woven unit cell is based on the pioneering study of Peirce (Peirce 1937). The yarns are considered flexible circular cylinders presenting a "just in touch" formulation in the cross points (see Figures 2.7 and 2.8).
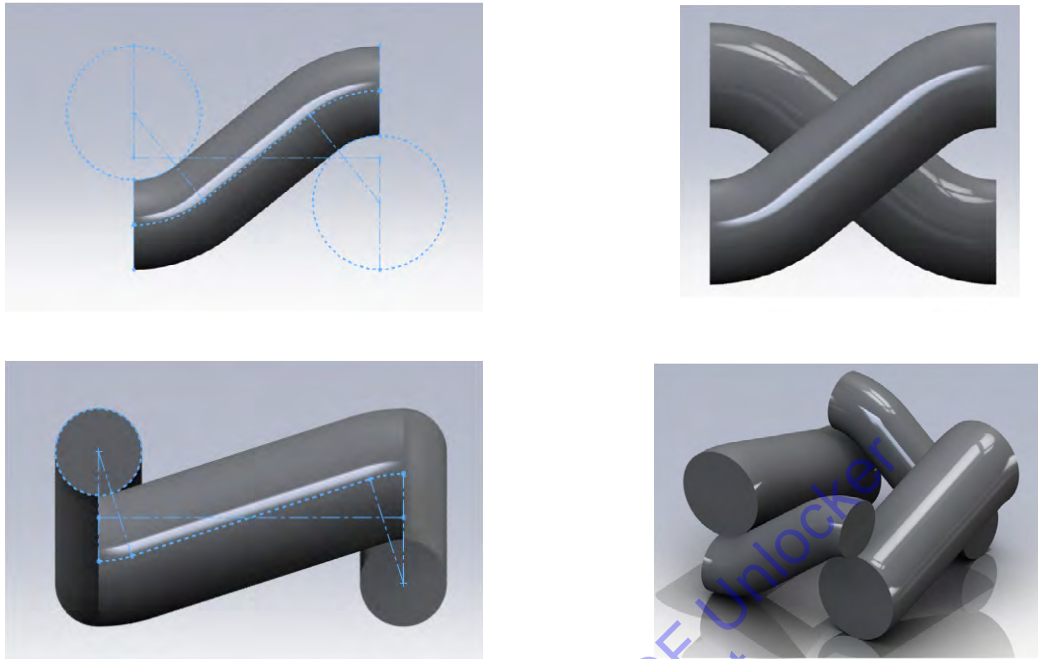
Figure 2.7: Geometrical representation of the plain woven unit cell.

The geometrical modelling is essential nowadays for the design of 3D woven fabrics used in composite materials and sandwich structures as reinforcements. The modern CAD software codes provide advanced numerical techniques (spline curves, NURBS surfaces) and easy-handling tools (features of symmetric or mirror parts and linear pattern) achieve the fast and easy geometrical modelling of complex textile structures.
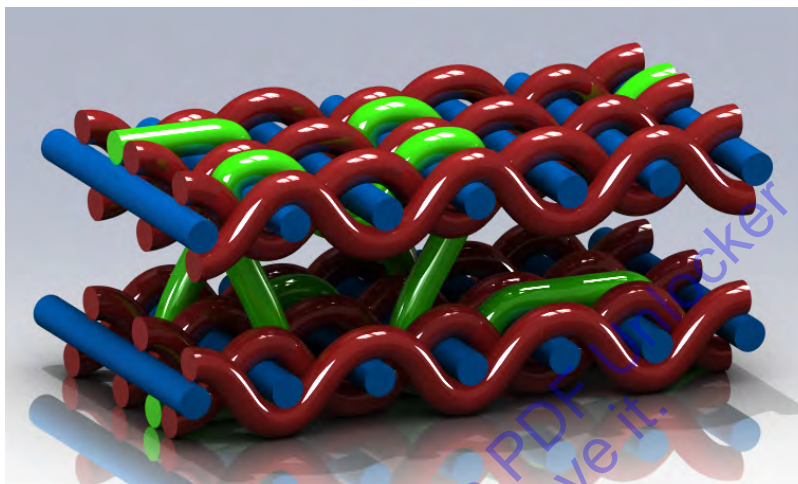
Figure 2.8: Geometrical representation of the unit cell of a 3D woven fabric.

2.4.3   Geometry of the weft knitted structures

In contrast to the 2D path of the threads (central axes) constituting the woven structures, the yarns of the knitted structures follow 3D paths. Thus the implementation of 3D CAD tools is requisite for the realistic modelling of the knitted fabric structure. In the current paragraph a general technique is presented for the modelling of the plain weft knitted unit cell. The calculation of the geometrical parameters for the complete definition of the structure based on the main structural parameters (course-spacing, wale-spacing and yarn thickness) is given in the literature (Vassiliadis *et al* 2007). The 2D representation of the loop central axis derives from the sketch of three circular arcs of equal diameter and the tangent lines connecting two of them as shown in the Figure 2.9. The sketch is projected onto the surface of a cylinder for the generation of the 3D sketch. The central axis of the cylinder lies on the mid-plane that is normal to the sketch.
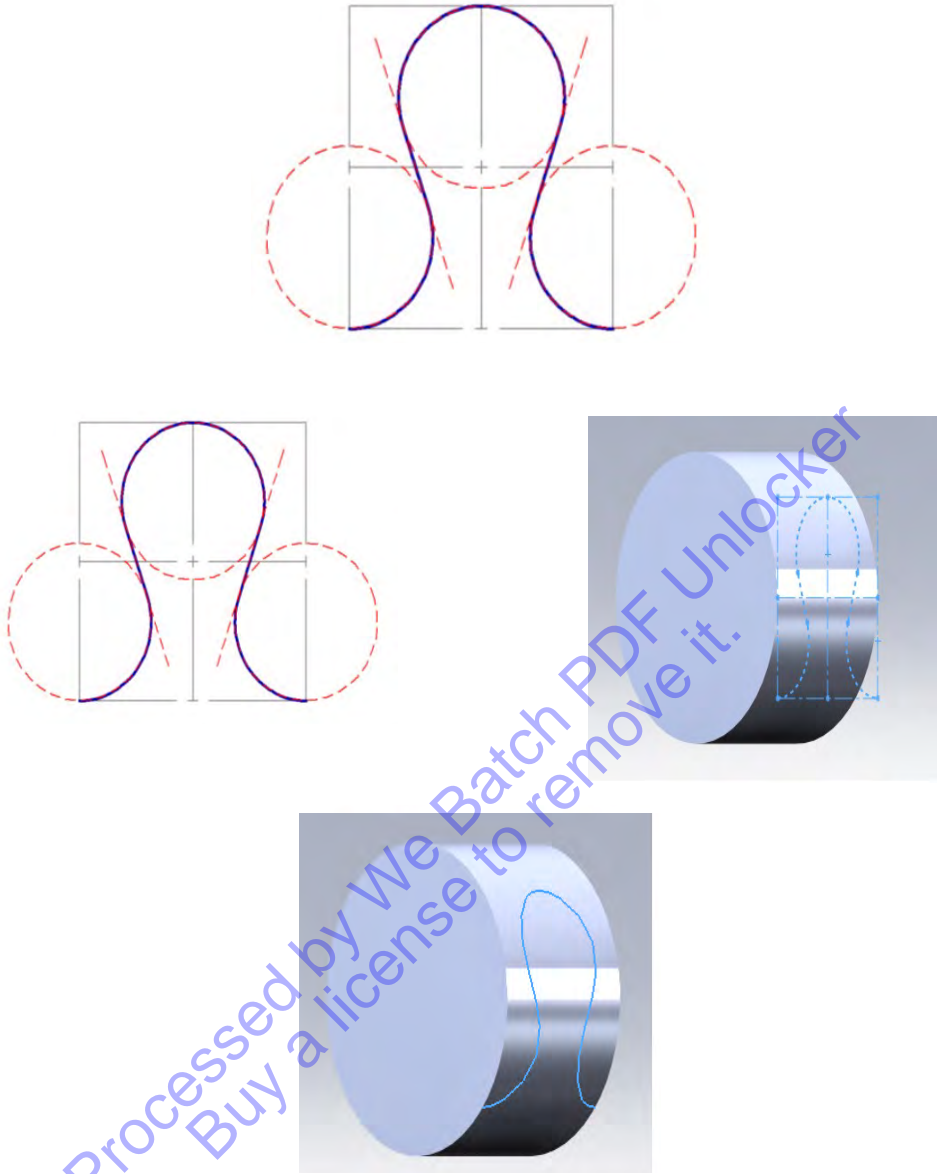
Figure 2.9: 3D sketch for the central axis of plain weft knitted loop.

The front and the side view of the loop are presented in the Figure 2.10. In order to obtain the unit cell of the structure, the adjacent loops are generated (along the wale direction) and the resultant model is cut at the dimensions: wale spacing × course spacing.

Figure 2.10: Modelling of the plain weft knitted loop and unit cell.

2.5   Implementing the FEM in the textile design

2.5.1   Tensile test of a multifilament yarn

The FEM using beam elements is implemented for the mechanical analysis of the multifilament twisted yarns (Vassiliadis *et al* 2010). For the simulation of the tensile test the one end of the modelled yarn is considered clamped. On the other end a uniform displacement is imposed along the yarn axis. The reaction developed in the clamped edge is calculated for the definition of the load – displacement.
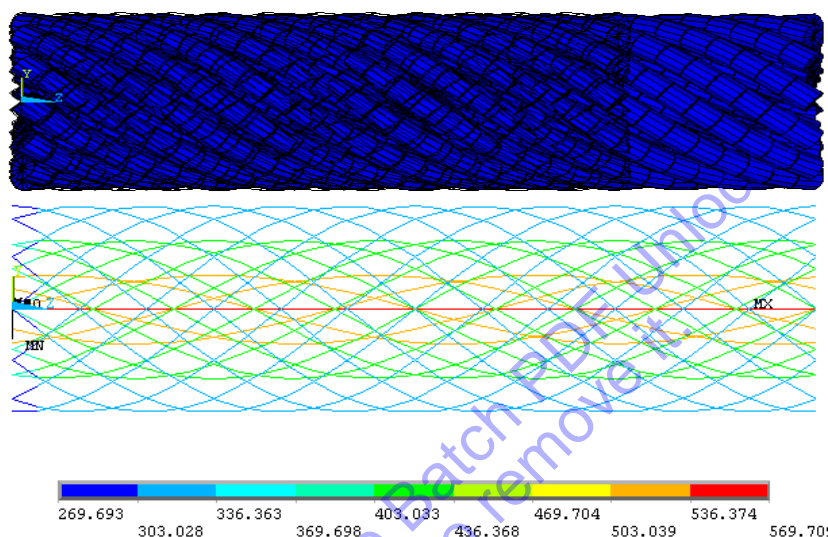
**Figure 2.11:** Deformed shape and axial stresses (N/mm²) resulting from the simulation of the tensile test of a 30-filament twisted yarn.

The nodes of the total model are restricted with zero radial displacement. This constraint precludes the reduction of the helix radius and the appearance of penetration between the filaments. Given that the tensile deformation of a single helix corresponds basically to the reduction of the helix radius, the proposed constraint is essential for the simulation. Thus a realistic deformed shape is derived.

The deformed and the free-state shape of the modelled yarn, such as the contour plot of the axial stresses (in N/mm²) developed in the constituent filaments are given in the Figure 2.11.

2.5.2   Drape test of a woven fabric

The drape of a fabric refers to the configuration resulting when it falls with gravity on a pedestal or a human body. Thus the prediction of the drape performance of a woven fabric is essential for the design and optimization of woven reinforced composite structures.

Geometrically the model consists of an orthogonal surface of the sample dimensions (200×200 mm) subtracting the surface of the circular pedestal. The part of the fabric supported by the table was subtracted by the model for computational simplification and the dofs constraints (simple support) were applied in the lower nodes of the circumference.

The 8-node solid-shell elements with 3 dofs (translational) per node were used for the analysis of the sheet in drape. The apparent elastic properties of the model were calculated experimentally by the respective bending rigidity the considering the model thickness (Provatidis *et al* 2009).

The load application consists in the definition of the apparent density (reflected value considering the model thickness) and the gravity acceleration (9.807 m/sec²). Thus the model was subjected to complex deformation (bending in double curvature) in low loading conditions (self-weight).

The modelling and the simulation were performed using the ANSYS commercial software code.
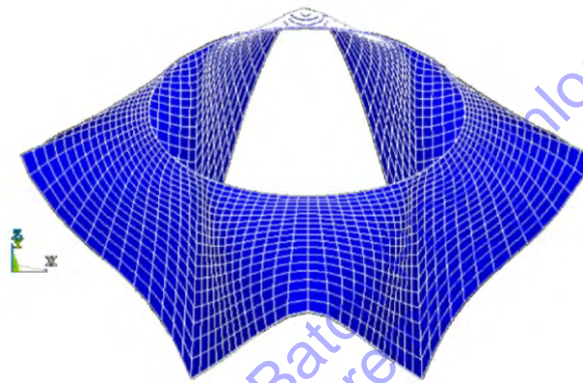
Figure 2.12: Deformed shape of the model resulted from the simulation of the drape test.

2.6   Literature

Hearle, J.W.S. 2004, "The challenge of changing from empirical craft to engineering design", International Journal of Clothing Science and Technology, 16(1/2): 141–152.

Lomov, S.V., Huysmans, G., Luo, Y., Parnas, R.S., Prodromou, A., Verpoest, I. & Phelan, F.R. 2001, "Textile composites: Modelling strategies", Composites – Part A: Applied Science and Manufacturing, 32 (10): 1379–1394.

Peirce, F.T., (1937) The geometry of cloth structure. Journal of the Textile Institute, 28(3): 45–96.

Provatidis, C., Kallivretaki, A. & Vassiliadis, S. 2009, "Fabric Drape using FEM", *2*nd *South East European Conference on Computational Mechanics*, Rhodes, Greece.

Vassiliadis, S., Kallivretaki, A. & Provatidis, C. 2007, "Mechanical Simulation of Plain Weft Knitted Fabrics", International Journal of Clothing Science and Technology , vol. 19 no. 2, pp. 109–130.

Vassiliadis, S., Kallivretaki, A. & Provatidis, C. 2010, "Mechanical modelling of multifilament twisted yarns", Fibers and Polymers, 11(1): 89–96.

3   e-textiles

by

D. Domvoglou and S. Vassiliadis

Department of Electronics Engineering, Technological Education Institute of Piraeus, Greece

3.1   Introduction

The effective incorporation of electric components on fibrous substrates constitutes an important research effort, aiming in the development of textile products with increased functionalities. The development of wearable electronic products has been successfully achieved in the past, at least in terms of functionality. The vision now lies in the fulfillment of the textile prerequisites such as washability, flexibility, comfort as well as acceptable aesthetics. Under these premises, research is now focused on the development of fully textile products with electronic functions, the so-called electronic textiles or e-textiles. Emphasis is thus given in the fibrous structure, which is now called to play an active role in the introduced electrical properties of the end product.

To produce an e-textile product, different technical components, unknown till now to the textile technologists, has to be used. Sensors, actuators, microprocessors, energy sources and the appropriate software are some of the elements that may be used to ensure efficient functionality of the end product. The internal communication of these components be guaranteed by the interfaces, ranging from conventional cables to conductive textiles and/or optical fibres. The external communication, on the other hand, is normally achieved by wireless technology, assisted by the presence of textiles antennas.

The transition from the development of wearable electronics to e-textile products has been reinforced by the increasing research effort in the field of conductive polymers. The fascinating world of conjugated polymers with conductive properties opens new routes in polymer and textile technology. Indeed, traditional insulators as textile fibres can now be modified and transformed into electric conductors.

The dynamic potentials of e-textiles in a future of clothing with integrated electronic properties, gain the attention of the research community, opening a discussion about the variety of the application fields of these innovative materials. Garments for military applications, wearable systems for telemedicine care as well as clothing with impressive aesthetic effects and improved functionalities can change the idea of traditional clothing, improving essentially peoples' quality of life.

This chapter provides an overview of the recent developments and the problems associated with these, in the field of e-textiles. Since the difficulties in e-textiles' study lies in their interdisciplinary nature, this chapter also hopes to provide some insight in their basic scientific disciplines, which can bring a future of personal assistant garments a step closer.

3.2   Electric conductivity-Background

Electric current expresses the flow or the interaction of a materials' free electrons. Actually when a voltage is applied from an energy source, an electric field is developed. This electric field forces the positively charged particles as well as the free electrons of the materials' chemical structure, to flow. The subsequent inability of the positively charged particles to move, results from their engagement into covalent bonds. Therefore, the free electron carriers are forced into an oriented flow, which is called electric current. The nature of electricity is best understood through the examination of the chemical structure of matter. It is thus known that matter is composed of atoms, consisted of electrons, protons and neutrons. The positively charged protons, as well as the uncharged neutrons, are in association and they are the elements that constitute the atoms' nucleus. The negatively charged electrons appear as cloud around the nucleus, orbiting in predetermined shells. Although oversimplified, Figure 3.1 shows a typical representation of the electron motion.
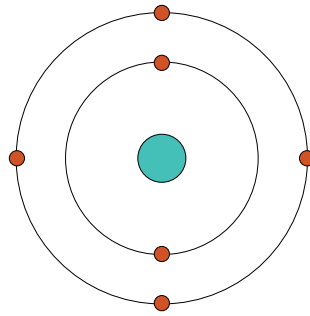
Figure 3.1: Electron's orbits around the atom's nucleus.

An extensive description of the quantum theory is beyond the scope of this chapter. However, it is of high value to refer to its general principles. Based on the above considerations, the energy of each orbiting electron depends on the combined effect of the specific shell properties as well as the possible interactions of the electron with other electrons and can thus be in a predetermined field of (energy) leves/states. Atoms interactions to form bonds would include the subsequent interaction of the free electrons' located in the outermost shell. In solids, things are more complex since a great number of atoms are bonded, forming crystalline solid materials. The independent atoms free electrons' can be located in many energy levels, depending on their chemical interaction with the surrounding atoms. The possible energy levels of the free electrons led to the development of the energy bands. The band corresponding to the outermost shell is called valence band. As expected and depending on the atom, the valence band can be fully occupied by electrons. On top of the valence band is the conduction band. The two bands are divided by a gap, called forbidden band, the size of which will determine the materials' electrical nature. The above theoretical consideration results in the categorization of materials according to their molecular structure. According to the aforementioned classifications, materials are divided into insulators, semi-conductors and conductors. Insulators in terms of band theory, have their valence band fully filled, leading to an inexistence of their atom structure's free electron and to a large forbidden band. The energy needed to promote electrons from the valence band to the energy band is large enough to be supplied by a weak electric field or by electrons' thermal vibration. On the other hand, in typical conductors such as metals, the size of the gap is small or non-existent, allowing free electrons to be easily promoted to the conduction band. Additionally, metals valence band is not filled, which also allows to the free electrons to easily "travel" from the valence band to the conduction band. In semiconductors, valence band is fully filled but the size of the forbidden gap is small enough for the free electrons to be promoted to the conduction band, at least at room temperature. The electrons vibration energy, a quantity highly depended on the temperature, would define the electrical behavior of semiconductors.
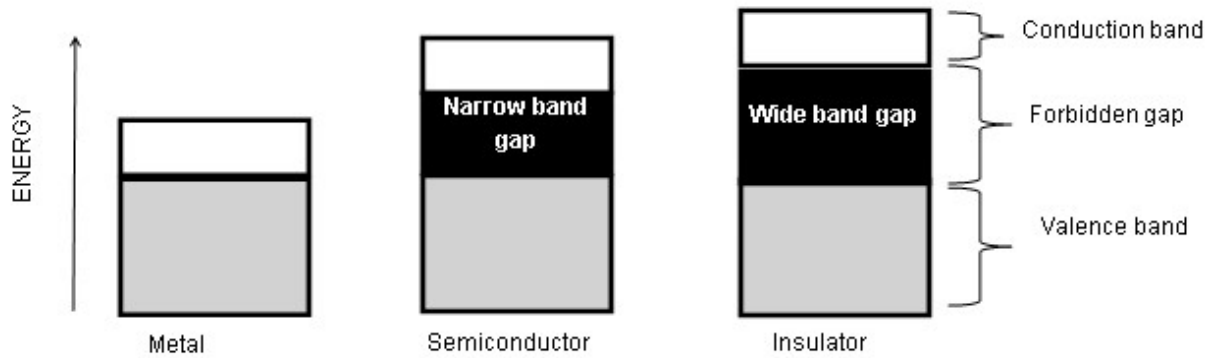
Figure 3.2: The band structure of a metal, a semiconductor and insulator (Wallace et al. 2009, p. 119).

The relation between the current flow through a conductor and the applied voltage is mathematically described by Ohm's law, one empirical and the most fundamental law in the study of the electric circuits.

$$I = \frac{V}{R}$$
(3.1)

where R is the electrical resistance measured in Ohms (Ω), V is the voltage applied across the conductor measured in Volts and I is the electric current which flow through the conductor, measured in Amperes.

The effect of the material's geometry in the material's electric behavior can be determined by a mathematical expression:

$$\rho = R\frac{A}{L} \tag{3.2}$$

where ρ is the resistivity measured in (Ω cm), l is the length of the sample and A is the sample's cross section.
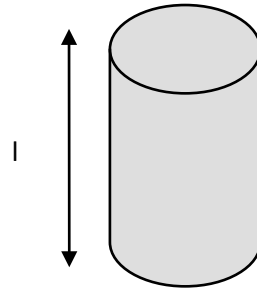
Figure 3.3: Geometrical representation of a fibre structure (Warner 1995, p. 253).

Electrical conductivity (σ), expressed in S m^{-1}, expresses the ability of the material to conduct the electric current and is the reciprocal of resistivity, ρ:

$$\sigma = \frac{1}{\rho} \tag{3.3}$$

The electrical conductivity depends on the carriers' flow as expressed in the corresponding mathematical equation.

$$\sigma = nq\mu \tag{3.4}$$

where n is the number of charge carriers, q is the carrier's charge and μ is the carriers' mobility.

Material	Resistivity (Ω m)
Superconductors	$<10^{-25}$
Metal Conductors	$\sim 10^{-8}$
Semi-Conductors	10^{-4}-10^{-10}
Insulators	10^{10}-10^{20}

Table 3.1: Typical resistivity values for superconductors, metal conductors, semiconductors and insulators (Harlin 2006, p. 217).

---

1.   The reciprocal of Resistance (R-1) is called conductance and is measured in Siemens (S) S=Ω-1.

| | 10^6 Ω⁻¹cm⁻¹ | Metals | 10^2 Ω⁻¹cm⁻¹ | Semi-conductors | 10^{-8} Ω⁻¹cm⁻¹ | Insulators | 10^{-18} Ω⁻¹cm⁻¹ |
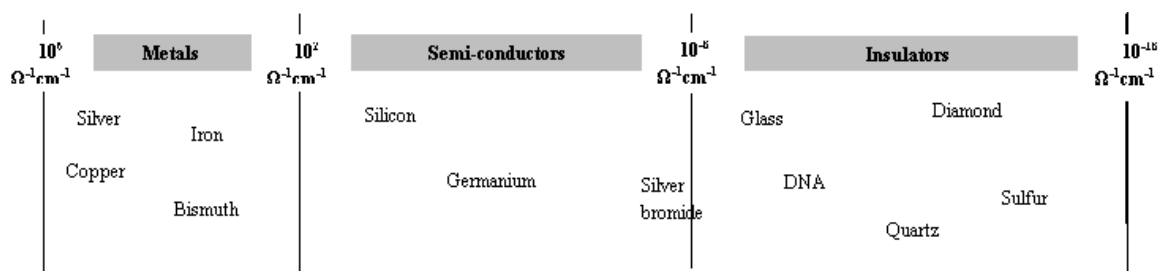
Figure 3.4: Comparison chart of conductivities in Scm^{-1} for conductive polymers, compared with metals, semi-conductors and conductors (Ghosh 2006, p. 239).

3.3   Conductive textiles

Our interest materials, textile fibers behave typically as electric insulators. This is because the chemical structure of polymers does not contain free electrons that would act as carriers to produce electric current upon application of an electric field. According to numerous studies (Kim et al. 2004; Dall' Acqua et al. 2004; Micusık et al. 2007; Knittel 2009) conductivity in textiles can be introduced via:

- Filling of fibres with carbon black or production of carbon fibres
- Interlacing in the textile structure metal , steel, or nickel wires or fibres
- Coating of textiles (fibres or fabrics) with conductive substances
- Modification of the polymer structure through the effective incorporation in the textile structure of intrinsically conductive polymers (ICP)

The superior conductivities of fabrics containing metal fibres are overwhelmed by the reduced flexibility, the increased weight, the cutting and processing problems as well as the increased cost of the end product. Additionally, the aesthetic priorities of textile products weaken the carbon filling method. Coating of textile substrates with metal salts usually reduces the wash resistance of the end product. Metallic and galvanic coatings have been also used, with limited success though (Meoli 2002; Tang 2006).

Intrinsically conductive polymers (ICP) were for a long time an unfulfilled dream of polymer scientists. Intense research interest has resulted to the successful development of polymers with acceptable conductivities and thus to a Nobel Prize in Chemistry in 2000. Scientists have concluded that the key for the development of conductive polymer lay in their conjugated structure, meaning the presence of alternative single and double bonds in the polymeric backbone. Polyaniline (PANI), polypyrole (Ppyr), polythiophene, poly(p-phenylene sulfide) as well as their derivatives are some of the most representative examples of conductive polymers. A critical evaluation of the relevant literature reveals that the unprecedented high levels of conductivities achieved by the aforementioned polymers; do not line with the limited environmental stability and the processability issues that they present. Polymeric chain conjugation introduces a degree of stiffness in the material's structure, which impedes the polymer's solubilization (Harlin 2006). Furthermore, an electro-conductive polymeric structure is normally susceptible to oxidation and to possible acid attacks which can lead either to the complete polymer degradation, or to the disruption of the conjugated structure (Das et al. 2010).

The reality of the ICSs synthesis is though to be correlated with the vision of the development of effective conductive textiles. Furthermore, while the development of ICPs with improved properties is at the center of the scientific research, ICPs effective application on textiles has also been the subject of a large number of studies (Kuhn et al. 1993; Lin et al. 2005; Micusík et al. 2007; Wu et al. 2009), ICPs can be applied in textiles substrates in the spinning dope, offering thus ICSs a "host body" with acceptable mechanical properties (Kaynak 2005; Harlin 2006). Another route that is steadily gaining ground is the development of conductive polymer coatings that can be easily applied on the fibre's or fabric's surface. Coating may provide solution in terms of the manufacture process, offer though doubtful durability of the desired conductive properties. Conductivity can be also introduced in textiles by conductive inks. Developments in digital printing are also beneficial, making printing with conductive inks possible. The undoubtful benefit of this method is the possibility of electrical circuits printing on conventional textiles (Tang 2006).

A competitive relation does exist between the innovative electro-conductive properties and the traditional textile properties as comfort, flexibility, durability, washability etc. Further research is defenitely needed in order to further explore this new class of materials and improve their properties. However, the commercialization of conductive polymers introduce textiles in a futuristic digital future, forcing them to rediscover their potentials.

3.4   Textile sensors and actuators

The electric signals' transmission in an e-textile system is assured by the use of conductive textiles. actually conductive threads replace the circuits' interfaces such as wires, offering increased comfort to the wearer. Technological advances have also led to the effective incorporation in the systems of electric components, which can transform the transmitted signals. It is known that the transformation of electric signals is possible due to two different electronic elements: sensors and actuators. Sensors are devices which transform physical phenomena such as light, intensity, sound, temperature etc., into a physical quantity – usually electric signals. On the other hand, actuators consists a components' category with the opposite functions, meaning the transformation of electrical signal into physical parameters. The transformation of one energy form to another is called transduction. The simplest wearable garment consists of conventional sensors and actuators connected with wires to power sources, all embedded in a textile substrate. A demand for functional wearable systems with textile properties moves the scientist interest in the development of electronic building blocks such as sensors and actuators compatible with textile priorities. Although progress in sensor technology minimized the size of sensors, it did not contribute a lot in the enhancement of their flexibility. Taking as granted the scientific principles in sensor technology, the interdisciplinary research in the field of e-textiles challenges the sensors' raw materials. The development of conductive polymers pushes forward the dynamics of this endeavor, making flexible sensors a reality.

Strain textile sensors have been developed from conductive coated textiles. Electrical conductance can be related to the conductor's geometry, according to the mathematical expression of Ohm's law (see equation 2). Fibres' extension between their elasticity limits, results in the material's cross-section reduction and in a consequently increase in its resistance (Langenhove et al. 2007, p. 106). A critical factor in the development of textile sensor is the fabric geometry as fibres' arrangement in a textile structure affects the structure's conductivity. Furthermore, problems associated with the response time and the durability of the developed products have been noticed, suggesting that further research is needed.

Textile pressure sensors are another scientific effort that has gained intense scientific interest. Various mechanisms are used to assure the soft sensor's functionality (Catrysse et al. 2004). A straightforward approach would consist of two layers of conductive fabric separated by a non-conductive mesh. An introduced pressure would allow the conductive layers' contact and the flow of the electric current, as illustrated in Figure 5. Alternative constructions based on the same scientific principles have also been developed, leading to the production of commercial products such as the "SoftSwitch", the "sensory jacket", the "Gorix" and others (Cho 2009, p. 582).

Application	Information Processing
Weighing Scales	Gravity-pressure-weight
Switch	Touch pressure-threshold-on/off
Respirometer	Respiration-chest volume-clothing pressure-respiratory rate
Gesture measurement	Acceleration by movement- dynamic gesture Changes of body surface-piezoresistive change-dynamic/static gesture
Accelerometer, vibroscope	Pressure change by inertia-acceleration/vibration

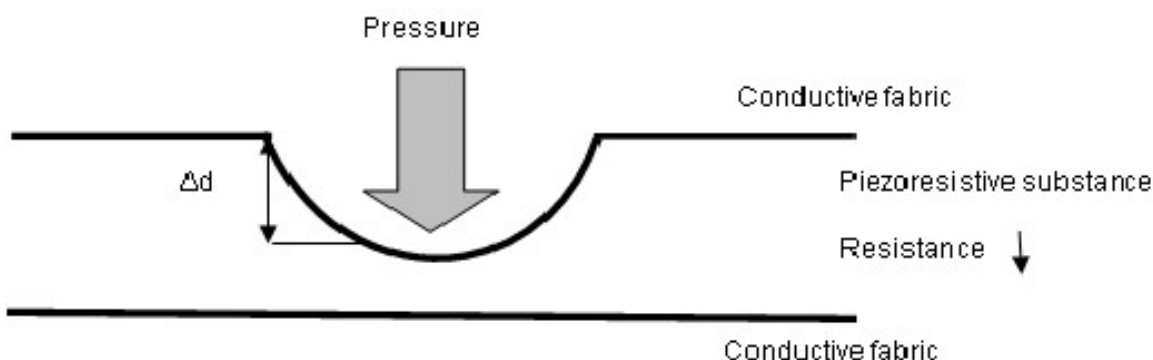**Table 3.2**: Application and information processing of a pressure sensor (Jeong 2010, p. 89).

Figure 3.5: Principles of piezoresistive sensor (Jeong 2010, p. 89).

Special mention deserves the development of textile electrodes for electrocardiogram (ECG) (Langenhove et al. 2007, p. 106; Jeong 2010, p. 89). Although textile electrodes offer improved comfort to the wearer, increasing the recording duration compared with conventional electrodes, they still produced signals with increased noise. "Textrodes", which are commercial available textile electrodes, consist of stainless steel fibres embedded in a belt. the belt is designed to be worn around the thorax (Catrysse & Puers 2007, p. 88).

Sensors make an electric circuit capable of "sense". The interpretation of the "senses" is assured by systems capable of delivering the "senses", such as actuators. It is thus obvious that sensors abilities should not be considered independent in a circuit, or treated as isolated building blocks of a system, but rather as electrical elements interrelated with other circuits' transductions. A medical garment with temperature sensors, for example, provides information regarding the levels of skin temperature. The subsequent transformation of the produced results into a physical action by the addition of an actuating device, such as a display, would maximize the circuit performance. In a more sophisticated version of the same product, the garment can incorporate a thermochromic function "programmed" to trigger when the skin temperature level exceeds a predetermined value.

Actuators that can be used in an e-textile system are textile displays, electroactive polymers as well as color-changing materials. Electric stimulation triggers electroactive or color-changing materials, which respond with the appropriate property change. Textile displays are more complex structures. Nevertheless, France Telecom has already developed a textile display using optical fibres.

The addition of sensors and actuators in an e-textile system push wearable technology in a different level. Improvements are needed but the route has been opened, making scientists dreaming of soft washable electric circuits.

3.5   Power supply sources for e-textiles

The operation of the electronic components described above (sensors, actuators, conductive textiles) presupposes the continuous provision of energy in the form of electrical power. Batteries – normally AAA or button – is the most widely used energy source, although they are bulky, heavy and with limited lifetime. The demand for e-textiles, which can provide comfort as well as functionality, led to the development of alternative power supply technologies or minimization of the size of the existing options. Lithium and rechargeable batteries can be considered as the most obvious option in this direction. Progress has also been noticed in the development of flexible batteries. Nevertheless organic photovoltaics, solar panels and other energy harvesting devices have been also considered as vital alternatives to conventional portable power sources. The vision now lies in the development of close energy e-textile systems, that can provide energy generated from the human body movement or temperature (Gho 2009; Min 2010, p. 214).

3.6   Processors/ Microprocessors

The data provided by the input devices, such as sensors are guided to a Central Processing Unit (CPU) which basically consist the brain of the system. Analysis of the data is performed by the CPU, which sends the new data to the output devices, such as actuators. Although the CPU has been minimized and sewable CPU has been commercialized, it is worth noticing the textile processors are not yet available.

3.7   Communication technologies in e-textiles

Communication of the different components of an e-textile product is essential for the functionality of system. Additionally, the information provided by the incorporated sensors and actuators have to be analyzed and communicated to the interest party. Three areas of analysis exist, as demonstrated in Figure 6: Personal Communications Networks (PCN), Wide Area Networks (WAN) and Information Systems (IS) (Lam 2009, p. 215). In a more straightforward categorization, the communication requirements can be internal (short-range communication) and external (long-range communication). Internal communication is normally assured by wired systems. In addition to conventional wires, conductive and optical fibres have been used, increasing the product's flexibility and thus comfort. Communication of the received data outside of the product is also possible with conventional wires but wireless technology is preferred due to the incomparable benefit they offer in terms of usability. It is obvious that wireless technology opens the potentials of e-textiles systems, especially for medical applications. The most frequent wireless technologies used in the field of e-textiles include IR (infrared), Bluetooth, Wi-Fi, GSM (Global System for Mobile Communications), GPRS (General Packer Radio Service), UMTS (Universal Mobile Telecommunications Systems) etc (Rantanen 2005, p. 198; Tang 2006; Cho 2009; Lam 2009, p. 205; Seymour 2009, p. 12; Seymour 2010, p. 10).
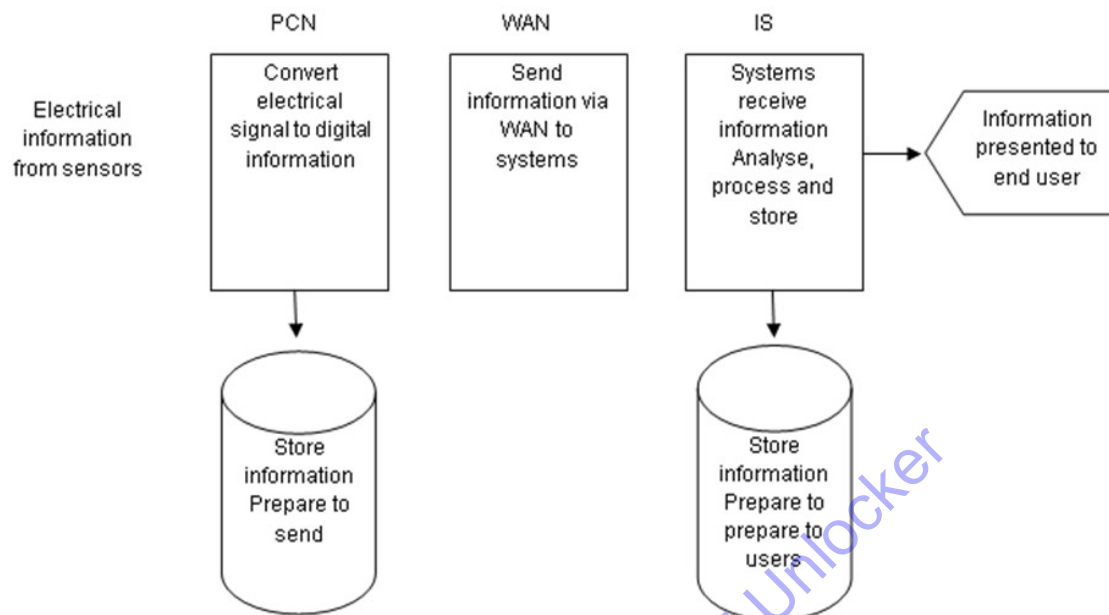
Figure 3.6: End-to-end process flow (Lam 2009, p. 205).

3.8   Conclusions

An overview of the main building blocks of an e-textile system was presented in the current chapter. The basic scientific principles of textile conduciveness are explained to give to the student a comprehensive fundamental understanding of these innovative structures. The difficulty of the current chapter is routed in the interdisciplinary nature of e-textiles. Innovations in this area do not derive from structural textile modifications textile modifications, rather than from a revolutionary re-appreciation of existent electronic technologies. A detailed investigation of the electronic technologies is beyond the scope of this chapter, however the reader can refer to the literature for a more in-depth study of the subject.

The effort is textile oriented and presents the preliminary research effort to introduce superior electronic functions to textiles. E-textiles systems were –till recently- made of conventional electronics embedded into a textile substrate. Progress in textile technology guided by the market demand for comfort textiles, showed that the realization of a fully e-textile structure is possible. However, the difficulties in the mass production of these systems and the increase in cost of the end-products cannot overrule the fascinating potentials of e-textiles, especially in sectors such as medicine, where they can use to significantly improve peoples' quality of life. The early steps in this endeavor moves e-textiles into a visionary cyber world.

3.9   References

Harlin, A. & Ferenets, M. 2006, Introduction to conductive materials. In: Mattila, H.R. ed. *Intelligent textiles and clothing*, 1st edn. Cambridge, England.

Kaynak, A. & Håkansson, E. 2005, "Generating Heat from Conducting Polypyrrole-Coated PET Fabrics", *Advances in Polymer Technology*, vol. 24, no. 3, pp. 194–207.

Kim, B., Koncar, V., Devaux, E., Dufour, D. & Viallier P. 2004 "Electrical and morphological properties of PP and PET conductive polymer fibers", *Synthetic Metals*, vol. 146, pp. 167–174.

Cho, G., Lee, S. & Cho, J. 2009, "Review and Reppraisal of Smart Clothing", *International Journal of Human-Computer Interaction*, vol. 25, pp. 582–617.

Knittel, D. & Schollmeyer, E. 2009, "Electrically high-conductive textiles", *Synthetic Metals*, vol. 159, pp. 1433–1437.

Meoli, D. & May-Plymlee, T. 2002, "Interactive electronic textile development: a review of technologies", *Journal of Textile Apparel, Technology Management*, vol. 2, no. 2, pp. 1–12.

Das, D., Sen, K., Saraogi, A., Maity, S 2010, "Experimental Studies on Electro-Conductive Fabric Prepared by In-Situ Polymerization of Thiophene onto Polyester", *Journal of Applied Polymer Science*, vol. 116, pp. 3555–3561.

Wallace, G.G., Spinks, G.M., Kane-Maguire, L.A.P. & Teasdale, P.R. 2009, *Conductive Electroactive Polymers – Intelligent Polymer Systems*, 3rd edn, Boca Raton.

Kuhn, H.H., Kimbel, W.C., Fower J.E. & Barry, C.N. 1993, "Properties and Applications of Conductive Textiles", *Synthetic Metals*, vol. 55–57, pp. 3707–3712.

Rantanen, J. & Hännikäinen, M. 2005, Data transfer for smart clothing: requirements and potential technologies. In: Tao, X ed. *Wearable electronics and photonics*, 1st edn. Cambridge, England.

Wu, J., Zhou, D., Looney, M.G.,Waters, P.J., Wallace, G.G. & Too, C.O. 2009, "A molecular template approach to integration of polyaniline into textiles", *Synthetic Metals*, vol. 159, pp. 1135–1140.

Jeong, K.S. & Yoo, S.K. 2010 Electro-Textile Interfaces Textile-Based Sensors and Actuators. In: Cho, G. ed. *Smart Clothing Technology and Applications*, 1st edn Broken Sound Parkway NW.

Dall'Acqua, L., Torin, C., Peila, R., Ferrero, F. & Catellani, M. 2004, "Performances and properties of intrinsic conductive cellulose–polypyrrole textiles", *Synthetic Metals*, vol. 146, pp. 213–221.

Langenhove, L.V., Westbroek, C.H.P. & Priniotakis, J. 2007, Textile sensors for healthcare. In: L. Langenhove, L.V. ed. *Smart textiles for medicine and healthcare-Materials, systems and applications,* 1st edn. Cambridge, UK.

Lam, P. 2009, The application of communication technologies in smart clothing. In: McCann, DBJ ed. *Smart clothes and wearable technology*, 1st edn. Cambridge, UK.

Catrysse, M., Pirotte, F. & Puers, R. 2007, The use of electronics in medical textiles. In: Langenhove, L.V. ed. *Smart textiles for medicine and healthcare-Materials, systems and applications*, 1st edn. Cambridge, England.

Catrysse, M., Puers, R, Hertleer, C., Langenhove, L.V., Egmond, H.V. & Matthys, D. 2004, "Towards the integration of textile sensors in a wireless monitoring suit", *Sensors and Actuators A*, vol. 114, pp. 302–311.

Mičušık, M., Nedelčev, T., Omastová, M., Krupa, I., Olejníková, K, Fedorko, P. & Chehimi, M.M., 2007, "Conductive polymer-coated textiles: The role of fabric treatment by pyrrole-functionalized triethoxysilane." *Synthetic Metals*, vol. 157, pp. 914–923.

Min, G. 2010, Power supply sources for smart textiles. In: Cho, G ed. *Smart Clothing Technology and Applications*, 1st edn. Broken Sound Parkway NW.

Tang, S. & Stylios, G. 2006, "An overview of smart technologies for clothing design and engineering", *International Journal of Clothing Science and Technology*, vol. 18, no. 2, pp. 108–128.

Seymour, S. 2009, *Fashionable Technology The interaction of design, science and technology*, 1st edn. Vienna, Austria.

Seymour, S. 2010, *Functional Aesthetics Visions in Fashionable Technology*, 1st edn. Vienna, Austria.

Ghosh, T.K., Dhawan, A. & Muth, J.F. 2006, Formation of electrical circuits in textile structures. In: Mattila, H.R. ed. *Intelligent textiles and clothing*, Cambridge, England.

Lin, T., Wang, L., Wang, X. & Kaynak, A. 2005, "Polymerising pyrrole on polyester textiles and controlling the conductivity through coating thickness", *Thin Solid* Films, vol. 489, pp. 77–82.

Warner, S.B. 1995, *Fiber Science,* 1st edn. Englewood Cliffs, New Jersey.

4 Acoustics and sound absorption issues applied in textile problems

by

S.M. Potirakis

Department of Electronics Engineering, Technological Education Institute of Piraeus, Greece

4.1 Sound and noise.

Although everyone is familiar with sound, since hearing is one of the traditionally recognized five human senses, it is difficult for a non-specialist to give a definition of sound. The common answer is that "sound is anything can be heard". However, a more appropriate definition could be the following:

"*Sound* is said to exist if a disturbance propagated through an elastic material causes an alternation in pressure or a displacement of the particles of the material which can be detected by a person or by an instrument." (Beranek 1986). From the physics point of view, the audible noise is not different from sound. There is only a psychological definition of *noise*: it is a disagreeable or undesired sound. Clearly,

Confining the study to sound propagating in fluids, e.g., in the atmospheric air, sound can be described as a spatiotemporal variation of pressure around the static pressure of the fluid, e.g., the atmospheric pressure, as shown in Fig. 4.1. This pressure variation is called *acoustic pressure*. Acoustic pressure is denoted by the lower case letter p, as opposing to the static pressure denoted by the capital letter P. Both of them are measured in Pascals (Pa), $[P] = [p] = 1\text{Pa} = 1\text{Nt/m}^2$.
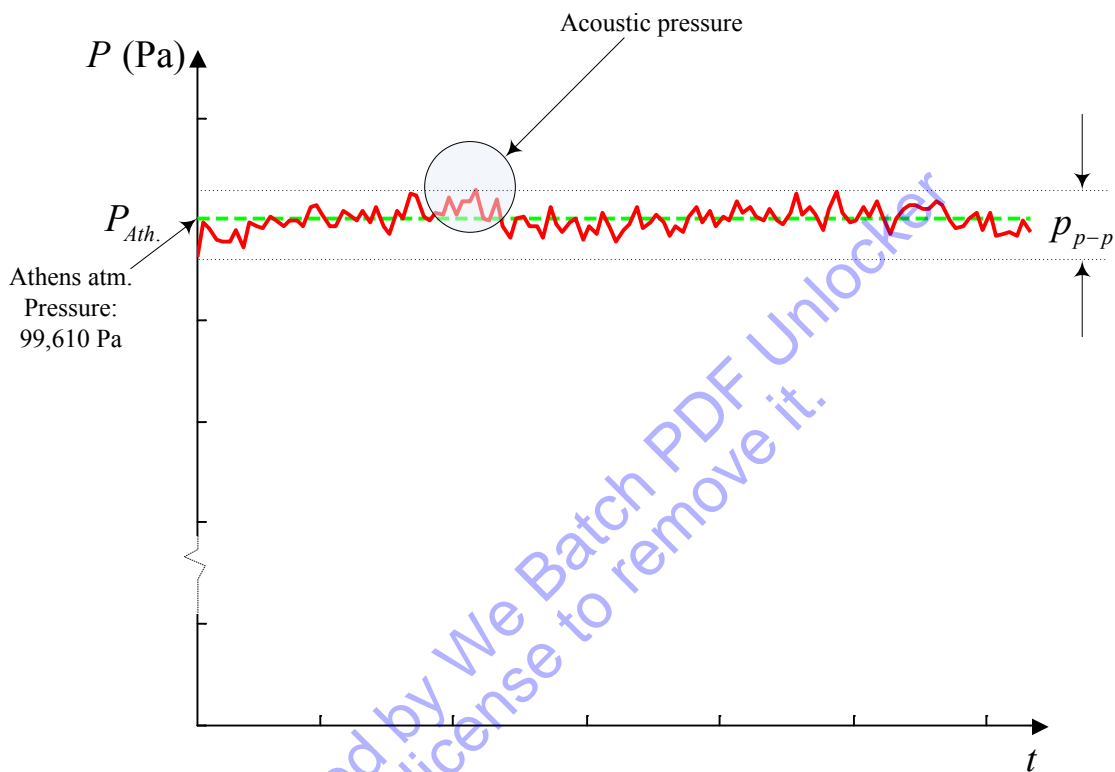

Fig. 4.1: The notion of acoustic pressure vs. static pressure, for example at the city of Athens (Greece). Only the temporal variation is presented here, since the pressure is monitored at a specific location (spatial point).

Acoustic pressure can be described as a sequence of alternating compressions and rarefactions of the particles of the fluid, as shown in Fig. 4.2 for a sinusoidal variation example. In the case of the (ambient) air example, the air particles are disturbed from their thermal random movement under the change of pressure. Therefore, each air particle can be considered to be displaced from its original position due to acoustic pressure. Then, the elastic forces among the air particles tend to restore it to its original position. Because of the inertia of the particle, it overshoots the resting position, bringing into play elastic forces in the opposite direction, and so on. However, the interaction between the specific particle and its neighboring particles disturbs their movement too, propagating the disturbance in space, without actually moving particles from their resting positions.
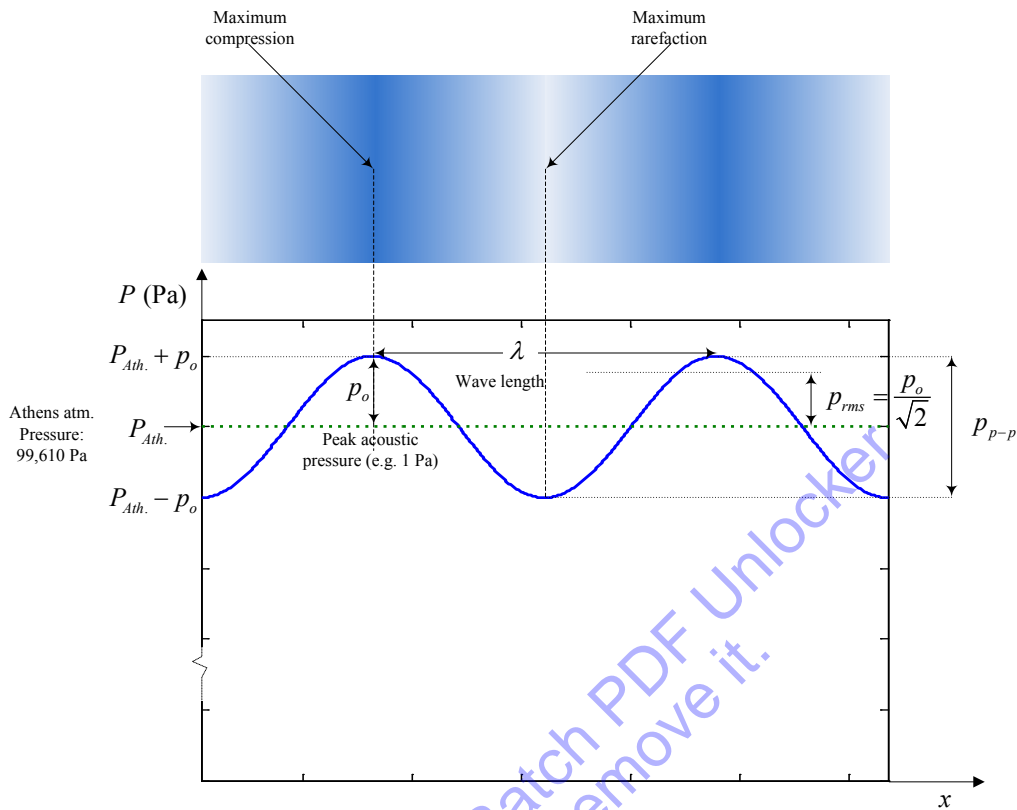
Fig. 4.2: Alternating compressions and rarefactions of the particles of a fluid around its static pressure (upper part), lead to acoustic pressure variations. On this, sinusoidal variation, example some of the characteristics of an acoustic wave are depicted.

It can be proved from basic principles (conservation of mass, 2nd law of Newton and compressibility) that sound as a propagating mechanical spatiotemporal disturbance satisfies the wave equation. The simplest wave case is that of *harmonic plane waves*, which propagate pressure disturbance along one dimension, say x, while being constant in the other two directions. In this case, sound satisfies the one-dimensional wave equation

$$\frac{\partial^2 p}{\partial t^2} = c^2 \frac{\partial^2 p}{\partial x^2},$$ (4.1)

where c is the velocity of acoustic waves, known as *speed of sound*, which is characteristic of a medium for a specific temperature.

Therefore, in a more informative way: *sound* is defined as the mechanical disturbance that propagates with a certain speed in a medium that can develop internal forces (e.g., elastic, internal friction) and has such a character that can excite the hearing mechanism and cause the auditory sense.
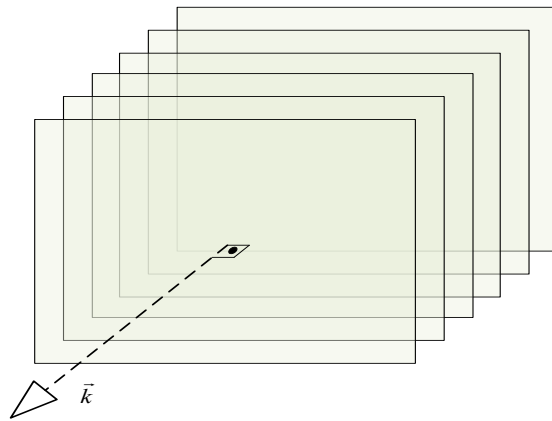
Fig. 4.3: Plane waves propagate along one dimension. Their wavefronts are infinite parallel planes normal to the direction of propagation.

Plane waves are depicted as in Fig. 4.3, by sequential infinite parallel planes perpendicular to the direction of propagation. These planes represent the wavefronts (surfaces of constant phase). Although it is not possible in practice to have a true (infinite extending) plane wave, many waves can be considered approximately plane waves in a confined region of space. The plane waves offer a simplified mathematical framework to study many basic problems in acoustics; they are of outmost importance for a number of applications as for example for the acoustic characterization of materials (see section 4.4).

It is finally noted that sound propagates in the form of *longitudinal waves*, i.e., particle motion is collinear to sound propagation direction, in liquids, plasma, and gaseous media such as air; in contrary to other waves like the mechanical waves propagating on a string or the electromagnetic waves which are *transversal waves*, i.e., the vibration is perpendicular to the direction of propagation. However, in solids sound is propagating through longitudinal, transversal and surface waves.

4.2   Sound measurement.

Sound measurement refers to the determination of basic characteristics of sound. Some of them are the following:

Period, T, is the time taken for one full cycle of a harmonic wave to pass a fixed point, $[T]=1\text{s}$. It is also referred to as cycle time.

Frequency, f, is the number of pressure variation cycles of a harmonic wave in a medium per second, and is expressed in Hertz (Hz), $[f]=1\text{Hz}=1\text{s}^{-1}$. It is the reciprocal of the period of vibration, $f=1/T$.

Angular frequency, $\omega = 2\pi f$, is defined as the rate of change in the phase of a sinusoidal waveform, $[\omega]=1\text{rad/s}$.

Wavelength, λ, is the distance travelled by the wavefront of a pressure plane wave during one cycle, i.e., during one temporal period, $[\lambda]=1\text{m}$. Alternatively, wavelength is called spatial period. In a harmonic wave it corresponds to the distance between two successive maximums or minimums of the acoustic pressure (Fig. 4.2).

By analogy with temporal angular frequency, ω, spatial angular frequency is given by $2\pi/\lambda$. This spatial frequency is termed angular *wavenumber* or just *wavenumber* and denoted by k, $k=2\pi/\lambda$. Therefore, wavenumber may be interpreted as the phase change per unit distance in a pure travelling wave. Wavenumber is the modulus of the *wavevector*, $\vec{k}=k\cdot\vec{n}$, which has the direction of propagation, $\vec{n}$, the direction normal to wavefront (Fig. 4.3).

Particle velocity (or flow per unit area), $\vec{u}$, is the velocity of the elementary quantities, e.g. air particles, of the propagation medium which vibrating around a resting position contribute to the development of a sound (propagating mechanical disturbance). Note that particle velocity (vector) does not relate to the average speed (scalar) of the associated molecules; the square of the latter is characterized by the local temperature of the fluid and it is a measure of the average molecular kinetic energy.

Volume velocity (acoustic volume flow), U, due to a sound wave is the flow rate of the propagation medium through a surface of area, $\vec{S}$, normal to flow direction. It is $U=\vec{S}\cdot\vec{u}$.

Speed of sound, c, is the velocity of the propagating mechanical disturbance in the elastic medium. The speed of sound in ambient air is approximately given as

$$c \approx 331.3 + 0.606 \cdot \Theta ,$$ (4.2)

where Θ is the temperature in ºCelsius.

Phase velocity, $\vec{u}_{ph}$, of a traveling harmonic wave is the velocity of a point of constant phase towards the direction of wavevector. In an isotropic acoustic medium which does not present the phenomenon of acoustic dispersion the phase velocity coincides with the speed of sound.

The speed of sound, the frequency, and the wavelength are related by the following equation:

$$c = \lambda f ,$$ (4.3)

therefore, the wavenumber may successively be expressed as

$$k = \frac{2\pi}{\lambda} = \frac{2\pi f}{c} = \frac{\omega}{c} .$$ (4.4)

Acoustic pressure is of course a central characteristic of sound. However, the instantaneous acoustic pressure, $p(t)$, is seldom the measured quantity, since sound power related quantities are usually pursuit. Therefore the *effective acoustic pressure*, p_{eff}, or *root-mean-square* (rms) *acoustic pressure*, p_{rms} is used instead, since p_{rms}^2 is proportional to energy or power related physical quantities,

$$p_{eff} = p_{rms} = \sqrt{\lim_{T \to \infty} \frac{1}{T} \int_0^T p^2(t) dt} .$$ (4.5)

If p_o is the peak value of the acoustic pressure (half of the peak-to-peak, p_{p-p}, value) for a harmonic sound wave, then the rms acoustic pressure (Fig. 4.2) is given by

$$p_{rms} = p_o / \sqrt{2} .$$ (4.6)

Sound "strength" (how loud it is) is usually expressed in decibels (dB). Although decibel is not expressing a physical quantity, but only a ratio relative to a reference quantity (e.g., the power gain of an amplifier is $G_{dB} = 10 \log\left(Power_{,out} / Power_{,in} \right)$ and reference quantity is the input power, $Power_{,in}$), if the reference quantity is known a priori, then decibels can be used to express physical quantities.

Therefore, *sound pressure level* (*SPL*), L_p, is defined using $p_{ref} = 20\mu\text{Pa}$ as reference quantity by

$$L_p = 10\log\frac{p_{rms}^2}{\left(p_{ref}\right)^2} = 10\log\frac{p_{rms}^2}{\left(20\mu\text{Pa}\right)^2} = 20\log\frac{p_{rms}}{20\mu\text{Pa}} , \qquad (4.7)$$

and is measured in dB_{SPL}, i.e., $\left[L_p\right] = 1\text{dB}_{SPL}$; it is noted that $p_{rms} = 1\text{Pa}$, corresponds to $L_p \approx 94\text{dB}_{SPL}$.

Sound intensity, $\vec{I}$, at a given point of an acoustic field in a specific direction is defined as the ratio of the average acoustic power that is transmitted through a unit area perpendicular to the considered direction at the specific point. It describes the amount and direction of flow of acoustic energy at a given position. $[I] = 1\text{W}/\text{m}^2$. For plane waves, the modulus of sound intensity is

$$I = \frac{p_{rms}^2}{\rho c} , \qquad (4.8)$$

where ρ is the density of the medium and c the speed of sound in the specific medium. Accordingly, considering $I_{ref} = 1\,p\text{W}/\text{m}^2$ as reference quantity for sound intensity, one can define intensity level (*IL*), L_I as

$$L_I = 10\log\frac{I}{I_{ref}} = 10\log\frac{I}{1\,p\,\text{W}/\text{m}^2} , \qquad (4.9)$$

and is measured in dB_{IL}, i.e., $\left[L_I\right] = 1\mathrm{dB}_{IL}$; it is noted that for specific frequency and density combinations $L_I \approx L_p$. For example for $\Theta = 22^{\circ}\mathrm{C}$ their difference is only 0.1dB. However, this fact should not lead to confusing the two levels, since they represent different physical quantities and not simple numerical factors without units.

The general solution of Eq. (4.1) reads

$$p(t) = p_{01}e^{j(\omega t - kx)} + p_{02}e^{j(\omega t + kx)} \tag{4.10}$$

If one is interested in the propagation along $+x$ direction only it becomes

$$p(t) = p_0 e^{j(\omega t - kx)} = p_0 e^{jk(ct - x)}, \tag{4.11}$$

and since only real quantities are observable, the real part of the above solution is

$$p(t) = p_0 \cos(\omega t - kx), \tag{4.12}$$

Using the definitions of ω, f, T, as well as Eqs (4.3) and (4.4), Eq. (4.12) could be rewritten as

$$p(t) = p_0 \cos 2\pi\left(\frac{t}{T} - \frac{x}{\lambda}\right), \qquad (4.13a) \qquad \text{or} \qquad p(t) = p_0 \cos\omega\left(t - \frac{x}{c}\right). \qquad (4.13b)$$

Interpreting the solution of the plane wave equation we note the following:

- The instantaneous acoustic pressure $p(t)$ is not a function of distance x, but depends only on time, t.
- In any position the sound has the same frequency, f.
- The only effect of distance is the phase delay, $-kx$. The energy levels that the plane acoustic waves carry (which is proportional to p_{rms}^2) remain unaltered with distance from the source.

4.3 Sound reflection, absorption, refraction.

In an acoustic system, the *cause* (or the stimulus) is the acoustic pressure, while the *effect* (or the result) is the movement of the acoustic medium "particles". Therefore, in direct analogy to the electric circuits, where impedance is defined as the ratio of the voltage (stimulus) to the current (result), one can define the *acoustic impedance*, Z, as the radio of the acoustic pressure, p, to the volume velocity (acoustic volume flow), U,

$$Z = \frac{p}{U}. \tag{4.14}$$

Z is frequency dependent and complex. Being also dependent on the area through which the flow is defined, it is not a property characteristic of the acoustic medium.

On the other hand, the *specific acoustic impedance*, z_s, sometimes referred to as unit area acoustic impedance, can be used to characterize an acoustic medium. It is defined as the ratio of the acoustic pressure, p, to the particle velocity (or flow per unit area), u, at a given point

$$z_s = \frac{p}{u}.$$ (4.15)

z_s is also complex and frequency dependent in general, $[z_s] = 1\,kgr/m^2s = 1\,rayl$. However, the *characteristic acoustic impedance*, i.e., the specific acoustic impedance under the assumption of harmonic progressive plane wave propagation, is real, frequency independent and given by

$$z_c = \rho c,$$ (4.16)

where, ρ is the density c and is the speed of sound in the specific medium. Characteristic impedance is one of the *bulk properties* of an acoustic medium.

Bulk properties are characteristic acoustic properties describing the interaction of a material with sound. They are independent of the material dimensions, e.g. thickness and area; therefore for an absorber they are independent of the absorber size. However, for anisotropic materials the bulk properties are a function of direction. Important bulk properties are the characteristic acoustic impedance, z_c, the *characteristic propagation wavenumber*, k_c, or alternatively the *effective density*, ρ_e, and *bulk modulus K_e*. The term *effective* is used to signify that this density refers to the density experienced by the sound wave and *not* the normal density of the medium (the mass by volume ratio). Bulk modulus is reciprocal to compressibility, i.e., it is defined as the ratio of the pressure applied to a material to the resultant fractional change in its volume. For a porous absorber, the effective density and bulk modulus are interrelated to the characteristic impedance and propagation wavenumber by the following equations

$$z_c = \sqrt{K_e \rho_e},$$ (4.17)

and

$$k_c = \omega \sqrt{\rho_e / K_e},$$ (4.18)

Once these bulk properties are known, the sound wave propagation within the corresponding acoustic medium can be predicted.

On the interface between two acoustic media, the specific acoustic impedance is usually referred to as *surface impedance* or *wall impedance*, implying that the specific impedance is estimated on the surface of a porous wall. In general, the impedance seen at the surface of an absorber depends on the porous media bulk properties, the geometry of the absorber and the mounting conditions of the absorber. The surface impedance is generally complex. Its real part (*acoustic resistance*) is related to energy losses, while the imaginary part (*acoustic reactance*) is associated with phase changes or energy storage mechanisms. Therefore, surface acoustic impedance provides more information for the absorbing properties of a material compared to the absorption coefficient (defined immediately following, see Eq. (4.19)).

Suppose two acoustic media 1 and 2, interfacing through a plane surface and characterized by surface impedances z_{s1} and z_{s2}, as depicted in Fig. 4.4.
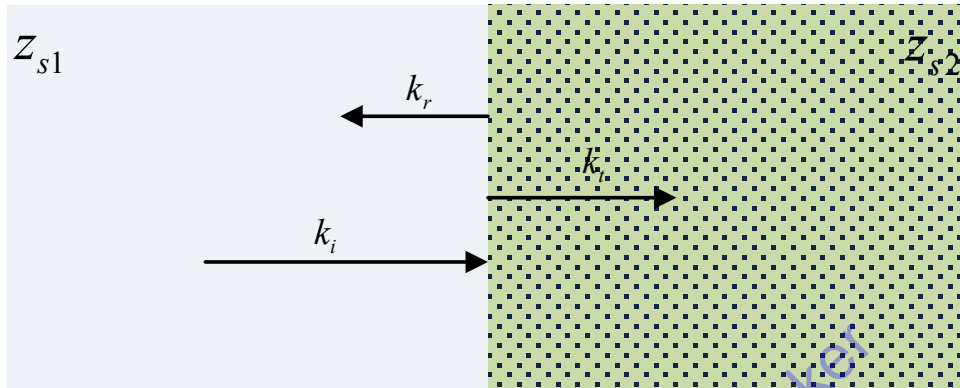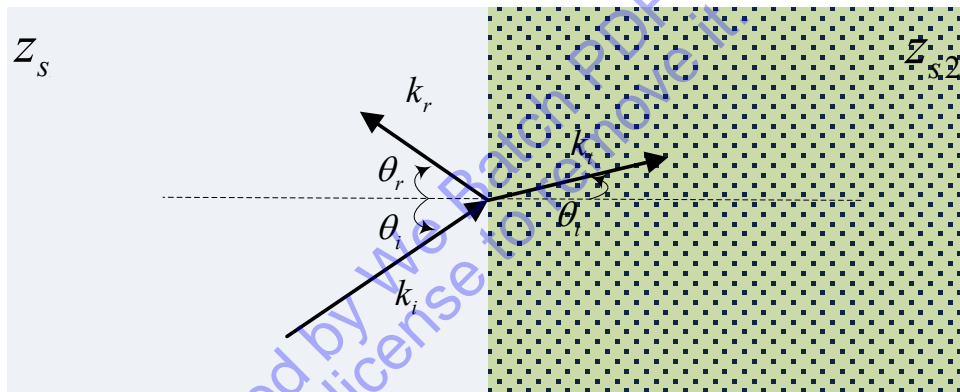
Normal incidence

Oblique incidence

Fig. 4.4: Reflection and refraction in case of normal (upper part) and oblique (lower part) incidence.

A harmonic progressive plane wave incident, $\vec{k}_i$, from medium 1 side to the interface is partly *reflected*, $\vec{k}_r$, back to medium 1, and partly *refracted* (transmitted), $\vec{k}_t$, to medium 2, assuming that interface surface is dimensionless and thus it is not absorbing. If the medium 2 is an absorber itself, then we could refer to the refracted sound as *absorbed* sound.

If the sound intensity moduli and sound energies corresponding to incident, reflected, refracted and absorbed sound are I_i, I_r, I_t, and I_a, and W_i, W_r, W_t, and W_a, respectively, then one can define the *reflection coefficient*, a_r, the *transmission coefficient*, a_t, or τ, and the *absorption coefficient*, a_a, or a, as

$$a_r = \frac{W_r}{W_i} = \frac{I_r}{I_i}, \ \ \tau = a_t = \frac{W_t}{W_i} = \frac{I_t}{I_i}, \text{ and } \ a = a_a = \frac{W_a}{W_i} = \frac{I_a}{I_i}, \tag{4.19}$$

For the case of normal incidence (upper part of Fig. 4.4), since from Eqs (4.8) and (4.16) it follows that

$$I = p_{rms}^2 / z_s, \tag{4.20}$$

substituting on the defining Eqs (4.19),

$$a_t = \frac{p_{t,rms}^2 z_{s1}}{p_{i,rms}^2 z_{s2}} \quad \text{and} \quad a_r = \frac{p_{r,rms}^2}{p_{i,rms}^2}, \tag{4.21}$$

and finally, employing the appropriate boundary conditions, one obtains

$$a_t = \frac{4 z_{s1} z_{s2}}{\left(z_{s2} + z_{s1} \right)^2} \quad \text{and} \quad a_r = \frac{\left(z_{s2} - z_{s1} \right)^2}{\left(z_{s2} + z_{s1} \right)^2}, \tag{4.22}$$

For the oblique incidence case, since the particle velocity continuation (one of the boundary conditions) at the interface surface, $x = 0$, is expressed as

$$\frac{p_i(0,t)\cos\theta_i}{z_{s1}} - \frac{p_r(0,t)\cos\theta_r}{z_{s1}} = \frac{p_t(0,t)\cos\theta_t}{z_{s2}}, \tag{4.23}$$

one obtains respectively,

$$\frac{p_t(0,t)}{p_i(0,t)} = \frac{z_{s2}\left(\cos\theta_i + \cos\theta_r \right)}{z_{s2}\cos\theta_r + z_{s1}\cos\theta_t}, \quad \text{and} \quad \frac{p_r(0,t)}{p_i(0,t)} = \frac{\left(z_{s2}\cos\theta_i - z_{s1}\cos\theta_t \right)}{\left(z_{s2}\cos\theta_r + z_{s1}\cos\theta_t \right)}, \tag{4.24}$$

and finally

$$a_t = \frac{4 z_{s1} z_{s2} \cos\theta_i \cos\theta_r}{\left(z_{s2}\cos\theta_r + z_{s1}\cos\theta_t \right)^2}, \quad \text{and} \quad a_r = \frac{\left(z_{s2}\cos\theta_i - z_{s1}\cos\theta_t \right)^2}{\left(z_{s2}\cos\theta_r + z_{s1}\cos\theta_t \right)^2}, \tag{4.25}$$

Since, on the interface surface no medium change happens, the tangential components of the wavevectors (Fig. 4.4) are equal: $k_i \sin\theta_i = k_r \sin\theta_r = k_t \sin\theta_t$. This means that since the incident and reflected waves are propagated in the same medium, the angle of reflection (angle between the direction in which the reflected wave is traveling and the direction perpendicular to the interface surface) is equal to the incidence angle (angle between the direction in which the incident wave is traveling and the direction perpendicular to the interface surface), i.e.,

$$\theta_i = \theta_r, \tag{4.26}$$

while for the transmitted and incident waves holds sequentially, using $c = \lambda f$ and knowing that frequency does not change when the medium changes, $\sin\theta_i / \lambda_i = \sin\theta_r / \lambda_r$, or

$$\frac{\sin\theta_t}{\sin\theta_i} = \frac{c_2}{c_1}. \tag{4.27}$$

Eqs (4.26) and (4.27) are the well known refraction laws of Snell-Descartes. Quite often Eq. (4.27) is called the *Snell's law*.

It is noted here that the ratio of the reflected by the incident pressure appearing in the right equation of Eq. (4.24), is usually referred to as the *pressure reflection coefficient* (or the *reflection factor*), R, and includes both amplitude and phase information from the reflected sound wave, p_r, and the incident sound wave, p_i,

$$R = \frac{p_r}{p_i}. \tag{4.28}$$

Moreover, for most absorbents, the speed of sound in the absorbent medium is much less than that the speed of sound in the air. Therefore, in the case that the incidence medium is the air, the angle of propagation in the propagation medium is smaller than in the air ($\theta_t << \theta_i$) and it is usually assumed that the propagation is normal to the interface surface, i.e. $\theta_t \to 0$.

Consequently, if in the case described by the lower part of Fig. 4.4 the left medium (medium 1) is the air, its surface impedance is the characteristic acoustic impedance and $z_{s1} = \rho_o c_o$, with ρ_o, c_o being the density of the (ambient) air and the speed of sound in the air. In the specific case, the right equations appearing in Eqs (4.24) and (4.25) may be rewritten as

$$\frac{p_r(0,t)}{p_i(0,t)} = \frac{(z_{s2}\cos\theta_i - \rho_o c_o \cos\theta_t)}{(z_{s2}\cos\theta_r + \rho_o c_o \cos\theta_t)}, \quad \text{and} \quad a_r = \frac{(z_{s2}\cos\theta_i - \rho_o c_o \cos\theta_t)^2}{(z_{s2}\cos\theta_r + \rho_o c_o \cos\theta_t)^2}, \tag{4.29}$$

furthermore, since $\theta_i = \theta_r$ and $\theta_t \to 0$ they become

$$R = \frac{p_r(0,t)}{p_i(0,t)} = \frac{\left(\dfrac{z_{s2}\cos\theta_i}{\rho_o c_o} - 1\right)}{\left(\dfrac{z_{s2}\cos\theta_i}{\rho_o c_o} + 1\right)}, \quad \text{and} \quad a_r = \frac{\left(z_{s2}\cos\theta_i - \rho_o c_o\right)^2}{\left(z_{s2}\cos\theta_i + \rho_o c_o\right)^2} = \frac{\left(\dfrac{z_{s2}\cos\theta_i}{\rho_o c_o} - 1\right)^2}{\left(\dfrac{z_{s2}\cos\theta_i}{\rho_o c_o} + 1\right)^2}, \quad (4.30)$$

Therefore,

$$\frac{z_{s2}}{\rho_o c_o}\cos\theta_i = \frac{(1+R)}{(1-R)} \tag{4.31}$$

and

$$a_r = |R|^2 \tag{4.32}$$

Remember that the interface is considered not to be absorbing, therefore $W_a = 0$ and, thus (energy conservation), $W_i = W_r + W_t$, i.e., $a_t + a_r = 1$. However, if medium 2 is an absorber, then the transmitted power is actually absorbed, so one could for convenience call the transmission coefficient, a_t, absorption coefficient, a. Consequently, in this case, the absorption coefficient, a, can be expressed as,

$$a = 1 - a_r = 1 - |R|^2 \tag{4.33}$$

Under the hypothesis of harmonic progressive plane wave propagation, the surface impedance is not frequency dependent; however it can be said to depend on the angle of incidence to the surface, in the sense that only the normal component of particle velocity is effectively contributing to the boundary conditions. If the wall material is locally reacting, the *effective surface impedance* at any angle is related to the surface impedance for normal incidence, the *normal surface impedance*, z_n by the formula

$$z_s(\theta_i) = \frac{z_n}{\cos\theta_i}, \tag{4.34}$$

since $z_s(\theta_i) = p/u_{eff} = p/u \cdot \cos\theta_i = z_n/\cos\theta_i$. This formula can be used to transform normal incidence results to oblique ones by simple substitution of z_n by $z_s(\theta_i)$, using Eq. (4.34). Although the aforementioned analysis regarding the reflection and the transmission coefficients for oblique incidence has been presented differently, one can obtain the same results (Eq. (4.25)), using the above transformation on the normal incidence results (Eq. (4.22)). Therefore, the determination of normal surface impedance is usually pursuit. Nevertheless, in order to characterize, or design, an acoustic medium the characteristic impedance is needed.

Suppose that a porous absorbing medium of thickness d and infinite (very large) area is mounted on a rigid wall as illustrated in Fig. 4.5.
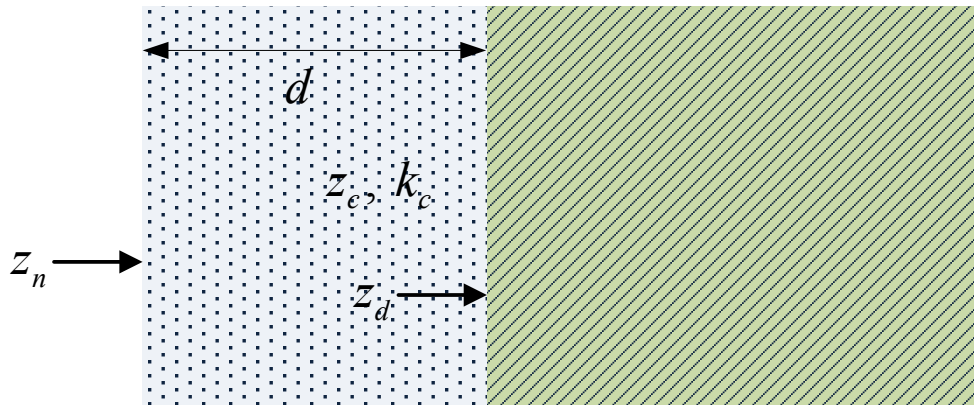
Fig. 4.5: Porous absorbing medium of thickness d mounted on a rigid wall.

The normal surface impedances at the outer interface surface of the absorbing medium (towards the air), z_n, and the inner interface surface (towards the rigid back), z_d, are interrelated through the formula

$$z_n = z_c \frac{z_d + j z_c \tan(k_c d)}{z_c + j z_d \tan(k_c d)}. \tag{4.35}$$

For $z_d \to \infty$, $z_n \to -j z_c \cot(k_c d)$; therefore, knowing z_n for two different thicknesses (d_1, d_2), the characteristic impedance and the characteristic wavenumber can be determined.

On the other hand, if the characteristic impedance and wavenumber of a material have been determined by other means, they can be converted to the surface impedance and absorption coefficient for a particular thickness of the porous material with known boundary conditions (on one side air and on the other side a rigid backing). First the normal surface impedance, z_n, is determined as

$$z_n = -j z_c \cot(k_c d), \tag{4.36}$$

while, since $\theta_i = 0$, R may be obtained from Eq. (4.31) as

$$R = \frac{\left(\dfrac{z_n}{\rho_o c_o} - 1 \right)}{\left(\dfrac{z_n}{\rho_o c_o} + 1 \right)}, \tag{4.37}$$

from which the absorption coefficient can be determined using Eq. (4.33).

4.4 Sound absorption measurement methods.

Various methods have been proposed for the characterization of the sound absorbing capability of different materials. From the application viewpoint, i.e., in order to use sound absorbing materials, it is usually important to know the random incidence absorption coefficient. On the other hand, from the design viewpoint, i.e., in order to be able to design these materials, a non-statistical, material-oriented parameter, like normal incidence absorption coefficient, seems to be more appropriate. Although both approaches can be found, the second one is far more frequently employed in the literature relevant to textile materials. The reason is that most of textile-oriented scientific articles deal with the study of the influence of textile parameters on the sound absorption properties, targeting to the understanding and modeling of the involved absorption mechanisms.

Normal incidence absorption coefficient is usually measured in the controlled conditions of an impedance tube, or Kundt's tube, where standing sound waves are developed. In order for the impedance tube methods to be applied successfully, the plane wave propagation approximation has to be fulfilled. This poses a number of limitations on the test setup:

- Since, ideally, plane waves propagate without attenuation, the losses into and through the tube should be minimized. This leads to heavy (thick) metal structures.
- The tube should have constant cross-section over the measurement section. They are usually circular.

- The loudspeaker should be a few tube diameters from the first microphone position, in order to ensure that the possible cross modes generated by the loudspeaker have not significant presence. Sometimes, absorbent is placed at the loudspeaker end of the tube.
- The microphone positions should not be too close to the sample so that any evanescent waves generated on reflection have had time to die away.
- The tube diameter has to be smaller than sound half wavelength (specifically $D < 0.586\lambda$), while its length longer than $3\lambda/4$.

4.4.1   Standing wave method

The standing wave method is historically the first proposed which is based on the use of impedance tube. The specimen under test is placed at the one end of the tube, while a sound source generates a single frequency sound at the opposite end. Assuming plane wave propagation conditions inside the tube and the specimen placed at the position $x = 0$ before a rigid termination, see Fig. 4.6, the overall resulting pressure after the interference between the two waves traveling in opposite directions (at steady state) is

$$p = A\left(e^{jkx} + \mathrm{Re}^{-jkx}\right), \tag{4.38}$$

where R, is the pressure reflection coefficient, see Eq. (4.28) and A is a complex constant. The first term of Eq. (4.38) corresponds to the incident while the second to the reflected wave. At the position where they are in phase, a maximum pressure, $p_{\max}$, is developed, Fig. 4.6. In contrary, a minimum pressure, $p_{\min}$, is developed at the position where they are completely out of phase. Since the amplitude of the reflected sound wave, is lower than the incident amplitude, the standing wave ratio, s, is defined as

$$s = \frac{p_{\max}}{p_{\min}} = \frac{|p_i| + |p_r|}{|p_i| - |p_r|} = \frac{1 + |R|}{1 - |R|}, \tag{4.39}$$

Rearranging Eq. (4.39) the magnitude of the reflection coefficient is obtained

$$|R| = \frac{s-1}{s+1}, \tag{4.40}$$

from which the absorption coefficient, a, results from Eq. (4.33).

Moving a pressure probe (microphone) along the impedance tube, the maximum and minimum pressure can be measured and therefore the standing wave ratio, and finally the absorption coefficient can be determined. For a specific frequency, with wavelength within tube range, the probe is moved on sound source axis (tube axis) starting from specimen's position towards the source. Although it is possible that a maximum of pressure is first detected as the probe is moving away from specimen, see Fig. 4.6, the first recorded value is always the first pressure minimum, and then the following maximum is also recorded. This minimizes the effect of tube losses, i.e., the specific procedure ensures that the recorded maximum is indeed a maximum and not an intermediate value. The same procedure is repeated for all frequencies of interest.
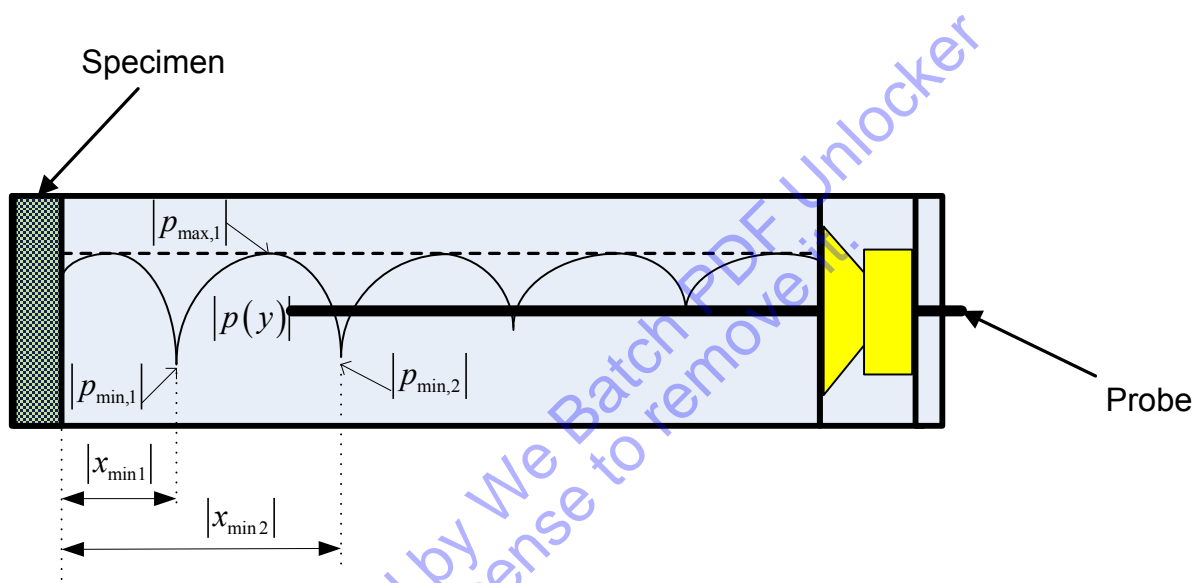

Fig. 4.6: Moving probe setup for the realization of the standing wave method.

Knowing the position of the first minimum, since the incident and reflected waves are there out of phase by exactly π, the phase angle of the pressure reflection coefficient can be calculated as

$$\angle R = 2kx_{min1} - \pi. \tag{4.41}$$

It is then possible, using Eq. (4.31), to obtain the normal incidence surface impedance as

$$z_n = \rho_o c_o \frac{1+R}{1-R}. \tag{4.42}$$

One of the key advantages of this method is that no calibration is pre-required for the measurement to be performed, provided that the apparatus is not changed during the measurement. The standard methods ISO 10534-1:1996 (1996) and ASTM C384-04 (2011) are based on the standing wave method.

4.4.2 Transfer function method

In the transfer function method, two pressure probes (microphones) are fixed at the positions $x = x_1$ and $x = x_2$ ($x = 0$ is the position of the specimen), see Fig. 4.7. The pressure transfer function between these two positions is

$$H_{21} = \frac{p(x_2)}{p(x_1)} = \frac{e^{jkx_2} + \mathrm{Re}^{-jkx_2}}{e^{jkx_1} + \mathrm{Re}^{-jkx_1}} \tag{4.43}$$

Solving Eq. (4.43) in regard to the complex pressure reflection coefficient R one gets

$$R = \frac{H_{21}e^{jkx_1} - e^{jkx_2}}{\mathrm{e}^{-jkx_2} - H_{21}\,\mathrm{e}^{-jkx_1}} = \frac{H_{21} - H_I}{H_R - H_{21}}e^{j2kx_1}, \tag{4.44}$$

where $H_I = e^{jk\Delta x}$, $H_R = e^{-jk\Delta x}$, and $\Delta x = x_2 - x_1$

Using Eq. (4.33) and (4.42) we calculate the absorption coefficient and the normal incidence specific acoustic impedance, respectively.
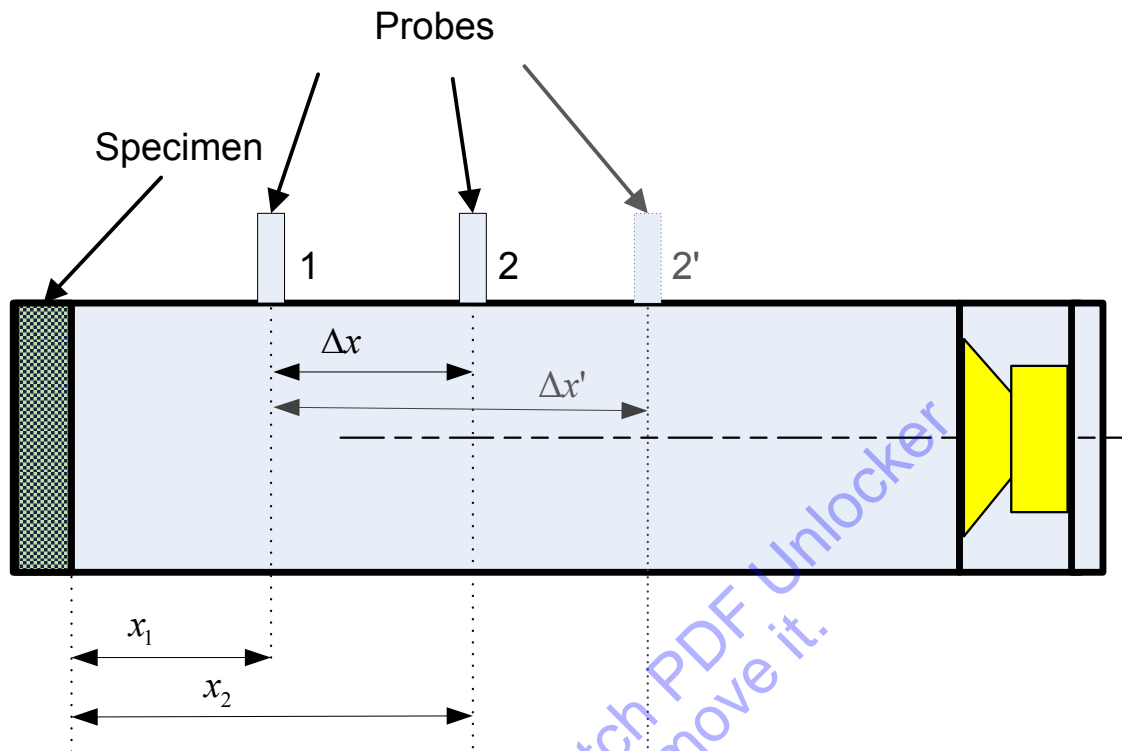
Fig. 4.7: Two microphones setup for the realization of the transfer function method.

In the transfer function method the two microphones used should be carefully positioned, because both a too close and a too distant spacing between them can lead to inaccurate measurements. If they are too close to each other, the pressure difference may be too small to be accurately measured and this leads to a low frequency limit $f_l > c_o/20\Delta x$. On the other hand, if their spacing is too wide there is a possibility to record almost identical pressure values at the microphones, as $\Delta x \to \lambda$. Therefore, an upper frequency limit is posed $f_h < 0.45c_o/\Delta x$. These frequency limitations are usually bypassed using more than two microphones to cover the frequency range of interest. The use of three microphones with appropriate spacing is typical.

The sound source can be reproducing either white noise or a deterministic signal like maximum length sequences (MLS) or log chirp (logarithmically swept sine). However, the first choice is more time consuming and troublesome since it involves an averaging based microphone matching process. Namely, each measurement is followed by a second one with microphones interchanged, to compensate for differences due to the mismatches in their responses.

A comparison between the standing wave method and the transfer function method seems to be in favor of the second, probably due to the accurate positioning of the microphones. The standard methods ISO 10534-2:1998 (1998) and ASTM E1050-10 (2010) are based on the transfer function method.

4.4.3   Transmission loss method

The transmission loss method is a variation on the standard impedance tube using two pairs of microphones. The microphones measure both reflected and transmitted waves to get the normal incident transmission loss, TL_n. The bulk properties characteristic acoustic impedance, z_c, and characteristic propagation wavenumber, k_c, with only one measurement can also be determined by this method. Although there are different variations of this method, the widely accepted variation of Song and Bolton (Song and Bolton 2000; Olivieri et al. 2006) is the one presented here.

As the sample of thickness, d, is placed in the tube, there are four plane acoustic waves with amplitudes, A, B, C, and D, relating to the material sample, as shown in Fig. 4.8. In anechoic conditions, i.e., if $D = 0$, it would be $TL_n(f) = 10\log_{10}(W_i/W_t)$, or $TL_n(f) = 10\log\left(\left|A^{anech.}/C^{anech.}\right|^2\right)$, where W_i and W_t are the airborne sound power incident on the specimen and the sound power transmitted through the specimen and radiated from the other side, respectively. Since different termination conditions would lead to different results, the transmission loss should be expressed in terms of the material under test. The basis for the method lies in the definition of the transfer matrix which is characteristic for an acoustic material.

The matrix relating the forward and backward traveling acoustic waves, **G**, is defined as

$$\begin{bmatrix} A \\ B \end{bmatrix} = \begin{bmatrix} G_{11} & G_{12} \\ G_{21} & G_{22} \end{bmatrix} \cdot \begin{bmatrix} C \\ D \end{bmatrix}, \tag{4.45}$$
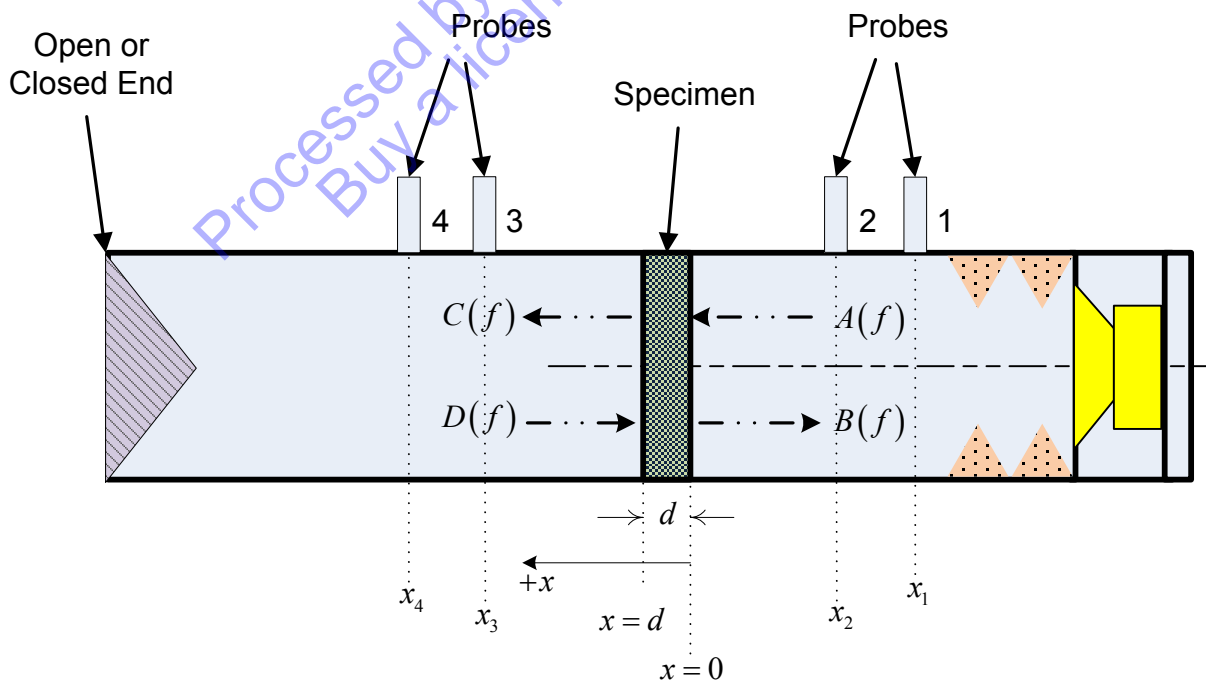

Fig. 4.8: Four microphones setup for the realization of the transmission loss method.

At each position x to the right of the sample, $x \leq 0$, the acoustic pressure, $p(x)$, and the modulus of particle velocity, $u(x)$, are

$$p(x) = A(f)e^{-jkx} + B(f)e^{jkx}, \quad \text{and} \quad u(x) = \left(A(f)e^{-jkx} - B(f)e^{jkx}\right)\Big/\rho_o c_o, \quad (4.46)$$

respectively, since pressure is a scalar physical quantity and particle velocity is a vector physical quantity. Similarly, to the left of the sample, $x \geq d$, it is

$$p(x) = C(f)e^{-jkx} + D(f)e^{jkx}, \quad \text{and} \quad u(x) = \left(C(f)e^{-jkx} - D(f)e^{jkx}\right)\Big/\rho_o c_o, \quad (4.47)$$

where ρ_o is the density, c_o is the speed of sound, f is the frequency, and k is the (complex) wave number for the (ambient) air inside the tube. Then, A, B, C, and D, can be expressed as

$$A = \frac{j\left(p(x_1)e^{jkx_2} - p(x_2)e^{jkx_1}\right)}{2\sin k(x_1 - x_2)}, \quad C = \frac{j\left(p(x_3)e^{jkx_4} - p(x_4)e^{jkx_3}\right)}{2\sin k(x_3 - x_4)},$$

$$B = \frac{j\left(p(x_2)e^{-jkx_1} - p(x_1)e^{-jkx_2}\right)}{2\sin k(x_1 - x_2)}, \quad D = \frac{j\left(p(x_4)e^{-jkx_3} - p(x_3)e^{-jkx_4}\right)}{2\sin k(x_3 - x_4)}. \quad (4.48)$$

Therefore, the amplitudes A, B, C, and D can be calculated by the four microphone measurements. Once these amplitudes have been determined, the acoustic pressure and particle velocity at $x = 0$ and $x = d$, i.e., at both sides of the specimen under test, can be estimated, using Eqs (4.46) and (4.47). Then, *the transfer matrix*, $\mathbf{T}$, can be defined as

$$\begin{bmatrix} p \\ u \end{bmatrix}_{x=0} = \begin{bmatrix} T_{11} & T_{12} \\ T_{21} & T_{22} \end{bmatrix} \cdot \begin{bmatrix} p \\ u \end{bmatrix}_{x=d} \tag{4.49}$$

Executing two sets of measurements under different termination conditions at the left end of the tube (Fig. 4.8), one obtains the components of $\mathbf{T}$ solving the linear system of equations

$$\begin{bmatrix} p^r & p^o \\ u^r & u^o \end{bmatrix}_{x=0} = \begin{bmatrix} T_{11} & T_{12} \\ T_{21} & T_{22} \end{bmatrix} \cdot \begin{bmatrix} p^r & p^o \\ u^r & u^o \end{bmatrix}_{x=d} , \tag{4.50}$$

where the superscripts o and r indicate the two different termination conditions, i.e., rigid and open end, respectively.

Moreover, the elements of the $\mathbf{G}$ matrix, defined by Eq. (4.45), can be determined from

$$\begin{bmatrix} A^r & A^o \\ A^r & B^o \end{bmatrix}_{x=0} = \begin{bmatrix} G_{11} & G_{12} \\ G_{21} & G_{22} \end{bmatrix} \cdot \begin{bmatrix} C^r & C^o \\ D^r & D^o \end{bmatrix}_{x=d} , \tag{4.51}$$

The element G_{11} corresponds to the transmission loss for normal incidence, therefore solving the system of Eq. (4.51), it is found that normal incidence transmission loss, TL_n, in dB, is

$$TL_n(f) = 20\log_{10}(G_{11}) = 20\log_{10}\left(\frac{A^r D^o - A^o D^r}{C^r D^o - C^o D^r} \right), \tag{4.52}$$

or, equivalently, after some algebraic manipulations employing Eqs (4.45), (4.46), (4.47), and (4.49),

$$TL_n = 20\log_{10}\left(\frac{1}{2} \left| T_{11} + \frac{T_{12}}{\rho_o c} + \rho_o c T_{21} + T_{22} \right| \right), \tag{4.53}$$

Knowing that (Ingard 1994; Allard 1993) the normal incidence transfer matrix for a finite depth, d, layer of a homogeneous, isotropic porous material (either rigid or limp) is

$$\begin{bmatrix} T_{11} & T_{12} \\ T_{21} & T_{22} \end{bmatrix} = \begin{bmatrix} \cos k_{c,p} d & j\rho_p c_p \sin k_{c,p} d \\ j \sin k_{c,p} d / \rho_p c_p & \cos k_{c,p} d \end{bmatrix}, \tag{4.54}$$

where $k_{c,p}$ is the characteristic wave number of the acoustic material, ρ_p is the density, and c_p is the speed of sound in the specific material.

Therefore, the characteristic wave number can be evaluated from Eq. (4.54) as

$$k_{c,p} = \frac{1}{d} \cos^{-1} T_{11}, \tag{4.55}$$

or

$$k_{c,p} = \frac{1}{d}\sin^{-1}\sqrt{-T_{12}T_{21}} \, , \tag{4.56}$$

while the characteristic acoustic impedance, $z_{c\,p} \quad {}_p c_p$, is

$$z_{c,p} = \sqrt{\frac{T_{12}}{T_{21}}} \, . \tag{4.57}$$

Finally, the speed of sound and density can easily be determined as $c_p = 2\pi f / k_{c,p}$ and $\rho_p = z_{c,p} / c_p$, respectively. We remind that since the characteristic impedance and wavenumber of the material have been determined, they can be converted to the surface impedance and absorption coefficient for a particular thickness of the porous material on a rigid backing, using Eqs (4.36), (4.37) and (4.33). The transmission loss method is described in the ASTM E2611-09 (2009) standard. An ISO standard is also under development.

4.5   Sound absorption mechanisms, porous materials.

One of the main sound absorbent classes is the *porous materials*. It encompasses all materials in which sound propagates through a network of interconnected pores in such way that acoustic energy is converted to heat mainly due to viscous boundary layer effects. For the absorption to be effective air should be able to pass through the material. Air is a viscous fluid, and thus sound energy is dissipated via friction with the pore walls. Moreover, flow changes during sound propagation through the irregular pores lead to a loss in momentum. Beyond viscous effects, there are losses due to thermal conduction from the air to the absorber material. All textile materials, nonwoven, woven or knitted, belong to this class. Typical textile materials used as sound absorbers are carpets, curtains, blankets, and cushions.

Porous absorbers are only effective at mid- to high frequencies (see Fig. 4.9). However, the ear is most sensitive at these frequencies and therefore their noise reduction effect is noticeable. Noise reduction is maximized if the maximum of the particle velocity is achieved within the porous material. This implies that in order to extend the noise reduction ability of porous materials to lower frequencies one has to increase their thickness. Another technique to extend to lower frequencies with a given thickness of absorbent is to place the porous material at a distance of quarter wavelength from a rigid back, e.g., from a room wall.
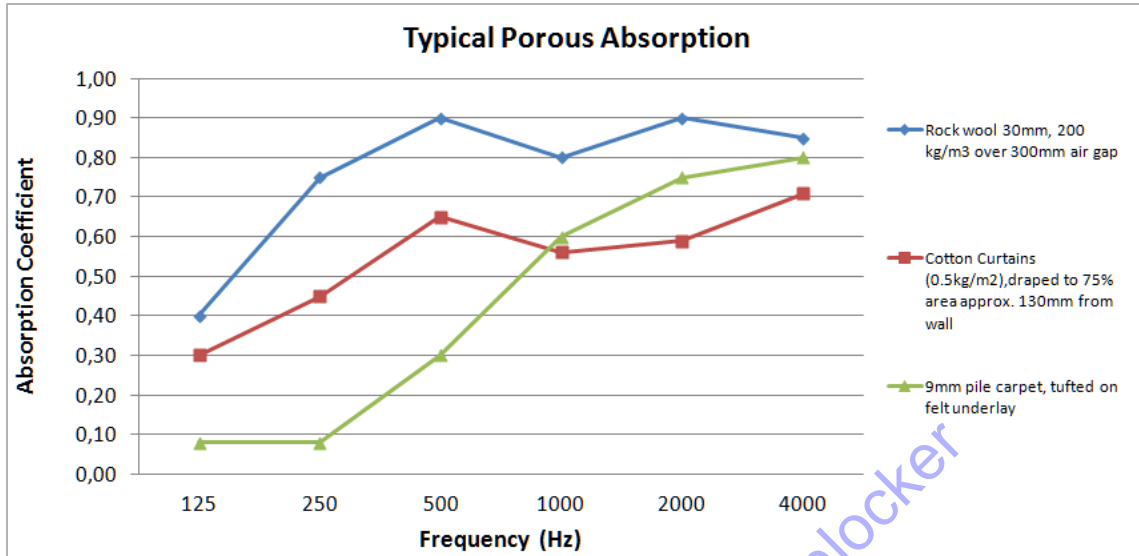
Fig. 4.9: Typical absorption of porous textile absorbers and rock wool fiber assembly.

The interaction of sound and the porous material is governed by the structural (geometric) details of the material. There are some material properties, known as *the microstructural properties*, which are closely related to the bulk properties of the porous material. The microstructural properties are used as design parameters for designing porous absorber with specific bulk properties. The key parameters for development or modeling are flow resistivity and porosity.

Flow resistivity, $\sigma = \Delta P / v_{fl} d$, where v_{fl} is the mean steady flow velocity, ΔP is the resultant pressure drop, and d is the thickness of the absorbent, $[\sigma] = 1 kgr/m^3 s = 1 rayl/m$, gives a measure of the resistance to air flow that the porous absorber poses. It provides some sense of how much sound energy may be lost due to boundary layer effects within the material. The porous material should have a low enough flow resistivity so the sound enters the absorbent, but not too low otherwise no dissipation occurs.

Porosity, ε, gives a measure of the amount of open air volume in the absorber available to sound wave propagation. It is a ratio of the total pore volume to the total volume of the absorbent. However, only the open connected pores, that allow air flow, should be included in the total pore volume. For many good porous absorbents it is possible to assume a porosity of $\varepsilon \approx 1$ (values near to 0.98 are usual).

It is noted that flow resistivity is related by empirical relationships to either bulk density, ρ_m, or to porosity of a fibrous porous material, $\varepsilon = \rho_m / \rho_f$, where ρ_f is the density of fibers. Although porosity and flow resistivity are the most important parameters in determining the sound absorption, other secondary parameters such as the shape factor and the tortuosity can be important.

Tortuosity, T_s, is defined as the ratio between the sound route through the pores and the thickness of the porous material. It is a parameter representing how the orientation of pores relative to incident wave affects sound propagation. The air that is forced to follow a tortuous path suffers accelerations which cause momentum transfer from air to the material. It is partly indicating the degree of complexity of the sound path through the material; the more complex is the propagation path, the higher is the absorption.

Characteristic lengths are parameters which refer to geometrical characteristics of the pores. Usually, pores have complicated shapes and this is why at least two geometric parameters (lengths) are needed to express shape influence to the sound propagation and consequently the absorption. Different pore shapes have different surface areas and hence have different thermal and viscous effects. The effective density of real porous absorbers is mainly determined by parts of the pores with smaller cross-sections, whereas the bulk modulus is more determined by larger cross-sectional areas.

Once the microstructural properties are known, it is then possible to calculate the characteristic acoustic impedance, z_c, and the characteristic propagation wavenumber, k_c, via appropriate models. The phenomenological theoretical models need more microstructural properties to be known than the macroscopic empirical models which consider a macroscopic view of the propagation, ignoring the details of propagation through each pore. This is the reason why the second ones, like the Delany and Bazley model, are more popular.

The macroscopic empirical model of Delany and Bazley offers very good accuracy under certain conditions. The empirical relations giving the characteristic acoustic impedance and the characteristic propagation wavenumber as functions of flow resistivity for a fibrous porous material are:

$$z_c = \rho_o c_o \left(1 + 0.0571 X^{-0.754} - j0.087 X^{-0.732}\right), \tag{4.58}$$

and

$$k_c = \frac{\omega}{c_o} \left(1 + 0.0978 X^{-0.700} - j0.189 X^{-0.595}\right), \tag{4.59}$$

where $X = \dfrac{\rho_o f}{\sigma}$, while c_o and ρ_o are the speed of sound in air and the air density, respectively.

The conditions under which the above model gives reasonable accuracy are: (a) The porosity should be close to 1, which most purpose built fibrous absorbers achieve. (b) $0.01 < X < 1.0$, which means that the validity is restricted within a defined frequency range. (c) The limits of the flow resistivity should be $1000 \leq \sigma \leq 50,000$ (in $rayl/m$).

Different phenomenological theoretical models are also used in the literature, like, for example, the model of Zwikker and Kosten (1949), which has been recently employed in textile materials (Shoshani and Yakubov 2000; Dias et al. 2007b). These models can also lead to the estimation of the characteristic acoustic impedance, z_c, and the characteristic propagation wavenumber, k_c, of the medium, via the effective density and the bulk modulus, using Eqs (4.17) and (4.18).

We remind that since the characteristic impedance and wavenumber of a material have been determined, they can be converted to the surface impedance and absorption coefficient for a particular thickness of the porous material on a rigid backing, using Eqs (4.36), (4.37) and (4.33).

4.6   Applications on textiles.

In a recent review article (Seddeq 2009, and references therein) the influence of various factors of a fibrous material on sound absorption have been summarized in the following points:

- Sound absorption coefficient increases with a decrease in fiber diameter, micro denier fibers with less than 1 denier per filament (dpf) provide a dramatic increase in acoustical performance.
- One of the most important qualities that influence the sound absorbing characteristics of a fibrous material is the air flow resistivity. In general, it can be inferred that, higher airflow resistivity always gives better sound absorption values but for airflow resistance higher than a limit the sound absorption is decreasing because of the difficulty of sound wave to pass through the materials.

- Tortuosity mainly affects the location of the quarter-wavelength peaks, whereas porosity and flow resistivity affect the height and width of the peaks. It has also been said that the value of tortuosity determines the high frequency behavior of sound absorbing porous materials.
- Fiber surface area and fiber size have strong influence on sound absorption properties; higher surface area and lower fiber size increases sound absorption.
- Less dense and more open structures absorb sound of low frequencies; denser structures perform better for frequencies above 2000 Hz.
- The creation of air gap increases sound absorption coefficient values in mid and higher frequencies. At the same time, creation of air gap presents minima at various frequencies for various air gap distances.
- Covering films such as PVC attachment increase sound absorption at low and mid frequencies at the expense of higher frequencies.

Textiles are typical examples of fibrous porous absorbers. Of course, different manufacturing techniques, different design, different raw materials and different treatments lead to different sound absorption characteristics. Several research articles have been published on the sound absorption properties of textile structures. The interest begun in the early 70s (e.g., Nute and Slater 1973; Dunlop 1974; Slater 1974, and references of these papers) when the focus was in evaluating common home textile items like curtains and carpets. However, the last years an increasing number of researchers, both from acoustics and textile side, focus their efforts on the acoustics of textiles. This trend is, to a great extent, caused by the evolution of new textile production methods and new textile materials. The textile products constitute an interesting sound absorbing alternative because of their two important advantages: low production cost and light weight. They are widely used in aviation, automotive and buildings. Further to the achievement of a high sound absorption performance the aesthetic aspect is also pursuit.

One could suggest two different classifications of the corresponding scientific literature. On one hand, the research works could be divided to the ones trying to achieve physical models of specific textile configurations and the ones trying to attain "black-box" models linking textile properties and acoustical properties. Both approaches involve sound absorption evaluation measurements, either to verify, or to lead to the models, respectively. On the other hand, the research works could be classified according to the textile structure under study. In this classification too, the acoustic evaluation measurements play a central role. Most of the publications use one of the widely accepted impedance tube methods for the involved acoustic evaluation.

Following the second classification scheme, one could identify four main categories corresponding to the study of: (a) raw materials in the form of fiber assemblies, (b) nonwoven fabrics, (c) woven fabrics, and (d) knitted fabrics. However, it should be noted that the majority of the published material deal with either nonwoven or knitted fabrics, mainly due to the associated lower production cost. The trend is to improve the acoustic performance of knitted fabrics and accordingly shift interest from nonwoven to knitted, which further provide a better aesthetic result.

In the case of *raw material* studies, the interest is focused on the comparison to standard porous fibrous absorbents like mineral wool and glass wool. The objective is usually to suggest eco-friendly (recyclable, biodegradable, natural) materials, not causing environmental pollution or danger for human health, with sound absorbing ability comparable to the one of the standard porous fibrous absorbents. (Ersoy and Küçük 2009; Yang et al. 2011).

Nonwoven fabrics are currently the most widely used textile materials in acoustic insulation products. This is due to their high total surface area, which is directly related to the denier and cross-sectional shape of the fiber. Nonwovens' fiber network structure provides enough degrees of freedom to permit acoustic design. Although they have only fibers and voids, which are filled by air, their structure is very complex. Voids, which are covered by fibers, are called pores in nonwoven structures and their size, number and shape is very important for the sound absorptive properties of nonwovens (Süvari and Ulcay 2011). The smaller the denier, the more fibers for the same material density, the higher the total fiber surface area is. This results to a higher chance for interaction between the sound wave and the fibers in the fabric structure. Another important parameter is the density of the nonwoven material, which affects the geometry and the volume of the voids in the structure. Ultra fine fibers enhance the mass per unit area, which contributes to an increase in the density and provides more chances for contact with the sound energy in the sound absorption nonwoven (Lee and Joo 2004). Moreover, web orientation, although marginally, is affecting sound absorption with unoriented web being more efficient (Lee and Joo 2003).
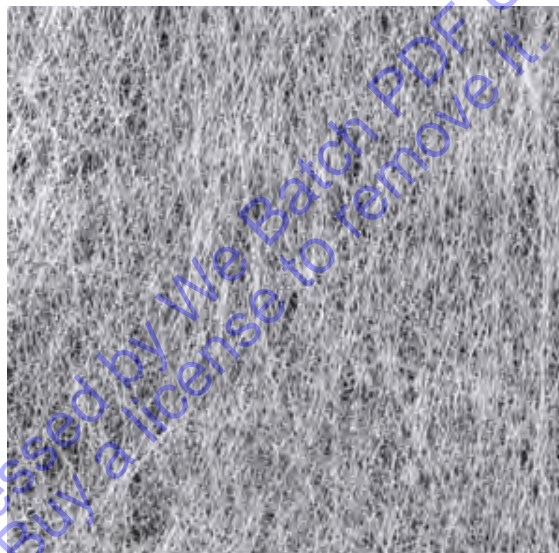
Fig. 4.10: Typical nonwoven fabric with sound absorption capability.

To a limit, the thicker a material, the more absorbent it becomes, particularly for low-frequency sounds (Rettinger 1968; Lee and Joo 2003; Na et al. 2007). Thinner materials, generally, require higher flow resistivity than thicker materials. One common method of increasing flow resistivity is the addition of a flow resistant scrim or film layer, which increases the air flow resistivity without adding too much weight or thickness. It is also possible to increase the flow resistivity by increasing the surface density of the material (adding density without changing the thickness); however, this method adds weight, which may be an issue in specific applications (Zent and Long 2007). Nevertheless, although the flow resistivity of a material may be increased to improve absorption at lower frequencies this is at the cost of lower absorption at higher frequencies (Lee and Joo 2003; Lee and Joo 2004; Zent and Long 2007).

Increasing the level of needle punching, using finer diameter or lower modulus fibers, and applying various coatings or sizing on nonwoven cellulosic composites improved their sound absorption (Parikh et al. 2001; Na et al. 2007). The surface roughness of nonwovens is also effective for increasing noise reduction performance. Roughness on the surface leads to resonance, and so appropriate roughness gives an increase in the sound absorption (Lee and Joo 2004). Nonwoven fabrics with a greater number of layers yielded higher noise absorption values (Rakshit et al. 1995; Shoshani 1990; Na et al. 2007). Heat-bonded materials are able to provide an equal sound absorption value at lower thickness than the needle-punched fabrics (Genis et al. 1990; Na et al. 2007). Acoustic barriers made of thermally bonded nonwovens can have several interesting applications, such as fillings inside walls separating neighboring apartments in wooden houses, noise shelters in the transfer industry, and acoustic enclosures for noise equipment in factories and workshops (Lee and Joo 2004).

An appropriate treatment, like carbonization, can also improve sound absorbing performance. For example, nonwoven composites with activated carbon fiber (ACF) nonwoven as a surface layer had significantly higher values of average transmission loss than glass fiber-surfaced composites above 600Hz (Chen and Jiang 2009). Furthermore, recent studies are considering the possibility of using natural fibers, like coir fibers, blends of bamboo, banana, and jute fibers with polypropylene (PP) staple fibers, or kenaf, waste cotton, and flax in blends with polypropylene and polyester (PET) as raw materials for nonwoven (Ayub et al. 2009; 2011; Thilagavathi et al. 2010; Parikh et al. 2006).

Concerning *woven fabrics*, the intrinsic parameters of the woven fabrics have a very little effect on their noise absorption coefficients in the low frequency domain ($f < 500 Hz$) but a significant impact at the higher examined frequency (e.g., $f > 2000 Hz$). It has been found (Shoshani and Rosenhouse 1990) that out of the intrinsic parameters examined, the cover factor had the most significant effect on sound absorption. The air gap behind the fabric has a very significant effect on the functional relations between absorption coefficient and the frequency (Shoshani and Rosenhouse 1990). The acoustic characteristics of woven hoses have been exploited in pipe noise reduction applications, like automotive intake systems, ventilation and air-handling systems (Dokumaci 2010). Interesting new ideas, like the construction of woven microperforated sound absorbers, have been possible since the introduction of woven three-dimensional fabrics (Onen and Caliskan 2010).
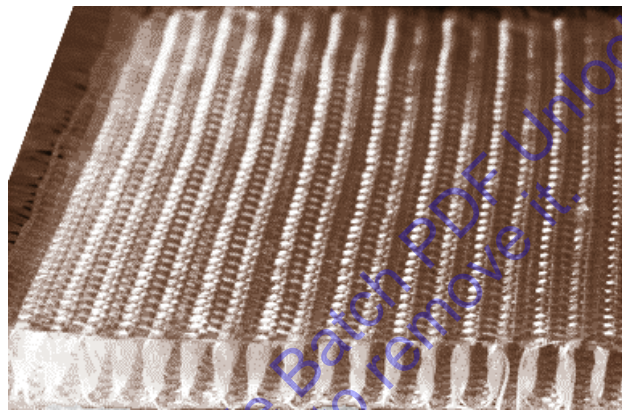
Fig. 4.11: Typical woven fabric with sound absorption capability.

Carpets, although usually referred to as a distinct category different from woven and knitted, could be seen as early three-dimensional woven fabrics. Carpets have been important sound-absorbing materials. Their effectiveness varies according to backing material, pile structure, yarn weight, pile thickness and underlay (Rossing and Fletcher 2003, pp. 256–270; Na et al. 2007). Pile characteristics including fiber content, pile density, pile height and air gap were reviewed with sound absorption of carpets (Shoshani and Wilding 1991; Na et al. 2007). The sound absorption of a carpet depends on its pile height, pile weight, type of backing material and whether the backing is coated with latex, loop or cut pile, and type and thickness of pad. Cut pile provides greater sound absorption than loop pile of otherwise identical construction. The type of pile fiber seems to has no significant effect on absorption (Na et al. 2007).

Nevertheless, the three-dimensional fabrics are mostly found in the form of *knitted spacer fabrics*, mainly due to their considerably lower cost compared to the corresponding woven fabrics. It has been shown that the fabric surface structure and thickness, spacer yarn type and their connecting ways, fabric combinations and their arrangement methods have significant effects on the sound absorbability (e.g., Öztürk et al. 2011). Sound absorption coefficient of fabrics increases with the increase in the number of miss stitches in knitted structure, because the total thickness of fabric increases. The results showed (Öztürk et al. 2010) that better noise absorption coefficient values can be achieved by using mini-jacquard knit instead of plain knit structure due to thicker face layer and consequently thicker spacer fabric. Besides, density has positive effect on sound absorption property of fabric. The sound absorbency of the fabric increases with the reduction in its porosity.
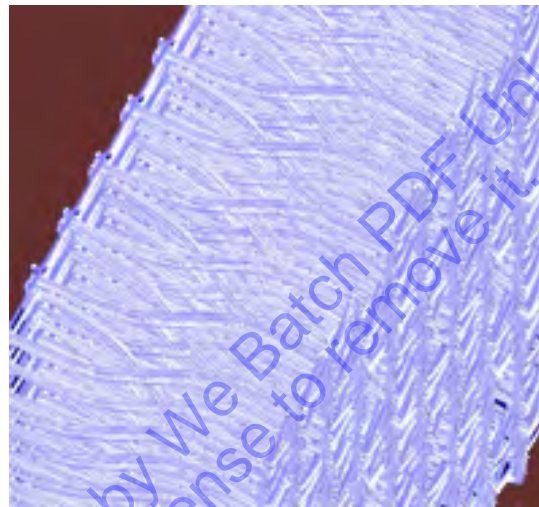
Fig. 4.12: Typical knitted spacer fabric with sound absorption capability.

The results also demonstrate that good sound absorbability could be achieved by using knitted spacer fabrics if suitable fabric structures and combinations are used. A recent research (Liu and Hu 2010) on several weft- and warp-knitted spacer fabrics yield interesting results. While the weft-knitted spacer fabrics exhibit the typical sound absorption behavior of porous absorber, the warp-knitted spacer fabrics exhibit the typical sound absorption behavior of microperforated panel absorber. The noise absorption coefficient increases with increase of the frequency for both kinds of fabrics. Both the weft-knitted and the warp-knitted spacer fabrics backed with the air-back cavity exhibit frequency-selected sound absorption with a resonance form. The sound absorbance can be improved by laminating different layers of fabrics. For the weft-knitted spacer fabric, the absorption increase by adding layers up to a number beyond which no more improvement is observed. However, for the warp knitted spacer fabrics, the absorption seems to continuously improve with increase of the fabric layers, but with a shift of the resonance region towards the lower frequency side. The combinations of weft-knitted and warp-knitted spacer fabrics can significantly improve their sound absorption, but their arrangement sequence has an obvious effect. At higher frequencies, the absorption coefficients of the warp-knitted spacer fabrics backed with weft knitted fabrics are much higher than those of the weft-knitted spacer fabrics backed with warp-knitted fabrics. However, at lower frequencies, the absorption of the warp-knitted spacer fabrics backed with weft-knitted fabrics is much lower than this of the warp-knitted spacer fabrics backed with weft-knitted fabrics. The air-back cavity can be replaced by multilayered warp-knitted spacer fabrics to achieve high absorption at low and middle frequencies.

Tuck spacer fabrics consists of top and bottom plain knitted layers. These two layers are interconnected with a mesh of yarn. This kind of fabric is a suitable alternative to utilizing several layers of plain knitted fabrics for achieving better sound absorbency. The sound absorption of these fabrics increases with both air flow resistivity and thickness. However, the effect of density is more predominant in terms of sound absorbency than thickness. The fabrics can be made denser by having more rows of the interconnecting yarn between a plain knitted course of the front and back beds (Dias et al. 2007a).

Another possibility investigated is that of thick knitted spacer fabrics. The results show better noise absorption when there is a thicker air gap between the front and back fabric layers of the spacer fabric and/or a thicker face layer. This type of a knitted structure is considered to be a promising material since it provides wide band sound absorption (Dias et al. 2007b).

Beyond knitted spacer fabrics, 2D knitted fabrics are also considered as a sound absorbent alternative, since their pros include, an aesthetic look and drapability compared with nonwovens. Therefore, if appropriately applied, they can supply a 3D seamless fabric with an attractive appearance (Honarvar et al. 2010). The sound absorption of plain knitted fabrics has recently been investigated (Dias and Monaragala 2006). It was found that knitted structures with smaller pore sizes (and a reduced porosity) with increased thickness, i.e. a thicker and denser knitted fabrics, have better sound absorbent properties (Dias and Monaragala 2006). Moreover, weft knitted fabrics produced in rib gating that is knitted on double jersey machines have also been studied (Honarvar et al. 2010). The samples with different numbers of knit and tuck stitches provide higher noise absorption than the samples with different numbers of knit and miss stitches (Honarvar et al. 2010).

Finally, a separate characteristic example is *microfiber fabrics*, which can be either woven or knitted. In any form, micro-fiber fabrics present an increased sound absorption because their fibers have a higher surface area than those of regular fiber fabrics, resulting in higher flow resistance (Na et al. 2007; Lee and Joo 2003).

4.7   References

Allard, J.F., 1993, *Propagation of Sound in Porous Media*, Elsevier Applied Science, London and New York.

ASTM C384-04(2011), 2011, *Standard Test Method for Impedance and Absorption of Acoustical Materials by Impedance Tube Method*, ASTM International, West Conshohocken, PA, USA.

ASTM E1050-10, 2010, *Standard Test Method for Impedance and Absorption of Acoustical Materials Using A Tube, Two Microphones and A Digital Frequency Analysis System*, ASTM International, West Conshohocken, PA, USA.

ASTM E2611-09, 2009, *Standard Test Method for Measurement of Normal Incidence Sound Transmission of Acoustical Materials Based on the Transfer Matrix Method*, ASTM International, West Conshohocken, PA, USA.

Ayub, M., Nor, M.J.M., Amin, N., Zulkifli, R., and Ismail, A.R. 2009, "A preliminary study of effect of air gap on sound absorption of natural coir fiber," in Proc. of the Regional Engineering Postgraduate Conference (EPC 2009), Putrajaya, Malaysia, 2009 October 20–21.

Ayub, M., Zulkifli, R., Fouladi, M.H., Amin, N.,and Nor, M.J.M., 2011, "A study on the acoustical absorption behavior of coir fiber using Miki model," Int. J. Mech. Mater. Eng. (IJMME), vol. 6 (3), pp. 343–349.

Barnard, A.R., and Rao, M.D., 2004, "Measurement of sound transmission loss using a modified four microphone impedance tube," in Proc. of the NOISE-CON 2004, Baltimore, Maryland, 2004 July 12–14.

Beranek, L., 1996, *Acoustics*, the Acoustical Society of America, American Institute of Physics, ISBN 10: 088318494X.

Chen, Y., and Jiang, N., 2009, "Carbonized and activated non-woven as high performance acoustic materials: part II noise insulation" Textile Res. J., vol. 79, pp. 213–218.

Cox, T.J., and D'Antonio, P., 2009, *Acoustic absorbers and diffusers: Theory, design and application*, 2nd Ed., Taylor & Francis, Abingdon, Oxfordshire, UK and New York, USA.

Dias, T., and Monaragala, R., 2006, "Sound absorbtion in knitted structures for interior noise reduction in automobiles," Meas. Sci. Technol., vol. 17, pp. 2499–2505.

Dias, T., Monaragala, R., Needham, P., and Lay, E., 2007a, "Analysis of sound absorption of tuck spacer fabrics to reduce automotive noise," Meas. Sci. Technol., vol. 18, pp. 2657–2666.

Dias, T., Monaragala, R., and Lay, E., 2007b, "Analysis of thick spacer fabrics to reduce automobile interior noise," Meas. Sci. Technol., vol. 18, pp. 1979–1991.

Dokumaci, E., 2010, "Sound transmission in pipes with porous walls," Journal of Sound and Vibration, vol. 329(25), pp. 5346–5355.

Dunlop, J.I., 1974, "Acoustic behaviour of carpets and fabrics", Journal of the Textile Institute, vol. 65(4), pp. 227–228.

Ersoy, S., and Küçük, H, 2009, "Investigation of industrial tea-leaf-fibre waste material for its sound absorption properties", Applied Acoustics, vol. 70, pp. 215–220.

Genis, A.V., Kostyleva, E. Yu., Andrianova, L.N., and Martem'yanov, V.A., 1990 "Comparative evaluation of acoustical properties of heat-bonded and needle-punched fibrous materials prepared from polymer melts," Fibre Chem., vol. 21(6), pp. 479.

Honarvar, M.G., Asgharian Jeddi, A.A., and Tehran, M.A., 2010, "Noise absorption modeling of rib knitted fabrics," Textile Res. J., vol. 80, pp. 1392–1404.

Ingard, K.U., 1994, *Notes on Sound Absorption Technology*, Noise Control Foundation, Poughkeepsie, NY.

ISO 10534-1:1996, 1996, *Acoustics – Determination of sound absorption coefficient and impedance in impedance tubes – Part 1: Method using standing wave ratio*, International Organization for Standardization, Geneva.

ISO 10534-2:1998, 1998, *Acoustics – determination of sound absorption coefficient and impedance in impedance tubes. Part 2: Transfer-function method*, International Organization for Standardization, Geneva.

Lee, Y.E., Joo, C.W., 2003, "Sound absorption properties of recycled polyester fibrous assembly absorbers", AUTEX Research Journal, vol. 3(2), pp. 78–84.

Lee, Y.E., Joo, C.W., 2004, "Sound äbsorption properties of thermally bonded nonwovens based on composing fibers and production parameters", Journal of Applied Polymer Science, vol. 92, pp. 2295–2302.

Liu, Y., and Hu H., 2010, "Sound absorption behavior of knitted spacer fabrics," Textile Res. J., vol. 80, pp. 1949–1957.

Muehleisen, R.T., 2007, "Measurement of the acoustic properties of acoustic absorbers," in Proc. Institute of Noise Control Engineering's Annual Conf. Noise-Con (Reno, NV USA).

Na, Y.-J., Lancaster, J., Casali, J, and Cho, G, 2007, "Sound absorption coefficients of micro-fiber fabrics by reverberation room method", Textile Res. J., vol. 77(5), pp. 330–335.

Nute, M.E., and Slater, K., 1973, "The effect of fabric parameters on sound- transmission loss", Journal of the Textile Institute, vol. 64(11), pp. 652–658.

Olivieri, O., Bolton, J.S., and Yoo, T., 2006, "Measurement of transmission loss of materials using a standing wave tube", in Proc. Inter-Noise 2006.

Onen, O., and Caliskan, M., 2010, "Design of a single layer micro-perforated sound absorber by finite element analysis," Applied Acoustics, vol. 71, pp. 79–85.

Öztürk, M.K., Negris, B., and Candan, C., 2011, "Development of a spacer knitted fabric for sound absorbent acoustic panel," in Proc. of the ICONTEX 2011, pp. 347–352.

Öztürk, M.K., Negris, B., and Candan, C., 2010, "A study on the influence of fabric structure on sound absorptiob behavior of spacer knitted structures," in Proc. of the 7th International Conference – TEXSCI 2010, September 6–8, Liberec, Czech Republic.

Parikh, D.V., Calamari, T.A., and Myatt, J.C., 2001, "Performance of nonwoven cellulosic composites for automotive interiors," in "IDEA 2001: The International Nonwovens Conference & Exposition, Your World Class Business Idea," Mar. 27–29, 2001, p. 5.

Parikh, D.V., Chen, Y., and Sun, L., 2006, "Reducing automotive interior noise with natural fiber nonwoven floor covering systems," Textile Res. J., vol 76(11), pp. 813–820.

Rakshit, A.K., Ghosh, S.K., and Thakare, V.B., 1995, "Optimization of blend of wool/polypropylene nonwoven fabric for sound absorption application," in "Proceedings of the 9th International Wool Textile Research Conference: Material Specification – New Products & Product Development," June 28–July 5, 1995, vol. 4, pp. 332–337.

Rettinger, M., 1968, *Acoustics: Room Design and Noise Control*, Chemical Publishing Co. Inc. New York.

Rossing, T.D., and Fletcher, N.H., 2003, *Principles of vibration and sound*, Springer, New York.

Seddeq, H.S., 2009, "Factors influencing acoustic performance of sound absorptive materials," Aust. J. Basic & Appl. Sci., vol. 3(4), pp. 4610–4617.

Shoshani, Y.Z., 1990, "Effect of nonwoven backing on the noise absorption capacity of tufted carpets," Textile Res. J., vol. 60(8), pp. 452.

Shoshani, Y., and Rosenhouse, G., 1990, "Noise absorption by woven fabrics," Applied Acoustics, vol. 30, pp. 321–333.

Shoshani, Y.Z., and Wilding, M.A., 1991, "Effect of pile parameters on the noise absorption capacity of tufted carpets," Textile Res. J., vol. 61(12), pp. 736.

Shoshani, Y., and Yakubov, Y., 2000, "Numerical assessment of maximal absorption coefficients for nonwoven fiberwebs", Applied Acoustics, vol. 59, pp. 77–87.

Slater, K., 1974, "Acoustic behaviour of carpets and fabrics – Reply", Journal of the Textile Institute, vol. 65(4), pp. 228–230.

Song, B.H., and Bolton, J.S., 2000, "A transfer-matrix approach for estimating the characteristic impedance and wave numbers of limp and rigid porous materials", J. Acoust. Soc. Am., vol. 107(3), pp. 1131–52.

Süvari, F., and Ulcay, Y., 2011, "Experimental investigation into sound absorptive properties of PET/PP high loft nonwovens", in Proc. of the ICONTEX 2011, pp. 368–373.

Thilagavathi, G., Pradeep, E., Kannaian, T., and Sasikala, L., 2010, "Development of natural fiber nonwovens for application as car interiors for noise control," J. Industr. Textiles, vol 39(3), pp. 267–278.

Yang, S, Yu, W, and Pan, N., 2011, "Investigation of the sound-absorbing behavior of fiber assemblies", Textile Res. J., vol. 0(00), pp. 1–10.

Zent, A., Long, J.T., 2007, "Automotive sound absorbing material survey results", SAE International, SAE Technical Paper 2007-01-2186, doi:10.4271/2007-01-2186.

Zwikker, C., and Kosten, C.W., 1949, *Sound Absorbing Materials*, Elsevier, Amsterdam.

5   Use of Digital Signal Processing in the textile field

by

Nicolas-Alexander Tatlas

Department of Electronics Engineering, Technological Education Institute of Piraeus, Greece

5.1   Introduction

Digital Signal Processing (often called DSP) has been rapidly evolving during the past years, covering a growing list of application domains, from factory automations to special effects in movies. The DSP wide adoption and use is mainly due to the development of microelectronic systems with greater computational power, smaller size, restricted power requirements and decreasing cost. The ever-increasing capabilities of hardware allow complex algorithms to be executed in real time even on mobile smart-phone type devices. The aim of this chapter is to provide the reader with an insight on basic principles, algorithms and techniques of signals, digitization and digital processing as well as its use in the area of textile production.

5.2   Signals and Digitization

A signal is defined as any physical quantity that varies with time, space or any other independed variables. In other words, a signal is a sequence or function depending on one or more variable, containing information about the property. Examples of everyday signals are speech, as a function of sound pressure over time, the natural light deviation, as a function of sun illumination over time or the decrease in temperature when climbing a mountain as a function of temperature over height.

(a)   (b)
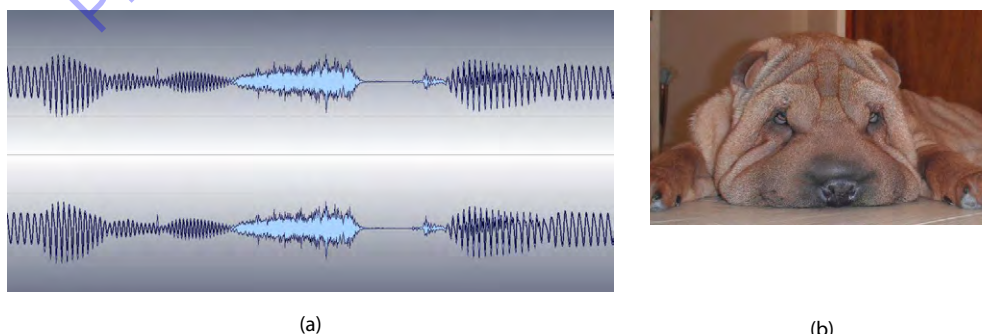
Figure 5.1: (a) One-dimensional signal (sound) (b) Two-dimensional signal (image).

Signals can be divided in different categories depending on the number and type of their variables. Depending on the number of independent variables signals can be of one dimension (one variable), two dimensions (two variables) and so on. An example of a one dimensional signal is music, where the one independent variable is time and the depended variable is sound pressure. A black-and-white picture is a typical example of a two dimensional signal, where the depended variable is luminance and the independent variables are X and Y coordinates of the picture. Figure 5.1 shows an example of a one dimensional and a two dimensional signal.

If the independent variable is continuous the signal is called a continuous signal whilst if the independent variable is discrete the signal is called a discrete signal. Usually the independent variable is time, so the classification is between continuous-time or analogue signals that are defined for every time value and discrete-time signals that are defined only at certain time values. The process of converting a continuous-time signal to a discrete-time signal is *sampling.* Figure 5.2 shows an example of a continuous and a discrete time version of the same sine-wave signal, where T_s is the sampling period, inversely proportional to the sampling frequency f_s.
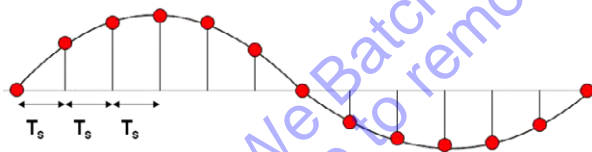
Figure 5.2: Continuous (black line) and discrete (red dots) time sine-wave signal.

According to Nyquist-Shannon sampling theorem, in order to accurately describe the original signal, the sampling frequency of the discrete signal must be at least twice the maximum frequency (f_{max}) contained in the continuous-time signal.

$$f_s \geq f_{max}$$ (Eq. 5.1)

Moreover, the actual values of a signal can be continuous, taking any possible values or discrete, taking values from a predetermined set. The conversion of a continuous to a discrete value signal is performed through quantization of the original values; this is done through some kind of approximation, such as truncation. Figure 5.3 shows a continuous (black line) and discrete (red line) value signal. The quantized signal in this example can have one of eight allowable values, while the continuous signal can have any permissible value. The distance between two consecutive discrete values is defined as the quantization step and is usually represented as Δ.

Figure 5.3: Continuous (black line) and discrete (red line) value sine-wave signal.

The error introduced by mapping continuous valued signals through a finite set of discrete values is called quantization error or quantization noise. The process of quantizing an analogue signal leads to information loss, because of the fuzziness introduced. Any sample that lies in an area $\Delta/2$ around a permissible quantization level is represented by the same value; the quantization error is generally a characteristic of the number of quantization levels L_q.

The final step of the quantization process in order to obtain a digital signal in the sample coding, where a unique binary number is assigned to every quantization level. Given that a binary word of length N can describe 2^N numbers, the number of coding bits N must satisfy the following Eq.:

$$2^N \geq L \tag{Eq. 5.2}$$

For example, the quantization process shown in Figure 5.3 can be coded using 3 bits describing 8 values. An approximation of the signal-to-noise ratio for a sine wave quantized signal depending on the sample bit depth is given by:

$$SNR = 6N + 1.76 dB \tag{Eq. 5.3}$$

Audio in music CDs is digitized with f_s=44,1KHz and N=16bits per sample. The sampling rate and bit depth selection is a trade-off between the signals accurate representation and the requirement for increased storage and processing, as explained in the following chapters.

5.3 Signal processing basics

Signal processing may refer to the analysis, or modification or other operation on a signal usually in order to extract information, such as a property. For example, the average luminance signal can be extracted from the images sensor of a digital camera and evaluated in order to decide if a flash light is necessary and determine its properties. Another example is the volume adjustment on any mobile phone: The incoming voice signal is either amplified or attenuated in order to meet the user requirements. Both the above examples have a common element, a device that is responsible for the processing: In DSP context, a *system* may be defined as the apparatus to perform any operation on a signal. The system may be mechanical, electrical, microelectronic or even software running on a computer. *Digital signal processing* refers to processing on digital signals, i.e. discrete time and discrete value signals performed by a digital system, realized in hardware or in software.

5.3.1 Digital vs Analogue Signal Processing

Electronic analogue signal processing was employed for decades, using circuit elements such as resistors, capacitors, diodes, transistors etc. The ability of analogue systems to provide functions such as derivatives, integrals as well as to solve differential equations was exploited in such systems. On the contrary, digital signal processing relies on numerical calculation. There are numerous of advantages in using DSP, such as:

(i) A digital processing system is extremely flexible. A software modification can radically change its operation. An analogue system would likely require to be redesigned.

(ii) The accuracy of a digital system is far greater. Even a slight tolerance on circuit elements induces an uncertainty towards the system precision, while digital systems accuracy is defined in a straightforward manner. Moreover, circuit element tolerance may be time-varying because of temperature fluctuations or aging.

(iii) Digital Signals can be stored and copied in magnetic, optical or solid state media without the possibility of degradation, offering the possibility of non-real time processing.

(iv) Complex processing algorithms requiring extremely high numerical precision may be realized in software.

(v) Usually the digital processing of a signal is cost-effective compared to the analogue processing, because of the decreasing prices of hardware and the restricted development effort required.

Of course, there are boundaries in digital signal processing, set by the restrictions in analogue-to-digital converter operating frequencies as well as the digital processors instruction speed capabilities. Thus, high bandwidth signals such as satellite television signals are usually pre-processed in the analogue domain.

5.3.2   Basic DSP system

Figure 5.4 shows a typical block diagram for a DSP system. As all natural signals are analogue, usually such a systems first part is an analogue to digital (A/D) converter, including a sampling and a quantization stage, as previously explained. The A/D output is a digital signal adequately describing the original signal attributes and appropriate as input to the Digital Processing stage. The processing can be performed using (a) Application specific hardware systems, or (b) Digital Signal Processor-based systems or (c) Generic computer systems, as well as systems that combine the above.
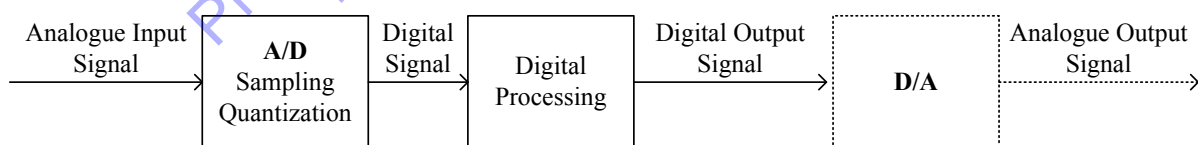
Figure 5.4: DSP system block diagram.

A hardwired implementation may be optimized resulting in lower costs and increased computational efficiency. On the other hand a software-based implementation usually requires less development time and is easily reconfigurable. Some applications require the output of the processing system to be given in an analogue form, such as audio signals, requiring an additional stage, that of a Digital to Analogue converter. However, in most cases this is not required, such as image processing where both static images and video are digitally captured.

5.4　　　Discrete Time Signals & Systems

It is obvious that DSP systems operate on discrete and quantized signals. In order to proceed, a short introduction on basic concepts regarding discrete signals and systems is presented in this paragraph. The following discrete signals are considered elementary:

a) Unit impulse sequence

$$\delta[n] = \begin{cases} 1, n = 0 \\ 0, n \neq 0 \end{cases} \tag{Eq. 5.4}$$

b) Unit step sequence

$$u[n] = \begin{cases} 1, n \geq 0 \\ 0, n < 0 \end{cases} \tag{Eq. 5.5}$$

c) Constant sequence

$$x[n] = A \tag{Eq. 5.6}$$

d) Linear sequence

$$x[n] = An \tag{Eq. 5.7}$$

e) Exponential sequence

$$x[n] = A^n \tag{Eq. 5.8}$$
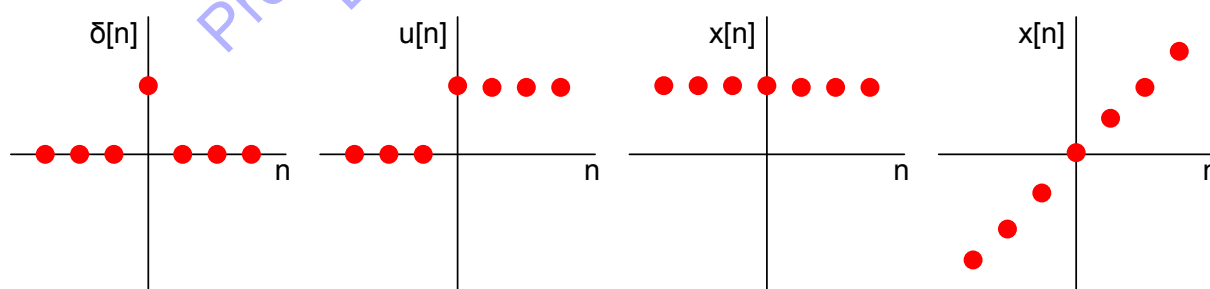
Figure 5.5: Elementary signals, (a) unit impulse, (b) unit step (c) constant and (d) linear sequences.

5.4.1   Basic Functions

Transformation of the independent variable

A signal s[n] may be time shifted by replacing the independent variable n with n-k. If k is positive a delay is introduced, while if negative the signal is advanced in time. Note that only a previously stored signal can be advanced in time. For example, a delayed unit step sequence would be:

$$u[n-k] = \begin{cases} 1, n \geq k \\ 0, n < k \end{cases} \qquad \text{(Eq. 5.9)}$$
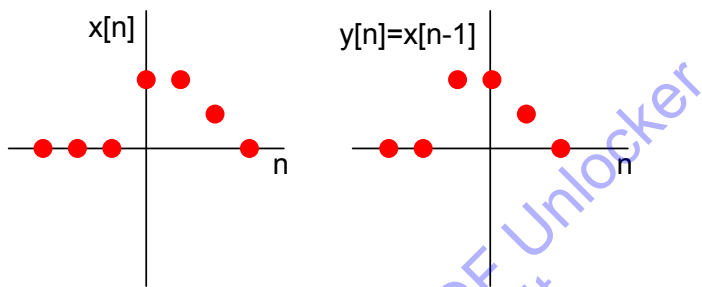
Figure 5.6: Example of signal delay.

Any discrete signal can be written as a sum of gain-adjusted and time-shifted impulse signals:

$$y[n] = \sum_{k=-\infty}^{+\infty} x(k)\,\delta[n-k] \qquad \text{(Eq. 5.10)}$$

Addition, multiplication and scaling

Amplitude scaling, meaning attenuation or amplification of signal by a constant is accomplished by multiplying every sample with that constant:

$$y[n] = Ax[n]$$ (Eq. 5.11)

The sum of two signals is given by the sums of their values sample-by-sample:

$$y[n] = x_1[n] + x_2[n]$$ (Eq. 5.12)

For example, mixing two different audio signals requires their addition according to the following equation. If the gain needs to be adjusted then each signal is first multiplied, then both are added.

Finally, the product of two signals is given by the product of their values sample-by-sample:

$$y[n] = x_1[n]x_2[n]$$ (Eq. 5.13)

5.4.2   Discrete-time systems

A discrete-time system is a system that accepts as input and produces according to a well defined set of rules as output discrete signals x[n] and y[n] respectively. The systems that are analyzed in this chapter have two fundamental features: they are Linear and Time-Invariant, and are thus named LTI systems. A *linear* system satisfies the superposition principle, meaning that the output of a system to a sum of signals is equal to the sum of the outputs for each individual signal, given that the signal is in a relaxed state. *Time-invariant* is a system whose behavior and properties remain constant over time.

Moreover, a system is *causal* if its output at any instance is a function only of the present and past inputs, thus does not depend on future inputs. Finally a system is *stable* if and only if every bounded input produces a bounded output.

If a LTI system in a relaxed state is stimulated with a unit impulse signal, its output characterizes the system; this output is the system *impulse response* h[n]. Given the impulse response of a LTI system, its output y[n] for any input x[n] is found through the convolution operation, symbolized as "*":

$$y[n] = h[n] * x[n]$$ (Eq. 5.14)

Given that a signal can be expressed as the sum of time shifted impulse signals, and that we are dealing with LTI systems, the previous equation can be also written as:

$$y[n] = \sum_{k=-\infty}^{+\infty} x(k)\, h[n-k]$$ (Eq. 5.15)

which is the description of linear convolution. Note that if K_1 is the length of one sequence and K_2 the length of a second sequence, the result of their convolution is of K_1+K_2-1 length.

5.4.3 Discrete-time system structures

The duration of the impulse response leads to two categories of LTI systems: an impulse that has a finite number of non-zero samples characterizes a Finite Impulse Response or FIR system; otherwise, the impulse belongs to an Infinite Impulse Response or IIR system. It is evident that the computation of the convolution of a signal with an infinite impulse requires an infinite number of operations. However, IIR systems can be practically implemented, using previous output values or recursive implementations.

5.4.4 Implementation of discrete-time systems

The implementation of discrete-time systems requires two block categories, (a) arithmetic units to perform basic calculations such as Eq. 5.11–Eq. 5.13, and (b) memory in order to store values, such as needed to implement Eq. 5.9. The usually employed blocks are four basic discrete-time systems shown in Figure 5.7. If the output of a system depends only on the input at the same instance, the system is called memoryless; otherwise it is called dynamic. However, the concept of memoryless systems should not be confused with the requirement for memory in an implementation, as memory is usually necessary to store intermediate values during any processing.
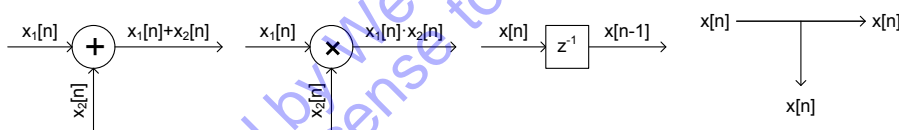
Figure 5.7: Basic implementation blocks (a) adder (b) multiplier (c) delay (d) splitter.

Block diagrams are commonly used for the implementation representation of discrete-time systems, used both for hardware and software implementation.

5.4.5   Frequency analysis

Analysis in the frequency domain of discreet time signals and systems provides an alternative regarding their design and implementation. In order to map a time series to a frequency domain series, a transition from the time to the frequency domain is needed. Periodical continuous signals can be analyzed in a series of sinusoidal signals (Fourier Series) or using other terms in an infinite number of discrete frequency spectrum components. If the signal is non -periodical, the expansions concept in the frequency domain is generalized and the Fourier Series is substituted by the Fourier Transform resulting in a continuous frequency spectrum. The Fourier Transform and the Inverse Fourier Transform are powerful tools, allowing the transition between the time domain and the frequency domain, without loss of the signal's information content. Especially when the signal is periodical and discrete the frequency spectrum is also periodical and discrete. In that case the transition is obtained by the Discrete Fourier Transform (DFT). The DFT for a finite sequence x[n] is given by:

$$X[k] = \sum_{n=0}^{N-1} x[n] e^{\frac{-j2\pi kn}{N}}, k = 0,1 \ldots, N-1 \tag{Eq. 5.16}$$

The inverse operation, or IDFT is given by:

$$x[n] = \frac{1}{N} \sum_{k=0}^{N-1} X[k] e^{\frac{j2\pi kn}{N}}, n = 0,1 \ldots, N-1 \tag{Eq. 5.17}$$

Direct computation of the N-point DFT requires computational cost proportional to N^2. The most important class of efficient DFT algorithms, known as the Fast Fourier Transform (FFT) algorithms, provide all DFT coefficients with a computational cost proportional to $N\log_2 N$.

5.5   Digital Image Processing

As mentioned in the introduction of this chapter, a digital image is two-dimensional signal. A black and white image can be expressed as a function of the luminosity for each x,y coordinate.

$$Luminosity = f(x,y)$$
(Eq. 5.18)

What is commonly named a "black and white" image is actually a grayscale image, having a number of different luminosity values. Larger values usually correspond to whiter areas whereas smaller values indicate darker parts of the image. Figure 5.8 shows the luminosity signal for the image in Figure 5.1(b). For example, the white spot from the flash reflection on the left part of the image is manifested as a peak in luminosity values.
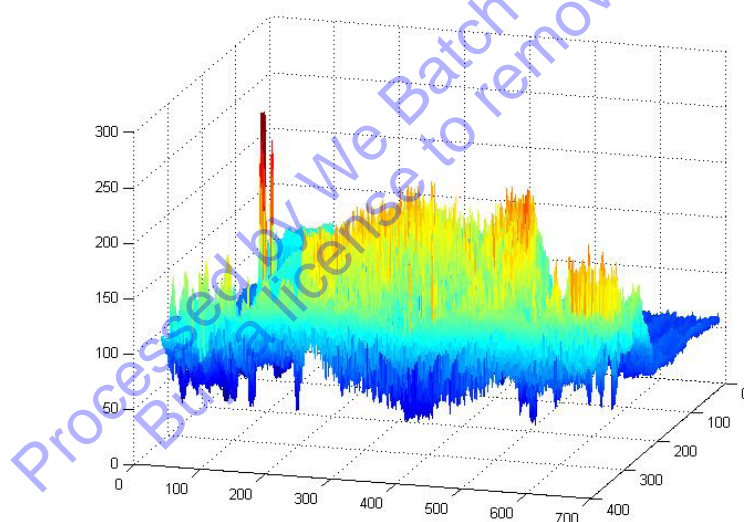
Figure 5.8: Luminosity representation.

The image digitization process does not differ from what was described for one dimensional signals. Equally distanced samples in the x,y space are obtained with the maximum distance of two sequential samples needs to be less than half the period of the faster changes in f(x,y). The samples are then quantized and coded, usually with N=8bits. The digital image samples are called picture elements or "pixels". Color images are represented in the same way; however three values are coded for each pixel, corresponding to the "amount" of each basic color, Red, Green and Blue.

An image that is of length N_1 and width N_2 contains $N_1 N_2$ pixels. The total space S (or memory) needed to store a color image is given by the following Eq:

$$S = 3NN_1N_2 (bits)$$
(Eq. 5.19)

It is obvious that increasing the resolution or bits per pixel allocation in an image (a) requires more space and (b) requires greater computational effort to process.

A number of stages are generally included in order to process a digital image, depending on the format and condition of the original picture as well as the required output. Figure 5.9 shows a general block diagram for an image dsp system. The digital image is captured or digitized from its analogue form in the acquisition stage. Depending on the image state, noise reduction or other algorithms to invert possible distortions are employed. The optimized picture is analyzed depending on the systems goal, such as to extract specific features from an image, such as boundary position, or to recognize objects, such as automobiles. Image compression in order to save storage space or increase transmission speed may be employed as a final stage.
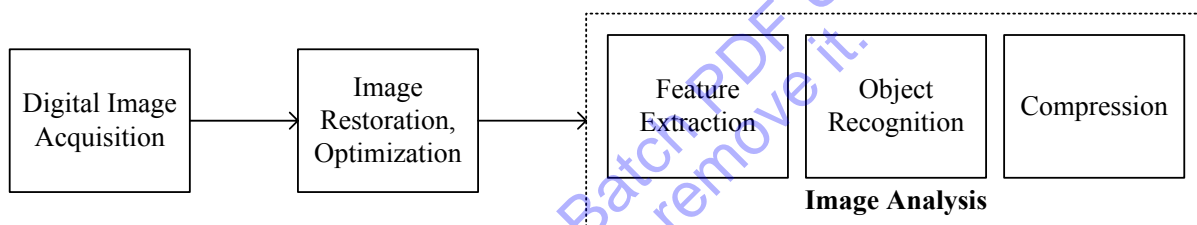
Figure 5.9: Image DSP general block diagram.

5.5.1 Image processing functions

An image processing stage may have as input or output either an image or a mathematical description. For example, any image compression software receives an image and outputs another image, while a Computer Aided Design (CAD) package is given coordinates and directives and outputs an image. The following analysis on image processing applies to algorithms that have both as input and output images. Functions in digital image processing provide values for output pixels based on the input pixels. Depending on the algorithm employed, these functions may be (a) Local, (b) Global and (c) Geometrical.

Local functions calculate the value of each output pixel with coordinates [n1,n2] using the value from the input image with the same coordinates as well as neighboring values. A neighborhood in an image is an area, usually a square of fixed size, centered on a pixel. A common local function is averaging where each pixel is results from an average of the input neighborhood pixel values. If the neighborhood of each pixel in the original image is not taken into account then the function is called a *point operation*. For example, point operations are Contrast adjustment, performed by multiplying each pixel value with a constant and Luminosity adjustment, performed by adding (or subtracting) each pixel value with a constant. Figure 5.10 shows an example for averaging, using a 9×9 neighborhood, contrast stretching using a constant of 3 and luminosity increase using a constant of 70.

(a)   (b)   (c)
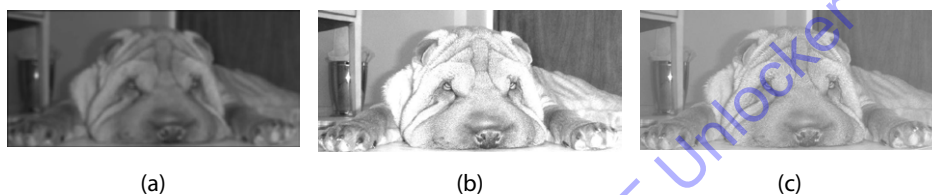
Figure 5.10: (a) Averaging (b) Contrast and (c) Luminosity adjustment.

Global functions utilize values from the whole original image to calculate each pixel value. These are usually transformation functions or adjustments, requiring for example knowledge of the maximum or minimum value encountered in the original image.

Geometrical functions apply to coordinate modifications, such as relocation, rotation and mirroring. These functions usually provide images of the same area with their original pixel values not altered, but moved to other positions.

5.6   DSP in textile quality control

A widespread use of DSP systems in textile production is that of quality control of woven fabric. The aim is to detect defects during the process. Generally, there are two types of defects in textiles, (a) structural, usually caused from faults during the weaving process and (b) tonal defects based on the presence of pollutants or a temporary error in the coloring process. However, a number of other defects can present, adding complexity to the detection procedure.

The general architecture for an automatic textile quality control setup in shown in Figure 5.11, including a digital camera and a motor/position sensor for the fabric conveyer connected through appropriate interfaces to a computer, running software for image acquisition and processing.
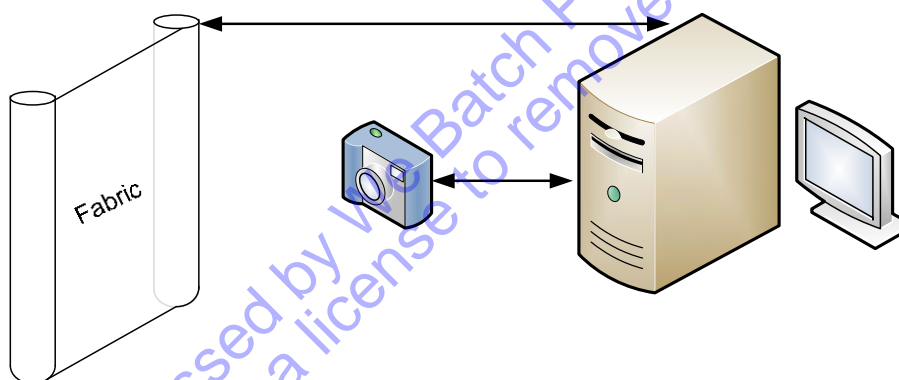
Figure 5.11: Automatic textile quality control system.

The fabric under examination is positioned between two axles adequately spaced to appropriately position part of the material for the digital camera to capture its image. The position of the fabric is controlled through the PC in order to synchronize each image obtained; a series of images is then automatically merged providing a digitized segment of the fabric for further processing. Upon the detection of a fault, an error message is created usually including a snapshot of the defect as well as the corresponding position of the axles.

Generally, there are two stages for operating such a processing system, (a) the training phase and (b) the recognition phase. During the training phase, the system is operated using a flawless fabric, in order to use the obtained images as reference. These images are first pre-processed with DSP algorithms that ensure distortion suppression, such as uneven brightness or contrast, following the extraction of specific textile features such as the color distribution, fiber unity etc. The same pre-processing and feature extraction stages are applied in normal operation; the system detects errors by comparing these features to the flawless set from the training phase. The challenge while operating such a system is (a) to select appropriate texture analysis features correlated to the detection of specific flaws (b) to fine-tune the process by introducing thresholds in order to minimize false positive events and maximize the detection capability.

The leading approaches to texture analysis are statistical and structural methods based on spatial frequencies. Statistical approaches are based on the analysis and characterization of patterns observed using statistical features, providing an overall features. The placement of textural sub-patterns, according to rules form the texture is the basis for structural methods, giving a detailed description of the surface under test. Moreover, the detection of flaws in texture images can be performed in two fundamental ways: The first is block-based processing method, where each block is compared to an error-free sample, as mentioned earlier. The second is to employ metrics based on whole images, requiring though a reference for every possible fault.

There are numerous specific techniques and algorithms that have been tested or are being employed in such systems, such as the Spatial Grey Level Co-occurrence (SGLC) and Cross correlation. The SGLC method utilizes matrices based on the second order probability for two pixels of different gray levels of given displacement to appear in an image. The method implementation requires the computation of the optimal image displacement vectors in terms of flaw detection capability, deeming it susceptible to errors from alignment mismatch of dimensional changes. Cross-correlation as a metric of similarity provides a clear way of detecting differences between the reference and inspected image, indicating a flaw. While computational intensive, in theory cross-correlation may detect any possible fabric defect as long as the test conditions are constant and/or pre-processing equalization stages are implemented. The reader is referred to (Bennamoun & Bodnarova, 2003) and (Kosek. 2005) for more information on detection methods as well as their efficacy and robustness.

5.7   References

J. Proakis & D. Manolakis, 1996, "Digital Signal Processing Principles, Algorithms and Applications", 3[d] edition Prentice Hall International, INC.

A.N. Skodras & B. Anastasopoulos, 2000, "Introduction to Digital Signal and Image Processing", University of Patras (in Greek).

D. Manolakis & V. Ingle, 2011, "Applied Digital Signal Processing", Cambridge University Press.

M. Bennamoun & A. Bodnarova, 2003, "Digital image processing techniques for automatic textile quality control", Systems Analysis Modelling Simulation, 43:11, 1581–1614.

Miloslav Kosek. 2005, "Efficient application of signal processing methods in textile science". Proceedings of the 4th WSEAS international conference on Applications of electrical engineering (AEE'05), p. 155–159.

6 RF Measurements and Characterization of Conductive Textile Materials

by

N. Stathopoulos, S. Savaidis and S. Mitilineos

Department of Electronics Engineering, TEI of Piraeus, Greece

6.1 Introduction

Conductive textile materials have been of great interest during the last decades, mainly due to their applications in the fields of human safety and health monitoring. Most of these applications are related in one way or another with sensor technology, where conductive textile materials are used in a wide range of low-power, low-frequency electronic applications. However, high frequency applications have also been proposed recently, mainly in the field of electrotextile wearable antennas (P.J. Soh, 2011) (Y.J. Ouyang, 2008). Wearable antennas could be useful for applications like life-jackets and RFID passive tags, although they have strong competition from the wearable, flexible metallic structures. Other applications, like electromagnetic shielding, have been successfully applied for the protection of human health from hazardous electromagnetic radiation.

Recently there have been efforts to evaluate the available conductive textile materials as well as to study their properties in high frequencies (D. Cottet, 2003) (Y.J. Ouyang a. W., 2007). It is critical here to recognize all the basic obstacles when using conductive textile materials in high frequencies. Specifically, all high frequency devices are very sensitive to the following properties: -dimensions, -geometry, -conductivity, -symmetry, -dielectric characteristics. Unfortunately, it is difficult for textiles to have inherently the appropriate properties and therefore be suitable for an HF application. On the other hand, how high could the frequency be in order to be used in conductive textiles effectively? Before we answer this question we have to discuss the influence of the frequency range on the operation of a device.

Actually for frequencies right above 1MHz, the influence of parasitic capacitance and the coupling between inductive elements is evident, while these influences become stronger as the frequency increases. Up to a few hundreds of MHz, passive elements like inductors and capacitors are discrete and can be connected to a circuit configuration as individual components. However, all parasitic and couplings should be taken into account, in order to keep the device within its specifications. The use of metallic shields is a very common technique in order to avoid undesired couplings in this range of frequencies. Furthermore, for frequencies higher than 1GHz, the pc-board with its track for component connections, acts as a part of the circuit and its material should have suitable dielectric characteristics in order to keep the device in operation.

Since the RF and microwave (MW) spectrum covers almost all frequencies, from a few hundreds KHz up to hundreds of GHz, the electro-textile materials herein are going to be tested and characterized only for the lower range of the RF spectrum (VHF and UHF range of frequencies). Practically, this will cover frequencies up to 3 GHz which means that the equivalent wavelength will not be less than 10 cm. In this range, the dimensions of textiles in use will be large enough for the tests.

Recently, a thorough work on electrotextile measurements for HF applications has been presented by Ouyang and Chappell (Y.J. Ouyang, 2008). Therein, the materials under test act as coupling components between two high frequency cavities. The shielding properties of conductive textiles are measured through the coupling power from one cavity to the other, while the tests have also been extended to microstrip resonators. A rather similar method has been described and applied within this chapter, but the textile material acts as a resonator itself in conduction with a copper microstrip transmission line. Although an extensive characterization method for textile transmission lines has also presented by Cottet et al. (D. Cottet, 2003), they focus on the transmission lines parameters, rather than a macroscopic study of their ability to conserve electromagnetic energy at a resonance frequency.

On top of the above, textile antennas have been introduced in order to integrate multiple transceiver components on textile substrates for HF frequencies applications and above. Textile antennas may consist of metallic plates over fabric substrate, but recently antennas fabricated with solely textile materials have been also introduced. The development of textile antennas can be traced back to the beginning of the new millennium, when wearable antennas partially based on textiles were first presented. Nowadays, textile antennas are considered a novel technology, but having already come up with certain design examples and constructions in several frequency bands. The respective research field is very active and ongoing research includes new materials and techniques for robustness, durability and credibility of designs.

The scope of this chapter is to present transmission lines and patch antennas layouts for (i) the evaluation of electrotextile materials in HF applications and (ii) the evaluation of electrotextile patch antennas in HF, RF and MW applications. The relative objectives are on the one hand the analysis of T-resonator devices and the experimental setups and measurements, and on the other hand the achieved VSWR, radiation pattern and gain of the antenna respectively. The chapter is organized as follows: In section 6.2, an elementary theory of transmission lines is roughly presented. This section has been considered necessary for the reader, in order to familiarize himself with the basic transmission line terminology. In section 6.3, a thorough presentation of coaxial T resonator and the relative measurements are presented, while in section 6.4 its microstrip version is presented. Section 6.5 includes a short introduction to antenna theory and microstrip antennas in order to familiarize the reader with the respective concepts, while in Section 6.6 early measurements results of textile antennas available in the literature are presented. The chapter concludes with Section 6.7.

6.2 Elementary transmission lines theory

6.2.1 Introduction

A transmission line is a system of conductors that is able to transfer electric power from a source to a load (this definition applies to any frequency range; minimum loss of power over the line is implied but not necessary). A typical application of transmission lines is that of the electric power distribution system where, the energy source is at a low frequency (eg 50 or 60Hz, without excluding the zero frequency). In this case we refer to the transmission of electrical energy produced by large or medium-sized production units, for distribution to residential and industrial consumers.

However, in many other applications, e.g. in telecommunications, the transmission of the electric power is carried out at high frequencies and the source should drive a load (e.g. an antenna) through a transmission line that has the form of a metallic rectangular waveguide i.e. quite different than the two parallel cables of the transmission lines in low frequencies. Moreover, at high frequencies, the transmission lines can be used in applications where their purpose in not to transfer energy from the source to a load. In these cases we exploit the distributed electrical characteristics of lines (distributed inductance and capacitance) to construct passive circuits that can not be constructed using discrete components.

Parallel conductors

Dielectric material
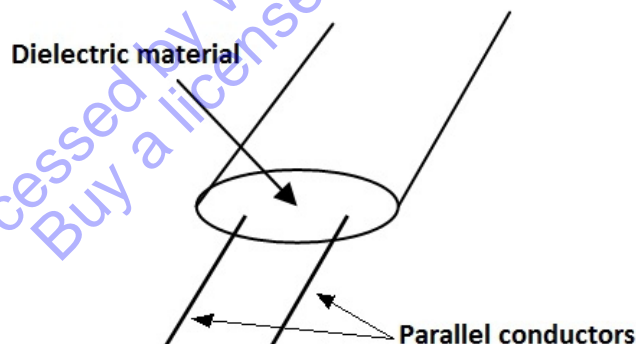
Figure 6.1: A cable of two parallel conductors.

The form of transmission lines used at high frequency applications (i.e. RF and MW), depends mainly on the operating frequency and can be categorized into the following cases:

- Cables with two parallel wires: They consist of two parallel cylindrical conductors at a specific distance between them, bounded by a low loss dielectric material. They have been used in the past for TV applications (receiver-antenna cable) in the VHF frequency range (Figure 6.1).

- Telephone and data transfer lines: These lines consist of twisted pairs of insulated conductors (Figure 6.2). By twisting the conductors we avoid electromagnetic interference and noise effects from the environment and thus support reliable data transmission in local computer networks (like e.g. Ethernet, wherein each cable contains 4 twisted pairs of conductors). The twisted pairs of cables are placed inside an insulating cylindrical shell which may contain an internal metal cover to shield from external interference. These cables are transmission lines capable of carrying high frequency data signals (typically up to 100MHz) at distances of up to 100m.
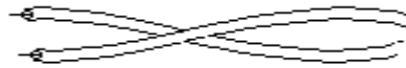
Figure 6.2: Twisted pair telephone cable.

- Coaxial cables for high frequencies: These cables (Figure 6.3) are used in a wide range of applications such as broadcasting of television signals between antenna and receiver, transmission of high-speed data (Ethernet) and many other applications that reach microwave frequencies. The basic type of coaxial cable used in practice is the RG type. For the purposes of Greek domestic TV cable, the RG-58 / U type is commonly used, while for Ethernet applications the RG-8 / U has been used.
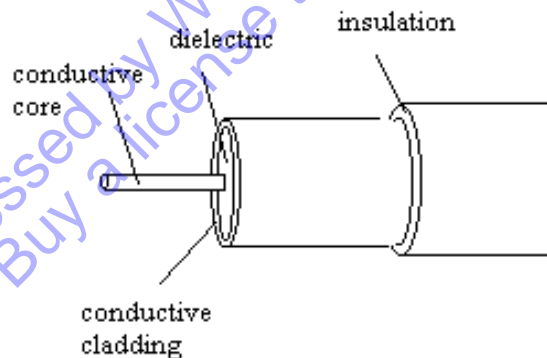
Figure 6.3: Coaxial cable.

- Microstrip lines (Figure 6.4): They are used for the connectivity and implementation of microwave passive networks that are going to be implemented on a pc-board that is made by high frequency, low-loss dielectric materials. With short or open termination, they are used as equivalent inductors or capacitors, while by using their self resonance characteristics they are applied as high frequency resonators. The pc-board dielectric materials are of great importance due to their low losses at high frequencies. For this reason the most common substrate materials in use are mainly Teflon-based.
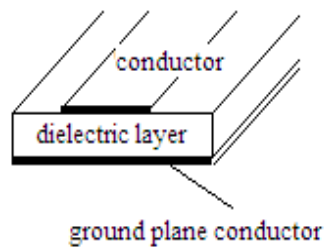
Figure 6.4: Microstrip transmission line.

- Metallic orthogonal waveguides (Figure 6.5): They are used in the microwave range of frequencies and their typical application is for the transfer of power from the high power transmitter to a high power antenna (e.g. a horn antenna). Their use also covers all the applications that are mentioned for the microstrip lines.
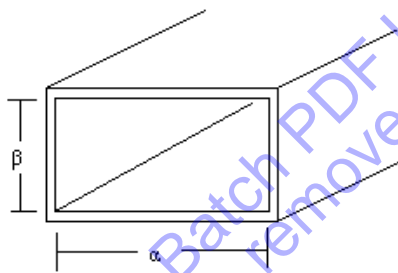

Figure 6.5: Microwave metallic orthogonal waveguide.

6.2.2   Transmission lines characteristics – distributed elements

A transmission line is characterized by four electrical parameters which reflect the behaviour at the steady state, provided that the construction is uniform throughout its length. These parameters are:

- Distributed inductance in series, that is expressed in H/m
- Distributed shunt capacitance in F/m
- Distributed ohmic resistance in series, that is expressed in Ω/m
- Distributed shunt conductivity, that is expressed in mho/m

The transmission lines' distributed elements can be approximately calculated for the aforementioned types of lines. Particularly, for the two parallel wires and coaxial cables, the following formulas for the distributed inductance could be used respectively:

$$L_{//} = \frac{\mu_0 \mu_r}{2\pi} \ln \frac{D^2}{r_1 r_2} \quad \text{in (H/m)},$$

where D is the distance between the parallel conductors and $r_1 r_2$ their radii.

$$L_{coaxial} = \frac{\mu_0 \mu_r}{2\pi} \ln \frac{D}{d} \quad \text{in (H/m)},$$

where D is the outer conductor diameter and d the core conductor thickness.

Furthermore, their distributed capacitance can be respectively calculated by the following approximate formulas:

$$C_{//} = \frac{2\pi\varepsilon}{\ln\left(\dfrac{D^2}{r_1 r_2}\right)} \quad \text{in (F/m)} \quad \text{and} \quad C_{coaxial} = \frac{2\pi\varepsilon}{\ln\left(\dfrac{D}{d}\right)} \quad \text{in (F/m)} \quad ,$$

where ε is the dielectric constant of the dielectric material.

The distributed ohmic loss across the line is a significant parameter that determines the power attenuation along the line. Although it is well known that the ohmic resistance of a conductor depends on its length, its cross section and its specific resistance, at high frequencies, the skin effect should be considered as a stronger contributor to ohmic losses.

6.2.3 Telegragh equations – Characteristic impedance and transmission constant

Using the distributed parameters of a transmission line, as they are described in section 2.2, we can simulate an elementary length Δx of the line through discrete elements at a distance x from the source, as it is illustrated in Figure 6.6. In this circuit R, L, C and G are the distributed resistance, inductance, capacitance and conductivity, respectively.
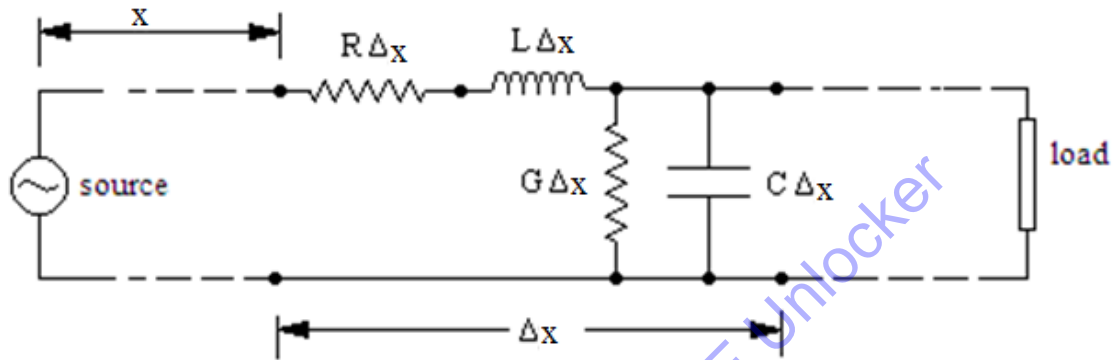

Figure 6.6: Equivalent circuit of an infinite homogeneous line's elementary length $\Delta \chi$.

For a sinusoidal steady state, with frequency ω, the equivalent element in series has an impedance of: $Z\Delta x = (R+j\omega L)\Delta x$, while the equivalent shunt element has an admittance of: $Y\Delta x = (G+j\omega C)\Delta x$. As a result, the equivalent circuit is that of Figure 6.7, where the current and voltage drop along the elementary length of the line could be calculated using elementary circuit laws.
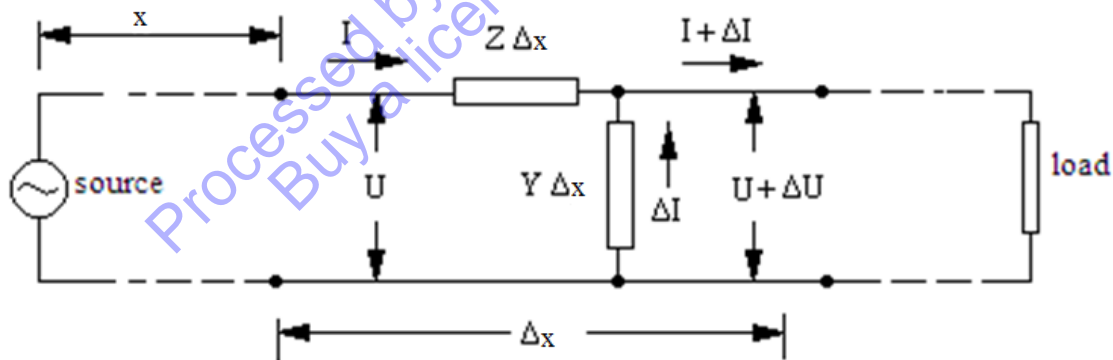
Figure 6.7: Voltage and current calculation for the equivalent circuit of Fig. 6.6.

By solving the circuit of Figure 6.7 the telegraph equations are deduced for the voltage and current along the line:

$$\frac{d^2U}{dx^2} = ZY\,U \tag{6.2.1.1}$$

$$\frac{d^2I}{dx^2} = ZY\,I \tag{6.2.1.2}$$

Taking into account the voltage and current initial values at the input of the line (U_0 and I_0), the solution of the equations (6.2.1.1–6.2.1.2) describe the linear combination between an incident ($e^{-\gamma x}$) and a reflected wave ($e^{\gamma x}$) as follows:

$$U(x) = \frac{1}{2}\left(U_0 - I_0 Z_c\right)e^{\gamma x} + \frac{1}{2}\left(U_0 + I_0 Z_c\right)e^{-\gamma x}$$

$$I(x) = -\frac{1}{2}\left(\frac{U_0}{Z_c} - I_0\right)e^{\gamma x} + \frac{1}{2}\left(\frac{U_0}{Z_c} + I_0\right)e^{-\gamma x} \tag{6.2.2}$$

Where, in the space of s=jω, the characteristic impedance is determined by:

$$Z_c = \sqrt{\frac{Z}{Y}} = \sqrt{\frac{R + sL}{G + sC}} \tag{6.2.3}$$

while the transmission constant is determined by:

$$\gamma = \sqrt{(R + sL)(G + sC)} \tag{6.2.4}$$

For transmission lines with a load Z_L as a termination, from equations (6.2.2) the following equations can be derived:

$$U = U_L \left[\cosh(\gamma x') + \frac{Z_C}{Z_L} \sinh(\gamma x') \right]$$

$$I = I_L \left[\cosh(\gamma x') + \frac{Z_L}{Z_C} \sinh(\gamma x') \right] \tag{6.2.5}$$

In (6.2.5) the current and the voltage at the termination load have been introduced, while the distribution along the line is determined by the distance x' from the load.

Using equations (6.2.5), the input impedance at any position on the line is calculated as follows:

$$Z_{in} = Z_C \frac{Z_L + Z_C\, tanh(\gamma x')}{Z_C + Z_L\, tanh(\gamma x')} \tag{6.2.6}$$

6.2.4   Lossy and lossless transmission lines

From equation (6.2.4) it is deduced that the transmission constant γ is in general a complex number that can be written in the form: $\gamma = \alpha + j\beta$ where α is the attenuation coefficient and β is the phase constant. The attenuation coefficient α is expressed in Np/km, while the phase constant β, which is the imaginary part of the transmission constant, is expressed in rad/km. Particularly, the unit Np (Neper) expresses the neper logarithm of a ratio of voltages or currents. For a transmission line, the attenuation coefficient α is usually expressed in dB of power loss along the line, where the conversion of Np into dB is conducted by multiplying the factor $20\log_{10} e = 8.686$.

For lossy transmission lines, both the transmission constant and the characteristic impedance are complex numbers, while for lossless transmission lines the transmission constant is purely imaginary ($\alpha = 0$) and the characteristic impedance is purely ohmic (a real number). In order to measure both the transmission constant and the characteristic impedance of a transmission line, its input impedance for short and open termination has to be measured respectively. From (6.2.6) it is easy to derive the following calculation formula based on the aforementioned measurements:

$$Z_c = \sqrt{Z_{in}^{(oc)} Z_{in}^{(sc)}} \tag{6.2.7}$$

$$\gamma D = \frac{1}{2} \ln \frac{\sqrt{Z_{in}^{(oc)}} + \sqrt{Z_{in}^{(sc)}}}{\sqrt{Z_{in}^{(oc)}} - \sqrt{Z_{in}^{(sc)}}} \tag{6.2.8}$$

where D is the length of the transmission line and $Z_{in}^{(oc)}$, $Z_{in}^{(sc)}$ are the input impedances for open and short termination respectively. Although any type of a transmission line should have a non zero attenuation constant, for high frequencies, short lengths (usually for a fraction of the wavelegth) and low loss dielectrics, are considered as lossless ($\alpha=0$). Thus, the aforementioned relations (6.2.5–6.2.6) could be simplified by substituting the hyperbolic functions with the corresponding trigonometric ones.

6.2.5   Reflection coefficient and standing waves in transmission lines

The characteristic impedance of a transmission line is of great importance, because it determines whether the reflective wave is present along the line or not. Particularly, if the termination of the line is different than the characteristic impedance, then part of the wave that is incident to the termination load is reflected back to the source. Thus, a fraction of the incident power will be transferred to the load, while the remaining power travels back to the source. The reflective wave is developed along the line and interferes with the incident wave. The result of this interference is a standing wave whose amplitude depends on the difference between the termination load and the characteristic impedance.

The standing wave is measured through the standing wave ratio (SWR) or voltage standing wave ratio (VSWR), while the reflection coefficient p determines the ratio between the reflected and incidence wave in any position of the line. The reflection coefficient at a distance x′ from the load is calculated for lossy lines as follows:

$$p = \frac{Z_L - Z_C}{Z_L + Z_C} e^{-2\gamma x'} \tag{6.2.9}$$

while for lossless lines (2.9) it is modified as:

$$p = \frac{Z_L - Z_C}{Z_L + Z_C} e^{-j2\beta x'} \tag{6.2.10}$$

The standing wave ratio can be expressed through the reflection coefficient for a lossless line as follows:

$$S = \frac{1 + |p|}{1 - |p|} \tag{6.2.11}$$

In the event that the line is terminated in its characteristic impedance, the reflected wave is zero, the standing wave degenerates and the line is considered as a *matched line.* In Figure 6.8 the amplitude of the voltage standing wave is illustrated for a lossy line. In the same Figure, the voltage amplitude is also illustrated for a matched lossy line. In both cases, the apparent exponential decay is due to the attenuation through the losses along the line.
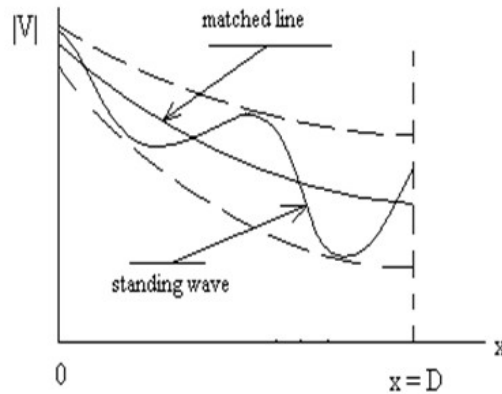
Figure 6.8: The amplitude of the voltage standing wave for a lossy line.

Furthermore, in Figure 6.9, the amplitude of the voltage standing wave is illustrated for a lossless line. This case is more important for high frequency applications when the length of the line is a few wavelengths long. Besides, the standing wave appears to be a periodic signal, with a period of half a wavelength ($\lambda/2$), whose accurate form is calculated from the assumption that at any point on the line, the voltage is $V_i + V_r = V_i(1+p)$, where V_i and V_r are the incident and reflected voltages at this point respectively.
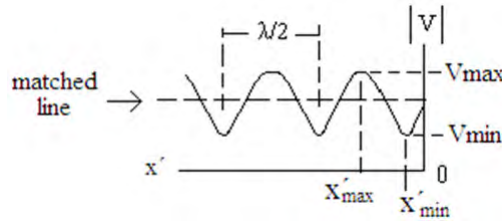
Figure 6.9: The amplitude of the voltage standing wave for a lossless line.

Particularly, the voltage amplitude along the line is calculated as follows:

$$|V| = |V_i|\sqrt{1 + 2|p|\cos\varphi + |p|^2}$$

(6.2.12)

where, $\varphi = \theta - 2\beta x'$, $\theta = \angle p_L = \angle \dfrac{Z_L - Z_C}{Z_L + Z_C}$ and $\beta = \dfrac{2\pi}{\lambda}$. The expression (2.12) is periodic in x′ with a period of λ/2, while its maximum and minimum values are:

$$|V_{\max}| = |V_i|(1 + |p|) \quad |V_{\min}| = |V_i|(1 - |p|)$$

(6.2.14)

Moreover, the first local maximum will be found at a distance: $x'_{\max} = \lambda\left[\dfrac{\theta}{4\pi} - \dfrac{k}{2}\right]$ from the termination load (with $k = 0, \pm 1, \pm 2, \cdots$) and the successive local minimum $x'_{\min}$ is located at a distance of λ/4 from the respective local maximum.

6.2.6   Power transfer from source to load

The standing wave along a transmission line is actually created from the interference between the incident and the reflected waves of voltage or current. Due to this phenomenon, the standing wave traps a fraction of the power that is transferred through the incident wave towards the load. As a result, the power that the termination load could dissipate is limited from the existence of the standing wave along the line. For a lossless line, the power that is dissipated from the load is calculated as follows:

$$P = \frac{|V_i|^2}{2Z_C}\left(1 - |p|^2\right) = P_i\left(1 - |p|^2\right)$$

(6.2.15)

The expression (6.2.15) determines that the fraction of the power that is trapped in the standing wave is $|p|^2$ and becomes zero when the reflection coefficient becomes zero. This is actually the reason why a transmission line has to be matched. Apparently, a matched line carries no reflective waves and consequently the reflection coefficient is zero. As a result, the incident power at its input will arrive and be dissipated in the load without any loss inside the transmission line due to reflections. Herein, it has to be clarified that the loss of power due to standing wave trapping, is different than the one that is derived from the ohmic losses along the line.

The aforementioned analysis has considered that the internal impedance of the source or the generator is equal to the line's characteristic impedance. This assumption enables the development of a standing wave only from the reflection at the line's termination load. However, in many applications, both the source's internal impedance and the termination load could be different than the line's characteristic impedance. In this case, the standing wave is developed from successive reflections from both the input side and the termination load.
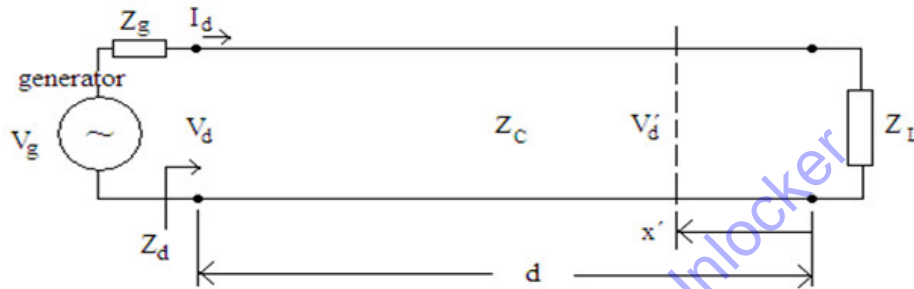
Figure 6.10: A doubly terminated transmission line.

For a doubly terminated transmission line (Figure 6.10), the power transfer from the generator to the load is now calculated as follows:

$$P = \left| \frac{V_g}{(Z_g + Z_C)(1 - p_d p_g)} \right|^2 \frac{Z_C}{2} \left(1 - |p_L|^2 \right) \tag{6.2.16}$$

where,

$$p_d = \frac{Z_d - Z_C}{Z_d + Z_C}, \; p_g = \frac{Z_g - Z_C}{Z_g + Z_C} \tag{6.2.17}$$

Evidently, with $Z_g = Z_C$, the expression (6.2.16) results to expression (6.2.15).

6.2.7 Quarter and half wavelength transmission lines

Energy trapping along a transmission line due to standing waves is not always a phenomenon that has to be avoided. Indeed, high frequency applications can take advantage of the energy trapping phenomena in short or open circuited lines in order to develop either inductive or capacitive elements or even more commonly, to use them as high frequency resonators.

The critical parameters for the development of high frequency elements using a particular type of a transmission line are the length (in wavelengths) and the termination load. More particularly, for a line with a length d, less than a quarter wavelength, zero or negligible losses and short circuited end (a shorted line also called a stub), the input impedance is calculated as follows:

$$Z_{in} = Z_C j \tan(\beta d) \tag{6.2.18}$$

Since the tangential argument is less than $\pi/2$ ($2\pi d/\lambda < \pi/2$) and Z_C is a real number, the expression (6.2.18) represents an equivalent impedance of a perfect inductor (Figure 6.11).
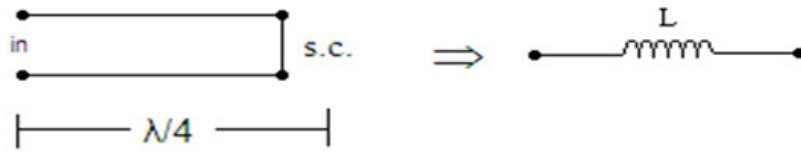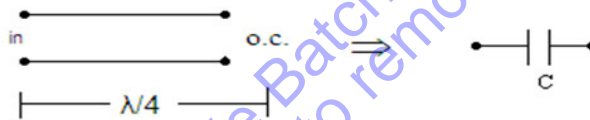

Figure 6.11: A short circuited transmission line with legth less than a quarter wavelength, is equivalent with a perfect inductor.

For a corresponding line with a length d, less than a quarter wavelength, zero or negligible losses and open end, the input impedance is calculated as follows:

$$Z_{in} = \frac{Z_C}{j\,tan(\beta x')} = -j\,\frac{Z_C}{tan(\beta x')} \tag{6.2.19}$$

Since the tangential argument is less than $\pi/2$ ($2\pi d/\lambda < \pi/2$) and Z_C is a real number, the expression (6.2.19) represents an equivalent impedance of a perfect capacitor (Figure 6.12).

Figure 6.12: An open circuited transmission line with legth less than a quarter wavelength, is equivalent with a perfect capacitor.

The properties now of a line with length equal to a quarter wavelength are based on its input impedance that is calculated as follows:

$$Z_{in}^{(\lambda/4)} = \frac{Z_C^{\ 2}}{Z_L}$$

(6.2.20)

If the quarter wavelength line is shorted at its end (Z_L=0) then the input impedance is infinite, Z_{in} = ∞. Consequently, a quarter wavelength transmission line with a shorted end is equivalent with an L//C resonator (see Figure 6.13). Furthermore, for a quarter wavelength transmission line with an open end (Z_L=∞), the input impedance is zeroed, Z_{in} =0, and its equivalent circuit is an L,C resonator in series.
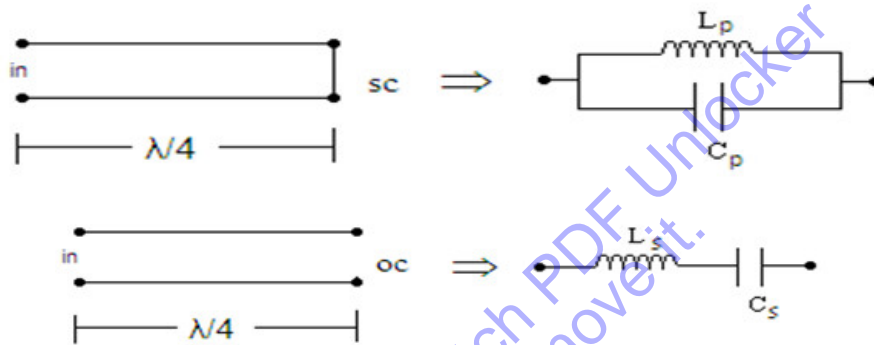
Figure 6.13: An open and short circuited transmission line with legth equal to a quarter wavelength, as a resonator.

The resonance properties of the quarter wavelength lines have a wide application in resosnance passive structures of RF and microwave networks. However, the standing wave form of Figure 6.13, provides resonance condition not only for the fundamental frequency but also for all its odd multiples. The odd multiples of the fundamental frequency are the well known *overtone* frequencies and they are present in any application of a quarter wavelength transmission line, which operates as a resonator in high frequencies.
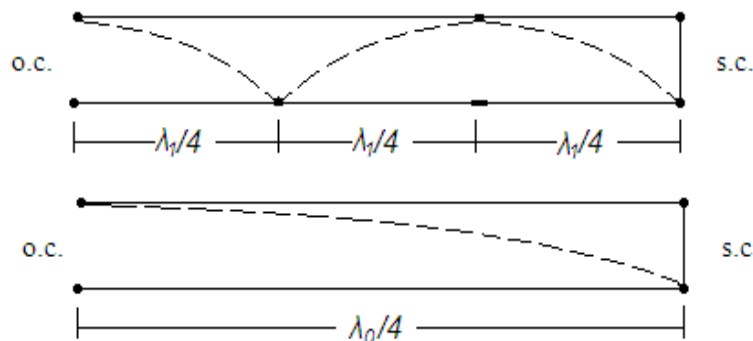
Figure 6.14: The standing wave along a shorted line in its fundamental and 3rd overtone resonance.

The resonance only for the odd overtones could be easily explained through the boundary conditions for the voltage at the two line terminations. Particularly, the line's open and short terminations, require maximum and zero voltage at the ends respectively.

In addition to the aforementioned analysis for a quarter wavelength line, similar results can be derived for a half wavelength transmission line. For a half wavelength line, the input impedance is equal with its load consequently, its self resonance appears when the line is terminated at open or short circuit at both ends. The overtones for a half wavelength line are all multiples of the fundamental frequency.

6.2.8   Smith Chart application on transmission lines

The Smith chart is a graphical method designed to calculate the functional characteristics of a transmission line. The need for the use of this method resulted from the complexity of the analytical calculations. The method is particularly useful in laboratory applications, where there is a need for fast and accurate calculations. The chart was published by the engineer P.H. Smith in 1939 and is designed on the domain of the reflection coefficient p. Through the chart, we can extract information about the line's input impedance, the coefficients of reflection and the standing wave. On the Smith chart, the reflectance at any point of the line is considered as a complex number in its cartecian form:

$$p = u + jv \tag{6.2.21}$$

Every point on the chart represents a normalized impedance, i.e. the input impedance of the line, at each point of it, normalized in respect to the line's characteristic impedance:

$$Z_n = \frac{Z}{Z_C} = \frac{R}{Z_C} + j\frac{X}{Z_C} = r + jx \tag{6.2.22}$$

There is analytical proof that the parameters u, v, r and x, are related to each other with the following equations that represent circles:

$$\left(u - \frac{r}{r+1}\right)^2 + v^2 = \frac{1}{(r+1)^2} \tag{6.2.23}$$

$$(u-1)^2 + \left(v - \frac{1}{x}\right)^2 = \frac{1}{x^2} \tag{6.2.24}$$

The equation (2.23) determines circles with centers at the points $u = \frac{r}{r+1}$, $v=0$ and radii $\frac{1}{r+1}$ (Figure 6.15). Every point on each circle is characterized by a constant r (r is ohmic part of the normalized impedance). All circles are tangent at point $u=1$, $v=0$, which represents $r=\infty$, while the outer circle represents all points with $r=0$. The circle $r=1$ is the matching circle, because it passes from the coordinates center, which is the point that represents the characteristic impedance. It is remarkable that all potential impedances can be represented by a point inside the outer circle $r=0$, consequently the Smith chart is enclosed by the outer circle.
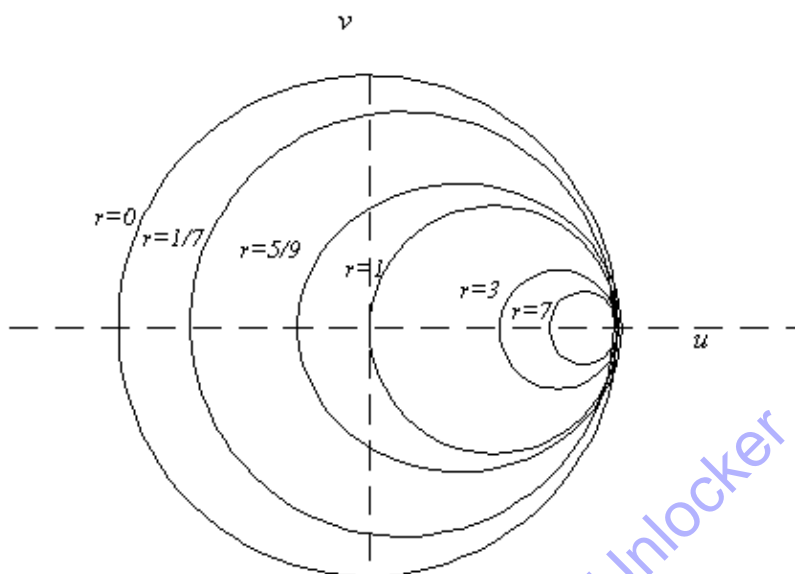
Figure 6.15: Circles that represent points on the chart with equal *r*.

The equation (6.2.24) determines circles with centers at the points $u=1$, $v = \dfrac{1}{x}$ and radii $\dfrac{1}{x}$. The centers of these circles lie on the line $u = 1$, and their arcs that are cut off from the outer circle of the chart, represent points with a constant imaginary part of impedance of the line.

Figure 6.16: Circular arcs that represent points on the chart with equal *x*.

For *x*=0 (pure ohmic resistance) the corresponding arc degenerates into a straight line, while for *x*=∞ (an infinite reactive part of the line's impedance) the corresponding arc degenerates into the point *u*=1, *v*=1. It is clarified here that the positive values of *x* (inductive loads) are placed in the upper semicircle, while the negative (capacitive loads) in the lower semi-circle.

The final version of the chart is that of Figure 6.17, where the bundles of circular arcs and circles are plotted in a dense grid. Therein, each constant *r* circle and each arc with constant *x* can be easily determined. Outside the chart's boundary circle, there is a concentric circle with external and internal ratings. The outer scales determine distances that correspond to movement toward generator (clockwise) and are expressed in wavelengths, while the internal ratings correspond to movement toward load (anticlockwise).
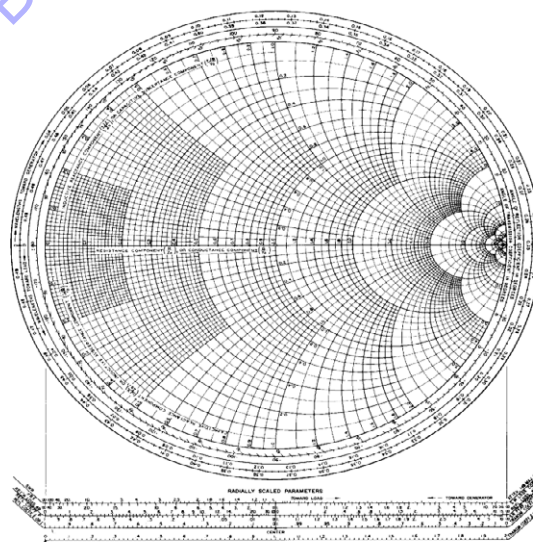
Figure 6.17: The complete form of the Smith chart.

For a lossless transmission line with given characteristic impedance ZC and termination load ZL, the normalized termination load will be equal to ZL/ZC = r+jx (point A in Figure 6.18); this is the "location of the load on the chart". The circle (0,0A) represents the lossless transmission line (line's circle). Moving along this circle, the line's input impedance can be determined from the location of each point on the circle (corresponding r and x values).
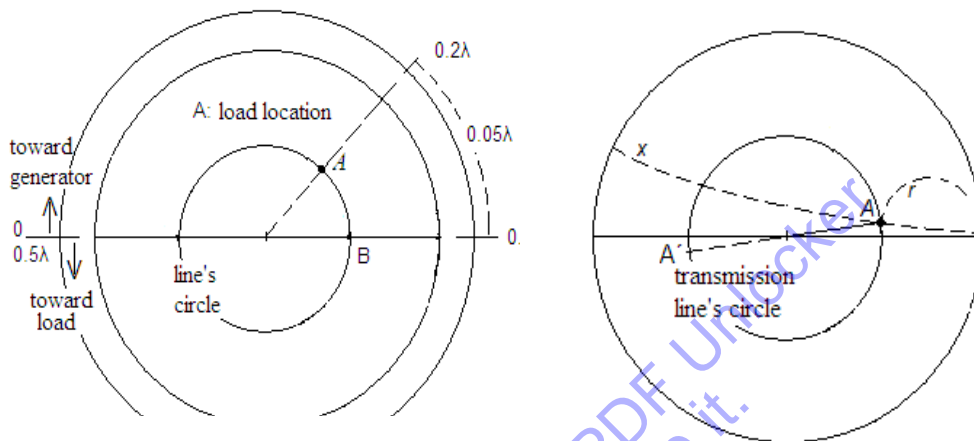

Figure 6.18: (Left)The circle of a lossless line – (Right) Covering distances along the line.

The Smith chart is useful for the study of the input impedance along the line. By covering a distance equal to e.g. 0.05λ from the load (see Fig. 6.18 –right side), we meet point B of the line. This point determines the input impedance of the line by reading its corresponding *r* and *x* values. Moreover, point B provides the value of VSWR that is readable on the horizontal axis. Consequently, as the line's circle gets smaller, the standing wave also decreases. Ideally, the perfect match can be achieved if the line's circle creates a single point at the center of the chart.

6.3   Coaxial cable T-resonator measurements results

A coaxial cable T-resonator (M. Dirix, 2012) (Y.H. Chou, 2008), is a two-port setup that uses two 50Ω coaxial cables, with a parallel connected coaxial resonating transmission line. This line should be either an open-ended quarter wavelength or a short-ended, half wavelength stub. Using a 50Ω Network Analyzer (Figure 6.19) and connecting its input and output ports to the ports of the T-resonator setup, we can analyze its frequency response for the UHF frequency range. A Network Analyzer (VNA) is a very common instrument for frequency analysis response of a passive network in RF. Particularly, the instrument's output operates as a frequency generator that scans a frequency-range defined by the user. The produced frequencies are driven through the passive network under test whose output is detected by the Network Analyzer's input. Internally, the instrument compares the input and output signals and displays the response of the passive network.
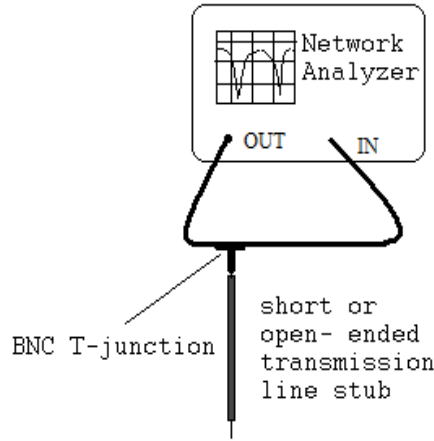
Figure 6.19 : Measurement setup using a 50Ω Network Analyzer.

If we use a resonating short-ended coaxial cable stub for the half wavelength frequency, as well as for its integer multiples, the stub's input appears to be a short circuit (for a half wavelength line with short-circuit termination, the input impedance is zero). The same effect also appears when we use an open-ended coaxial cable for the quarter wavelength frequency and its odd integer multiples (for a quarter wavelength line with open termination, the input impedance is zero). As a result, for these discrete frequencies, a strong attenuation will appear on the Network Analyzer's input port.

If we assume a lossless coaxial cable, then we can analyze theoretically the proposed T-resonator two-port frequency response, by using the lossless transmission line theory. The frequency analysis for a short-ended stub with 0.5m length and 66.6% propagation velocity, is illustrated in Figure 6.20. Each resonance frequency is an integer multiple of the fundamental f_0 which can be calculated as follows:

$$f_0 = \frac{c_0}{2\ell\sqrt{\varepsilon_r}} \tag{6.3.1}$$

where for propagation velocity 66.6% , $\sqrt{\varepsilon_r} = 1.5$ and ℓ is the stub's physical length.
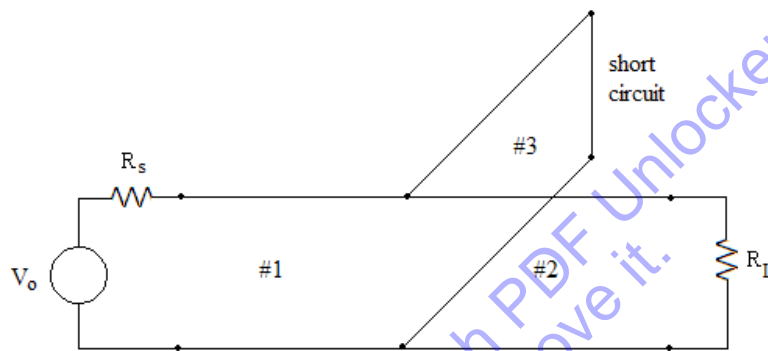
Figure 6.20: The equivalent lossless transmission line circuit.

By considering the instrument internal impedance $R_s = 50\Omega$, the power loss from input to output can be calculated as follows:

$$Loss(dB) = 10\log\left(1 - |p|^2\right), \tag{6.3.2}$$

where the reflection coefficient is provided by the standing wave along line #1, while line #2 is matched. Consequently, the calculation of p for short-ended line #3, is as follows:

$$p = \frac{Z_L - Z_c}{Z_L + Z_c} \text{ , with } Z_L = Z_c \mathbin{/\!/} jZ_c \tan(\beta d) = \frac{jZ_c \tan(\beta d)}{1 + j\tan(\beta d)} \quad . \tag{6.3.3}$$

whereas, for open-ended line #3 the reflection coefficient p is calculated as follows:

$$p = \frac{Z_L - Z_c}{Z_L + Z_c} \text{ , with } Z_L = Z_c \mathbin{/\!/} Z_c / j\tan(\beta d) = \frac{Z_c}{1 + j\tan(\beta d)} \quad . \tag{6.3.4}$$
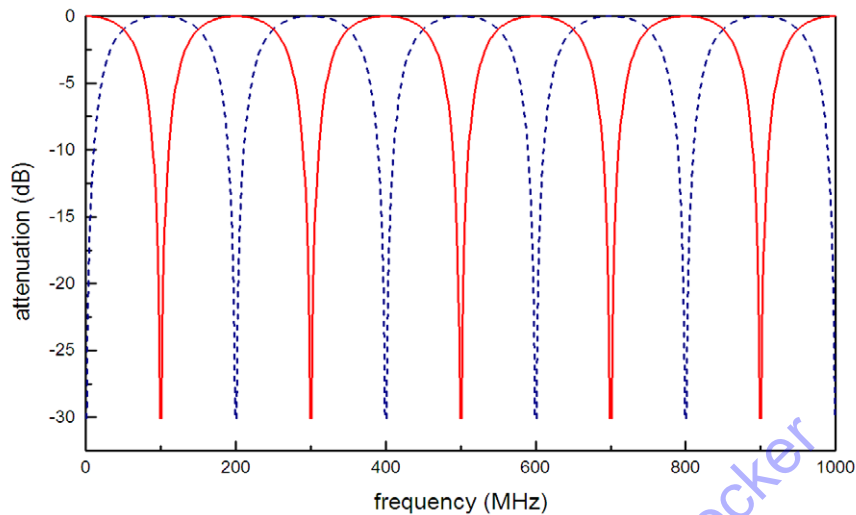
Figure 6.21: T-resonator frequency response for lossless transmission lines with 66.6% propagation velocity and a 0.5m parallel connected coaxial cable with short termination (dashed line), and open termination (solid line).

In the context of the above described theoretical framework and due to the absence of attenuation losses along the lines, the Q factor for each resonance appears to be infinite. Evidently, this result can be obtained from the determination of the loaded Q factor ($Q_L = f / BW_{3dB}$), where for a lossless resonance, BW_{3dB} tends to a zero limit value (see also Figure 21). Apparently, finite Q factors for lossy transmission lines are expected.

6.3.1 Coaxial Cable Experimental Measurements and Results

Next, using the aforementioned setup, we measure the frequency response of two coaxial cable stubs (half wavelength) with 0.5m length, the one with a copper shield and the other with an electrotextile shield (Vassiliadis, 2011). In Figure 6.22 (a) and (b), the Network Analyzer's frequency response snap shots are illustrated for both the copper shield and the electrotextile shield coaxial cables, respectively. The finite depth of the resonance nulls indicates the level of attenuation losses, whereas the 3 dB bandwidth, the Q factor value. The basic remark from Figure 6.23 (a) is that the loaded Q for the first 4 resonance frequencies is approximately the same, whereas, in Figure 6.23 (b), the second resonance frequency has an evidently higher Q. In particular, from Figure 6.23 (b), we notice that the electrotextile coaxial cable presents a Q comparable with that of the corresponding copper coaxial cable, but only for the resonance frequency of 400MHz.
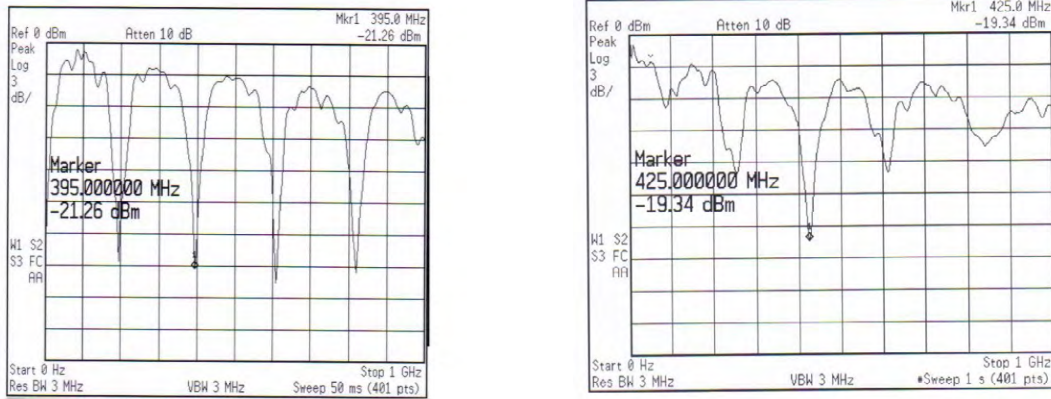
Figure 6.22: (a) Frequency response of a coaxial 'T' resonator   with a copper shield and
(b) Frequency response of a coaxial 'T' resonator with an electrotextile shield.

In Figure 6.22 (a) and (b) the resonance response arround 400MHz is illustrated for a smaller frequency span, in order to measure the 3dB bandwidth and the maximum attenuation level more accurately.
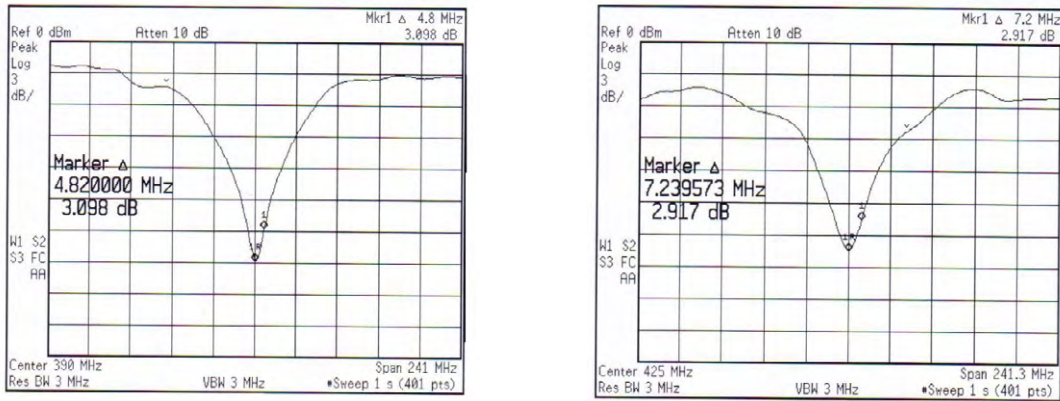
Figure 6.23: (a) Notch characteristics for a coaxial 'T' resonator with a copper shield
(b) Notch characteristics for a coaxial 'T' resonator with an electrotextile shield.

Using the same span settings we measure the relative 3dB bandwidth and the maximum attenuation for the first three resonance frequencies of the T-coaxial resonators. In Table1 the measurement results are tabulated, considering that the reference instrument power is 0dBm.

	Coaxial cable with copper shield				Coaxial cable with textile shield		
	f(MHz)	L_A(dB)	BW(MHz)	Q_L	f'(MHz)	L_A'(dB)	BW'(MHz)
F_0	200	-20	+/-2.5	40	250	-12	+/-25
$2F_0$	400	-21	+/-4.8	41.6	425	-19	+/-7.2
$3F_0$	600	-22	+/-5	60	620	-12	+/-12

Table 1: Tabulated measurement results for the copper reference cable and the cable with conductive textile shield under test.

Evidently, from Table 1, in the first three resonance frequencies of the copper coaxial cable, the loaded Q slightly increases at higher frequencies, whereas for the electrotextile, the higher Q appears only at the second overtone (400MHz).

Consequently, it is reasonable to examine the attenuation characteristics of the electrotextile coaxial cable in this range of frequencies.

6.3.2   Calculation of the electrotextile coaxial cable attenuation constant

From the measurement results of Table 1 we can calculate the unloaded Q factor for the 400MHz resonance frequency as follows (M. Dirix, 2012):

for the copper coaxial cable: $Q_0 = \dfrac{Q_L}{\sqrt{1 - 2 \times 10^{L_A/10}}} = 41.3$ (6.3.5.1)

for the electrotextile coaxial cable: $Q_0' = \dfrac{Q_L'}{\sqrt{1 - 2 \times 10^{L_A'/10}}} = 29.9$ (6.3.5.2)

The unloaded quality factors from expressions (6.3.5) comprise of the loss effect from the conductors and the dielectric losses, since radiation losses are negligible:

$$\frac{1}{Q_0} = \frac{1}{Q_c} + \frac{1}{Q_d} \tag{6.3.6.1}$$

$$\frac{1}{Q_0'} = \frac{1}{Q_c'} + \frac{1}{Q_d} \tag{6.3.6.2}$$

where, Q_c is the quality factor of the conventional cable due to copper conductor losses, Q_c' is the quality factor that corresponds to the losses of the cable shielded by an electrotextile, and Q_d is the quality factor due to dielectric losses, which are common for both cables. From expressions (3.6) the quality factor due to electrotextile losses, is calculated through the unloaded Q of both resonators as follows:

$$\frac{1}{Q_c'} \cong \frac{1}{Q_c} - \left[\frac{1}{Q_0} - \frac{1}{Q_0'} \right] \tag{6.3.7}$$

For a smooth copper coaxial cable RG58 C/U, we calculate the quality factor which corresponds to copper conductor losses, as follows:

$$Q_c = \frac{\beta}{2a_c} = \frac{\pi\sqrt{\varepsilon_r}}{\lambda_0 a_c} \ , \tag{6.3.8}$$

where a_c is the copper conductor attenuation constant which is calculated as follows for a coaxial cable (Pozar, 2005) :

$$a_c = \frac{R_s}{2\eta \ln\left(\frac{b}{a}\right)} \left(\frac{1}{a} + \frac{1}{b} \right) \tag{6.3.9}$$

In (6.3.9), parameters a and b are the core and shield radii. For the RG58 C/U cable a=1mm and b=4mm, whereas $\sqrt{\varepsilon_r} = 1.5$ and $\eta = \frac{120\pi}{\sqrt{\varepsilon_r}}$ Ω is the impedance of the dielectric insulator. The surface resistivity R_s of the copper conductor could be calculated by considering the skin effect depth $\delta_s = \sqrt{2/\omega\mu\sigma}$ from the expression:

$$R_s = \frac{1}{\sigma\delta_s} = \sqrt{\frac{\omega\mu_0}{2\sigma}} \tag{6.3.10}$$

Considering smooth copper conductor with $\sigma = 5.813 \times 10^7$ S/m we calculate the attenuation constant as $a_c = 3.6 \times 10^{-3}$ Np/m = 0.03 dB/m. The relative Q_c that is then calculated from (6.3.8) is ≈ 1745 and is valid only for smooth copper conductors. Taking into account the conductor's surface roughness and the woven type of the shield conductor, the aforementioned value of quality factor is significantly reduced. However, its final value should be higher than the quality factor of resonators unloaded Q ($Q_c \gg Q_0, Q_0'$) and the following approximation is justified:

$$\frac{1}{Q_c'} \cong \frac{1}{Q_0} - \frac{1}{Q_0'} \Rightarrow Q' = 108 \tag{6.3.11}$$

As a result, from (6.3.11) and (6.3.8) we calculate the attenuation constant for the electrotextile coaxial cable: $a_c' = 0.058 \text{Np/m} = 0.5 \text{dB/m}$.

6.4   Microstrip T-resonator measurements results

An alternative measurement setup layout for the evaluation of electrotextile materials in RF frequencies is proposed herein. The coaxial lines that have been examined in section 3 of this chapter, are replaced by microstrip lines. The proposed layout is illustrated in Figure 6.24 and consists of a copper microstrip line that connects the input and output of the Network Analyzer through SMA connectors. In the middle of the copper microstrip line, an open-ended line is connected, with its upper conductor consisting of a conductive textile material.
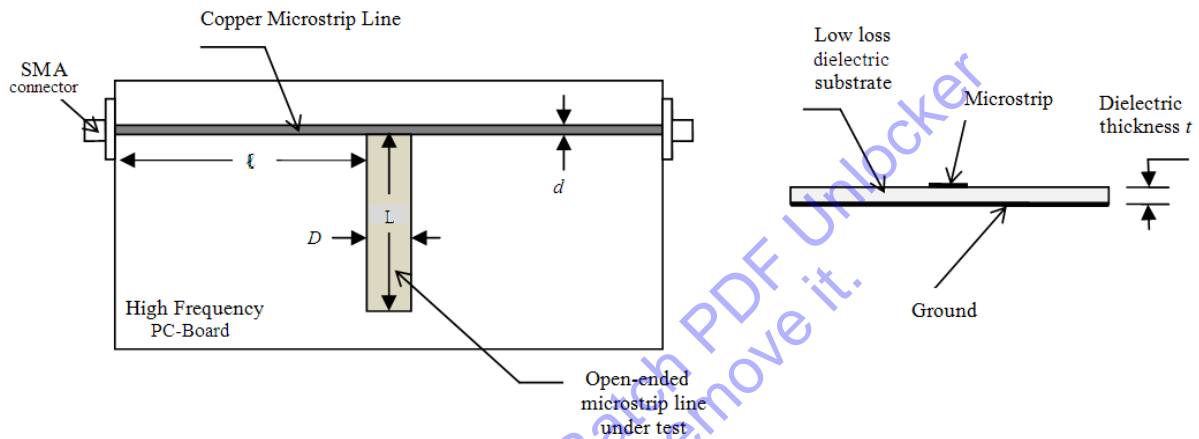
Figure 6.24: A microstrip T-resonator layout (left) and its cross section (right).

According to the analysis that is presented in the previous section, a similar frequency response using the same calculation scheme is expected. Moreover, the proposed layout should be more adequate for a measurement setup, despite the expected difficulties of copper-textile connection and the adhesion between the textile and the dielectric substrate.

6.4.1   Design and analysis

The characteristic impedance of a microstrip line depends on the thickness and the dielectric constant of the low-loss dielectric substrate; the width of the upper conductor; as well as the thickness of the conductive material. The pc-board material is selected with ε_r=10 and thickness t=1.2mm, while the copper microstrip line is 5mm wide (d=5mm) and 30cm long (ℓ=15cm). The calculation of the characteristic impedance for the aforementioned data, gives an approximate value of Z_c=20Ω. Although for matching with the Analyzer's ports' impedance the characteristic impedance should be 50Ω, this is not always achieved. In order to increase the characteristic impedance Z_c the thickness t should be increased or the width d should be decrease. However, due to practical limitations, Z_c could be different than the matching impedance.

Regarding the open-ended line under test, its width D=1cm and its length L=15cm. These dimensions have been considered as suitable for the evaluation of conductive textile pieces in RF frequencies. However, precautions should be taken, in order to keep the conductive item stick on the pc-board. For this reason, a double sided tape could be used, or another adhesive method that keeps the item in contact with the substrate. Using the aforementioned dimensions and considering initially a copper conductor, the characteristic impedance should be approximately 12.5Ω.

As far as the analysis is concerned, we adopt the circuit that describes the problem, if R_s=R_1=50Ω, the characteristic impedance of lines #1 and #2 is 20Ω and the characteristic impedance of line #3 is 12.5Ω with its termination open. In the event that the calculation takes into account the connection cables without any calibration procedure that compensates their involvement, then the formulation of expressions (6.2.16–6.2.17) is required.
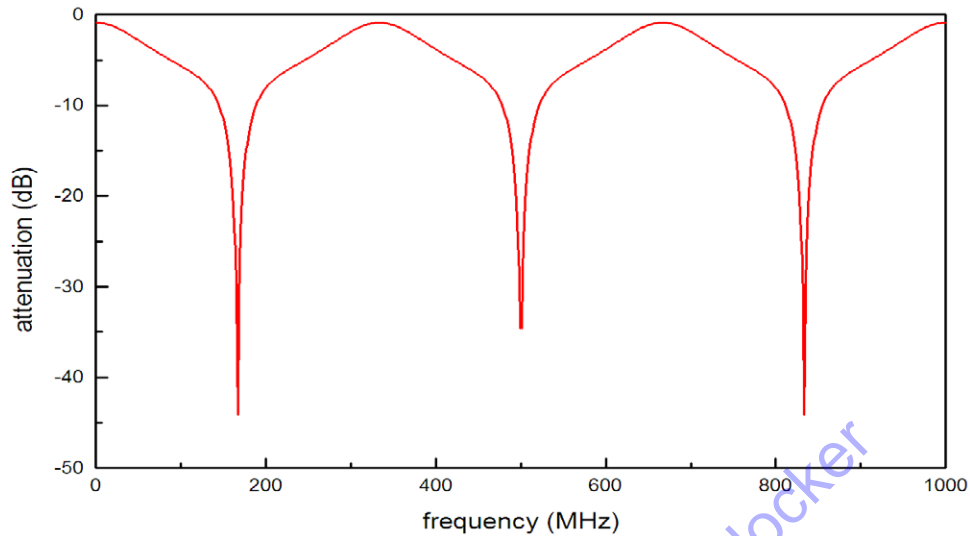
Figure 6.25: T-resonator frequency response (see details in the text).

However, the VNAs can be calibrated either manually or automatically. The calculations could be simplified and based on the procedure that is described through expressions (6.3.2–6.3.5). As a result of the application of the latter procedure, the frequency response is illustrated in Figure 6.25.

It is evident from the analysis, that the frequencies of resonance are independent from the characteristic impedance of lines #1 and #2. The fundamental frequency of resonance, is at approximately 170MHz for copper conductors and lossless dielectric materials, and also supports all odd overtone frequencies.

6.4.2 Experimental Measurements and Results

The aforementioned layout has been prepared and tested with a high frequency Network Analyzer within the 0 to 1.5GHz frequency range. The test is conducted for a copper open-ended line in order to register the measurements as reference. It is necessary to calibrate the instrument for the measurement, in order to isolate any discrepancies from the connections through the test cables. The calibration procedure could be conducted either manually or automatically (electronic calibration) for the new generation of VNAs.

The frequency response is illustrated in Figure 6.26 and it is evident that there is a good agreement with the theoretical results. However, a drift of frequency toward higher frequencies is observed (the theoretical fundamental frequency is 170MHz, whereas the measured is 205MHz). This drift is justified by the imperfect way the copper open-ended line has been positioned on the dielectric substrate (a copper strip on a double sided tape has been used). Specifically, areas where the copper leaves a void between its surface and the substrate, reduce the effective dielectric constant ε_r. Therefore, the fundamental and the overtone frequencies will drift upwards, as it is predicted by expression (6.3.1). As it will appear later on, this discrepancy will be more intensive for the textile conductor, because its texture enhances the aforementioned effect. Although, this is an inconvenient remark for the measurement setup, it will not affect the measurement of the quality factor (as described in section 6.3).
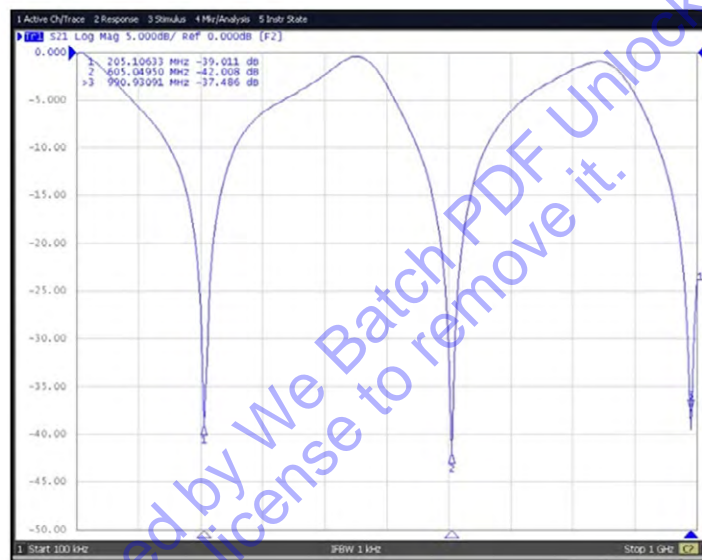
Figure 6.26: Frequency response for copper open-ended line under test.

In Figure 6.26 supplementary information about the transmission line circuitry has been provided. Specifically, the Smith chart for the input impedance is illustrated. There is no line crossing the center of the chart and the input is not matched at 50Ω, as confirmed theoretically. However, for the resonance frequency (see marker 1) the input impedance is close to the infinity point of the chart.
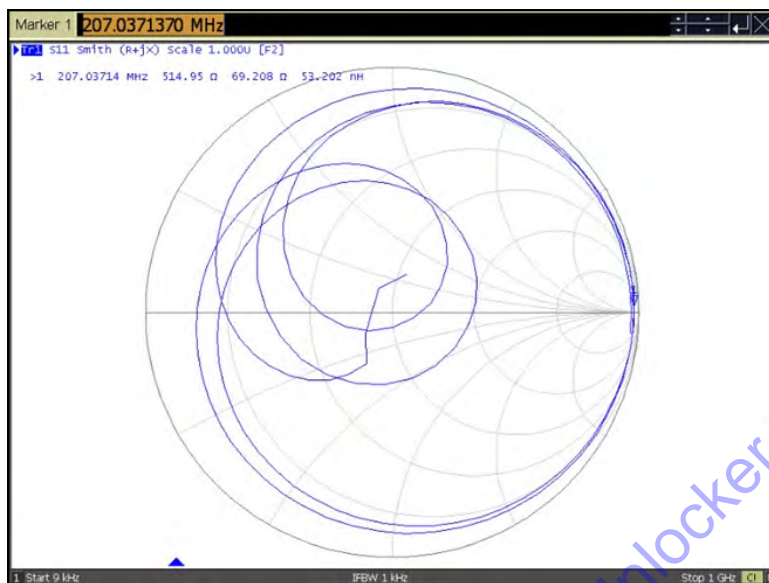
Figure 6.27: The Smith chart for the input impedance with copper open-ended line under test.

In Figure 6.27, the Smith chart for the input-output impedance is illustrated. Since the output impedance that is seen from the instrument's port at the resonance frequencies is approximately 50Ω, the corresponding instrument port is matched (notice that $2\ell=\lambda/2$). Consequently, three lines are crossing the center of the chart and correspond to the three resonance frequencies that are captured by the instrument's frequency span.

Next, the copper conductor is replaced by a conductive textile material with the same dimensions. The frequency response is illustrated in Figure 29. Therein, six different lengths (15, 14, 13, 12, 11 and 10cm) have been tested and their fundamental frequency corresponds to markers 1 to 6 respectively.
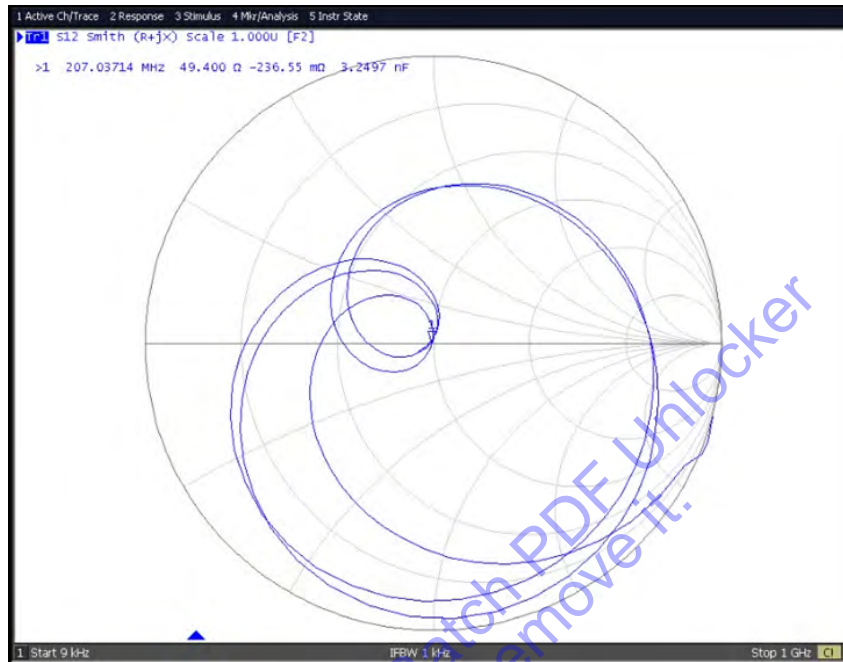

Figure 6.28: The Smith chart for the input-output impedance with copper open-ended line under test.

Evidently, and due to the aforementioned effect, the frequencies are found higher than the copper and quite higher than the theoretical. However, the Q factor can be easily measured through the bandwidth and the center resonance frequency.
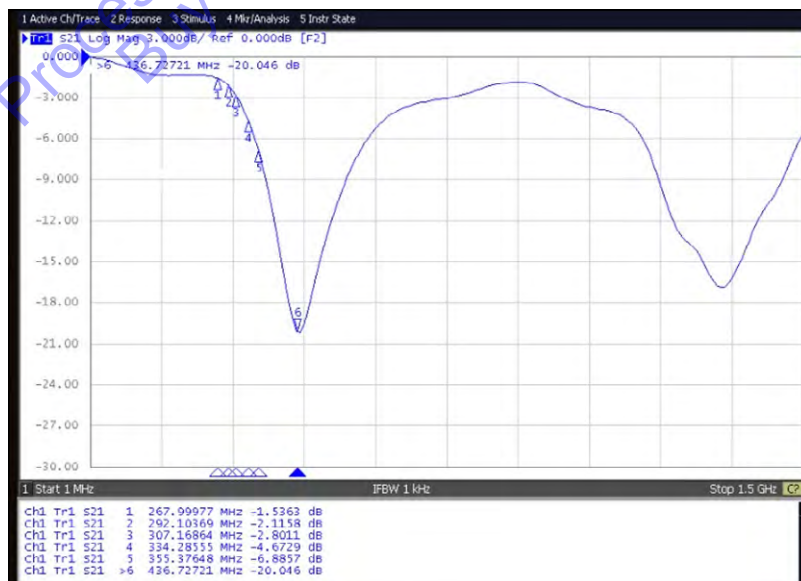

Figure 6.29: Frequency response for textile open-ended line under test and 4 different lengths.

6.5 Antenna fundamentals

6.5.1 Radiation mechanism

In essence, antennas are devices that transform an electric current or voltage on a conductive material to an electromagnetic wave propagating in the air, or vice versa. The IEEE definition of antennas includes the transmission or reception of electromagnetic waves (S.P. Savvaidis, 2011). Nevertheless, antennas may also transmit and receive electromagnetic waves in the vacuum or other dielectric environments, as illustrated in Figure 6.30.
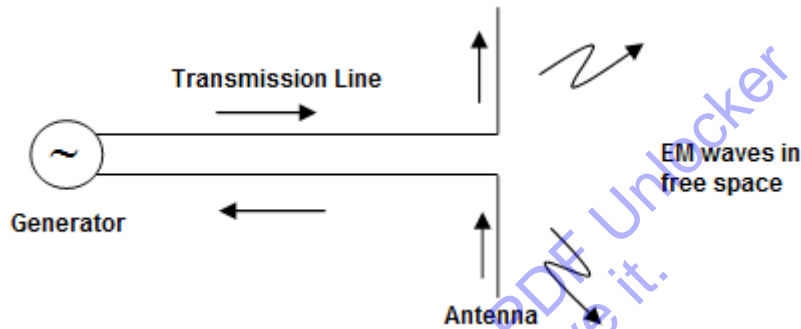

Figure 6.30: A simplified diagram of an antenna connected to a transceiver.
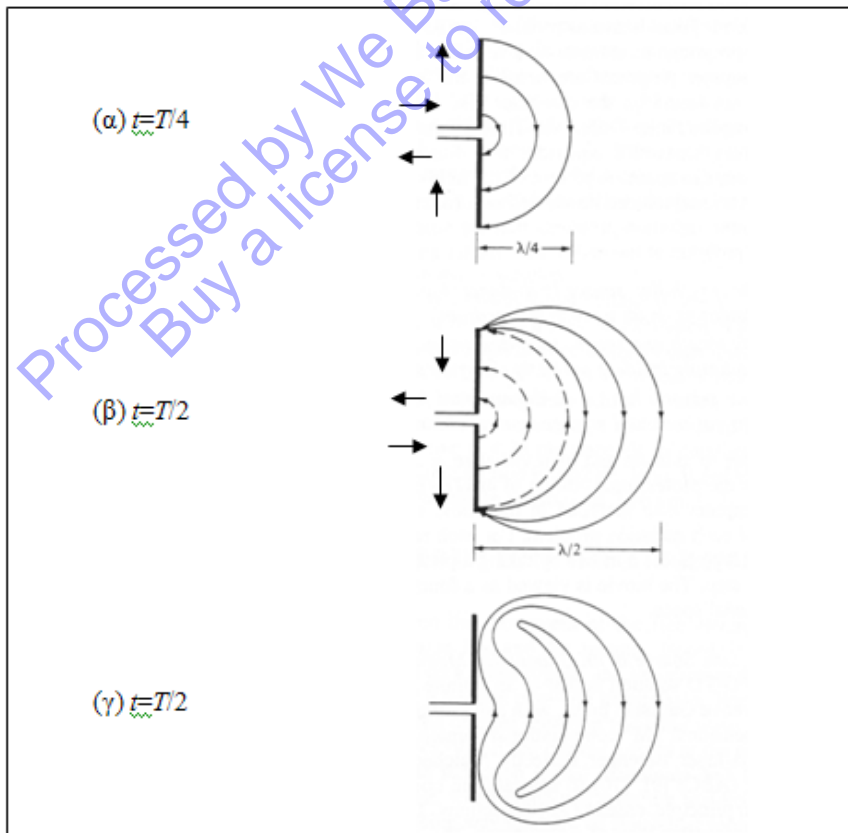

Figure 6.31: Concept of operation of an antenna device (Balanis, 2005).

More specifically, the antenna illustrated in Figure 6.30 above is a so-called *dipole antenna* and consists of two wires positioned in parallel on the same axis. The voltage or current coming from the generator through the transmission line creates a current flow on the antenna, and then electromagnetic waves are generated in free space due to the well-known Maxwell equations (Mitilineos, 2006).

The concept of operation of an antenna is further illustrated below using Figure 6.31 (Balanis, 2005). Consider a thin dipole antenna with a sinusoidal current flowing on its surface, i.e. a current of the form $I=I_o\sin(2\pi ft)= I_o\sin(2\pi t/T)$, I_o being the amplitude, f being the frequency and T being the current's time period. The current flow direction on the antenna is indicated by arrows. During the first quarter time period, the electric field induced by the antenna to the nearby free space environment is indicated by the curves in Figure 6.31(a), covering a region of up to a quarter wavelength in distance. During the other quarter time period, newer electric field lines are introduced in the free space, while the previous ones have propagated another quarter wavelength in distance. Note that the direction of current and electric field is inverted during this time frame. Interestingly enough, at the time where $t=T/2$, the current on the antenna surface is equal to zero; thereupon, the electric field lines are detached from the antenna surface and configure closed loops, as indicated in Figure 6.31 (c).

The aforementioned procedure is repeated infinitely for as long as there is a current flowing in the antenna. Electric field lines are propagating further and further away from the antenna, reaching distant targets or other antennas acting as receivers.

The specifics of antenna theory and the respective equations and analysis comprise a scientific field with extreme breadth and depth, and will not be analyzed here for the sake of brevity and readability. The interested reader is referred to the referential work of C.A. Balanis, where a complete list of further literature can also be found (Balanis, 2005). Furthermore, the concept of smart antennas has been recently introduced in order to describe antennas that dynamically adapt to environmental conditions. This offers adaptive radiation patterns and input impedance, as well as a series of other specifications and applications, such as the estimation of the direction-of-arrival of the incoming signal; the aid in developing multiple-access information schemes; the advancement of the channel capacity; and others. Smart antennas consist of a number of simple antenna elements, that when combined with a smart processing circuitry, configure the smart antenna system. Further literature on the field can be found in (Mitilineos, 2006). In the following, a brief introduction to the main terminology and concepts of antennas and antenna arrays is cited in order to aid the interested reader in familiarizing with antenna fundamentals, including radiation patterns, gain and directivity, bandwidth and polarization.
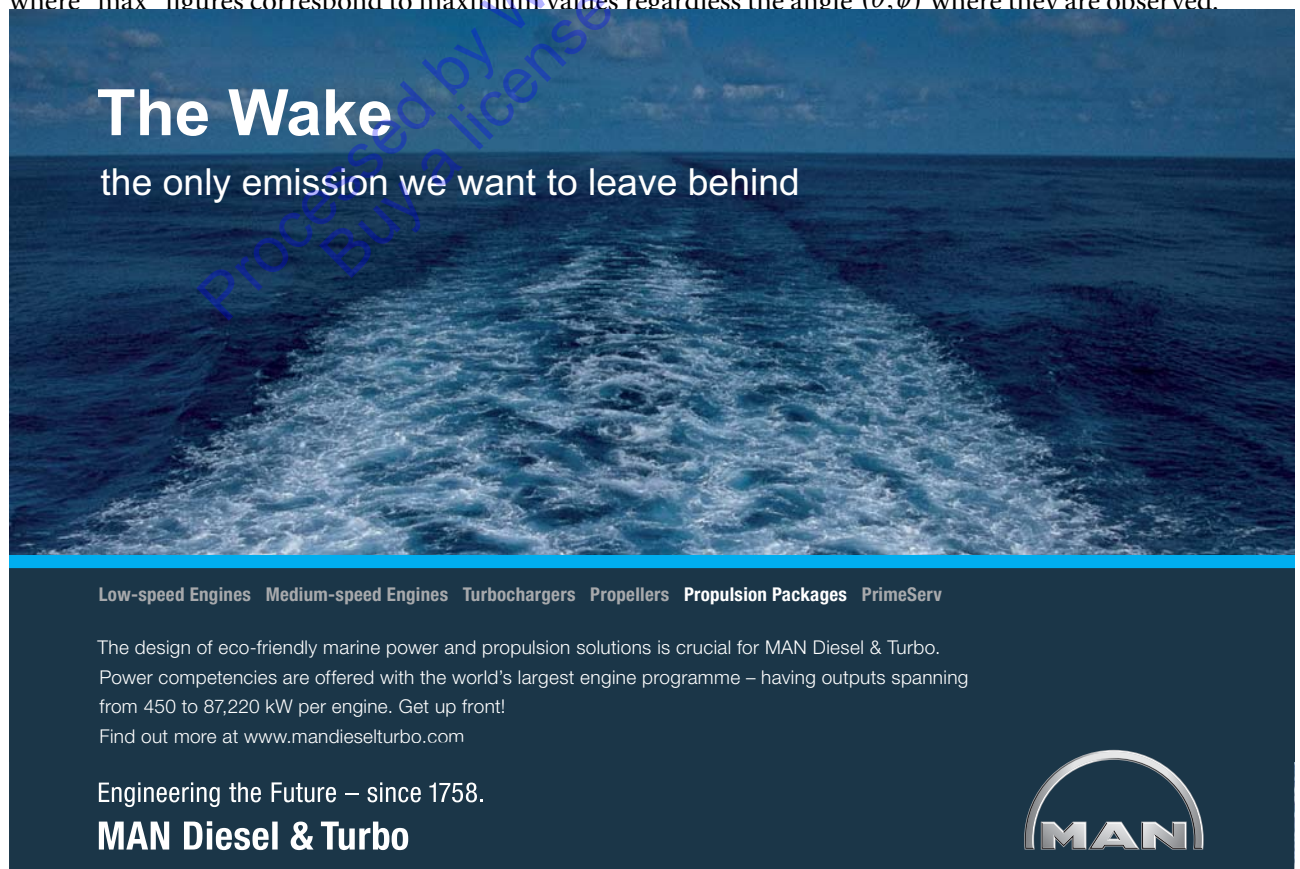
6.5.2 Antenna radiation patterns

Perhaps the most important characteristic of an antenna is the way it converts the power delivered from the generator to electromagnetic waves propagated to various directions in space. The *antenna radiation pattern* is defined as "a mathematical function or a graphical representation of the radiation properties of the antenna as a function of space coordinates. In most cases, the radiation pattern is determined in the far-field region and is represented as a function of the directional coordinates. Radiation properties include power flux density, radiation intensity, field strength, directivity, phase or polarization" (Balanis, 2005). Often, field and power patterns are normalized with respect to their maximum value, yielding normalized patterns.

Regardless the specific antenna type, the radiated power attenuates inversely proportional to the square distance to the transmitter. Thereupon, antenna radiation characteristics may be summed up to the way a specific antenna radiates towards directions in space, *(θ,φ)*. In this sense, a radiation pattern may be calculated using (all of the following correspond to a closed curve or surface at a distance *R)*:

- the received power $W_r(\theta,\varphi)$ (Watt)
- the Poynting vector, P_{av} (Watt/m^2)
- the radiation intensity $U(\theta,\varphi)=R^2 P_{av}$ (Watt/sr)
- The respective normalized patterns may be calculated as in the following:

$$P(\theta,\phi) = \frac{W_r(R,\theta,\phi)}{W_r(R,\theta,\phi)_{\max}} = \frac{P_{av}(R,\theta,\phi)}{P_{av}(R,\theta,\phi)_{\max}} = \frac{U(\theta,\phi)}{U(\theta,\phi)_{\max}} , \qquad (6.5.1)$$

where "max" figures correspond to maximum values regardless the angle (θ,ϕ) where they are observed.

Radiation patterns are three dimensional; nevertheless, it is very common to use only one or two two-dimensional patterns over a predefined closed line at a distance *R*, e.g. for constant *θ* or constant *φ*. The most widely used 2D patterns are the ones referring to the so-called *E-* and *H-* planes (principal patterns). Figure 6.32 displays some of the most interesting antenna characteristics related to radiation patterns:

- **radiation lobes** are included between directions of minimum radiation. Lobes are designated as Main lobe, side lobes and back lobe. The main lobe includes the maximum radiated power direction. All other lobes are designated as "side lobes", while the back lobe radiates towards the opposite direction with respect to the main lobe.
- the half-power or 3-dB radiation points, correspond to the angles where the radiated power is exactly the half with respect to the maximum one. The aperture between the left and right 3-dB points is called the 3-dB beamwidth.
- Null points are angles at which the radiation is minimized (not necessarily dropping to zero).
- Side-lobe level is the ratio of power radiated from side lobes with respect to the power radiated from the main lobe.
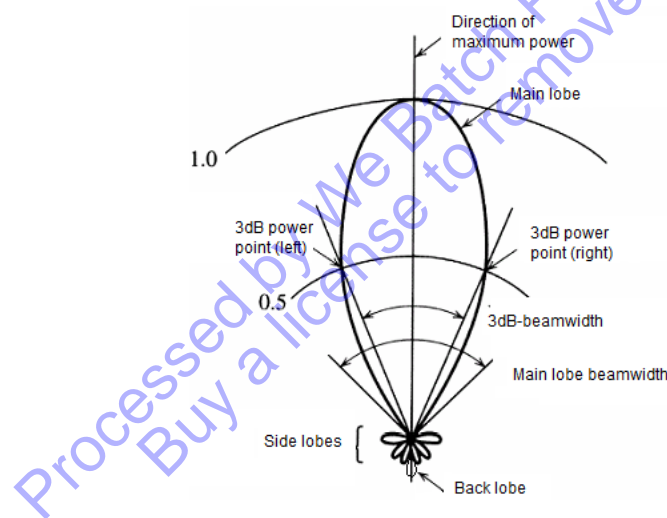

Figure 6.32: Normalized polar power pattern (S.P. Savvaidis, 2011).

In order to better understand the aforementioned terminology, consider an example of an antenna with a gain equal to 100, or equivalently 20dBi (see sub-section 5.1.2 for a definition of antenna gain). What does it take to read on such an antenna's radiation pattern? In the following we take a closer look to the most commonly used pattern types, namely the polar, the dB-, and the Cartesian patterns.

6.5.2.1 Polar radiation pattern

Figure 6.34 displays an example of a polar *power* radiation pattern. The specific antenna has a direction of maximum directivity towards 22.5°. For any given angle, φ, the normalized value of the gain is equal to the distance between the origin of the coordinates system and the respective point on the pattern. E.g., for Figure 6.34 and an angle equal to φ the normalized gain is equal to 0.8. Given a gain of 100, it is concluded that the gain at angle φ is equal to 80.

Furthermore, the 3dB-beamwidth is graphically calculated using the directions at which the respective length equals 0.5. For the specific figure, the 3dB-beamwidth is designated as Δ3dB.
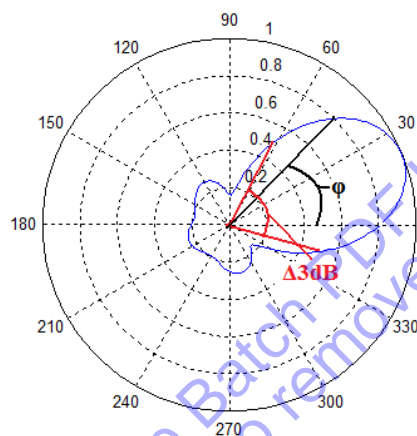

Figure 6.33: Polar radiation pattern example (S.P. Savvaidis, 2011).

6.5.2.2 Polar radiation pattern in dB

Figure 6.34 displays an example of a polar *power* radiation pattern in dB.
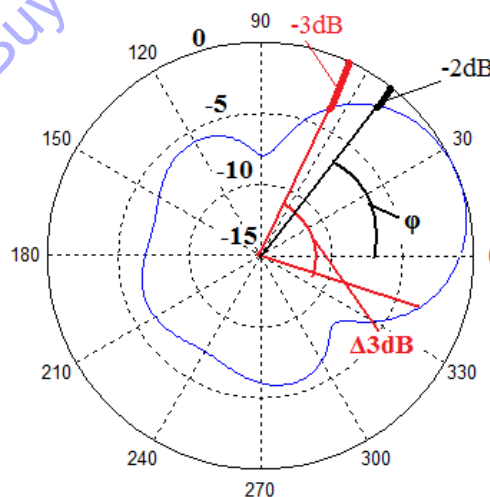

Figure 6.34: Radiation pattern of Figure 6.33, transformed in dBi (S.P. Savvaidis, 2011).

In contrast to Figure 6.33, the above figure is characterized by that:

The minimum gain value in dB is defined by the user, and in this example is equal to -15dB (most inner circle in figure). Evidently, the gain value of -15dB is selected so as no direction corresponds to a smaller gain.

A normalized polar pattern range of values is between 0 and 1. Correspondingly, the values of the pattern in dB range between $-\infty$ and 0, respectively.

- The pattern in dB seems to be somewhat more stretched out with respect to the natural pattern.

Finally, in contrast to the previous procedure, the gain value at a given angle is calculated using the distance towards the most outer circle. E.g. for the angle φ in the figure, the distance towards the most outer circle is -2dB, thereupon the normalized gain at this angle is equal to -2dBi. Given the maximum gain to be equal to 20dBi, it turns out that the gain at this angle is equal to 20dBi -2dB = 18dBi = 63.1.

6.5.2.3 Cartesian radiation pattern in dB

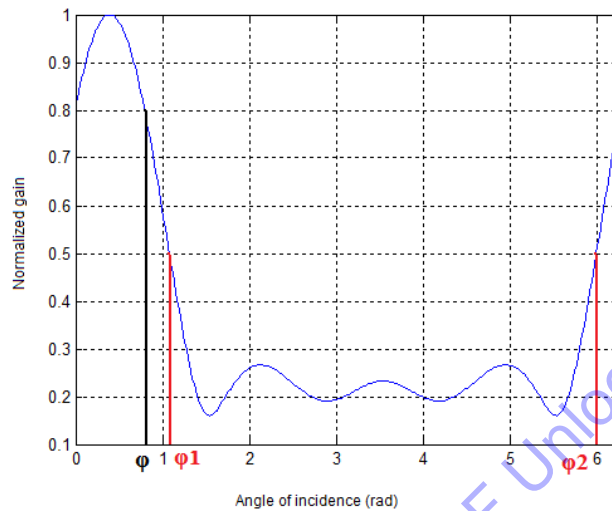Figure 6.35 displays an example of a cartesian *power* radiation pattern.

Figure 6.35: Radiation pattern of Figure 6.34 in Cartesian coordinates (S.A. Savvaidis, 2011).

The Cartesian pattern is the easiest to read, but the least used in practice nevertheless. Its use is straightforward, with every angle corresponding to a normalized gain indicated on the vertical axis, as in Fi.

6.5.3   Antenna gain and directivity

The *Antenna Gain* is a characteristic figure of antennas that corresponds to the antenna's capability of aiming a narrow solid angle, or, similarly, of an antenna's capability of collecting electromagnetic waves from narrow solid angles. The higher the antenna gain, the larger the current induced to a receiving antenna for a given distance and angles of transmission and reception. Moreover, it is empirically proven that the higher the antenna gain, the narrower the 3dB-beamwidth, and vice versa.

The isotropic radiator is used as a reference antenna in order to define gain. The isotropic radiator does not exist in nature but is rather a conceptual definition; it is supposed to be a radiator that radiates uniformly towards all directions, and its radiation pattern is a sphere. Furthermore, it is noted that since the gain of an antenna is compared to that of an isotropic radiation, the notation used in dB dictates that the antenna gain is given in dBi, "i" standing for "over isotropical".

The gain of the isotropic radiator is defined to be unity, i.e. equal to 1. The gain of any antenna towards a given direction, (θ, φ), corresponds to the ratio of the Poynting vector of the field generated by the antenna at a distance R, versus the Poynting vector of the field that would have been generated by the isotropic radiator at the same distance and with the same input power. Given that the isotropic radiator's gain is unity, the latter is calculated to be equal to $W_{in} / 4\pi R^2$. Thereupon, the antenna gain at any given angle (θ, φ) is given by

$$g(\theta, \phi) = \frac{P_{av}(\theta, \phi)}{W_{in} / 4\pi R^2} = \frac{4\pi R^2 P_{av}(\theta, \phi)}{W_{in}} = \frac{4\pi R^2 P_{av}(\theta, \phi)}{W_{rad} + W_{loss}} ,$$

(5.2)

where W_{in} corresponds to the power that **enters the antenna** (not the power that is incident to the antenna, since a fraction of the latter is reflected back to the source; neither the power transmitted by the antenna, W_{rad}, since part of W_{in} is dissipated by the antenna producing mostly heat that is represented by W_{loss}).

It is usually implied that the "gain" corresponds to the maximum gain, regardless the direction where it appears. Thereupon, the "gain" in most textbooks is defined by

$$G = g(\theta, \phi)_{max} = \frac{4\pi R^2 P_{av}(\theta, \phi)_{max}}{W_{in}} .$$

(6.5.3)

In order to discriminate W_{in} to W_{rad}, **directivity** is defined similarly to gain, but now the calculations are referenced back to the radiated rather than the fed power, i.e.

$$d(\theta, \phi) = \frac{P_{av}(\theta, \phi)}{W_{rad} / 4\pi R^2} = \frac{4\pi R^2 P_{av}(\theta, \phi)}{W_{rad}} ,$$

(6.5.4)

and, again, directivity is usually described as the maximum directivity, i.e. $D = d(\theta, \phi)_{max}$.

Moreover, the **efficiency** of an antenna is defined as

$$n = \frac{W_{rad}}{W_{rad} + W_{loss}} = \frac{G}{D} .$$

(6.5.5)

Finally, another metric of gain or directivity is indirectly given by the **effective area** of an antenna that is defined by $a_e(\theta, \phi) = \dfrac{W_r}{P_{av}(\theta, \phi)}$, while, similarly as above, $A_e = a_e(\theta, \phi)_{max}$. It is given that $A_e = \dfrac{\lambda^2}{4\pi} G$.

6.5.4 Antenna bandwidth

Antenna bandwidth is usually defined in terms of the respective reflection coefficient's bandwidth. More specifically, an antenna may be considered as a load connected to a transmission line. Following the analysis of earlier sections on transmission lines, the antenna bandwidth is usually defined as equivalent to the corresponding reflection coefficient's bandwidth. And, the reflection coefficient's bandwidth is defined as the frequency range within which the coefficient's amplitude remains within the limit of at most 3dB larger than its minimum value. A more loose but certainly most popular definition of bandwidth that is more usually used by field and development engineers is one that uses a maximum value of the reflection coefficient's value. E.g., the most widespread corresponding value is -10dB, which means that the bandwidth of the antenna is defined as the frequency range within which the reflection coefficient's amplitude is smaller than -10dB.

Another definition of antenna's bandwidth relates to the antenna's gain or directivity, and states that the antenna's bandwidth is the frequency range within which the gain remains within the limit of at most 3dB smaller than its maximum value.

Finally, a definition of antenna bandwidth that is unique for this class of devices is one that relates to the antenna's radiation pattern. More specifically, the antenna bandwidth may be defined as the frequency range within which the antenna's 3dB-beamwidth remains within certain limits with respect to its value at the central frequency (e.g. not varying more than 10%).

6.5.5   Antenna polarization

Finally, antenna polarization is defined according to the direction of the propagated electric field vector with respect to the horizontal plane (x-y plane, or ground plane) or a plane that is characteristic to the specific antenna type (e.g. dipole axis, larger side of a horn antenna, etc.). In this sense the terms horizontal or parallel, and vertical or perpendicular are used.

More specifically, if the lines of force of the electric field are in right angles with respect to the Earth's surface, then the wave is vertically polarized, whereas if the lines of force are parallel to the Earth's surface then the wave is horizontally polarized. For any other reference surface different to Earth, the respective definitions are "perpendicular" and "parallel" polarization respectively.

At times, the electric field's lines of force are neither horizontal neither vertical, nevertheless do have a constant direction; this is a linear polarization. Nevertheless, it is very usual that electric lines of force rotate; in such cases there may exist either the circular or elliptical polarization schemes, which are not further discussed herein.

6.5.6   Microstrip patch antennas

As long as textile antennas are concerned, it can be easily figured out that there are certain limitations on the available designs due to inherent limitations of the material on which such antennas are crafted (i.e. textile material). More specifically, due to the fact that textile antennas are actually intended to be used as *wearable* antennas, it happens that all the available designs and constructs in the literature refer to **textile patch antennas**. Thereupon, a short discussion on patch antennas is given below.

Microstrip patch antennas were first introduced during the second half of the twentieth century and are based on the observance that microstrips may radiate electromagnetic waves effectively given certain limitations (Mitropoulos, 2005). An example of a patch antenna is depicted in Figure 6.36. In the left side of the figure, the width and length of the patch are illustrated, together with the feeding transmission line (the line is connected to the source). Also, there is a substrate of thickness h, and a ground plane. The substrate has a relative permittivity equal to ε_r, while the thickness of the patch is equal to t.
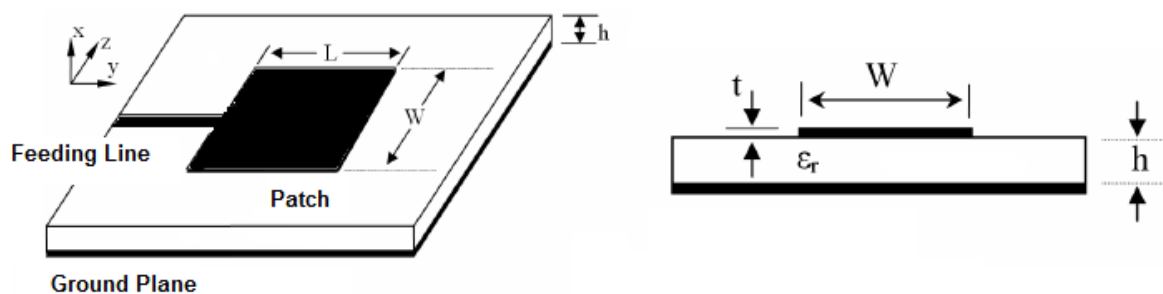

Figure 6.36: Patch antenna design example (Angle and side views).

Due to inherent design limitations, patch antennas usually radiate most effectively towards the direction that is perpendicular to the substrate surface and opposite to the ground plane. Different patch layouts are proposed in the literature, yielding rectangular, circular, ring, or other complex patch layouts. More specifically, there are analytic expressions yielding the appropriate width and length of a rectangular patch like the one in Figure 6.36 according to the desired frequency of operation; nevertheless the simple shape of the patch in Figure 6.36 results in a narrow bandwidth and linear polarization. In order to achieve circular or other polarization schemes, various patch shapes are introduced, like the circular ring patch in Figure 6.37(a). Other shapes that are more appropriate in order to achieve higher bandwidths include asymmetric patch corners and metal cut-outs at the point where the transmission line enters the patch, like in Figure 6.37(b).

Furthermore, a patch antenna may be fed using a microstrip or coaxial probes (see), or even using sophisticated techniques of induced fields due to proximity to nearby transmission lines etc. (Balanis, 2005) (Mitropoulos, 2005). Feeding a patch antenna also plays an important role on the achieved polarization, i.e. asymmetric feeding may result to circular or other polarization according to design requirements.
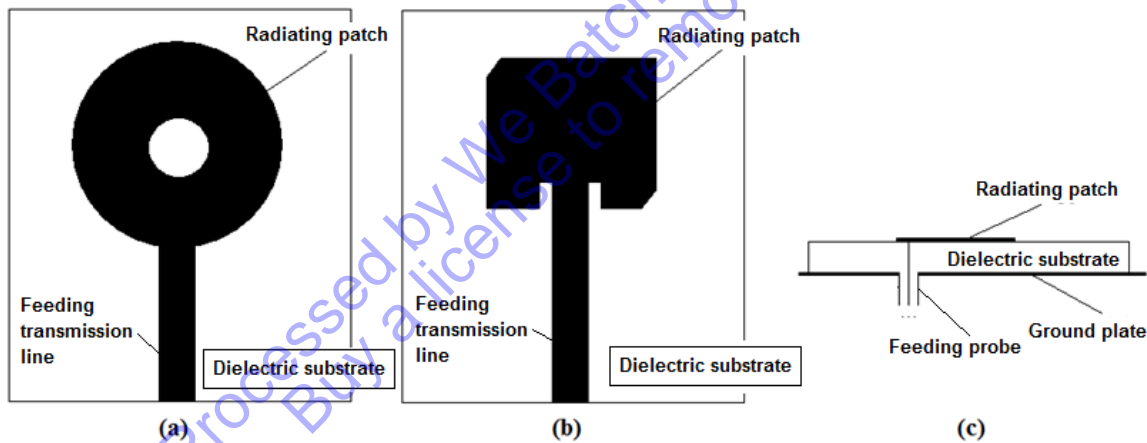

Figure 6.37: Various patch shapes and feeding techniques.

The length and width of a patch usually range between $\lambda/2$ and $3\lambda/2$, while the relative permittivity ranges between 2 and 12. Large thickness values and lower permittivity values are in general more efficient, in that they yield larger bandwidth and efficiency antennas (Mitropoulos, 2005). In the following Section, a more detailed discussion on textile patch antennas is given.

6.6 Textile antennas

6.6.1 Textile antennas in the literature

Research and technology development on textile antennas followed the introduction of the smart textiles concept in the nineties. Smart textiles are a generic term implying textiles with advanced functionality (mainly with respect to certain electrical-related characteristics) that can be applied to any industry from home to automotive and industrial applications; on the other hand, wearable smart textiles and thereby wearable sensors, antennas, chips etc. correspond to a specific applications area related to clothing and clothing materials. In recent years there has been an extensive research activity on the field of wearable computing, with passive and active components sewn on fabric and offering the means for developing wearable communications modules.

The main idea behind this concept is that smart textiles may be used as a platform carrying smart sensory and actuator systems, mainly for developing applications around a person or groups of persons. Smart wearable textiles are being made available today due to the availability of micro-electronics on the one hand and of new textile materials on the other, and according to Hertleer are classified as passive, active, and smart textiles. Passive textiles host sensors that collect data regarding biological, environmental and other data, active textiles may on top of passive actuate external switches and functions, and smart textiles may adapt their behavior according to the environmental and other circumstances (Hertleer C. , 2009). One particular area of research on the field is the design and development of antennas and antenna arrays on conductive fabric surfaces (textile antennas), i.e. using the cloth itself as the communication module rather than as a module host.

A wearable textile system will ideally comprise several components, like sensors, actuators, processing units, energy supplies, and a communication system. Ongoing research aims at developing circuit components and, eventually, integrated data processing and communication units out of clothing material. Up to day and to the best of our knowledge, only sensors and antennas have been successfully implemented using solely textile materials. Moreover, out of all the available design approaches, planar patch antennas are the most suitable, when using textile materials for antenna development, since they allow an easy integration with conventional clothing. Thereupon, textile antennas available in the literature currently solely employ planar patch designs.

It is widely considered that the development of textile antennas will be greatly beneficial to end-users like civil protection units, first responders etc., elderly users or patients in hospitals, or even everyday users for widespread commercial applications and smart networking. Indeed, textile antennas will greatly leverage performance and comfort of smart textile systems, by offering higher gain and operability with respect to integrated antennas while at the same time offering comfort and ease of use with respect to external but rigid antennas.

The feasibility of higher-than-normal antennas is also legitimate, mainly due to the large area of deployment that is available on the cloth surface giving the designer many choices and large margins from an antenna design point of view. Actually, the available area on a cloth's surface allows possibilities like using co-planar structures and/or planar arrays with antenna elements that may be selected from a wider set of different antenna types, as well as employment of different diversity schemes. However, the wearable character of the antenna obliges the designer to also examine the physical and physiological properties of the end product in order to avoid comfort problems which would potentially limit the success of the wearable textile based antennas.

Research and technology development regarding textile antennas can be traced back to the beginning of the new millennium, when wearable antennas partially based on textiles, were presented by Salonen et al. (P. Salonen, 2004). In particular, Salonen et al. dealt with the match performance and radiation characteristics of the antenna, as well as with the power absorbed by the human body. In consequent publications, Salonen et al. presented a dual-band E-shaped patch textile antenna, as well as specific studies on the behavior of an antenna under certain circumstances like bending etc. Furthermore, hybrid antennas using both metallic parts and fabrics were presented by Klemm, Santas and Nurul (M. Klemm, 2006), (J.G. Santas, 2007) and (H.M.R. Nurul, 2010).
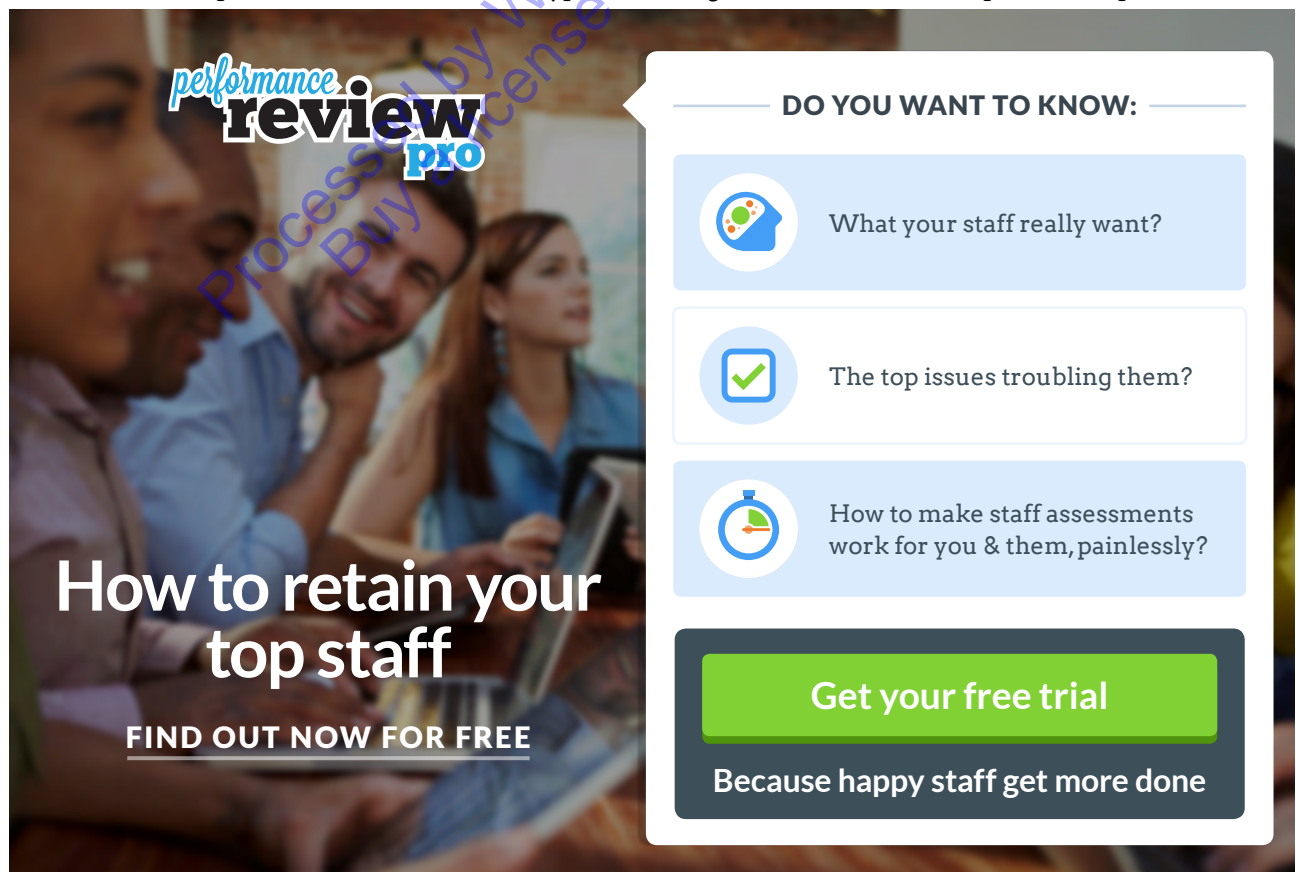
On the other hand, pure textile microstrip antennas have been investigated for employment in various frequency bands. Hertleer et al., as well as Vallozzi et al. reported 2.4GHz antennas for fire fighter garments that are made purely of textile-material (Hertleer, 2009) (L. Vallozzi, 2010). Santas et al. introduced a textile antenna for UHF-VHF bands (J.G. Santas, 2007b), while discussed the effects of variations in material property on a textile antenna performance. Dierk et al. proposed a textile patch antenna suitable for the GPS L1 band at 1.57542GHz in (A. Dierck, 2010). Furthermore, Alomainy et al. provided a parametric study of wearable antennas on various distances from the body (A. Alomainy, 2007). Distance from the bearer's body may have a substantial effect on an antenna's performance; backwards radiation may be suppressed using ground planes, but then additional elements need to be used in order to cover the entire azimuth plane. Dual-band textile antennas have also been reported, like an antenna for the 2.4GHz and 5GHz bands on EBG substrate by Zhu and Langley (S. Zhu, 2009) The effect of bending and crumpling has been also investigated by Bai and Langley that made an extensive study on the effects that bending may have on an antenna's efficiency, radiation pattern, gain and matching (Q. Bai, 2009).

Other research results towards the development of textile antennas include certain research projects, like an undergoing ESA project aiming at developing textile antennas for Iridium operating frequencies that require antennas with circular polarization. Furthermore, the European project ProeTex aims at developing smart electro-textile garments for firefighters and first responders at security missions (http://www.proetex.org/). The SFIT cluster is a European initiative and comprises a cluster of EU funded research projects, aiming to bring together projects addressing the area of Smart Fabrics, Interactive Textile (SFIT) and flexible wearable systems (http://csnej106.csem.ch/sfit/). Furthermore, SYSTEX is a coordination and support action project aiming at enhancing the research on wearable microsystems and e-textiles (http://www.systex.org).

Evidently, textile antennas despite comprising a relatively new technology have already come up with certain design and development examples, in several frequency bands, while various issues have been studied or confronted, like bending, textile substrate electrical characteristics robustness, dual band and wide band operation etc. Nevertheless, textile antennas are still an immature technology, and there are certain issues of particular interest that an interested designer needs to take into account, on top of concerns related to classical antenna design and development.

First of all, it is still unclear what are the electrical characteristics and properties of woven, knitted, sewn or embroidered conductive and dielectric fabrics. It is important to test and evaluate market-available conductive fabrics of various types, with respect to their electrical characteristics and their eligibility to be used as a basis for antenna development, as well as with respect to their properties as clothing materials. Specific and detailed models are needed, since the aforementioned characteristics are subject to change with respect to fabric density, waving techniques used, moisture absorbed by the fabric etc. Then, an antenna design should be tested in simulation regarding its behaviour under various bending and crumpled conditions, as well as change of electrical characteristics due to moisture and sweat absorption by the material.

Furthermore, conductive fabrics should posses a low and stable electrical resistance in order to suppress non-radiative losses i.e. Ohmic or reactive losses. A fabric with a resistance less than 1 Ohm/sq.m is considered as a rough limit for feasible operation (I. Locher, 2006). Furthermore, the fabric should be flexible enough to provide wearing comfort while at the same time the mechanical properties should allow a reasonably low degree of deformation of the antenna shape and, consequently, of its radiation properties. On the other hand, dielectric fabrics may be used as a substrate material. Electrical permittivity and permeability of the dielectric fabric should be carefully measured and apparently the dielectric fabric should exhibit the lowest possible conducting losses, i.e. a low loss tangent, in order to increase the antenna's efficiency. Furthermore, low permittivity is desired since it generally provides better efficiency and better bandwidth (Balanis, 2005) (I. Locher, 2006). Finally, a thickness of a few millimetres is desired, whereas the anticipated thickness variation of typical clothing materials should be kept as low as possible.

Besides the electric properties of the conductive and dielectric fabrics, additional fabric properties – depending on the role of the fabric and its contribution in the final garment's structure – must be taken into account: a) Mechanical properties (Tensile, tearing, etc.) b) Comfort properties (hand evaluation, thermal properties, water vapour permeability, etc.), c) Appearance properties (colour stability, shrinkage, etc.). The final design and fabrication decisions should consider implementation parameters in the garment, making sure that it will conform to rules of industrial scale production and ensuring that multifunctional garments will be available under feasible cost conditions and in adequate quantities.

6.6.2 Numerical and measurements results

In order to demonstrate the feasibility and applicability of textile antennas design and development, two test cases are presented herein that can be found in the literature. The first is a rectangular-ring shaped antenna for firefighter garment introduced by Hertleer et al. (Hertleer C.V.-L., 2007), and the second is a linear polarization patch antenna on felt substrate for 2.4 GHz communications introduced by Locher et al. (I. Locher, 2006).

6.6.2.1 A rectangular-ring shaped antenna for firefighter garment (Hertleer C.V.-L., 2007)

In this work, Hertleer et al. presented a textile antenna developed on aramid fabric with the purpose of integrating it on a firefighter's garment for short range communication to transmit the fire fighter's life signs to a nearby base station. The antenna's shape was that of a rectangular ring (see Figure) and it was optimized for operation within the entire 2.4-2.4835 GHz frequency band. More specifically, a bandwidth of return loss lower than -10dB was required, while the antenna gain should be maximized for the aforementioned frequency band.

The proposed antenna in realistic operational conditions was supposed to be covered with several layers of textile material (comprising the protective garment of the firefighter) that would affect the antenna's characteristics. Furthermore, the antenna should operate in the presence of a body, which further affects the antenna. According the Hertleer, the proposed antenna provides enough robustness to preserve its characteristics under these circumstances.

Reproduction and Original Electrical Characteristics		Reproduction Results		Original Results
Substrate thickness	1.73 mm	Gain	3.6 dBi	Gain
Ground plane	10cm x 10cm	-10dB return loss bandwidth	125 MHz	-10dB return loss bandwidth
ε_r	1.85	3-dB beamwidth	66°	3-dB beamwidth
$\tan \delta$	0.015			

Table 6.2: Electrical characteristics and results comparison between reproduction and the antenna reported in (Hertleer C.V.-L., 2007).

In order to verify Hertleer's allegation, we reproduced the proposed antenna in a commercially available simulator and extracted numerical results regarding its return loss and gain radiation pattern. Herein, by "reproduced" we mean that we extracted the patch dimensions and electrical characteristics, designed a similar patch in the simulator and analyzed the proposed antenna in order to get the numerical results that are presented herein.

The dimensions and electrical characteristics of the reproduction were based on data included in the work of Hertleer. The former are illustrated in Figure 6.38 (upper left), while the latter are included in Table 6.2. According to our results, the antenna gain is equal to 3.6 dBi at boresight, with a 3-dB beamwidth equal to 66° and a -10dB return loss bandwidth equal to 125 MHz (the band 2.4-2.4835 GHz included). The corresponding results of the original antenna were reported as in the following: gain equal to 4.36 dBi and 3.83 dBi (antenna uncovered or covered with protective garment respectively), -10dB return loss bandwidth slightly over 100 MHz, and 3-dB beamwidth equal to 71.1° and 70.2° (uncovered and covered respectively). Furthermore, the antenna gain measured in proximity to a human body was found to be equal to 3 dBi. According to the above, it is concluded that (i) the reproduced antenna's radiation characteristics are similar to the ones reported for the measured prototype and (ii) the proposed antenna is suitable for 2.4 GHz ISM band applications.
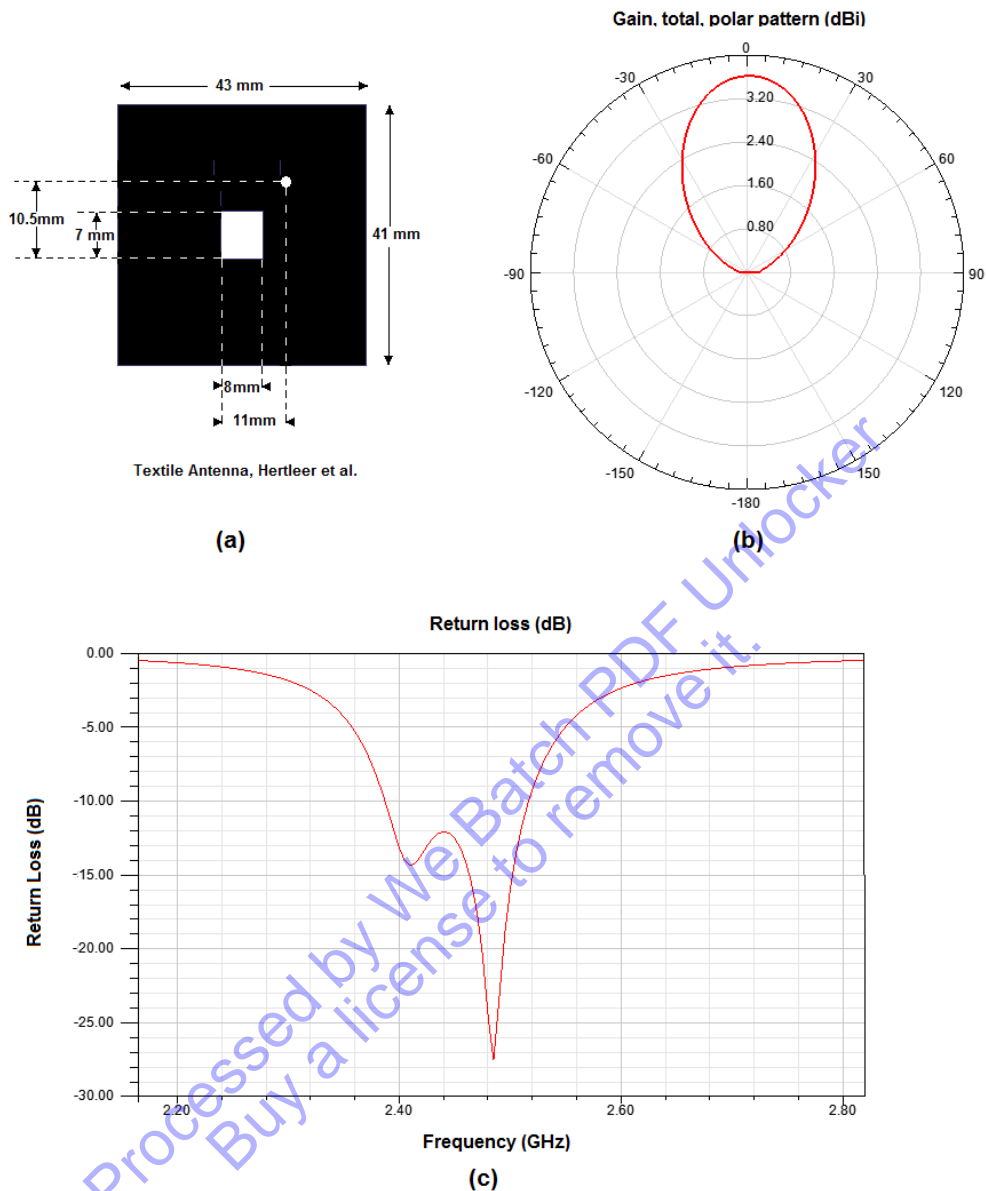
Figure 6.38: Reproduction and simulation results of a textile antenna
for firefighter garments at 2.45 GHz (Hertleer C. V.-L., 2007).

6.6.2.2 A linear polarization patch antenna on felt substrate for 2.4 GHz communications (I. Locher, 2006)

In this work, Locher et al. presented a detailed study on the design and characterization of purely textile patch antennas, including characterization of the electrical properties of several substrate materials available for the development of textile antennas. In this context, four textile antennas are presented, based on various substrates and with different polarizations. All antennas are fed via a microstrip line and are designed to operate in the 2.4 GHz ISM band. According to the authors, a microstrip feed not only guarantees a flat structure, but also allows the assembly of electronic components directly on the fabric in antenna proximity.

Out of the four antennas presented in this work two of them are circularly polarized, and two of them are linearly polarized. Furthermore, two of them are developed over a felt substrate with a thickness of 3.5 mm, and two of them are developed over a spacer substrate with a thickness of 6 mm. For comparison purposes, we have reproduced the linear polarized antenna over a felt substrate, using a commercially available simulator, and numerical results are presented herein.
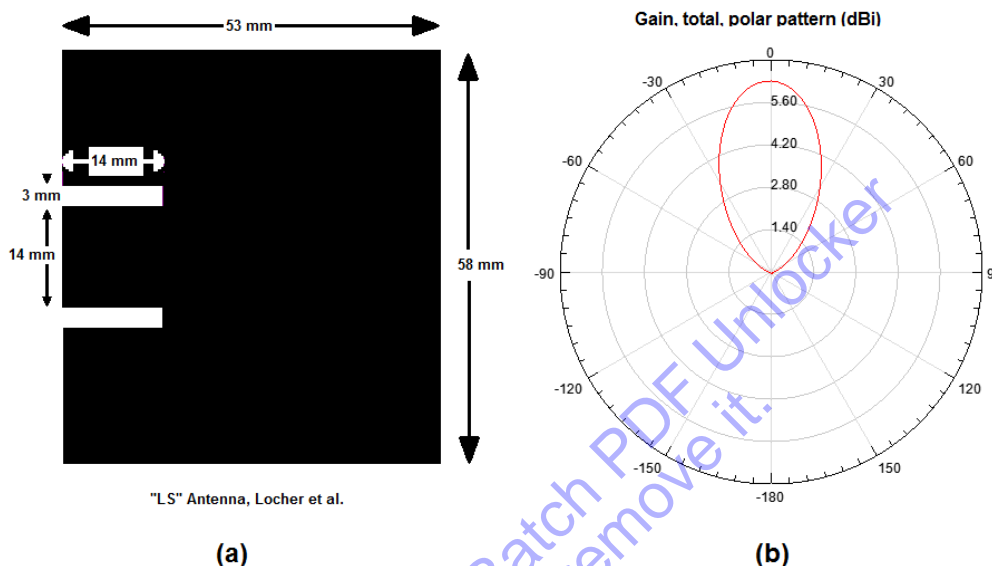

Figure 6.39: Reproduction and simulation results of a textile antenna
with felt substrate and linear polarization at 2.4 GHz (I. Locher, 2006).

Reproduction and Original Electrical Characteristics			Reproduction Results		Original Results
Substrate thickness	3.5 mm		Gain	6.3 dBi	Gain
ε_r	1.45		3-dB beamwidth	58°	3-dB beamwidth
$\tan \delta$	0.02				

Table 6.3 : Electrical characteristics and results comparison between reproduction and the antenna reported in (I. Locher, 2006).

In order to verify Locher's design, we reproduced the linear polarized antenna case over a woolen felt substrate and extracted numerical results regarding its return loss and gain radiation pattern. Again, by "reproduced" we mean that we extracted the patch dimensions and electrical characteristics, designed a similar patch in the simulator and analyzed the proposed antenna in order to get numerical results.

The dimensions and shape of the antenna are illustrated in Figure 6.40 (left), while the electrical characteristics of the patch and substrate are tabulated in table 6.3 above, together with numerical and compared measurements results. According to our results, the antenna gain is equal to 6.3 dBi at boresight, with a 3-dB beamwidth equal to 58°. Correspondingly, the original antenna was measured with a gain of 5.5 dBi in the case where a conductive fabric was used, and 9.0 dBi in the case where a copper foil was used, while the 3-dB beamwidth when using the conductive fabric was measured equal to 57° and 78° under flat and bent conditions respectively. Again, it is concluded that the reproduced antenna's radiation characteristics are similar to the ones reported for the measured prototype, while at the same time the proposed antenna is suitable for 2.4 GHz ISM band applications.

6.7   References

(A. Alomainy, 2007) Alomainy, A., Yang, H., and Davenport, D.M.,"Parametric study of wearable antennas with varying distances from the body and different on-body positions", *IET Seminar on antennas & propagation for body-centric wireless communications*, London, April, 24, 2007.

(Q. Bai, 2009) Bai, Q., and Langley, R., "Crumpled textile antennas", *Electronics Letters*, Vol. 45, p. 436, 2009.

(Balanis, 2005) C.A. Balanis, *Antenna Theory: Analysis and Design*, John Wiley & Sons, Hoboken, New Jersey, USA, 2005.

(D. Cottet, 2003) D. Cottet, J. Grzyb, T. Kirstein and G. Troster, "Electrical characterization of textile transmission lines", *IEEE Transactions on Advanced Packaging*, Vol. 26, No 2, 182–189, (2003).

(Y.-H. Chou, 2008) Y.-H. Chou, M.-J. Jeng, Y.-H.Lee and Y.-G.Jan, "Measurement of RF PCB dielectric properties and losses", *PIER Letters*, Vol. 4, 139–148, (2008).

(A. Dierck, 2010) Dierck, A., De Keulenaer, T., Declercq, F., and Rogier, H., "A wearable active GPS antenna for application in smart textiles", *32nd ESA Antenna Workshop on Antennas for Space Applications*, pp. 1–4, Noordwijk, The Netherlands, October, 5–8, 2010.

(M. Dirix, 2012) M. Dirix, O. Koch 'Conductivity Measurements of Silverpastes' Acta Polytechnica, Vol. 50 No. 4 (2010).

(Hertleer, 2009) C. Hertleer, *Design of Planar Antennas Based on Textile Materials*, Ph.D. Dissertation, Ghent University, Belgium, 2009.

(Hertleer C.R., 2009) Hertleer, C., Rogier, H., Valozzi, L., and Van Langenhove, L., "A textile antenna for off-body communication integrated into protective clothing for firefighters", *IEEE Transactions on Antennas and Propagation*, Vol. 57, No. 4, p. 919, April 2009.

(Hertleer C.T., 2008) Hertleer, C., Tronquo, A., Rogier, H., Van Langenhove, L,"The use of textile materials to design wearable microstrip patch antennas", *Textile Research J.*, vol. 78, no. 8, pp. 651–658, Aug 2008.

(Hertleer C.V.-L., 2007) C. Hertleer, L. Van-Langenhove, H. Rogier, and L.A. Vallozzi, "A textile antenna for firefighter garments", *Proceedings of AUTEX 2007*, Tampere, Finland, 26–28 June 2007.

(T.F. Kennedy, 2009) Kennedy, *T.F.,* Fink, *P.W.*, Chu, *A.W.*, Champagne, N.J., Lin, G.Y. and Khayat, M.A, "Body-Worn E-Textile Antennas: The Good, the Low-Mass, and the Conformal", IEEE Transactions on Antennas and Propagation, Vol. 57, No. 4, April 2009.

(M. Klemm, 2006) Klemm, M., Troester, G., "Textile UWB antennas for wireless body area networks", *IEEE Transactions on Antennas and Propagation*,Vol. 54, No. 11, pp. 3192–3197, Nov 2006.

(I. Locher, 2006) I. Locher, M. Klemm, T. Kirstein, and G. Troster, "Design and characterization of purely textile patch antennas", *IEEE Transactions on Advanced Packaging*, Vol. 29, No. 4, pp. 777–788, November 2006.

(J.C.G. Matthews, 2009) Matthews, J.C.G., Pettitt, G., "Development of Flexible, Wearable Antennas". 3rd European Conference on Antennas and Propagation, Berlin, Germany, March, 23–27, 2009.

(Mitilineos, 2006) S.A. Mitilineos, *Multipath Fading Mitigation Using Smart Antennas*, PhD Dissertation, NTUA Press, Athens, Greece, 2006.

(Mitropoulos, 2005) G.K. Mitropoulos, *Development of Integrated Patch Phased Array on Variable Permittivity Substrates*, PhD Dissertation, NTUA Press, Athens, Greece, 2005.

(H.M.R. Nurul, 2010) Nurul, H.M.R., Malek, F.S., Vandenbosch, G.A.E., Volski, V., Ooi, S.L., and Adam, I., "Evaluation of a wearable hybrid textile antenna", *Loughborough Antennas and Propagation Conference*, p. 337, Loughborough, UK, November, 8–9, 2010.

(Y.J. Ouyang a. W., 2007) Y. Ouyang, W. Chappell, "Measurement of electrotextiles for high frequency applications," Proc. IEEE MTT-S Int. Microwave Symposium, pp.1679–1682, 2005.

(Y.J. Ouyang, 2008) Y. Ouyang, W.J. Chappell. "High frequency properties of electro-textiles for wearable antenna applications", *IEEE Trans. Antennas and Prop.*, Vol. 56, No 2, 381–388 (2008).

(Pozar, 2005) D.M. Pozar, *Microwave engineering*, 3rd ed. Wiley, (2005).

(P.J. Soh, 2011) P.J. Soh, G.A.E. Vandenbosch, X. Chen, P.S. Kildal, S.L. Ooi, H. Alikbarian, "Wearable textile antennas' efficiency characterization using reverberation chamber", IEEE, AP-S/URSI 2011.

(P. Salonen, 2004) Salonen, P., Rahmat-Samii, Y., and Kivikoski, M., "Wearable antennas in the vicinity of human body", *IEEE Antennas and Propagation Society Symposium,* June, 20–25, 2004.

(S. Sankaralingam, 2010) Sankaralingam, S., and Gupta, B., "Development of textile antennas for body wearable applications and investigations on their performance under bent conditions", *Progress In Electromagnetic Research B*, Vol. 22, pp. 53–71, 2010.

(J.G. Santas, 2007) Santas, J.G., Alomainy, A., and Yang, H., "Textile antennas for on-body communications: techniques and properties", *European Conference on Antennas and Propagation*, pp. 1–4, Edinburgh, UK, November, 11–16, 2007.

(S.P. Savvaidis, 2011) S.A. Savvaidis, and S.A. Mitilineos, *Antennas, Radio Propagation and Radar Laboratory Notes*, TEI of Piraeus, Athens, Greece, 2011.

(L. Vallozzi, 2010) Vallozzi, L., Van Torre, P., Hertleer, C., Rogier, H., Moeneclaey, M., and Verhaevert, J., "Wireless communication for firefighters using dual-polarized textile antennas integrated in their garment", *IEEE Transactions on Antennas and Propagation*, Vol. 58, No. 4, pp. 1357–1368, April 2010.

(S. Vassiliadis, 2011) S. Vassiliadis, N. Stathopoulos, K. Prekas, S. Savaidis, "Behaviour of the conductive yarns and fabrics in high frequencies", *ITMC 2011 International Conference, Casablanca, 2011.*

(S. Zhu, 2009) Zhu, S., an d Langley, R., "Dual-band wearable textile antenna on an EBG substrate", *IEEE Transactions on Antennas and Propagation*, Vol. 57, No. 4, pp. 926–935, 2009.

7 Programmable Logic Controllers (PLC)

by

Kl. Prekas and S. Vassiliadis

Department of Electronics, Technological Education Institute of Piraeus, Greece

7.1 Introduction

The textile processes are often characterized by their complexity. Therefore specific control systems are necessary to supervise and rule the operations of the production activities. Additionally, since the various production steps are in sequential order, they require synchronization and control of the interconnection between the various phases of the production lines. The automation systems receive signals from the sensing and measuring devices, they process them and they generate commands to activate correspondingly the actuators, which in turn change the operation conditions of the machines.

According to the initial approach the control systems were realized through electronic circuits. The inputs of them received the signals of the sensing devices located on the machines and their output was driven the actuators. The decisions were made according to logical correlations between the values of the inputs, which were realized by the design details of the electronic system. Often this method of construction of a control system is known as wired logic approach. As it is expected, the logic relationships between the inputs and the outputs could not be changed easily since they require the hardware change of the electronic systems. Practically a new system should be designed in order to obtain the new characteristics demanded by the user.

A later alternative to the wired logic systems became possible after the spread of the use of the microcomputer systems in the industry. Industrial computer systems with specific characteristics have been designed to serve as general purpose control systems. The inputs of that systems can receive the signals of the sensing devices and the outputs can drive small loads or they can activate relays to drive heavier loads. The control logic i.e. the logical correlation of the inputs and the outputs ir realized through the applications software of the microcomputer system. This category of the industrial control systems are known widely as programmable logic systems (PLC's). The use of the PLC's has been spread rapidly and they have supported highly the automatization of the textile processes. The processes can be automated by the use of the PLC's without any need of extremely specialized electronic engineers as it was necessary for the design of the wired logic systems. The implementation of the PLC's presupposes two major actions: a. the selection of the suitable PLC among the existing models in the market or the selection of a specific configuration in the case of modular systems and b. the development of the application software according to the control logic to be realized. Often the software is developed using a symbolic graphics language, so that the elimination of the need of highly skilled programming personnel to be achieved.
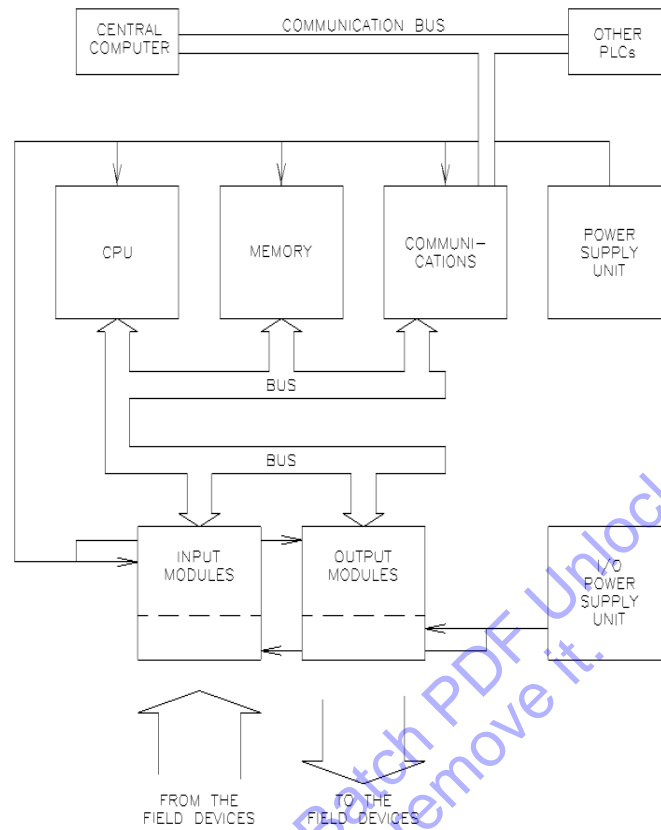
Figure 7.1: PLC's block diagram and its interconnections.

7.2   PLC characteristics

From the structural point of view, the PLC's form two major categories: the compact and the modular systems. The two types are used in applications with considerable different requirements and they are not competitive to each other.
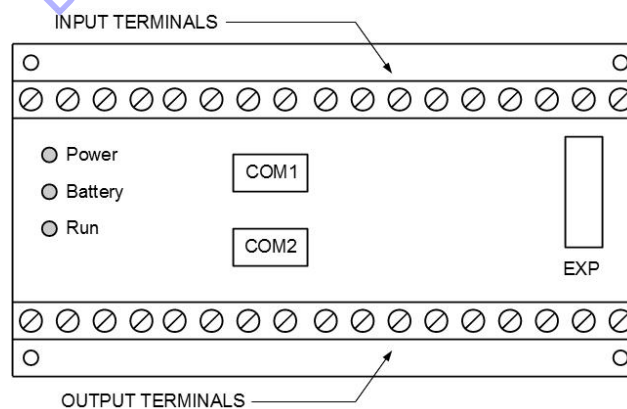

Figure 7.2: Typical outline of a compact PLC.

The compact PLC's physically are located in a single box with connecting strips for the input and the output signals. The case of the PLC is suitable for industrial use. The compact PLC's have a standard number and kind of inputs and outputs per specific model and constructor. As a rule, they can not be changed i.e. the user can not add or remove inputs and outputs. Thus it is essential to select the proper PLC by forecasting the possible future needs, in order to avoid change of the PLC due to lack of inputs or outputs in a next development phase of after a necessary change. Newer and sophisticated architectures permit the cascade connection of more that one PLC, allowing the development of higher capacity systems based on compact units. The compact PLC's are relatively of low prices and they are available in various configurations concerning the inputs and the outputs number available to the user. Typical number of inputs and outputs characteristic for compact PLC's is up to 20. Apart of the control inputs and outputs the compact PLC's are equipped with communication lines, power inputs etc. The software development can be made through specific consoles of from personal computers equipped with the necessary development software. The final version of the application code is downloaded to the compact PLC using the communication ports existing for this specific operation.
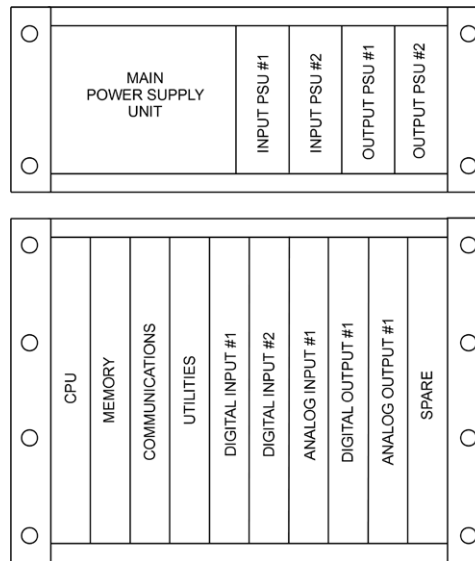
Figure 7.3: Typical outline of a modular PLC.

The modular PLC's are made to support the necessary expansion needs of the application. They consist of various modules of different kinds. They are placed on industrial racks and the correct selection of the type of the modules concerning their kind and their capacity results in the desired configuration. The initial configuration can be changed by removing and adding modules, of course within usually wide limits. Typically the number of the inputs and the outputs can be in the range of many decades or hundreds. The modular systems are usually more expensive than the compact ones and they are suitable for applications of higher complexity. The user selects the number of the inputs modules taking in account the type and the number of the inputs available in each specific module. In the same sense the output modules are selected and the final configuration will be available for the programming phase. In addition to the control input and outputs modules, there are available communications, power etc. modules.

7.3   Input and output characteristics

The inputs and the outputs can be of different kind designed to serve different needs of the users. However in order to support the industrial components and systems compatibility, the inputs and the outputs are standardized and a certain palette of them is being used in the industrial applications.

The inputs can be digital or analog. The digital inputs are simpler and they can receive signals corresponding to the logical levels "0" and "1". The analog inputs are more sophisticated and they can receive signals which are varying within certain limits. The analog input receives the signal, it conditions it and finally it samples it for the conversion of its amplitude in a digital word. This numerical value series generates the digital form of the signal to be used by the PLC. The analog inputs can receive either voltage or current signals. The typical standardized variation ranges for the voltage signals is 0–5 V and 0–10 V. For the electrical current signals is 0–20 and 4–20 mA. For the outputs of the PLC the categorization is the same as in the case of inputs.

The developer must take the output characteristics of the sensing devices and the input characteristics of the actuators in order to conclude to the final architecture of the PLC system and to define the exact number and kind of the single inputs and outputs or the respective number of the input and output modules.

7.4   Software development

The typical programming can be made using the graphical programming language known widely as "Ladder", due to the characteristic ladder-like structure of the programming graphics. However it is possible to use typical programming assembly or higher level languages coding tools as well. Every PLC is equipped with a certain firmware, a kind of simple operational system allowing the up- and downloading of the applications software, the start and stop of the operation etc.

The electrical signals are transmitted to the PLC over wires, which are connected to the inputs of the device. For a digital input the corresponding logical level is stored in a variable, able to be used by the program. The variables have standard format per PLC constructor. A typical format is "I1.2" corresponding to the second input of the first input module. The respective format exists for the outputs i.e "O2.3" declaring the third output of the second output module.

The values of the signals are represented and values of variables and they are used by the application software of the PLC in order to perform the control procedure. The application software realizes the logic of the correlations between the inputs and the outputs of the system i.e. the control algorithm. Any kind of change on the control algorithm can be made only by changing the application software of the PLC, without any hardware changing.

7.5   Operation of the PLC

The PLC is located in a suitable electrical box for the protection of it and of the cables and connectors. After the downloading to it of the final form of the application software, the PLC is ready for its industrial operation. The execution of the software starts by the dedication of specific values to the input variables according to the level of the signals connected on them. The execution of the control software uses the initial values of the variables. They remain constant even if the value of the signal changes during the execution of the control software. Any new value of the input will pass in the respective variable only after the end of the current control cycle and before the execution of the next control cycle. As it is obvious the fast response of the system to external changes, depends directly to the short duration of the control cycle of the software. The longer and complex the control software, the longer the execution time of the code and thus there will be a delay of the reaction of the system to the external changes.

7.6   A case study

A characteristic example of the use of PLC's has been selected in order to give the practical aspects of their implementation. The scenario of the application is as follows:
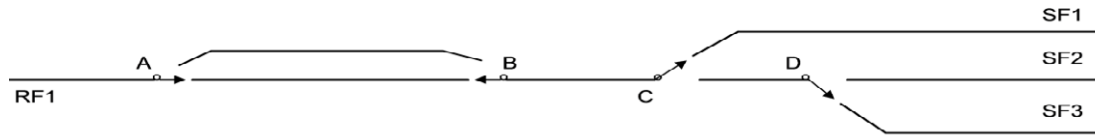
Figure 7.4: The bobbins transportation layout between roving and spinning frames.

In a spinning mill the transfer of the bobbins from the roving frame (RF1) to the ring spinning frame (SF) is automated. It is considered that a roving frame feeds three ring spinning frames (SF1, SF2 and SF3). The bobbins are transferred hanged on trains, which move on rails. On the branching of the rails there are remote controlled shunts. They take the proper positions so that the train will find the right path. The topology of the installation is as follows. There are four trains on the rails.

Upon the loading of the full bobbins on the ring spinning frame, the empty ones are transferred on the train. The ring spinning frame sends a train replacement request signal. The shunts take a proper position, so that the empty bobbin train will travel to the bypass rail between A and B. It stays there for a while. The shunts take a position which permits the full bobbin train to travel to the ring spinning frame. Then the shunts change their position again, so that the empty bobbin train waiting in the bypass rail will arrive in the roving frame rail.
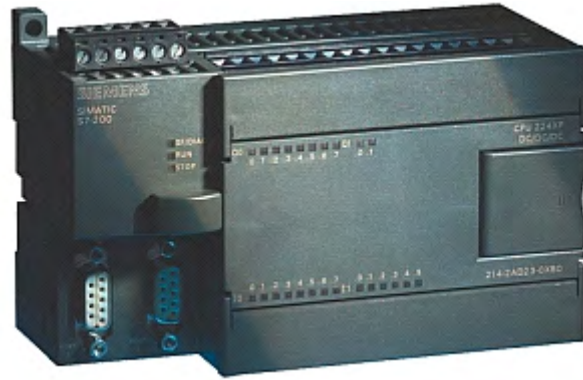
Figure 7.5: The SIMATIC-S7 PLC of Siemens.

In order to give a realistic solution on the above technical implementation, a PLC of Siemens has been selected. The SIMATIC-S7 is widely used and it has a very good technical support. From the family of SIMATIC-S7 the CPU 224 is used. We suppose that the input signals are connected to the SIMATIC-S7, the CPU evaluates their values, applies the combinational and sequential logic rules and finally activates the corresponding outputs. The outputs of the PLC drive the respective actuators for the control of the installation.
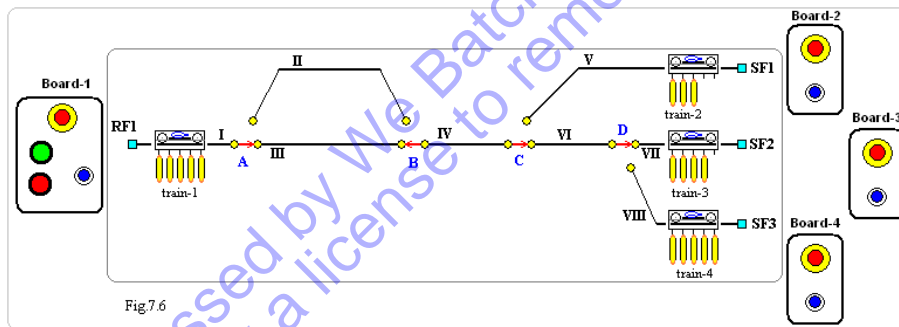
Figure 7.6: The operation buttons activate the inputs of the PLC.
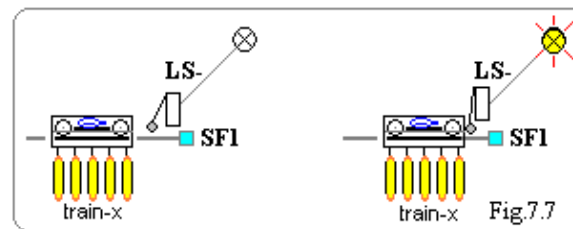
Figure 7.7: The arrived train activates the limit switch which in turn acts on the input of the PLC.
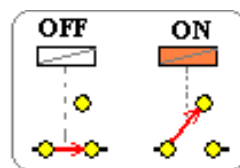
Figure 7.8: The shunts are activated by the outputs of the PLC through solenoids.

In the previous figures the interfaces of the inputs and the outputs of the PLC for the current application are indicated. The transportation system equipped with the input/output (I/O) signaling devices (switches and actuators) is given in the Figure 7.9.
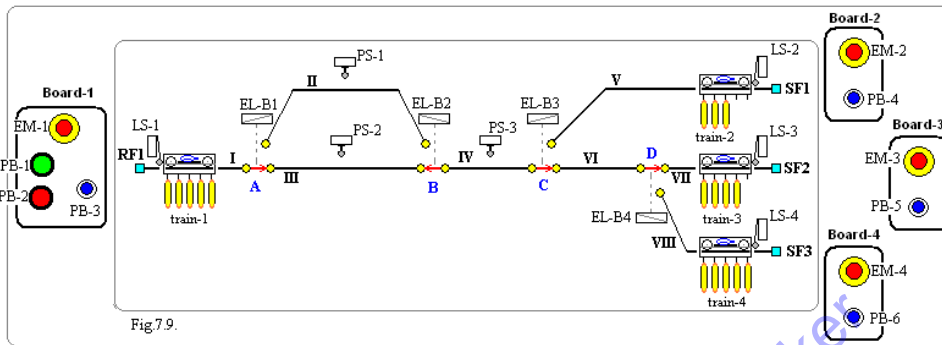
Figure 7.9: The outline of the installation with the I/O devices.

The input switches and the actuators are mapped on the inputs and outputs of the PLC, as in the following table 7.1. It is worth to mention that the physical signal caused by the pressing of the emergency switches is allocated on the input I0.0. In the software of the PLC, the emergency signal will be handled as the value of the input I0.0 (1 or 0, true of false etc).

Inputs			Outputs		
Mnemonic	Description	Inputs PLC	Mnemonic	Description	Outputs PLC
EMS	Emergency Stop	I0.0	D-1	Direction Train-1	Q0.0
PB-1	Start System	I0.1	M-1	Electromotor Train_1	Q0.1
PB-2	Stop System	I0.2	D-2	Direction Train-2	Q0.2
PB-3	Train on area RF1 ready.	I0.3	M-2	Electromotor Train_2	Q0.3
PB-4	Button Call from area 1	I0.4	D-3	Direction Train-3	Q0.4
PB-5	Button Call from area 2	I0.5	M-3	Electromotor Train_3	Q0.5
PB-6	Button Call from area 3	I0.6	D-4	Direction Train-4	Q0.6
LS-1	Limit Switch Area 1 (RF1)	I0.7	M-4	Electromotor Train_4	Q0.7
LS-2	Limit Switch Area 2 (SF1)	I1.0	EL-B1	Electromagnet of Shunt-1	Q1.0
LS-3	Limit Switch Area 3 (SF2)	I1.1	EL-B2	Electromagnet of Shunt-2	Q1.1
LS-4	Limit Switch Area 4 (SF3)	I1.2	EL-B3	Electromagnet of Shunt-3	Q2.0
PS-1	Pressure Switch Line-AB	I.1.3	EL-B4	Electromagnet of Shunt-4	Q2.1
PS-2	Pressure Switch Line-AB′	I1.4			
PS-3	Pressure Switch Line-CD	I1.5			

Table 7.1: Mapping table of the I/O signals on the inputs and outputs of the PLC.

After the hardware connections of the input and output devices to the PLC, the next step is the software development. The code can be written in the classic way, based on programming script or in a graphics based programming language, the ladder.
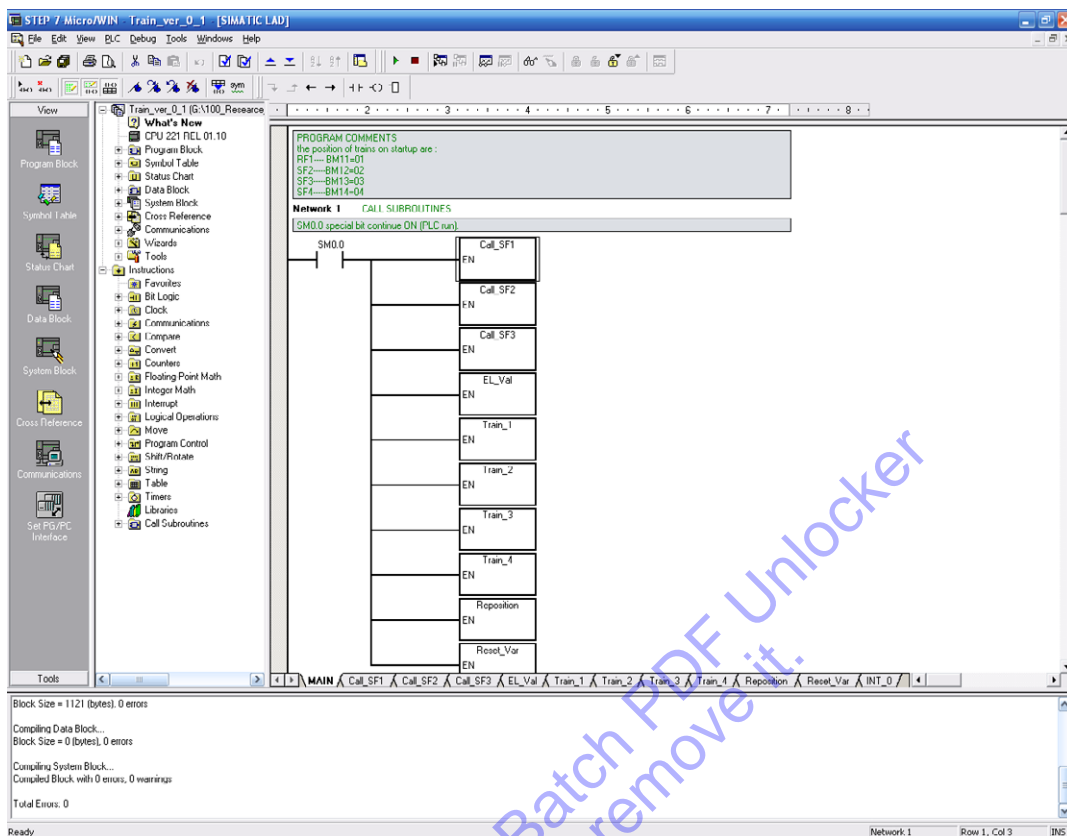
Figure 7.10: The V4.0 STEP 7 MicroWIN programming environment.

The programming environment used for the software development is the V4.0 STEP 7 MicroWIN of Siemens. It allows fast and reliable programming supporting the visual realization of the code.
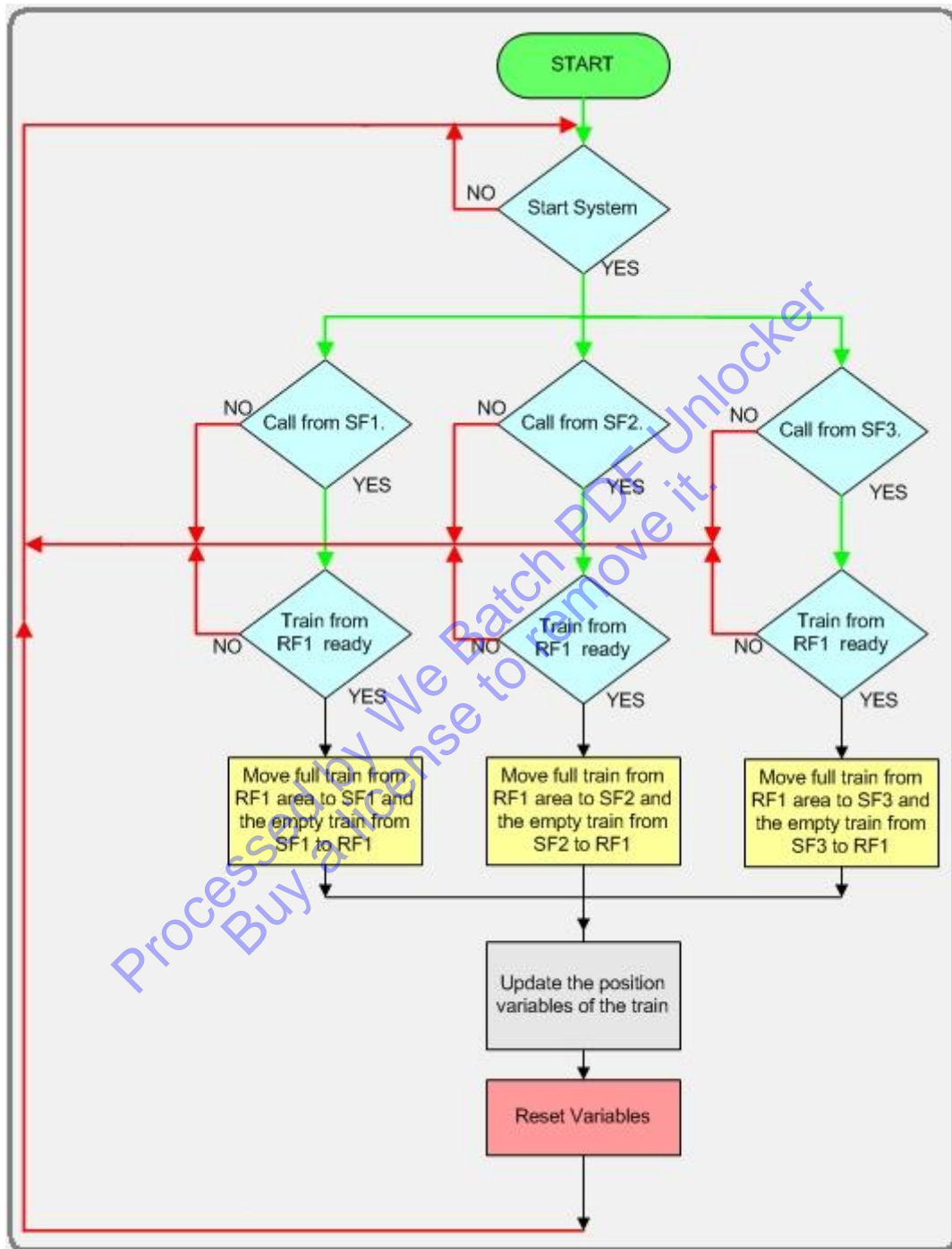

Figure 7.11: The block diagram of the application software.

The software is structured and it consists of the main part and the subroutines. In the main part exist the initialization, the start and stop procedures. Also the call wait stage is characteristic of the operation of the main part. The CallSF subroutine is managing the transportation of the train to the spinning frame and the return of the empty train to the roving frame. It acts on the shunts and receives signals from the limit switches and intermediate variables. The subroutines TrainX rules the motion of the trains taking in account their positions and the requested actions. Some other routines like Reset_Var, Re_position and El_Val are supporting parts. Figure 7.11 gives the total structure of the application software in the form of a block diagram.
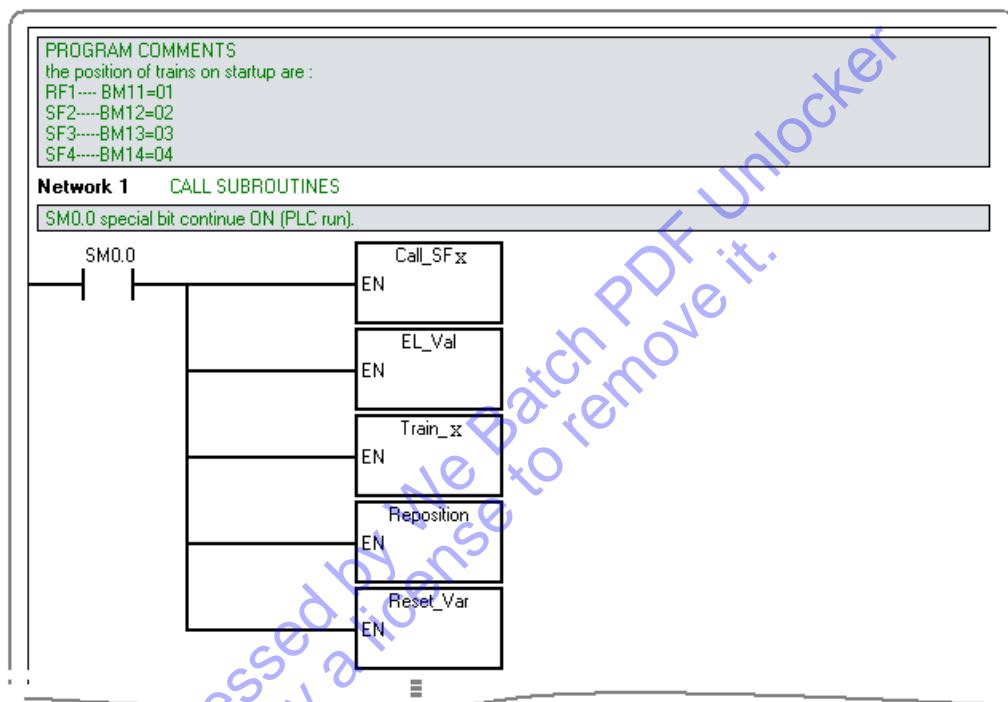
Figure 7.12: The main part of the program (In real there are 3 different Call_SFX and four Train_X routines).
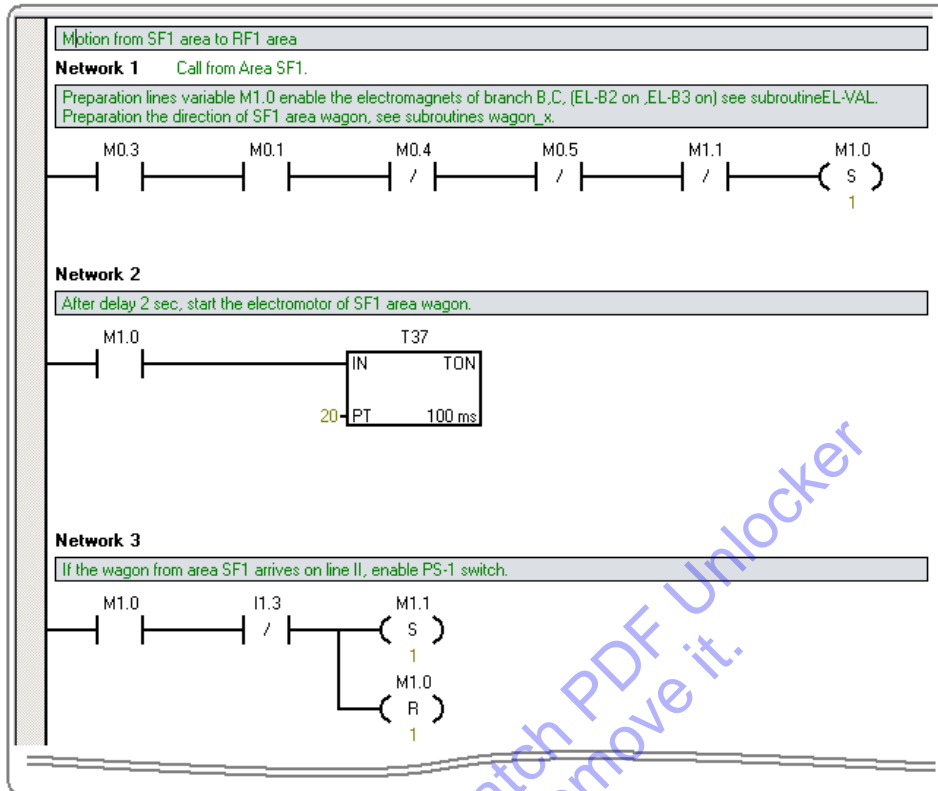
Figure 7.13: The first part of the Call_SFX subroutine. It continues in the same sense for the various parts of the route.
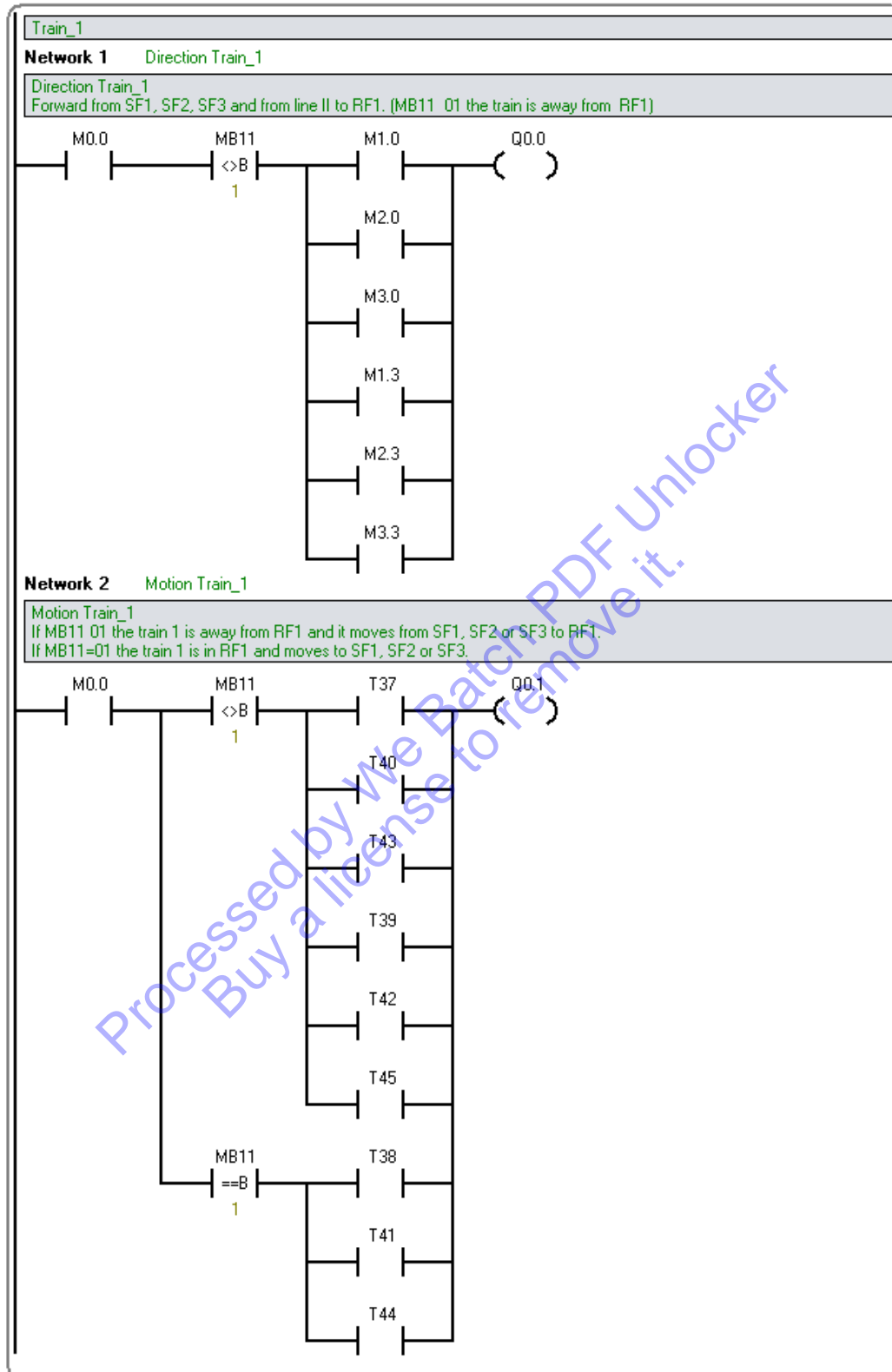
Figure 7.14: The Train_1 subroutine. The rest derives by the cyclic rotation of the indices.

The above figures present the structure and partly the realization of the application software code for the development of a bobbin transportation system between the roving frame and the spinning frames. There are many similar applications in the textile production processes. Thus this example is indicative and characteristic for the wide field of use of the Programmable Logic controllers in the textile industry. If a reader wants to access the full code of the present case study, he/she is kindly invited to contact the authors.

As it is shown, the use of the Programmable Logic Controllers gives a satisfactory solution to many technical problems and applications of the textile processes. The hardware wiring is not complicated and the software programming can be successfully performed by the user or by any other skilled person. The PLC's can be replaced without essential difficulty in the case of a damage or malfunction. The use of the PLC's has been widely spread all over the world and it is a de facto technological standard for the automatization of the operation of production machines, transportation systems, testing instruments etc.

7.7   Acknowledments

The publication of the pictures related to the SIMATIC-S7 has been possible only after the kind permission of the producing company Siemens. Obviously, any other kind of use is not permitted (indicative cases: copy, reproduction, publication etc), without the explicit permission of Siemens.

Explicitly and unconditionally it is recognized that these pictures and any other related informative material contained in this chapter its an exclusive property of Siemens. Any improper use of it by any means and without the explicit permission of Siemens is illegal and thereby Siemens may demand the recovery of any direct or consequential damage may having occur.

7.8   References

http://www.automation.siemens.com/mcms/programmable-logic-controller/en/simatic-s7-controller/s7-200/software/Pages/Default.aspx

Vassiliadis S., "Automation and the Textile Industry", EUROTEX, Portugal, 1996.

8 Wireless Body Area Networks and Sensors Networking

by

D. Goustouridis and E.D. Kyriakis-Bitzaros

Department of Electronics Engineering, Technological Education Institute of Piraeus, Greece

8.1 Introduction

The rapid development of the microelectronics and micromechanics, both in design and manufacturing, within the last decades allowed for huge advancements in the areas of sensing devices and systems. These advancements make possible:

- The development of new generation of sensors based on Micro & Nano ElectroMechanical Systems (NEMS & MEMS), or even Micro OptoElectroMechanical Systems (MOEMS).
- The miniaturization of electronics devices, with minimal requirements in power consumption
- The realization of various types of autonomous wireless networks.

These developments are critical for the design and implementation of the so call Body Area Networks (BANs) or Wireless Body Area Networks (WBANs) (Yang, 2006). In these networks a wide variety of sensors could be attached on clothing, on body or even under the human skin and transmit the environmental and/or body signals, through the network to specified control and decision points. Furthermore, in addition to the sensors a series of actuators could be also included in the WBAN, thus the network in addition to the collection of data from the environment and/or body it is capable of reacting with the environment and change the current conditions.

The wireless nature of the networks, the increased capabilities of the contemporary mobile devices (smart phones, PDAs etc.) and the wide variety of the sensors that could be used, offer numerous innovative applications not only for special application domains such as military, aerospace etc., but even for everyday life and for everyone's use. The most important of these applications is health care improvement, in a more efficient and cheaper way, in order to ameliorate the quality of life and extend life expectancy.

8.2   Sensor Networks. Why?

Electronic devices and computers are able of processing a wide range of diverse signals and act accordingly. These signals coming from the environment or the human body are analogue in nature and cover a wide range of parameters including temperature, pressure, humidity, odors, chemical or biological properties, sound, light (or images) etc. As they are recorded and processed by the electronic modules not only give information about the conditions of a certain area of the outside world or even about the conditions inside the body but could be further used for interaction with the monitored environment or the body and solve tune or recalibrate unwanted situations and events.

The events that a WBAN should handle are very similar to the events that the human brain should care of. For example if a person smells smoke from one direction decides to take an alternative path, or if he/she feels sick decides which medication he/she will use. This is exactly the situation that a WBAN try to emulate: A WBAN that is fitted on a patient body, collects important data such as heart rate, blood pressure, biochemical parameters etc. and alerts the patient itself, and/or the doctor at his office several kilometers away.

Three are the most critical parameters in a WBAN:

- The sensors and the electronic devices should be as small as possible, to be wearable without disturbing the everyday activities.
- The required power to operate the WBAN should be as small as possible in order to allow the use of small weight batteries that last very long time or even better the WBAN should collect energy from the environment (energy harvesting), so to be battery-less.
- The communication protocols should be implemented in a very efficient way to guarantee security and high throughput of information with low energy consumption.

8.3   WBAN Applications

Health Applications, Point of Care

The main use of WBANs is for health applications monitoring the physiological status of a patient either in the hospital environment or at home. For example patient monitoring is of high importance in the waiting areas of emergency departments or at the recovery phase after a surgery, to prevent lack of attention of a patient's health deteriorating rapidly. Applications of WBANs at home include monitoring of a patient with chronic diseases (e.g. pneumonological, cardiovascular diseases etc.), or during the recovery phase at home. Moreover, WBANs could also be used as diagnostic tools for monitoring physiological parameters (e.g. blood pressure, glucose) at home or outdoor environment during everyday activity.

The most common areas of use are:

- *Cardiovascular diseases,* to prevent myocardial infarction, monitor episodic events etc.
- *Cancer detection,* by monitoring the nitric oxide emitted from cancer cells.
- *Asthma,* by monitoring of allergic agents in the environment.
- *Diabetes,* glucose level monitoring, by monitoring in real time the glucose level and inject insulin automatically.
- *Alzheimer, depression and elderly people,* by detecting any abnormal situation (i.e. via accelerometers and positioning system to monitoring the activity of the person).
- *Epileptic Seizures Strike early warning,* by monitoring the EEG activity.
- *Telemedicine systems,* to support unobtrusive ambulatory health monitoring for long period of time.

Sport training

WBANs can be used to identify specific postures and provide biometric and technical feedback in many sports, to improve the performance of both elite and amateur athletes and prevent from injuries due to incorrect postures.

Military

WBANs can be used in the battlefield to connect the soldiers, report their activities to the commander and monitor their physical status (stress etc.).

Vehicle drivers

WBANs can be used to monitor driver behavior, i.e. blink-rate, yawning, eyebrow raise, chin-drop, head movement, or physiological signals such as EEG, to determine the alertness level of the driver and to prevent sleeping episode by alerting the driver.

8.4   WBAN Architecture

A WBAN is a particular case of a WSN (Wireless Sensor Network) that has certain special requirements and constrains (Latre et.al. 2011, p. 2):

- A conventional WSN is composed of a large number of sensors that, usually are distributed in large areas and sometimes at not easily accessible places (Akyildiz et.al. 2002, p. 394). For that reasons in most cases the WSN employs redundant nodes to cope with diverse types of failures. In contrary, a WBAN consists of a limited number of sensor/actuator nodes placed strategically on the human body, or hidden under clothing.
- In WBANs the transmission of sensor's data is critical and it is accomplished, usually in regular intervals, without the employment of redundant nodes, directly to a central personal server (PS), while the data exchange in a general purpose WSN is event driven, which means that data transmission takes place in an irregular time base, when an event occurs and multihop paths do exist. Furthermore, due to the personal and confidential character of the data within a WBAN, data encryption offering high-level of security and confidentiality is required.

- While energy conservation is definitely beneficial, the power consumption of the WBAN nodes it isn't as critical as for the WSN, since the replacement of the batteries is much easier. However, due to the proximity of the WBAN with the user's body, low-power transmission is mandatory to avoid hazardous influences.
- As a WBAN user moves around, the WBAN shares the same mobility pattern, while in many case the network may interfere with the WBANs of other users. In contrary a WSN is usually considered stationary.

Figure 8.1 illustrates a simplified WBAN configuration with its connection to the outside world. The WBAN consists of a number of Sensor Nodes (SN) and Actuator Nodes (AN). The sensor/actuator nodes communicate with a Personal Server (PS) that is a special node responsible for building and controlling the overall body network. The PS node could be a specifically designed node, or a general purpose device such as a smart phone or a PDA with a special application built-in. The PS transmits the measurement data to the Wireless Personal Area Network (WPAN) that consists of the user's house internet modem/router or other wireless connected home devices. Through the WPAN the WBAN is connected to the internet to enable remote access of user data, e.g. a physician, an emergency station or a hospital could monitor or alarmed for a user/patient physiological conditions.
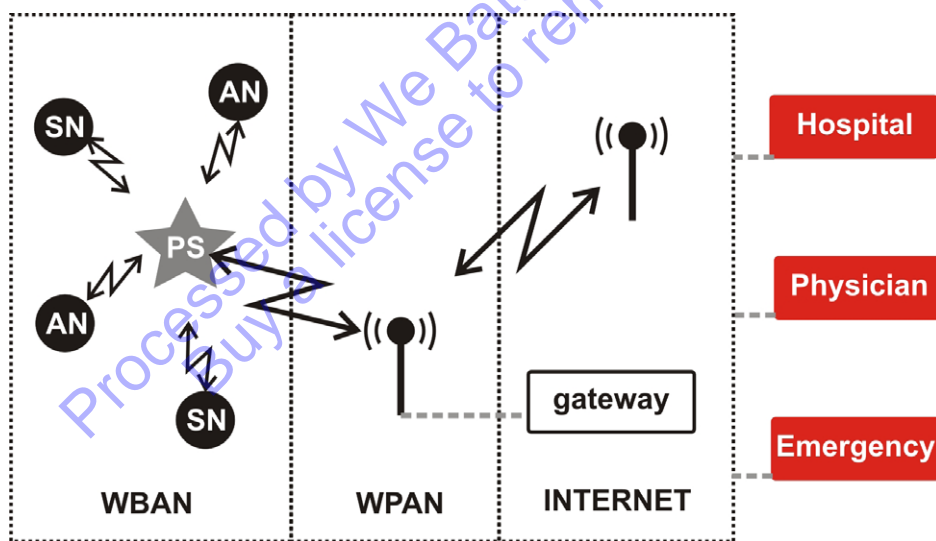
Figure 8.1 WBAN configuration and wireless connection with the internet.

8.4.1   Sensor and Actuator Node

The heart of an SN or an AN is a low-power microprocessor, which is responsible for the control of the RF, the memory and the sensor or actuator modules, respectively, as well as for the implementation of the power management scenario, which is required to maximize node autonomy. Figure 8.2, illustrates the typical structure of an SN or an AN of a WBAN, however, in many cases complex nodes acting as both sensors and actuators do exist in a WBAN. A description of the components comprising an SN or an AN is given bellow.
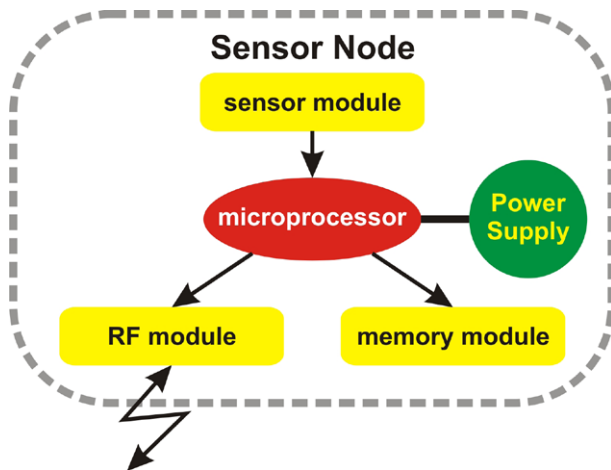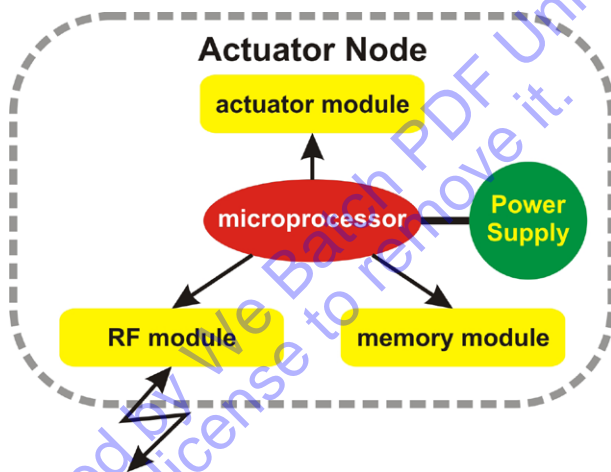
Figure 8.2a. Typical configuration of Sensor Node

Figure 8.2b. Typical configuration of Actuator Node

Sensor/Actuator Module

Sensor and Actuator module is the key component of a WBAN node. These modules connect the physical world (analogue-physiological signals) to the electronic systems (monitoring, analysis and decision taking through the appropriate software). The SNs and ANs are usually exposed directly to or even implanted inside the human body in order to be able to measure the physiological signals and parameters. For example, to monitor the blood pressure or the blood glucose the sensing area of the sensor module must be directly exposed to blood stream. For that reason: a) the size of the modules must be small enough to preserve the normal operation of the body and b) the module area exposed to the body must have physical compatibility to human tissues, especially in the case of the implantable ones. For that in most cases the development of new manufacturing techniques and the synthesis of novel biocompatible materials are of crucial importance in the design and implementation of bio-sensors. In some other cases e.g. temperature measurement, electrical activity etc. the biocompatibility issue is not so crucial.

Actually, the sensor module comprises of two subsystems: a) the sensing element that converts the physicochemical signal to an electrically measurable signal and b) the conditioning circuit that amplifies and converts the weak and susceptible to noise sensing element's signal to a more stable one such as voltage, current or frequency. Depending on the electrical property used to sense the parameter under measurement two major categories of sensors exist, namely, capacitive and resistive ones (Tsoukalas et.al. 2006, p. 1). In capacitive sensors the physicochemical signal under measurement is converted to capacitance changes, while the condition circuit converts that capacitance changes to frequency or voltage changes. In resistive type of sensors the measurement signal is converted to resistivity changes, while the condition circuit converts that resistivity changes to current or voltage changes.

According to how sophisticated the condition circuit is different tasks can be implemented such as temperature compensation, calibration etc. In some cases mixed analogue/digital circuits are used, so that the sensors' output could be an insensitive to noise digital signal. In the case of the sensors that measure the body electrical signals (ECG, EEG, EMG) (Nemati et.al. 2012), the sensing element is an electrode while the condition circuit amplifies and stabilizes the weak electrode signals. A very important parameter of the sensor/actuator modules is the measurement accuracy of the physiological signal, while this accuracy determines the measurement accuracy and reliability of the whole system.

Microcontroller

In the Sensor Node the main task of the microprocessor is to read the sensors' data and then transmit them, after processing if necessary to the PS. In the case of an Actuator Node the microprocessor when receives an order from the PS, triggers the actuator to perform an operation, e.g. to inject some drug.

Moreover, the microprocessor of the SN or AN is responsible for the implementation of the power management scenario aiming to extend the autonomous and service-less operation time of the node. Finally, it runs the necessary diagnostics ensuring the correct operation (health) of each node and enable through their results the PS to check the health of the entire WBAN. Usually, the on-board processing requirements are low, so simple, low-cost and low-power microcontrollers such as Texas Instruments' MSP430™ Ultra-Low Power series (TI 2012), ATMEL's tinyAVR picoPower series (Atmel 2012) or equivalent are used.

Memory module

The memory module usually on-chip flash memory or RAM) is used for storing the firmware of the node as well as for temporally storage of the network and personal data and the measurements. The memory requirements are very much application dependent and range from a few Kbytes to several hundreds of Kbytes.

Power source

The SN and AN consume power for sensing or actuating, communicating and data processing. Most of the energy is consumed for data communication. The power is stored either on batteries (rechargeable or not) or capacitors. In some systems special energy harvesting subsystems are used for renew their energy. In such systems (Huang et al 2009) an amount of energy can be harvested from the environment (vibrations, heat, light radiation, electromagnetic fields etc.) and then stored to a capacitor or rechargeable the battery, so the sensor/actuator node could be fully or partially autonomous in energy. While a fully energy autonomous approach (with no battery) is very attractive, it is very difficult to implement in applications where a high data rate transmission is required. In any case the microcontroller is responsible for the power saving policies (power management) by shutting down the subsystems that are in an idle state.

RF module

The RF module is responsible for the wireless communication within the WBAN and consist of the transceiver and the antenna. The antenna is the one of the most critical components of the node, since its design influences considerably the efficient operation of the WBAN. The transceiver RF of the RF module is responsible for the transmission/reception of data between the SN/AN and the PS. Several issues must be taken into account in the design of the RF module, mainly the frequency and the emitter RF power that are used. First of all body sensors/actuators are placed on or even in the human body, so the propagated electromagnetic wave could be diffracted around the body or absorbed from it. The transmission signal must be of low power, but with enough bandwidth for the required data rate, to insure low Specific Absorption Rate (SAR) from the tissues according to international SAR regulations. Further issues that should be taken into consideration are the location of the WBAN, which could be indoors or outdoors and how severe is the interference from other users in proximity. The design of the antenna and the material to be used is very crucial for the communication of the node and depends on the node placement and the allowable volume that usually is very limited. The RF module is the most power consuming one, so must be in idle or shutdown mode when it is not in use.

Finally, according to the sensor type and the WBAN application continuous or burst mode data transmission at different rates is required, so the communication protocol implemented must have different specifications (please refer also to section 8.5). The most widely used sensors in WBANs, their applications and the associated data rate requirements (Latre et.al. 2011, p. 4, Chen et.al. 2011, p. 177, Ullah et. Al. 2009, p. 801) are summarized in Table 8.1.

8.4.2   Personal Server

The Personal Server is a device that gathers the information acquired by the sensors, activates the actuators, processes the data and informs the users (patient, doctor, hospital etc.) via an external gateway (i.e through the internet, cellular phone infrastructure, etc.) or a display. It consists of the power unit, an efficient general purpose processing unit, memory and a transceiver. The software of the PS may be complicated enough to take decisions for certain situations and send commands to the ANs to resolve them or could receive external orders by the person monitoring the WBAN user. In many implementations a PDA or a smart phone, offering access to the cellular infrastructure, with a specially developed application could be used as a PS for a WBAN.

Sensor Type	Application	Data rate
Accelerometer & gyroscope	To recognize and monitor body posture, for applications such as virtual reality, health care, sports, and electronic games.	High
Blood glucose	To monitor the amount of glucose circulating in the blood.	High
Blood pressure	To measure the systolic and diastolic human blood pressure.	Low
CO_2 gas sensor	To monitor changes of gaseous carbon dioxide levels and/or oxygen concentration during human respiration.	Very low
ECG sensor	To record the heart's electrical activity, to diagnose a heart disease or to monitor the effectiveness of heart medications.	High
EEG sensor	To record electrical activity within the brain.	High
EMG sensor	To record electrical signals produced by muscles contraction or at rest, for healthcare in nerve and muscles disorders.	Very high
Pulse oximetry	To measure the oxygen saturation in the blood, usually in patients with pneumonological diseases.	Low
Humidity & Temperature	To measure the temperature of the body and the ambient humidity.	Very low

Table 8.1. Typical applications and data rate requirements of sensors in WBANs.

8.5   Communication Protocols / Platforms

For the reliable and secure operation of a WBAN the communication protocols and the platform that is used is a very critical issue. The WBAN is a network that is part of a wireless (or wired) personal area network (PAN/WPAN) at the home (or the area) where the user of the WBAN lives. That network may include the personal computer, a PDA, a smart phone, home cinema, peripherals like printers etc. The PAN is connected via the router to the local area network (LAN/WLAN) that could be the network of the building, the office or the hospital where lives, works or stays the person of interest. The LAN is connected to a metropolitan area network (MAN/WMAN) and then to the wide area network (WAN). This situation is illustrated in figure 8.3.

As it is obvious, the transmission of the WBAN data over the internet as described above should be strictly private and confidential so data encryption is mandatory to protect the user's privacy. Moreover, in health care applications, the WBAN must be accessible in cases when the user is not capable to give authorization, i.e. to guarantee accessibility in trauma situations and at the same time should also guarantee the confidentiality of unauthorized persons. The data encryption becomes more difficult due to limitations in energy consumption since security and privacy protection mechanisms require a significant amount of energy.
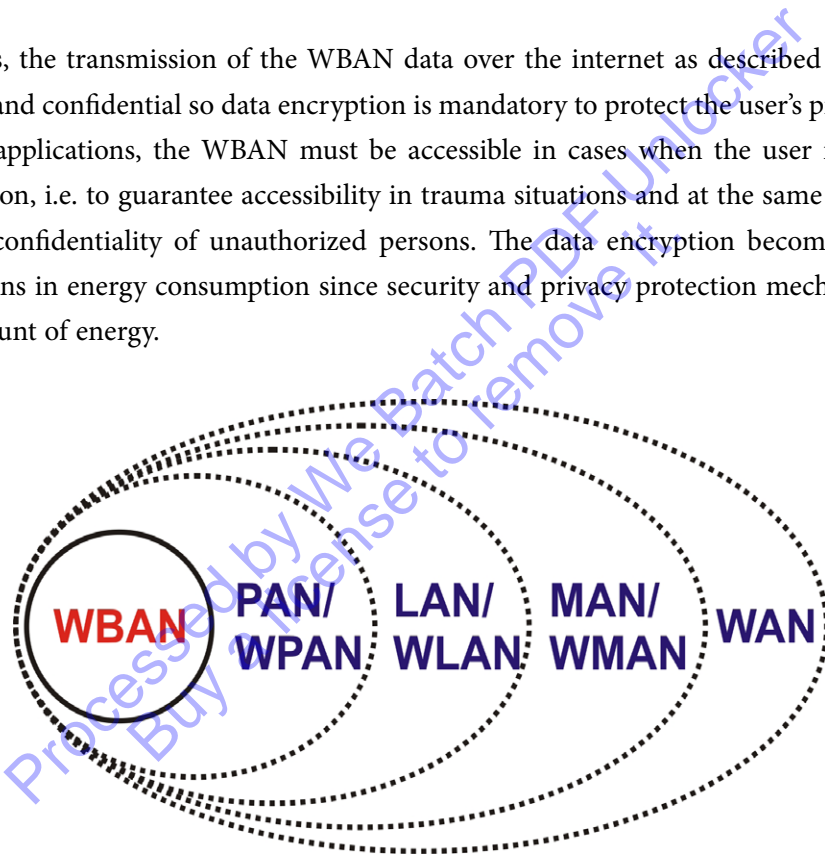
Figure 8.3. WBAN hierarchy in comparison with other networks

Another very critical parameter of the used communication platform is the supported data transmission bandwidth. In Table 8.2 data rates, power consumption and privacy of various applications are given (Ullah et. Al. 2009, p. 801). While in most sensor nodes the required data rate is relative small, in a WBAN that may consists of tenths of nodes the overall data rate that the personal server should manage can be easily rose to several or tenths of Mbps , so the communication platform must be able to handle such relatively high data volume.

Application type	Sensor Node	Data Rate	Power Consumption	Privacy
In-Body Applications	Glucose monitor	~2 Kbps	Very LOW	HIGH
	Pacemaker	~2 Kbps	LOW	HIGH
	Endoscope capsule	~2 Mbps	LOW	MEDIUM
On-Body Medical Applications	ECG	~ 100 Kbps	LOW	HIGH
	EEG	~50 Kbps	LOW	HIGH
	EMG	~300 Kbps	LOW	HIGH
	Blood Pressure	~10 bps	HIGH	HIGH
	Blood Saturation	~20 bps	LOW	HIGH
	Temperature	~100 bps	LOW	MEDIUM
	Motion Sensors	~50 Kbps	LOW	HIGH
	Cochlear implant	~100 Kbps	LOW	HIGH
	Artificial Retina	~500 Kbps	MEDIUM HIGH	HIGH
On-Body non Medical Applications	Audio	~1 Mbps	MEDIUM HIGH	LOW
	Voice	~100 Kbps	MEDIUM LOW	MEDIUM
	Social Network	~200 Kbps	LOW	HIGH

Table 8.2. Data rate, power consumption and privacy requirements for WBAN medical applications.

The available media access control (MAC) communication protocols that can be implemented in a WBAN are quite limited. As described above, they must comply simultaneously to the requirements of high data rate and low power consumption, low SAR, high encryption and reliability. In figure 8.4 the features of existing MAC protocols are illustrated. The most widely used and emerging radio technologies for WBANs and WPANs (IEEE 802.15 working group) are the Bluethooth (IEEE 802.15.1), IEEE 802.15.4 and ZigBee, UWB (ultra wide band, eg. wireless USB) and IEEE 802.15.6. An overview of MAC protocols designed for wireless sensor networks (WSNs) can be found in (Akyildiz et.al. 2002).
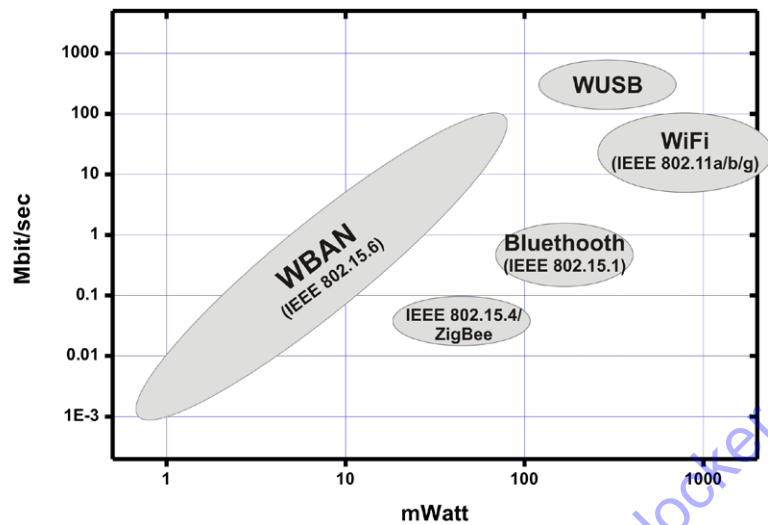
Figure 8.4. WBAN MAC requirements compared with available wireless protocols.

The Bluetooth (IEEE 802.15.1) and the Bluetooth Low Energy (BLE previously known as WiBree), operates in the 2.4GHz ISM band, covers a range of 1m–100m and at version 2.0 +EDR supports a maximum data rate of 3Mbps at relatively high power consumption. The low energy version support a maximum data rate of 1Mbps. Although some implementations of WBANs use Bluetooth (Johansson et.al. 2001), due to the relative high energy consumption and the complex protocol stack is not a suitable MAC protocol for WBANs applications.

The IEEE 802.15.4 and the based on that standard ZigBee protocol is the most widely used MAC protocol for WBAN implementations (Zigbee, Timmons & Scanlon, 2004, Li & Tan 2005). It operates on one of three possible unlicensed frequency bands: 868 MHz, 902-928 MHz and 2.4GHz, and can support a data rate up to 250Kbps (at 2.4GHz). It has very low power consumption and it covers a range up to 10m. While it has limited data rate, up to now is the best solution for low data rate WBANs.

The general conclusion is that neither the IEEE 802.15.1, nor the IEEE 802.15.4 was designed to support WBANs as described above, so a specialized MAC protocol is needed. Such effort is given from the IEEE 802.15 task group 6 (IEEE 802.15.6) that started in 2007. As describes itself, *the scope of IEEE 802.15 task group 6 is development of a communication standard optimized for low power devices and operation on, in and around the human body (but not limited to humans) to serve a variety of applications including medical, consumer electronics / personal entertainment and other* (IEEE802.15.6, Kwak et.al, 2010). The IEEE 802.15.6 will likely employ UWB protocols (at frequencies 3.1–10.6 GHz), however the time frame for product commercialization incorporating this standard still remains unknown. Table 8.3 summarizes the WBANs draft requirements.

Distance	2m standard, 5m special
Piconet density	2–4 nets / m2
Devices per network	max. 100
Net network throughput	100 Mbit/s max
Power consumption	~1mW / Mbps (@ 1 m distance)
Startup time	< 100 μs
Latency (end to end)	10 ms
Network setup time	< 1 sec

Table 8.3. WBAN requirements as in IEEE 802.15.6 protocol.

8.6   WBANS projects

Bellow the most relevant projects in the field of WBANs are summarized:

CodeBlue (Shnayder et.al. 2005)
In this project implemented at the Division of Engineering and Applied Sciences of Harvard University, several types of body sensors (e.g., pulse oximeter, ECG sensor) are individually connected to Zigbee-enabled radio transmitters, where patients' sensor devices publish all relevant information directly to an access point. The physicians subscribe to the network by multicasting and they can specify the information they need, such as the identification of the patient(s) of interest, and the types of body signals that need to be collected. It also has a flexible security model, in addition to the ability to prioritize the critical.

AID-N (Gao et.al. 2007)

In this project, although the WBAN utilizes a similar mesh structure as done in CodeBlue, its application scenario is different. Instead of deploying access points on the wall, wireless repeaters are located along a predefined emergency route. When an emergency situation happens, medical staff can recognize the correct emergency route. Due to its application as a medical emergency response system, a GPS module is included to the PS to provide an outdoors location service. The body sensor(s) are first connected to a PS through cable(s), whose signals can be delivered to a remote database by the PS through a WiFi or cellular network.

SMART (Curtis et.al. 2008)

In this project were monitored the physiological signals from patients in the waiting areas of emergency departments. There have been various cases in which the medical team has found that the patient's health deteriorates rapidly while waiting in an emergency room. Since time is of an essence in this situation, patients' lives cannot be risked because of the lack of attention provided in emergency rooms. The SMART system can be used to collect data from various patients waiting in an emergency room, and wirelessly send it to a central computer that collects and analyzes the data. This way, patients can receive treatment before the condition worsens.

ALARM-NET (Wood et.al, 2006)

Alarm-Net is a wireless sensor network for assisted-living and residential monitoring. It integrates environmental and physiological sensors in a scalable, heterogeneous architecture. It creates a medical history log, while preserving the patient's privacy. Authorized care providers may monitor resident health and activity patterns, such as circadian rhythm changes, with a automatic 24/7 monitoring system, which may signify changes in healthcare needs. Wearable sensor devices can sense even small changes in vital signals that humans might overlook, such as heart rate and blood oxygen levels, boosting accuracy.

HipGuard System (Soini et.al. 2008)

HipGuard system is developed for patients who are recovering from hip surgery. This system monitors patient's leg and hip position and rotation with embedded wireless sensors. Alarm signals can be sent to patient's Wrist Unit if hip or leg positions or rotations are false, and hence HipGuard system can provide useful real-time information for patient rehabilitation process.

MobiHealth (Mobiheatlh, Neves et.al. 2008)

Mobihealth is a mobile healthcare project funded by the European Commission, to create a generic platform for home healthcare using WBAN based sensors. In this project GPRS/UMTS wireless communication technology for transferring data, are used to provide continuous monitoring to patients outside the hospital environment. MobiHealth targets, improving the quality of life of patients by enabling new value added services in the areas of disease prevention, disease diagnosis, remote assistance, physical state monitoring and even in clinical research. The patients wear a lightweight monitoring system which is customized to their individual health needs. Therefore, a patient who requires monitoring for short or long periods of time doesn't have to stay in hospital for monitoring. With the MobiHealth BAN the patient can be free to pursue daily life activities.

IBBT IM3 (IBBTIME)

The Flemish IBBT IM3-project (Interactive Mobile Medical Monitoring) focuses on the research and implementation of a wearable system for health monitoring. The solution consists of four elements or zones: a) The patient zone, including mobile sensors for registering the physiological parameters: Electrocardiogram, heartbeat, respiration, etc. b) A medical hub: A cell phone or personal digital assistant (PDA), which collects the data registered for the patient and transmits it. c) An IM3 backend server, which securely stores and processes the data; including customised algorithms and event managers, which can give a first interpretation of the data and fulfils privacy regulations. d) The biodata viewer, which can be used by care personnel for remote monitoring of patients. Patient data is collected using a WBAN and analyzed at the medical hub worn by the patient. If an event (e.g. heart rhythm problems) is detected, a signal is sent to a health care practitioner who can view and analyze the patient data remotely.

LifeShirt (LifeShirt)

LifeShirt although it isn't a WABN system that collects and transmits wireless data, it is presented here due to the fact that it is a commercially available system. LifeShirt comprises of a comfortable and lightweight garment with embedded sensors that continuously collect information on a range of cardiopulmonary parameters, such as blood pressure, EEG, audio, temperature and blood oxygen saturation. The LifeShirt Recorder™ is a mobile device that continuously encrypts and stores the subject's physiologic data on a compact flash memory card. It enables healthcare professionals and researchers to accurately monitor more than 30 vital life-sign functions in the real-world settings where patients live and work.

Finally in (De Rossi et.al. 2003) is presented the implementation of a truly wearable, instrumented garments which are capable of recording biomechanical variables. Although it isn't a WBAN system, comfortable garment devices (a smart shirt, a leotard and a glove) which can read and record vital signs and movements with sensors fabricated together with the garment are presented. The sensing function is based on piezo-resistive fabric sensors, based on carbon-loaded rubbers (CLR) and different conductive materials.

8.7   Concluding Remarks

The use of WBANs brings together technological advances in diverse areas ranging from electronic devoces and wireless networks to new sensing materials and multifunctional fabrics giving the possibility to make the every day life of anyone safer and more comfortable. Especially, the area of health monitoring and telemedecine has attracted the interest of the research community and a lot of efforts have been devoted to it in order to increase life expectancy and quality of life at a reduced cost.

Two are the main issues that should be resolved to enable the wide adoption of WBANs in many application domains. The development and commercialization of a protocol standard, like the IEEE 802.15.6 and the evolution of industrial processes for the incorporation of sensors and actuators in fabrics and therefore to comfortable garments, which will have the capability to record vital signals and movements and interact with the humans without any disturbance to the user's routine.

8.8 References

(Akyildiz et.al. 2002) Akyildiz, I.F., Su, W., Sankarasubramaniam, Y. & Cayirci, E. 2002 'Wireless sensor networks: a survey', *Computer Networks*, vol.38, pp. 393–422.

(Arshak et.al. 2007) Arshak, K., Jafer, E., McGloughlin, T., Corbett T., Chatzandroulis S., & Goustouridis, D. 2007, 'Wireless Measurement System for Capacitive pressure Sensors Using Strain Compensated SiGeB', *IEEE Sensors 2007*, October 28–31, 2007.

(Atmel 2012) Atmel Corp., Online Doc., http://www.atmel.com/products/microcontrollers/avr/tinyAVR.aspx

(Chen et.al. 2011) Chen, M., Gonzalez, S., Vasilakos, A., Cao, H., & Leung, V. 2011 'Body Area Networks: A Survey', *Mobile Netw Appl* vol.16, pp.171–193.

(Curtis et.al. 2008) Curtis, D., Pino, E., Bailey J., Shih, E., Waterman, J., Vinterbo S., Stair, T., Guttag, J., Greenes, R., & Ohno-Machado, L. 2008 'SMART – An Integrated Wireless System for Monitoring Unattended Patients', *J. of the American Medical Informatics Association*, vol. 15, no 1, pp. 44–53.

(De Rossi et.al. 2003) De Rossi, D., Carpi, F., Lorussi, F., Mazzoldi, A., Paradiso, R., Scilingo E.P., & Tognetti, A. 2003, 'Electroactive Fabrics And Wearable Biomonitoring Devices', *AUTEX Research Journal*, Vol. 3, No. 4, pp. 180–185.

(Gao et.al. 2007) Gao T., Massey T., Selavo L., Crawford D., Chen B., Lorincz, K., Shnayder V., Hauenstein L., Dabiri F., Jeng J., Chanmugam, A., White D., Sarrafzadeh M., & Welsh, M. 2007 'The advanced health and disaster aid network: a light-weight wireless medical system for triage', *IEEE Trans Biomed Circuits Syst*, vol.1, no 3, pp. 203–216.

(Huang et.al 2009) Huang, L., Ashouei, Yazicioglu, F., Penders, J., Vullers, R., Dolmans, G., Merken, P., Huisken, J., de Groot, H., Van Hoof, C., & Gyselinckx, B. 2009 'Ultra-Low Power Sensor Design for Wireless Body Area Networks: Challenges, Potential Solutions, and Applications', *International Journal of Digital Content Technology and its Applications*, vol. 3, no 3, pp. 136–148.

(IBBTIM3) IBBT-IM3 project, http://www.ibbt.be/en/projects/overview-projects/p/detail/im3

(IEEE802.15.6) IEEE 802.15 WPAN TG 6 Body Area Networks. http://www.ieee802.org/15/pub/SGmban.html.

(Johansson et.al. 2001) Johansson, P., Kazantzidis, M., Kapoor, R., & Gerla, M. 2001 'Bluetooth: an enabler for personal area networking', *IEEE Network*, vol. 15, no. 5, pp. 28–37.

(Kwak et.al, 2010) Kwak, K.S., Sana Ullah, S., & Ullah, N. 2010 'An Overview of IEEE 802.15.6 Standard', *ISABEL 2010* (*Invited),* Rome, Italy.

(Latre et.al. 2011) Latre, B., Braem, B., Moerman, B.C., & Demeester, P. 2011 'A Survey on Wireless Body Area Networks', *Wireless Networks*, vol.17, no 1, pp. 1–18.

(Li & Tan 2005). Li, H., & Tan, J. 2005 'An ultra-low-power medium access control protocol for body sensor network', *27th Annual International Conference of the Engineering in Medicine and Biology Society*, IEEE-EMBS, Shanghai, 2005, pp. 2451–2454.

(LifeShirt) LifeShirt from VivoMetrics, http://vivonoetics.com/products/sensors/lifeshirt/

(Mobiheatlh) Mobihealth project, http://www.mobihealth.org.

(Nemati et.al. 2012) Nemati, E., Deen, M.J. & Mondal, T. 2012 'A Wireless Wearable ECG Sensor for Long- Term Applications', *IEEE Communications Magazine*, pp. 36–43

(Neves et.al. 2008) Neves, P., Stachyra, M., & Rodrigues, J. 2008 'Application of Wireless Sensor Networks to Healthcare Promotion', *Journal of Communications Software and Systems,*Vol.4, No.3, pp. 1845–6421.

(Shnayder et.al. 2005) Shnayder, V., Chen B., Lorincz K., Fulford-Jones T.R.F., & Welsh M. 2005 'Sensor networks for medical care' *Harvard University Technical Report TR-08-05.*

(Soini et.al. 2008) Soini, M., Nummela, J., Oksa, P., Ukkonen, L., & Sydänheimo, L. 2008 'Wireless Body Area Network For Hip Rehabilitation System', *Ubiquitous Computing and Communication Journal*, vol. 3, no. 5, pp. 42–48.

(TI 2012) Texas Instruments, Online doc. http://www.ti.com/lsds/ti/microcontroller/16-bit_msp430/overview.page

(Timmons & Scanlon, 2004) Timmons, N.F., & Scanlon, W.G. 2004 'Analysis of the performance of IEEE 802.15.4 for medical sensor body area networking', *First Annual IEEE Communications Society Conference on Sensor and Ad Hoc Communications and Networks*, Oct. 2004, pp. 16–24.

(Tsoukalas et.al. 2006) Tsoukalas, D., Chatzandroulis, S., & Goustouridis, D. 2006 'Capacitive Microsensors for Biomedical Application', *Encyclopedia of Medical Devices and Instrumentation, 2nd Edition*, John Wiley & Sons, vol. 2, 2006 pp. 1–12.

(Ullah et. Al. 2009) Ullah S., Khan, P., Ullah, N., Saleem, S., Higgins, H. & Kwak, K.S. 2009 'A Review of Wireless Body Area Networks for Medical Applications', *International J. of Communications, Network and System Sciences (IJCNS)*, vol. 2, no. 8, pp. 797–803.

(Wood et.al, 2006) Wood A., Virone G., Doan T., Cao Q., Selavo L., Wu Y., Fang, L., He Z., Lin S., & Stankovic, J. 2006 'ALARM-NET: wireless sensor networks for assisted-living and residential monitoring', *Technical Report CS-2006-11*, Department of Computer Science, University of Virginia.

(Yang, 2006) Yang, GZ 2006, *Body Sensor Networks,* Springer-Verlag, London.

(Zigbee) ZigBee Alliance, Offcial webpage, http://www.zigbee.org.

9 Electronic and computer applications in the knitting design and production

by

Mirela Blaga

Faculty of Textiles, Leather and Industrial Management, "Gheorghe Asachi" Technical University of Iasi, Romania

Abstract

The chapter introduces the basic information about knitting technology and knits applications, as a short introduction to the knitting field. The main benefits of the electronics and information technology to the knitting production efficiency and to the high quality of the products are outlined. The unlimited knitting design and production possibilities are strongly related to the CAD and CAM systems, whose action ensures the huge potential for innovations, production management and control.

9.1 Knitting Principles

Knitting is a fabric forming process that converts yarns into fabrics and accounts more than 30% from the total textile production According to the yarn feeding system, two knitting techniques are known, namely weft and warp. By weft knitting, the loops are formed from a single thread within the same row (figure 9.1), whereas the warp knitting produces a fabric from warp yarns that run vertically and parallel to each other (figure 9.2) (Choi, W. & Powell, N., 2005, p. 2).

Weft knitted fabric	**Characteristics**	**Warp knitted fabric**	**Characteristics**
	High resilient, more open, with rich design possibilities.		Less resilient, more cover, lighter weight and higher productivity.
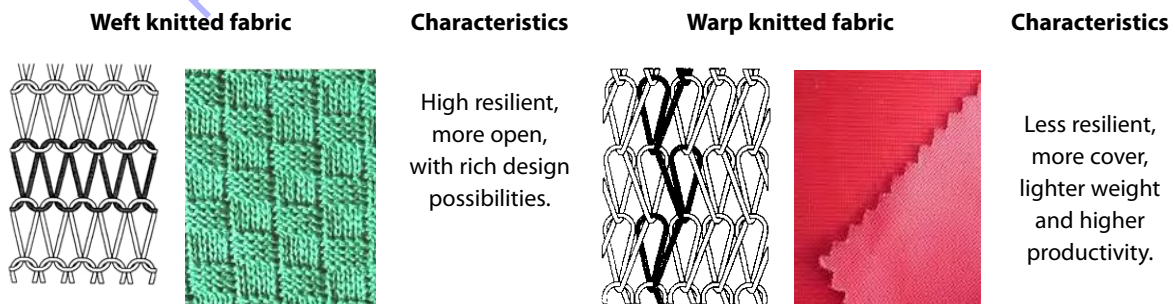
Figure 9.1: Weft knitting.

Figure 9.2: Warp knitting.

Weft knitted loops tends to distort under tension and yarn can freely flow between loops under greater tension, a characteristic which deals with elastic recovery properties. Warp knitted threads have an approximately vertical path through the structure, which makes the warp threads less likely to fray or unrove (Spencer, D.J. 2001, p. 48). Due to the machine's mechanisms, the fabrics are producing from dimensionally stable to highly elastic without necessarily changing the type of yarn.

Engineering of knitted fabrics is a complex activity, based on the perfect match of some individual pieces, like: end use, product design, fabric structure, shape, yarns, knitting machine and finishing. All these, should fill-in the puzzle of one ready to use product production cycle (figure 9.3).
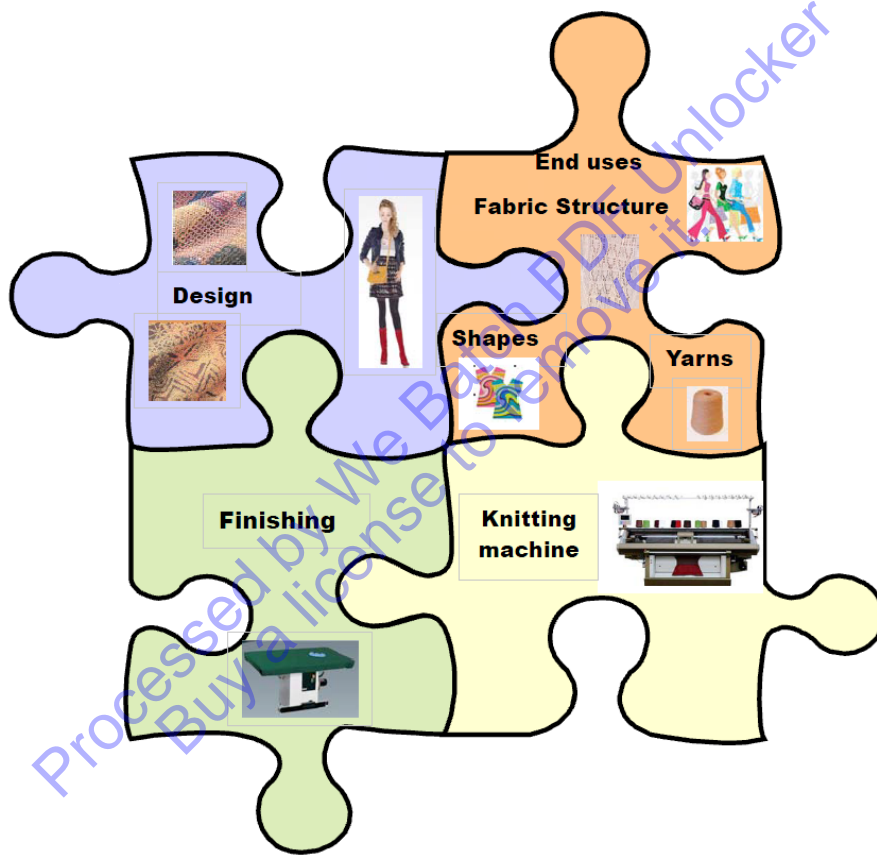
Figure 9.3: Engineering Process of Knitted Garments.

From yarn characteristics to complex structures, a finished knitted garment must be carefully engineered to provide the required attributes customized to the activity and the shape of its user (Lamar, W., & Powell, N. 2009, p. 7).

9.2   Knitting machines

The machine contains and co-ordinates the action of a number of mechanisms and devices, each performing specific functions that contribute towards the production and efficiency of the knitting action (Spencer, D.J. 2001, p. 18).

Knitting machines are basically categorized according to the: yarn feeding system, needle movement, arrangement of needle bed and binding groups. Table 9.1 displays the main classes of the knitting machines, according to these criteria.

Single yarn system			Warp yarn system	
Simultaneous needle movement	Individual needle movement (weft knitting)		Simultaneous needle movement (warp knitting)	
	Flat Knitting	Circular knitting	Flat Knitting	Circular Knitting

Table 9.1: Classes of knitting machines.

The main parts of one knitting machine, either circular or rectilinear, weft or warp knitting, are illustrated in the example chosen in figure 9.4.

Figure 9.4: Main parts of a circular knitting machine (Maier&Cie).

- The *frame*, which is an independent stand, designed to accommodate the majority of machine's mechanisms.
- *The yarn feed* consists of the yarn package or warp beam, tensioning devices, yarn feed control and yarn feed carriers or guides.
- *The knitting area* includes the knitting elements, needle beds, drive and control, as well as pattern selection.
- *The fabric take-down mechanism* includes fabric tensioning, wind-up and accommodation devices.
- *The quality control system* includes stop motions, fault detectors, automatic oilers and others, according to the machine developments.
- *The machine control* and *drive system* generating the power driving the devices and mechanisms.

9.3 Production of knitted garments

The production of a knitted garment from yarn to ready made product consists of several processes, depending on the machinery used and the production methods that a company have employed.

The flowchart of knitted garments production made on circular knitting machines is presented in table 9.2.
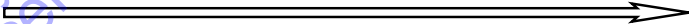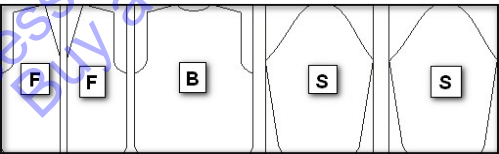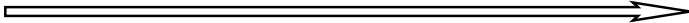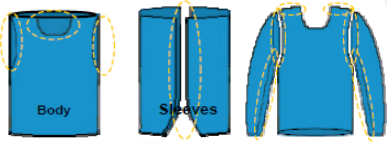
Technology	Production method	
	Cut & sew ⟶	
		The characteristic of knitted fabric made on circular machines is the form of tube. After finishing, the fabric is cut according to a pattern and sewn together.
	Seamless garment ⟶	
	(Peterson, J.& Ekwall, D. 2007)	The complete garment created on circular knitting machines joins one body tube, two sleeves tubes and finshed edges, made in a single stage on the machine.

Table 9.2: Manufacturing of knitted garments on circular machines.

The manufacturing process of knitted garments made on flat technology can be divided in four different production methods, as represented in table 9.3.
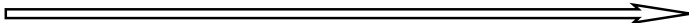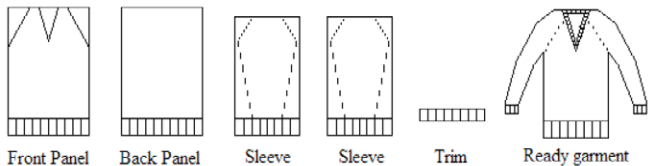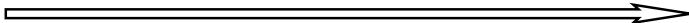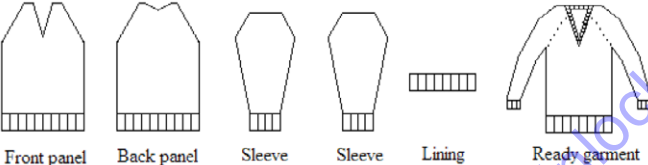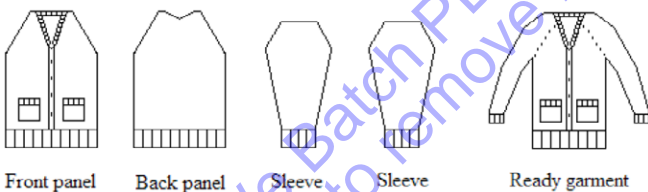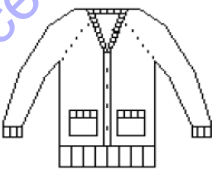
Technology	Production method	
	Cut & sew	
	Front Panel Back Panel Sleeve Sleeve Trim Ready garment	Rectangular flat knitted panels are cut to the required shapes, which are sewn together.
	Fully fashion	
	Front panel Back panel Sleeve Sleeve Lining Ready garment	Front, back and sleeve pieces are knitted in the right shape directly in the knitting machine.
	Integral knitting	
	Front panel Back panel Sleeve Sleeve Ready garment	Trimmings, pockets, buttonholes and other accessories are directly knitted in the fully fashion produced panels.
	Complete garment	
	Complete garment	The entire garment is ready made directly in the flat knitting machine with no additional processes such as cutting and sewing.

Table 9.3: Manufacturing of knitted garments on flat machines (Peterson, J. & Ekwall, D. 2007).

9.4   Use of knitted fabrics

Created either in flat, tubular or three-dimensional form, from a variety of raw materials, exhibiting special properties, knitwear are suitable for a big range of applications, from apparel to the field of technical and composites. It is possible to be manufactured elasticized, stable, strong, fine, thick, open or closed structures, as well as three dimensional shapes, desirable for technical applications.

Generally, the new developments were centered on three main objectives: to improve patterning possibilities, to increase production efficiency, and to ensure a high quality to the products, as being detailed in the schematic view from Table 9.5.

Sports	Medical	Hometextiles	Industrial	Geotextiles

Table 9.4: Applications of knitted fabrics.

9.5   Introduction of electronic elements and devices

Knitting machines have been developed with mechanically controlled and operated movements. The limitations of mechanical movements, their high manufacturing costs, the slow speed in operation, difficulty to adjust, the friction and wear tendency, became incompatible with the requirements of advanced knitting technology. Electronic selection or machine control is compatible with higher running speeds and eliminates complex mechanical arrangements. It provides greater versatility as regards design parameters, simplifies the modification of repeat sequences and size, style and pattern-changing operations, being capable of changes even during the machine running. Electronics offer also the decisive advantages of convenient power-supply, compatibility with existing mechanical components, micro-miniaturization of circuitry, and economical data storage (Spencer, 2001, p. 136).

Along with the introduction of electronic and computers controls into most aspects of modern life, the first attempts to integrate the primitive computers into the circular knitting machines have been made during late sixties (Raz, 1993, p. 342). The knowledge derived from these developments has been gradually transferred to flat knitting, as a prepared technology to increase its potential. Thus, the machines controlled by punched cards were replaced by electronic devices.

The electronics elements and devices have been successfully introduced to textile field, due their specific features: their small size, less response time, high capacity and sensitivity, easy to transport and less power consumption (Chandra Ray, 2012, p. 213). The introduction of electronics and information technology gained significant improvements for most components and systems of the knitting machines, but keeping the basic concept of the stitch formation (Shaikh, 2004, p. 122).

Generally, the new developments were centered on three main objectives: to improve patterning possibilities to increase production efficiency, and to ensure a high quality to the products, as being detailed in the schematic view from Table 9.5.

Patterning possibilities	Production efficiency	Product quality
Pattern design preparation-CAD	Production manufacturing-CAM	Yarn feeding system
Electronic needle selection	Monitoring the settings and specific technical motions	Stitch length control
Pattern mechanisms	Operational data acquisition	Shaping of the product
Take-down adjustements	Cylinder temperature and oil pressure	Online quality control

Table 9.5 Applications of electronics in knitting.

Adapted to various technologies, these general objectives were particularized and became more specific, as described bellow.

The most important functions controlled by the computer on a *weft flat knitting machine* (Raz, 1993, p. 343) are related to:

6. Individual needle selection, required for creation of unlimited patterns;
7. Cam movements necessary to operate the needles for producing various stitch types and structures;
8. Size of the loops for the quality and flexibility of patterns;
9. Size of the carriage movement, in order to reduce at minimum the knitting time and to increase the machine productivity;
10. Amplitude of the needle beds racking to produce complicate patterns;
11. Quality control systems to ensure the high quality and standards of garments.

The most important functions controlled by the computer on a *weft circular knitting machine* (Iyer et. all, 1995, p. 106) can be summarized as:

12. Individual needle selection systems, for unlimited size patterns, flexible patterns to fashion demands;
13. Electronic yarn feeding device;
14. Take-down systems with an incorporated electronic control;
15. Reduction of standstill times, thus increasing the machine efficiency.

In case of *flat warp knitting machines*, the specific electronic controlled concern the: yarn feeding unit, patterning mechanism, fabric take-up mechanism and data collection (Raz, 1997, p. 145).

The latest generation of computer controlled V-bed flat knitting machines, are the most complicated and sophisticated textile equipment ever produced. With its comprehensive patterning and garment shaping facilities, offers the greatest challenges and opportunities for the application of a CAD/CAM system (Spencer, 2011, p. 136). Therefore, this technology has been chosen as example, to identify most of the benefits of the electronics and IT applications.

The application of electronics and information technology has generated important improvements for most of the components of the flat knitting machines, but keeping the basic concept of stitch formation unchanged.

There are certain advantages of implementing the computer-controlled electronic systems in the machine structure, such as: easy operation of the machines, high speed of the programming and control of majority of machine functions.

Figure 9.6 exhibits some of the features of an electronic flat knitting machine that ensure that high quality fabric is knitted at high speed with the minimum of supervision. The main electronic parts and it functions are briefly described, to outline the potentialities of computer controlled machines.
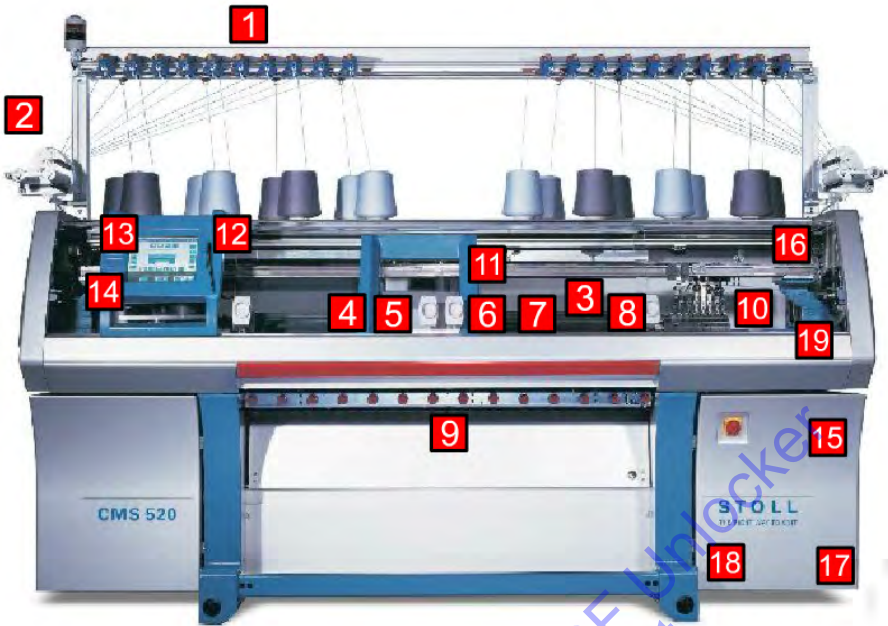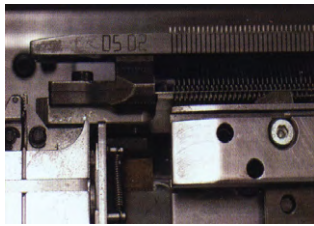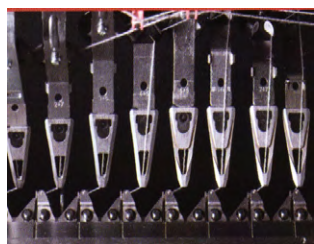
Figure 9.6: General view and components of a computer controlled flat knitting machine [www.stoll.de].

The main components incorporated by the flat knitting machine are detailed presented in table 9.6 [Stoll].

No	Component part	Name of the component/features
1.		**1. Yarn control units** Allow an easy yarn insertion, setting also the yarn tension. Separate knot detectors for small and large knots are located in the same area.
2.		**2. Friction feed wheel** Provides low and constant tension during yarn feeding, especially for yarns with special properties.
3.		**3. Needles of CMS Stoll machines** The machines are equipped with pelerine spring-transfer needle with spring-loaded latch and conical hook, with a high level of safety during operation. The main advantage is the low level of needle consumption.
4.		**4. Combined knitting/transfer systems** The 'heart' of the machine is the knitting system with the three-way technique or simultaneous transfer of the loops. The highest production output is possible.
5.		**5. Electronic selection system** Stoll selection systems are maintenance-free and have two selection points for each system in each direction.
6.		**6. Stitch length control** The stitch cams allow several tensions in one stitch row, being quickly adjustable with power tension setting. Long and short stitches on the same course are possible to be achieved dynamically during carriage movement.
7.		**7. Holding-down jacks** High-quality stitch appearances are provided by Stoll holding-down technology, which allows a soft knocking over of the fabric for knitting the most sophisticated pattern under a good quality control.

No	Component part	Name of the component/features
8.		**8. Large needle bed racking** The needle bed is equipped with a racking device with a maximum racking course of four inches and a programmable racking speed. Various patterns with special effects given by the inclined loop positions can be achieved.
9.		**9. Stoll – multiflex fabric take-down system** The take down mechanism is composed of freely programmable and adjustable roller segments**.** The motion is controlled by automatic devices which adjust the take-down tension, according to the number of working needles, to avoid differences in stitch densities when knitting fully fashioned fabrics.
10.		**10. Thread cutting/clamping device** 16 yarn feeders by thread cutting/clamping device provided as standard on both sides of needle beds.

No	Component part	Name of the component/features
11.		**11. Extraction device suction** Suction effect created by an electrical turbine, ensure a good cleaning of the needle beds during knitting operation, thus a blockage or slow running of the carriage being avoided.
12.		**12. Main drive** Programmable speed with flexible speed adjustment using starting bar is available. Variable stroke with Power-RCR system (Rapid Carriage Return), especially useful at short strokes for narrow garments, binding off and narrowing is a special feature of this technology.
13.		**13. Display slide with color monitor** The monitor enables to enter machine commands while maintaining eye contact to the fabric. Colour display 800x600 pixels and touch screen.
14.		**14. Stoll-touchcontrol®** An individual user interface and intuitive menu guidance enables entering pattern changes easily and directly at the machine.
15.		**15. Main computer has** 256 MB memory
16.		**16. USB port** Easy to reach device and facile transport of data to machine.
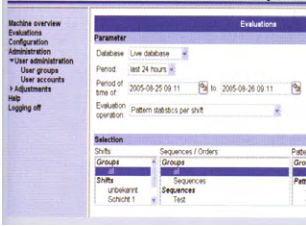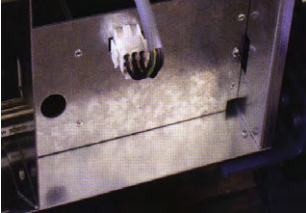
No	Component part	Name of the component/features
17.		**17. Intranet connection** Allows the network between knitting machines, controlled by the main server.
18.		**18. Battery back-up** After power failure it is possible a correct continuation of the knitting process.
19.		**19. Guaranteed safety** Valid EU directives relating to the design and safety of machines are precisely observed.

Table 9.6: Components of electronic flat knitting machines.

9.6   Computer-aided designing (CAD)

The textile Computer-Aided Design (CAD) represents a computerized design facility for designing, simulating the fabric on a personal computer and delivering the particular programs for manufacturing the product on the machine (Chandra Ray, 2012, p. 215). Computer-Aided Design (CAD) and Computer-Aided Manufacturing (CAM) have revolutionized the knitting industry, since seventies, being commercially available for small and medium sized companies, from 1980.

Designers are employing the CAD systems to create product designs, which are then transferred to CAM machines for manufacturing the final product. CAD/CAM technology replaced the mechanical patterning and shaping devices on machines with electronic controls.

Each machine builders are developing their own software solutions, to manufacture the knitted products on the associated machines. The provided packages computer – machines are developed according with the specific features of the machines.

The design of patterns and preparation for knits production are accomplished today with the help of equipments and systems based on electronic data processing. The core of such system is a personal computer, with keyboard or graphic pencil, one of two monitors and data storage units (Iyer, 1995, p. 111).

The latest software packages developed by the machine builders are dominating the world market and present common features, which are going to be discussed in the following.

The M1 plus software from Stoll machine builders consists of one unit, two monitors for simulation the fabric in technical view and real fabric view, one keyboard, mouse and an USB stick for transferring the program into machine memory for manufacturing (figure 9.7). The MKS system for developing knits on circular knitting machines, allows the design of patterns via one computer with one monitor, keyboard and mouse, the programs being transferred to the machine via a diskette along with all the parameter details that are created automatically (figure 9.8).
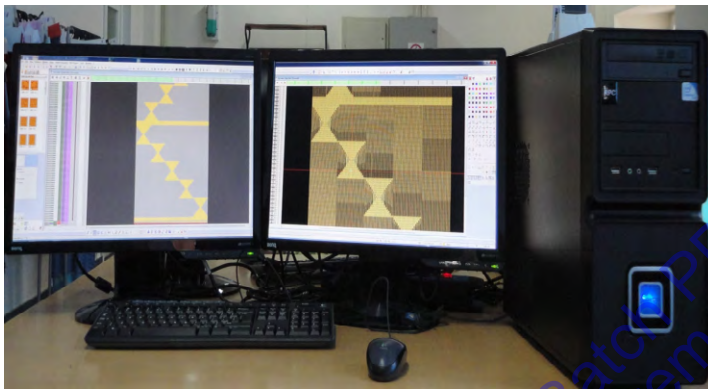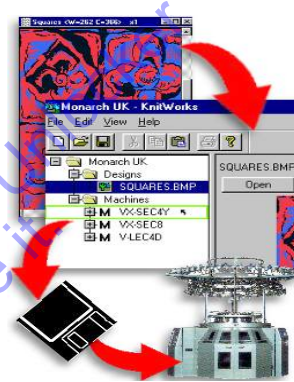

Figure 9.7: M1 plus for flat machines, Stoll.

Figure 9.8: MKS for weft circular knitting machines, Monarch.

These systems contain also black-and-white or color printers and self-operating pattern registration units via video camera or digital scanner.

Following the example of CAD system developed by Shima Seiki Company, presented in figure 9.9, the most important features of the design systems can be stated briefly as follows:

16. Creating a database with yarn specifications, colors, gauges, nature, for various fabrics;
17. Designing, filling of patterns and pictures. The software contains drawing tools, colors and symbols, to facilitate the structure representation. Database with ready-made structure modules are generally at the programmer disposal.
18. Designing the programs for knitting machines with various gauges and technologies, prepared manually or automatically.
19. Pattern making, according to the desired sizes, using the facilities offered by the soft.
20. 3D simulation of the final product before knitting, which offers clear advantages, concerning the quality of the product, the waste and reduction. Full visual design is available on the monitor, changes in color, structure, shape can easily be made.
21. On-line transfer of the machine programs to knitting machine.
22. Marketing, e-commerce, sales promotion, by using a wide range of design tools for creating various promotional items.
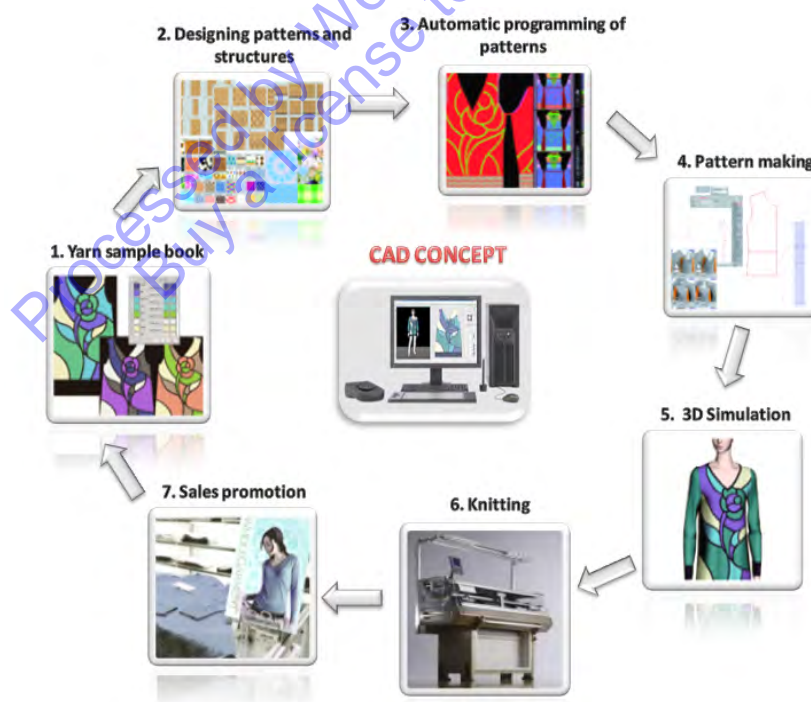

Figure 9.9: Pattern design stages [www.shimaseiki.jp].

Some conclusions can be summarized from the above mentioned features, as general advantages of the computerized design activity:

f) The reduced time necessary for creating pattern design, by using powerful drawing tools;

g) Immense potential for innovative combinations of colors, knitted structures, yarn, complex fabrics, various fabric shapes;

h) Simulation of the product on the virtual model, before manufacturing with a great flexibility of making changes in real time;

i) Easy storage of manufacturing data and documents, and the direct interface connection with the knitting machine for transfer of the programs.

9.7 Computer-aided manufacturing (CAM)

Computer Aided Manufacturing (CAM) is the concept defining the use of computers and computer technology to manage, organize, and manufacturing the industrial knitting production. This involves the use of some algorithms for manufacturing process planning and management.

In practice, the two components, CAD and CAM, are combined, i.e. a designer creates a pattern, and then the computer automatically schedules the instructions for making the knitted fabric and controls the manufacturing.

CAM in knitting technology performs the main activities:

- Monitoring, control and manage the flow of manufacturing raw materials;
- Development of programs for knitting and adjusting the machine parameters;
- Command and control the machines;
- Production management and planning.

The *Shima Total Design System* is a totally-integrated knit production system that allows all stages – planning, design, evaluation, production, and sales promotion – to be integrated into a smooth work-flow, explained below and based on the scheme from figure 9.10 (Spencer, 2011, p. 144).

- The designer, using computer-graphic paint software and a pressure-sensitive airbrush, creates concept drawings. Scanned-in images can be also used to create a pattern. The working pattern is then displayed using *KnitPaint* software. Courses and wales are converted into numbers of loops. Jacquard, intarsia and structure patterns can be created separately.
- The pattern is automatically converted into usable knitting data, customized to the required *Shima* machine;
- The *loop simulation programme* uses yarns either scanned or painted and the simulated knit pattern can then be draped onto models, created by a mesh grid, in conformity to the fully fashioned piece. A database of models wearing various types of knitwear (V-neck, crewe neck, cardigan, etc.) for which the mesh grids are ready-made is available;

- The system ensures a smooth production flow to the cutting room, where a selection of cutting widths and thickness are available;
- This is an optimal system for all types of print applications for apparel, innerwear manufacturers, interior designers, towel manufacturers and sundry goods manufacturers.

Data created on this system is sent to the production line, which includes state-of-the-art computerized knitting machines and fabric cutting machines.
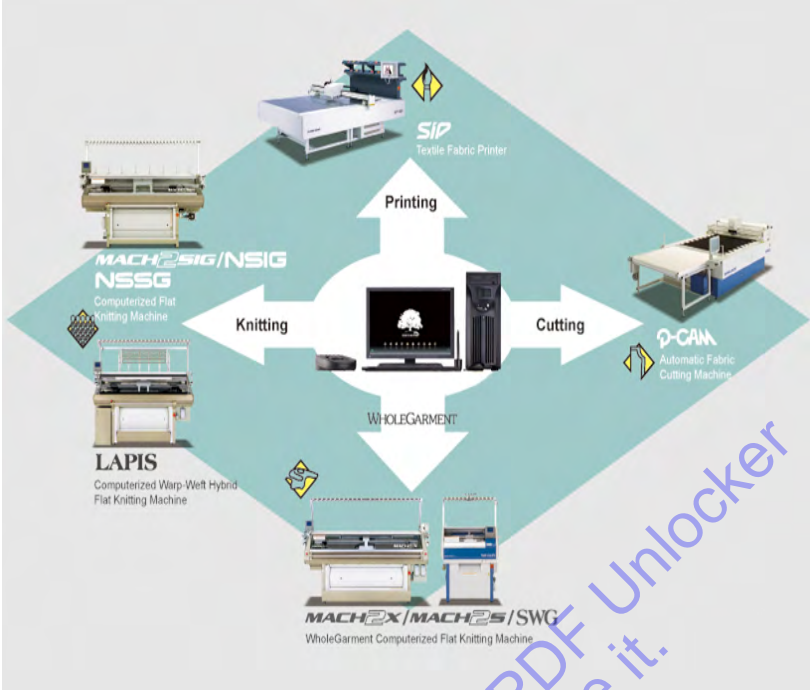
Figure 9.10: Shima Seiki CAM solution [www.shimaseiki.jp].

CAM system is facilitated by the existence of modular equipment, consisting of computers, printers, data storage units, communication networks, microprocessors, as exemplified in figures 9.11–9.12.

CAM components used by Stoll Company include on-line graphics station M1 knitting machines, cable network and a network hub to hub, as represented in figure 9.11, which show types of connections between CAM system components.

Figure 9.11: Connection between M1 pattern stations with CMS machines [www.stoll.de].

Central computer is used for function and data server. Other networked computers are used for: drawing, writing and knitting simulation programs, cutting, grading of the samples.

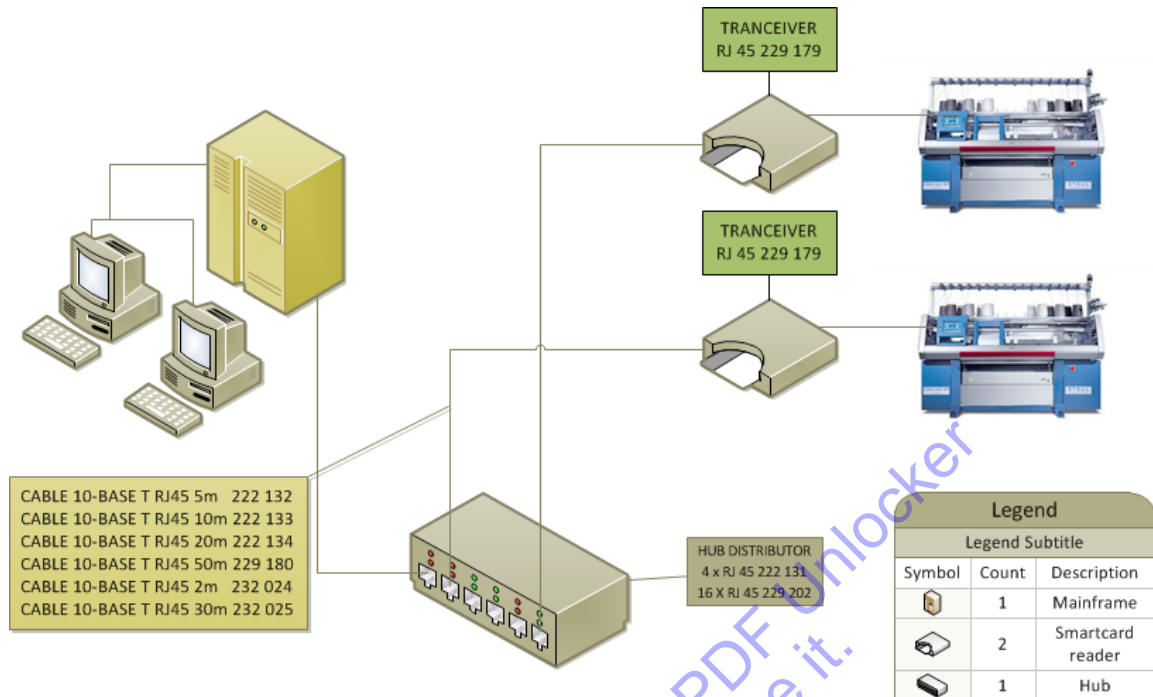In figure 9.12 the core of the communication network is one server connected via T-switch to M1 and M1 plus pattern stations, command being then sent to a particular machine via peripheral Selan. If the server is connected to the Internet via Modem peripheral, knitting machine control can be done in real time.

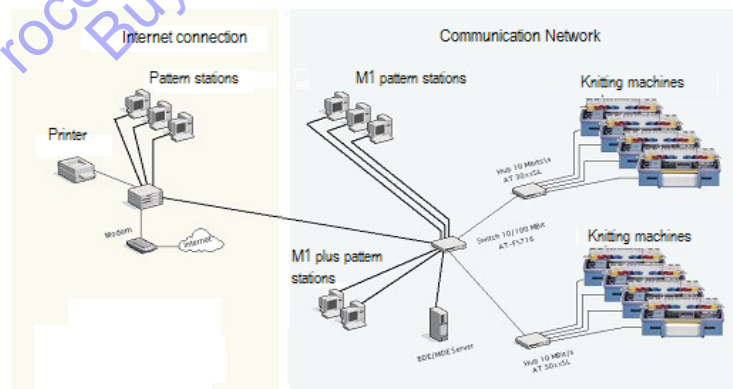**Figure 9.12:** Internet communication network with CMS knitting machines [www.stoll.de].

The communication network can be connected and output peripherals, such as printer, plotter. The printer can be connected to the network and it is used for printing on paper the results: pattern drawings, knitted structures, knitting programs, pattern grading, working resorts of machines or worker, yarns consumption.

9.8   References

Blaga, M., Dan, D., Ciobanu, R., Ionesi, D. 2011 *Interactive application for Computer Aided Design of 3D Knitted fabrics*, the 7th International Scientific Conference eLearning and Software for Education, Bucharest, ISSN 2066-026X.

Choi, W., Powell, N. 2005, 'Three-dimensional seamless garment knitting on V-bed flat knitting machines', *Journal of Textile and Apparel,* NC State University, volume 4, issue 3.

Iyer, C., Mammel, Schach, W. 1995, *Circular knitting, Second edition,* Meisenbach Bamberg, Germany.

Peterson, J. & Ekwall, D. 2007, 'Production and business methods in the integral knitting supply chain', *AUTEX Research Journal*, Vol. 8, No. 4, AUTEX.

Ray, S.C. 2012, *Fundamentals and Advances in Knitting Technology,* Woodhead Publishing India Pvt. Ltd.

Raz, S. 1993, *Flat Knitting Technology,* Universal Machinenfabrik, Germany.

Raz, S. 1997, *Warp knitting production*, Melliand Textilberichte, Germany.

Shaikh, I.A. 2004, *Pocket Knitting Expert, A Practical Handbook on Textile Knitting*, editor&publisher Irfan Ahmed Shaikh.

Spencer, D.J. 2001, *Knitting technology: A comprehensive handbook and practical guide* (3rd ed.). Cambridge, England; Lancaster, Pa.: Woodhead Publishing Limited.

http://www.stoll.de/

www.karlmayer.com

www.shimaseiki.com/product/cadcam/sdsone

www.monarchknitting.co.uk

10 Electronic and Computer Applications in the Clothing Design and Production

by

Serkan Boz and M. Çetin Erdoğan

Emel Akın Vocational Training School, Ege University, Izmir, Turkey
Department of Textile Engineering, Ege University, Izmir, Turkey

10.1   Introduction

Considering the recent conditions, apparel producers must produce quality products in a short period with low costs to be able to compete in the world market. Also, you must research and develop many products and make production time shorter in order to get a share in the apparel market. This situation, makes it a must to change the production phases and pre-production phases from human-based to automation by computer aided design, computer and electronic aided manufacturing systems.

The intense competition in the foreign markets forces apparel producers to analyze their inputs that form the costs. Hence, there are certain improvements about automation which reduce the costs. Automation can be defined as the process of reducing the human work in the production phase. With the help of automation, the addiction to worker becomes lessened and switches the quality dependence from worker to the machine which is easier to adjust and to control.

In general, the advantages of all Computer Aided Design (CAD) / Computer Aided Manufacturing (CAM) systems are as follows:

- Allowing flexibility in production
- Better quality of production
- More sophisticated quality-control facilities
- Reduction in production times
- The opportunity to work fewer stocks (Groover, 1996)

10.2   Electronics and Computing In Modelling Department

CAD systems are used in preparation stages of model design, pattern making, marker planning and grading in clothing industry.

10.2.1 Model Design

CAD systems are equipped with functions to create fashion illustrations. Some of these functions are as follows:

- Free drawing
- Graphics drawing
- Pattern design templates
- Design enlarge or shrink
- Regional deformation or bending the pattern
- Color changes on the pattern
- The infinite possibilities of shading on design and model
- Dressing prepared design on garment model
- All drawings, designs and models drawn on paper or fabric can be transferred by scanners (Öndoğan, 1997)

10.2.2 Computerized Pattern Design, Grading And Marker (Cutting Plan) Making

After completion of model design, measurement of the design and patterns must be prepared. The body size results of previous studies are used during operation of measurement. Then the patterns are prepared according to these measurements for garment production.

The necessary arrangements on the main pattern are made. Then the pattern grading is made according to the measurement table which is already prepared.

Cutting plan preparation means placing the model patterns according to number specified in the order of production, and fabric characteristics. The system provides the chance to place of patterns during preparation of the cutting plan. The user is able to change the places of model and patterns manually (Öndoğan, 1997).

Another convenience provided by CAD systems is saving the patterns and cutting plans in a digital environment. Patterns and cutting plans can be stored and reused if needed (Öndoğan, 1994).

10.3 Electronics and Computing In Cutting Department

Cutting room is a critical department which affects the quality of the product and is where the cutting, spreading and arrangement of the fabric is made. Modernization in the cutting room has started with fabric spreading machines and has continued with computerized cutting planning systems has come to cutters which shortens the time and effort requiring cutting processes.

10.3.1 Automatic Fabric Spreading Machines

The automatic fabric spreading machines move on the railed system which combine two spreading tables and can be used on both tables at the same time. The fabric spreading process in the automatic fabric spreading machines can be automatically made by entering the parameters.

The spreading process must be started by using a control panel and the layers must be controlled by the operator. The machine has back and forth motion to make spreading. Automatic fabric spreading machines have types, which the operator standing or sitting in an armchair (Taylor, 1995, Erdoğan, 2003).

Figure 10.1: Fabric Spreading Machine (www.astasjuki.com)

Fabric spreading machines consist of the following sections;

- The engine
- Fabric tension control
- Photocell
- Worker carrying mechanism
- Electronic counter
- Cutter
- Fabric roll carrying mechanism
- Optional lighting
- Right and left spreading

10.3.2   Computer Aided Cutting Systems

Correct cutting process increases the productivity in the sewing room. NC cutter (numerically controlled cutter) is used in 1969 for the first time. With CAM (Computer Aided Manufacturing) systems, it's possible to get a fast and sensitive cutting and hence the time loss caused by operators who match the fabric pieces, is gone. CAM system also allows you to cut the pieces which touch or are really closer to each other, perfectly. This lets you save fabric in total. When you do the cutting with CAM system, there will be no difference between the layers of fabric; hence the productivity of the sewing room increases (Taylor, 1995).

Computer aided cutters are divided into two basic groups; electronic cutters and mechanical cutters. Classical round knives and upright-knifed cutters form the mechanical cutters. Round knives are used on low surfaces or on only one layer of fabric. Laser cutters make the cutting process by burning the fabric. Laser cutters are used on one single layer of fabric because with more layers of fabric, melting yarns may stick to each other and decrease the sensitivity of cutting. Water-jet cutters use the high pressured water. Water-jet is common for cutting leather and rubber surfaces (Erdoğan, 2003).

Computer aided fabric cutters cut fabrics according to marker plans which are prepared before. Machine can be connected to marker plan system online or offline. Computer aided cutters make a more sensitive and faster cut than manual systems. Cutting process is done by machine head which is rotated by computer to x and y directions. The other parts of cutter are table, control panel, command panel and vacuum system.

Figure 10.2: Computerized Fabric Cutting Machine (www.astasjuki.com)

10.4   Electronics and Computing In Sewing Room

In the production of apparel, the sewing time in a standard machine is 17% of the whole time. Rest of the time is spent on taking the piece, placing fabric into the machine and making adjustments. Technological developments and the necessity of doing good work in short time, lead the apparel producers to automation in the sewing room as well.

10.4.1   Electronics In Sewing Machine

Electronic lockstitch sewing machines are a part of automation as well. These machines allow you to adjust the speed of sewing at the beginning and hence the quality increases.

The operations in this machine are controlled by the operation panel. The places of the keys on the panel are easy to remember and use.

Figure 10.3: Electronic Sewing Machine (www.brothertr.com)

On automatic lockstitch sewing machines there are following features;

- Adjusting the diving time and speed
- Stopping the needle anywhere
- Hardening automatically (back tack stitch)
- Adjusting the sewing length
- Ending the sewing with photocell which sense the end of fabric
- Starting with slow start button
- Automatic thread trimming
- Automatic presser foot lifting

Another group of machines that supply the automation in the sewing room are computerized sewing machines. As you know, the worker starts the operation in computerized sewing machines and prepares the next piece while the sewing processes. There are many newly developed computerized sewing machines depending on the wide range of products. Computerized sewing machines are mostly used in factories that produce shirts, trousers and suits.

Some of these machines:

- Computerized pliers sewing machines
- Computerized hip pocket sewing machines
- Computerized flap pocket sewing machines
- Computerized belt loop sewing machines
- Computerized belt sewing machines
- Computerized side sewing machines…etc. (Taylor, 1995)

Figure 10.4: Hip Pocket Automaton (www.astasjuki.com)

Figure 10.5: Belt Loop Automaton (www.astasjuki.com)

The most common computerized sewing machines are buttonhole, button and bar tacking computerized sewing machines.

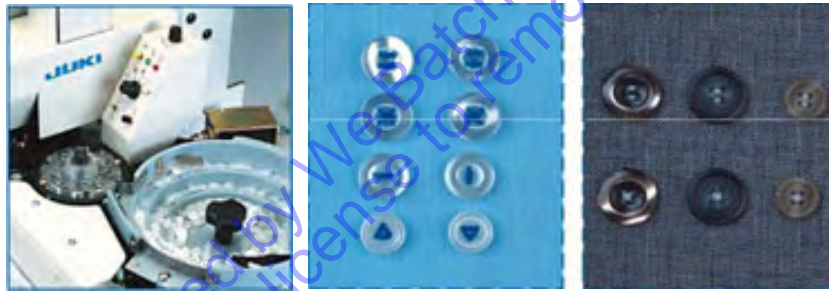**Figure 10.6:** Button sewing automaton (www.astasjuki.com)

10.4.2   Computerized Embroidery Machines

From past to present Embroidery machines have a major technological development. The first examples of these machines run with jacquard principle. Today these machines are computer aided. Embroidery machines have program packages. The machine works automatically with pre-designed patterns.

Figure 10.7: Computerized Embroidery Machines (www.brothertr.com)

Embroidery machines are lock stitch machines. Pattern formation is possible with the movement of the machine pulley (pantograph). Needle and looper are moved by the movement of main motor shafts arm. Stitch formation is related with this motor. Pattern formation is related with the pulse (step) motors. These motors are more numerous than one. According to the design of the pattern, pulse motors move the pantograph right to left and front to back. Patterns in computer language are converted to stitch design thanks to the pulse motors. Pulse motors guide the pulley for new location after the needles are come out of the fabrics. Pulley doesn't move when the needles are inside the fabrics.

It is possible to work with different colors in pattern belongs to the number of needles. Every needle works with each color in turn. It is viewed that only one needle works on each machine head during the machine running. The machine stops automatically when the thread is finished or broken thanks to electronic sensors. There is also an electromechanical system that cuts the thread in the end sewing embroidery.

10.5   Computerized Movers

The process of moving doesn't enrich the product even though moving is required in each stage of production. Therefore, it's aimed that the minimum cost, to be flexible and efficient, should minimize the need for personnel and space by using movers. Especially the small quantity orders, a wide variety of styles and quick response requirements make the moving process more complex (Tait, 1997).

During the process of moving, the products are moved by hangers. Therefore, the system has these advantages;

- Less wrinkle and staining (less ironing and stain removal)
- Less preparation time for workers
- No interferences of models and colors
- Transferring the production data every time to managers

Figure 10.8: Computerized Movers (www.astasjuki.com)

During computerized moving, each hanger unit is numbered with barcodes. Following info can be given on barcodes;

- Stations
- Process
- The model name
- Standard duration of transactions
- Type of operation
- The daily target
- The number of clothing on each hanger unit,
- Size
- Color
- The customer name…etc.

This information is given by production number in loading stations. The hanger unit is unloaded and the garment is sent to packaging unit, after all transactions completed. Empty hangers are returned to loading station. After loading, hanger units go to their destinations without any intervention.

10.6   Computerized Production Management and Control

Production management and control means to assemble materials, machinery and labor resources to provide the production and controls of the desired qualities, quantities and efficiency with the lowest time and cost (Özaltay, 2002).

The apparel companies must use the information technology, automation to achieve their goals. A variety of software was developed for apparel companies. Companies can check the new models, new collections and the status of their orders over the internet. This software, allows apparel companies to get information about all processes from preliminary costs to delivery.

Computer aided production management and control, can be used in a textile company for the following processes;

- Security
- Preliminary cost
- Proforma cost
- Customer management
- Marketing and sales
- Material requirements planning
- Time planning
- Order management
- Stock control
- The purchase
- Production follow-up
- Production management
- Delivery
- Packing list
- Current accounts
- The actual cost (Çepoğlu etal, 1997)

The production management and control can be done correctly thanks to this system. The companies will use these systems more efficient to preserve their place in competitive market.

10.7   Conclusion

Nowadays, apparel producers have to follow the fast improving technology in order to get a place in the world market. This situation requires automation in all steps of the process. But ready-made clothing producers should be careful with their choice of machine and go for the most suitable one for the factory and product range. And the producers should also watch out for the reliability of the company.

10.8   References

Çepoğlu, R., Karabay, G., 1997, Software Used In Apparel Companies For Production Management And Control, Tekstil ve Konfeksiyon, Vol. 3.

Erdoğan, M. Çetin, 2003, Apparel Machinery Lecture Notes.

Groover, M.P., 2007, Automation, Production Systems And Computer İntegrated Manufacturing, Prentice Hall Press.

Öndoğan, Z., 1994, CAD/CAM Systems In Apparel Industry, Tekstil ve Konfeksiyon, Vol. 5.

Öndoğan, Z.,1997, The Accordance Of Computer Aided Design Pattern Model Application And Marker Making Systems To Apparel Companies, PhD Thesis, Ege University Natural And Applied Science Institute.

Özaltay, M., 2002, Software Used In Apparel Companies For Production Management And Control, Thesis Study, Ege University Engineering Faculty Textile Engineering Department.

Tait, N., June 1997, Cost Effective Workflow Systems, Apparel International.

Taylor, P., 1995, Computers In Clothing Industry.

http://www.astasjuki.com/

http://www.brothertr.com/